BORNEO JOURNAL OF RESOURCE SCIENCE AND TECHNOLOGY

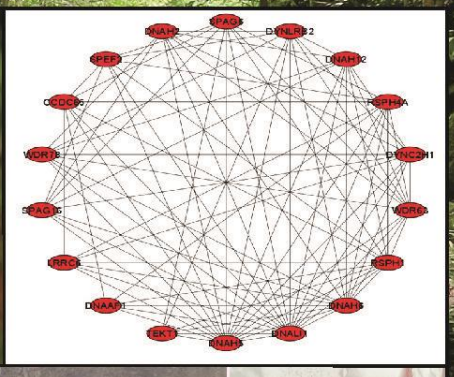

Volume 14 Number 1, June 2024
ISSN : 2229-9769
eISSN : 0128-2972

UNIMAS
UNIVERSITI MALAYSIA SARAWAK
PUBLISHER

BORNEO JOURNAL OF RESOURCE SCIENCE AND TECHNOLOGY

Borneo Journal of Resource Science and Technology (BJRST) publishes scientific articles in all fields of resource sciences. The journal welcomes the submission of manuscripts that meet the general criteria of significance and scientific excellence from but not limited to Borneo. Acceptance for publication is based on contributions to scientific knowledge, original data, ideas or interpretations and on their conciseness, scientific accuracy and clarity.

BJRST publishes scientific articles in all fields of resource sciences including land and forest resources, aquatic science, biodiversity and ecology, biotechnology and molecular biology, chemistry, microbiology, bioinformatics, plant science and zoology. It offers a forum for the discussion of local issues that are of global concern. It is a double-blind refereed online journal published bi-annually. Currently it is indexed by Scopus, MyCITE (Malaysian Citation Index),UDL edge Beta, DOAJ Directory of Open Access Journals, Index Copernicus, MyJurnal and Google Scholar.

When submitting the work, contributors are requested to make a declaration that the submitted work has not been published, or is being considered for publication elsewhere. Contributors have to declare that the submitted work is their own and that copyright has not been breached in seeking the publication of the work.

Views expressed by the author(s) in the article do(es) not necessarily reflect the views of the Editorial Committee.

Manuscripts can be submitted via https://publisher.unimas.my/ojs/index.php/BJRST

Correspondence on editorial matters should be addressed to: Prof

Dr Edmund Sim Ui Hang
Chief Editor
Borneo Journal of Resource Science and Technology
Faculty of Resource Science and Technology, Universiti
Malaysia Sarawak
94300 Kota Samarahan
Sarawak
Malaysia
uhsim@unimas.my

Contents

Borneo Journal of Resource Science and Technology (2024), 14(1): 1-17
DOI: https:doi.org/10.33736/bjrst.6065.2024

The Comparison between Pollution Index and STORET Methods in Determining Post-Mining Lake Water Quality in Lati Petangis Forest Park, Paser, East Kalimantan after Reclamation

NAUFAL HAFIDH MAHDI SUJARWO PUTRA[1], TRI RETNANINGSIH SOEPROBOWATI*[1,2,3] & JUMARI JUMARI[1,3]

[1]Department of Biology, Faculty of Science and Mathematics, Diponegoro University, Jl. Prof. Soedarto, SH, Tembalang, 50275 Semarang, Indonesia; [2]School of Postgraduate Studies, Diponegoro University, Jl. Imam Bardjo No. 3-5, 50241 Semarang, Indonesia; [3]Cluster for Paleolimnlogy (CPalim), Diponegoro University, 50241 Semarang, Indonesia.
*Corresponding author: trsoeprobowati@live.undip.ac.id
Received: 10 September 2023 Accepted: 15 April 2024 Published: 30 June 2024

ABSTRACT

Lati petangis Forest Park is a post-mining forest park located in Paser, East Kalimantan, Indonesia. This area has been through the stages of reclamation and post-mining lake has been formed. Monitoring activities are needed to determine the success of post-mining management. This study aims to assess the water quality of post-mining lake in Tahura Lati Petangis based on the Pollution Index and STORET methods. The research was located at 3 observation stations, which were station 1 (Pit Lake I Saingprupuk Erai), station 2 (Natural Lake Gentung Dayo), and station 3 (Pit Lake II Saingprupuk Duo). At all observation stations, *in-situ* water quality observations were made in the form of Dissolved Oxygen (DO), pH, and water temperature at 4 points sites. Water sampling was also carried out at 4 sites in each station for *ex-situ* quality testing. The determination of water quality status based on the Decree of the Minister of Environment of the Republic of Indonesia No. 115/2003 with lake water quality standards following the Government Regulation of the Republic of Indonesia No. 22/2021. The results showed that the STORET method is more sensitive than the Pollution Index. Determination of general water quality status shows that station 1 and 2 are only usable for agricultural activities (class IV). Station 3 is unable to be used for all four designation classes based on DO, BOD, COD, phosphate, phenol, and zinc parameters that are not meeting the quality standards. The STORET method is recommended to be used in determining water quality based on periodic and time progression.

Keywords: Pollution Index, Post-Mining Lake, STORET

INTRODUCTION

Paser District is located in the southern region of East Kalimantan Province, Indonesia, making the mining sector one of the sources of regional economic income, especially coal mining. Coal production in 2017 reached 32,879,307 tons, and in 2018 the production increased to almost 2 million tons (BPS Kab.Paser, 2022). High production as a source of long-term economic income needs to be considered because it can have a negative impact on the environment.

Lati Petangis Forest Park (Tahura Lati Petangis) is nature reserve located in Paser District, East Kalimantan, Indonesia. The area was previously former coal mining concession of PT BHP Kendilo Coal Indonesia, which ended its operations in 2002. Reclamation and revegetation activities have been carried out based on the principle of an area borrow-to-use system (DLH Kab. Paser, 2017). The area borrow-to-use system is a way to grant permits to use forest areas for mining activities without changing the function and designation of the forest area by taking revegetation and reclamation steps after the permit expires, and it will be returned to the local government as the landowner. Post-mining activities, such as reclamation and revegetation are efforts to improve land functions and provide ecological and economic benefits (Pratiwi *et al*., 2021). The establishment of the Lati Petangis Forest Park (Tahura) was based on the Decree of the Minister of Environment and Forestry of Republic Indonesia No. SK. 4335/MenLHK-PKTL/KUH/2015 on September 08, 2015 (DLH Kab.Paser, 2017).

The impacts of mining activities cause major changes to the landscape and land use (Redondo-Vega *et al*., 2021). Coal mining generates hazardous waste, such as heavy metal substances during production, washing, and several other processes. These hazardous wastes produce acid mine drainage with low pH and harmful for human consumption (Park *et al*., 2017; Zhou *et al*., 2020). Pollution from mining processes is an interaction between anthropogenic activities, hydrological activities and mineral rock weathering. The process that occurs will reduce the quality of waters and harm the living biota (Nyirenda *et al*., 2016; Dan-Badjo *et al*., 2019; Verma *et al*., 2019; Zhu *et al*., 2020; Punia *et al*., 2021).

The condition of Lati Petangis Forest Park is diverse, consisting of natural forest areas, revegetation areas, open areas, native lakes and post-mining lakes. The natural lake is the largest lake in that area and there are seven post-mining lakes (DLH Kab.Paser, 2017). Post-mining lakes are formed from mining pit dredging activities, which are filled by groundwater, surface water flow, and rainwater (Sakellari *et al*., 2021). Post-mining lakes are characterised by having an acidic pH, containing heavy metals, depths ranging from tens to hundreds of meters, so they have a dangerous risk of being used. Generally, the status of post-mining lakes is oligotrophic, although post-mining lakes have the potential to provide ecosystem and economic services (McJannet *et al*., 2019; Lund *et al*., 2020; Blanchette & Lund, 2021). Stability of post-mining lake water quality requires time that may range up to decades (Sakellari *et al*., 2021).

The previous research in the Lati Petangis Forest Park showed differences water quality in each lake. Ammonia and phenol were identified to exceed the water quality standards in all lakes (DLH Kab.Paser & FPIK Unmul, 2020). The high ammonia is caused by incomplete nitrogen cycle. This can reduce water quality through increasing the organic load of waters (Risacher *et al*., 2018; Nizzoli *et al*., 2020; Qian *et al*., 2021; Zhao *et al*., 2021). In addition, as a post-mining lake, there is concern that it still contains dangerous heavy metals.

The potential development of post-mining areas is related to economic value, ecology, education, and ecosystem safety characteristics (Soni *et al*., 2014). One of the considerations is water quality. Water quality is a condition of water quality that is measured or tested based on certain parameters and certain methods based on applicable laws and regulations (Government Regulation of Republic Indonesia No. 22/2021). Determination of lake water quality status is related to the function of its use class.

Based on the Decree of the Minister of Environment of Republic Indonesia No. 115/2003 about concerning guidelines for determining water quality status, the Pollution Index and STORET methods are recommended for determining the status of environmental pollution in Indonesia. Both methods are included in the Water Quality Index (WQI) method using the U.S. Environmental Protection Agency (US-EPA) value system. The use of the pollution index is only capable of describing water quality on temporary scale because it can be sourced from a single observation. The STORET method can be used to describe water quality consistently because the data is based on periodic development and time (Saraswati *et al*., 2014; Barokah *et al*., 2017). Comparison of water quality determination of the two methods may provide a suggestion of the suitable method to be used.

Terrestrial ecosystems and clean water, proper sanitation are two areas that need attention for the Sustainable Development Goals (SDG's). Some of the goals of these development sectors are to protect, restore and enhance the sustainable use of terrestrial ecosystems, restore land degradation, and ensure the availability and management of clean water (UNDP, 2015; Bappenas RI, 2021; Tyas *et al*., 2021). Research that aligns with sustainable development goals can help formulate follow-up strategies for regional development (Gebrehiwot *et al*., 2021; Thakur *et al*., 2022).

Lati Petangis Forest Park as post-mining area with the function of forest park has been running for approximately 20 years. Therefore, it is necessary to monitor and evaluate the post-mining development. The focus of the study was on the quality of post-mining lake waters.

MATERIALS AND METHODS

Description of the Study Area

The research was located in the Lati Petangis

Forest Park (Tahura Lati Petangis), Paser District, East Borneo, Indonesia, which has an area of 3,445.37 Ha. Geographically, it is located from north to south between 116°3'40.996″BT - 116°6'21.502″BT and 2°2'30.786″LS - 2°9'24.983″LS. As regards the administrative division, Lati Petangis Forest Park located in three villages, namely Saing Prupuk Village, Petangis Village, and Teberu Simpang Damai Village, Batu Engau, Paser District, East Kalimantan. The area has eight lakes, consisting of one natural lake and seven former mining exploration lakes (pit lakes).

The focus of the research was on lakes located in the Saingprupuk Village administration, namely Saingprupuk Erai Pit Lake I (Pit Lake I) and Saingprupuk Duo Pit Lake II (Pit Lake II) as post-mining lakes. While one other lake is a natural lake Gentung Dayo which is not included in the reclamation area of PT BHP Kendilo Coal Indonesia (Table 1).

Table 1. Characteristics of research sites

Station Number	Location Name	Coordinate Point	Size	Depth	Water Volume
Station 1	Pit Lake I Saingprupuk Erai	116°6'17.349″ E – 2°2'87.800″ S	1,31 Ha	10,5 m	94.975,00 m^3
Station 2	Natural Lake Gentung Dayo	116°5'48.730″ E – 2°3'49.080″ S	12,74 Ha	11,6 m	1.153.383,59 m^3
Station 3	Pit Lake II Saingprupuk Duo	116°5'50.558″ E – 2°4'32.902″ S	5,79 Ha	11,67 m	898.438,90 m^3

Source: DLH Kab.Paser & FPIK UNMUL, 2020

The study was held in January 2023 at the three observation stations (Figure 1). Water sampling was taken by purposive random sampling, and the three lakes each had four observation sites. At each station, water quality was measured based on temperature, pH, and dissolved oxygen (DO). Water samples were collected to analyze Chemical Oxygen Demand (COD), Biological Oxygen Demand (BOD), Ammonia (NH_3-N), Nitrate (NO_3-N), Nitrite (NO_2-N), Total Phosphate, Phenol, Dissolved Zinc (Zn), Dissolved Manganese (Mn), Dissolved Iron (Fe), Dissolved Lead (Pb), Dissolved Copper (Cu), Sulfide as (H_2S), and Sulfate.

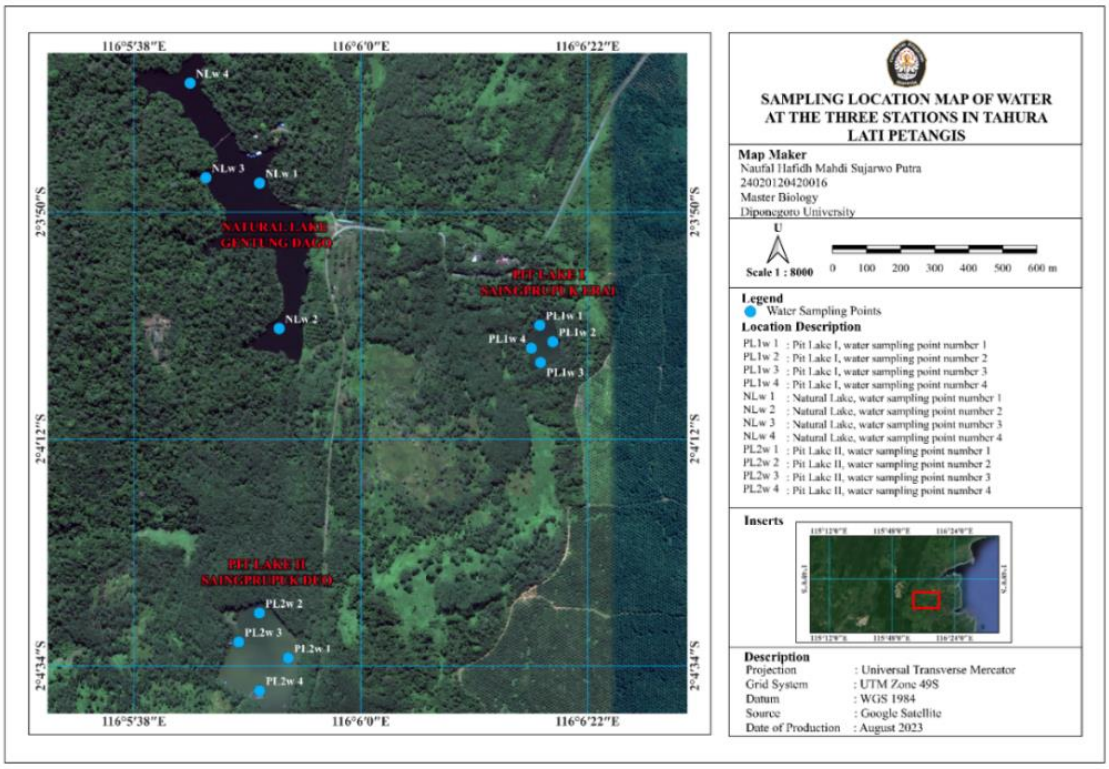

Figure 1. Research location of lakes in Lati Petangis Forest Park

Data Analysis

In-situ water quality measurements of pH, temperature, and Dissolved Oxygen (DO). Ex-situ measurements were made by taking 5 litres of water samples on the lake water surface at each research stations with 4 collection points. Lake water samples were tested at the Laboratory of Samarinda Industrial Research and Standardisation Centre, East Kalimantan. The *ex-situ* measurement parameters and Indonesian Standard Test methods used are as follows (Table 2).

Table 2. *Ex-Situ* parameters and testing methods for water quality parameters of Lati Petangis Forest Park Lakes

No	Parameters	Indonesia Standard Testing Methods
1	*Chemical Oxygen Demand* (COD)	SNI 6989.2.2019 (Spectrophotometry)
2	*Biological Oxygen Demand* (BOD)	SNI 6989.72:2009
3	Ammonia (NH_3-N)	SNI 06-6989.30-2005
4	Nitrate (NO_3-N)	SNI 06-2480-1991
5	Nitrite (NO_2-N)	SNI 06-6989.9-2004
6	Total Phosphate (PO_4)	SNI 06-6989.31-2005
7	Phenol (C_6H_6O)	SNI 06-6989.21-2004
8	Dissolved Zinc (Zn)	SNI 6989-84:2019
9	Dissolved Manganese (Mn)	SNI 6989-84:2019
10	Dissolved Iron (Fe)	SNI 6989-84:2019
11	Dissolved Lead (Pb)	SNI 6989-84:2019
12	Dissolved Copper (Cu)	SNI 6989-84:2019
13	Sulfide as (H_2S)	SNI 19-6964.4-2003
14	Sulfate	SNI 6989.20-2019

Source: Samarinda Industrial Standardisation and Services Centre, 2022

Pollution Index

The Pollution Index method is an easy assessment method and is able to produce calculations of the level of pollution to water quality standards (Suriadikusumah *et al*., 2021). The formula of PI as follows:

$$PI_j = \sqrt{\frac{(C_i/L_{ij})_M^2 + (C_i/L_{ij})_R^2}{2}} \qquad \text{Eq (1)}$$

where: *PIj* = pollution index for designation j; *Ci* = concentration of water quality parameter i; *Lij* = concentration of water quality parameter i listed in the standard for water designation j; *M* = maximum; *R* = average.

The maximum Ci/Lij is obtained from the Ci/Lij equation depending on the number of water quality parameters measured, and the value of the largest Ci/Lij is selected. The average Ci/Lij is obtained from the values of the Ci/Lij equation for each parameter summed up and divided by the number of water quality parameters measured.

Pollution Index was based on 17 water quality parameters, namely temperature, pH, and dissolved oxygen (DO), Chemical Oxygen Demand (COD), Biological Oxygen Demand (BOD), Ammonia (NH_3-N), Nitrate (NO_3-N), Nitrite (NO_2-N), Total Phosphate, Phenol, Dissolved Zinc (Zn), Dissolved Manganese (Mn), Dissolved Iron (Fe), Dissolved Lead (Pb), Dissolved Copper (Cu), Sulfide as (H2S), and Sulfate. The first step in determining water quality used the pollution index (PI) method to calculate the value as in Equation (1), then the evaluation of the PI value was included in Table 3.

Table 3. Status of water quality criteria in Pollution Index

Score Range	Water Quality Status
$0 \leq PI \leq 1,0$	Meets quality standards
$1,0 < PI \leq 5,0$	Lightly polluted
$5,0 < PI \leq 10$	Moderately polluted
$PI > 10$	Heavily polluted

Source: Decree of the Minister of Environment of Republic Indonesia No. 115/2003

STORET water quality index

STORET method principally compares water quality data with water quality standards in accordance with its designation. This method is usually through periodic measurements over time to form time series data. The way to determine the status of water quality is by using the value system from the US-EPA (U.S. Environmental Protection Agency) (Decree of the Minister of Environment of Republic Indonesia No.115/2003).

This research uses the calculation of water quality data for 2017, 2020, and 2023. If the measurement results meet the water quality standard value, the score is 0, and if the measurement results do not meet the water quality standard value, the score is given according to Table 4. Water quality parameters can be divided into physical, chemical, and biological parameters. The three types of parameters have different score systems.

Table 4. The water quality scoring system

Number of parameter samples used	Value	Parameter		
		Physical	Chemical	Biological
< 10	Maximum	-1	-2	-3
	Minimum	-1	-2	-3
	Average	-3	-6	-9
> 10	Maximum	-2	-4	-6
	Minimum	-2	-4	-6
	Average	-6	-12	-18

Source: Decree of the Minister of Environment of the Republic Indonesia No. 115/2003

The measurement of water quality parameters through maximum, minimum, and average values is compared with the quality standard value. The number of negatives (the calculation value does not meet the quality standard) of all parameters is calculated and the quality status is determined from the number of scores obtained using a score system. The values obtained are then classified into four classes of water quality status as follows (Table 5).

Table 5. Water quality classification in STORET method following US-EPA grading system

Class	Score	Characteristic of water quality
A	0	Meets quality standards
B	-1 to -10	Lightly polluted
C	-11 to -30	Moderately polluted
D	≥ -30	Heavily polluted

Source: Decree of the Minister of Environment of Republic Indonesia No. 115/2003

Determination of the designation of water quality standards is carried out by comparing the results of water quality measurements with the water quality standards listed in Government Regulation of Republic Indonesia No. 22/2021. Water quality classification is determined into four classes, namely:

1) Class I, water intended for drinking water raw water and or other designations that require the same water quality as these uses.
2) Class II, water intended for water recreation infrastructure / facilities, freshwater fish farming, animal husbandry, water for irrigating crops and or other designations that require the same water quality as these uses.
3) Class III, water intended for freshwater fish cultivation, animal husbandry, water for irrigating crops and or other uses that require the same water quality as these uses.

4) Class IV, water intended for irrigating crops and or other uses that require the same water quality as these uses.

RESULTS AND DISCUSION

By referring to Indonesian water quality standards, this study generally determined that water quality of station 1 (Pit Lake I Saingprupuk Erai) and station 2 (Natural Lake Gentung Dayo) are only suitable for agricultural or irrigation activities (class IV), while station 3 (Pit Lake II Saingprupuk Duo) is not suitable for all four use classes based on Government Regulation of Republic Indonesia No. 22/2021. Parameters that have not met the general water quality standards were Dissolved Oxygen (DO), Chemical Oxygen Demand (COD), Biological Oxygen Demand (BOD), Total Phosphate, and Phenol. In addition, specifically for Dissolved Zinc (Zn) at station III (Pit Lake II Saingprupuk Duo) the value has not met the quality standards.

pH

Station 1 and Station 2 had more alkaline water pH categories compared to Station 3 which was more neutral (Figure 2). Even so, the values shown from three observation stations meet the lake water quality standards for all classes. The pH value will increase along with the natural neutralization process and correlates with the age of the lake. An increase in the pH value of post-mining lake water is generally followed by decrease in the concentration level of aquatic minerals, and also increase in the concentration of aquatic nutrients (Oszkinis-Golon *et al.*, 2020; Pukacz *et al.*, 2020; Gąsiorowski *et al.*, 2021).

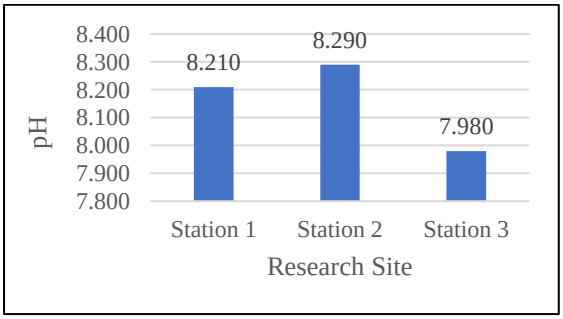

Figure 2. pH at three observation stations of lakes in Lati Petangis Forest Park

Temperature

Temperature measurements showed that the lake water quality standards were met for the designation of all classes based on Government Regulation of Republic Indonesia No.22/2021 (Figure 3). Water temperature is very important in measuring water health and determining the process of nutrient release. Water temperature also supports the life and development of biota species in the environment (Peng *et al.*, 2022).

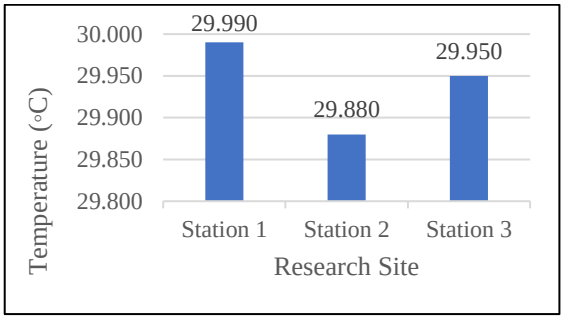

Figure 3. Temperature at three observation stations of lakes in Lati Petangis Forest Park

Dissolved Oxygen (DO)

The DO values obtained from the three observation stations were only be used for fish farming and agricultural activities (class III and IV) (Figure 4). Dissolved oxygen (DO) is influenced by water temperature as one of the abiotic factors. Higher water temperature causes lower dissolved oxygen. The lower dissolved oxygen value, the worse the water quality. Dissolved oxygen plays a role in supporting metabolic processes of aquatic biota and biogeochemical processes (Wilson, 2010; Carey & Woelmer, 2020; Febiyanto, 2020; Handoko & Sutrisno, 2021).

Chemical Oxygen Demand (COD) & Biological Oxygen Demand (BOD)

The COD values of the three observation stations meet the water quality standards for class II, class III, and class IV designations. BOD value for station 1 meets the quality standards for all classes, while the BOD values for stations 2 and 3 only meet the quality standards for class II, III, and IV designations (Figure 4). COD is a total organic water whose value is inversely proportional to dissolved oxygen (DO). COD is the level of water pollution by organic substances that can be oxidized, causing a reduction in dissolved oxygen content (Mafuyai *et al.*, 2020; Abdullahi *et al.*, 2021). COD values are always higher than BOD. Comparison of COD and BOD values can

determine the number of organic compounds that are persistent and cannot be degraded by aquatic microorganisms. Thus, it is able to investigate the source of origin of organic contaminants (Mafuyai *et al*., 2020; Abdullahi *et al*., 2021; Qi *et al*., 2021).

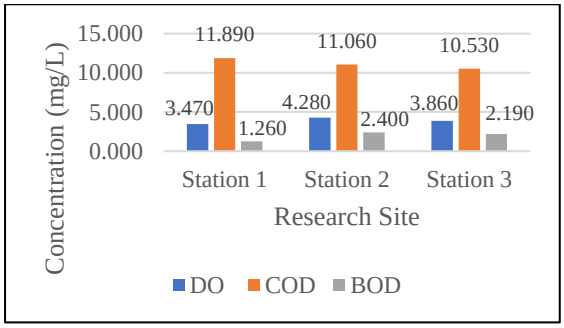

Figure 4. Dissolved Oxygen (DO), Chemical Oxygen Demand (COD), and Biological Oxygen Demand (BOD) at three observation stations of lakes in Lati Petangis Forest Park

Ammonia, nitrite, & nitrate

Ammonia, nitrite, and nitrate in waters are generally other forms of compounds from the decomposition of nitrogen by microorganisms. Sources of high nitrogen concentrations in waters can come from anthropogenic activities as well as litter from plants around the waters (Baker *et al*., 2017; Roland *et al*., 2018; Zhang *et al*., 2022). Nitrate values are always higher than ammonia and nitrite, but ammonia and nitrite are much more toxic in waters than nitrate. The process of changing from ammonia to nitrite is much slower than the change of nitrite to nitrate. Nitrite concentrations in drinkable waters range from 0.01 - 0.1 mg/L and ammonia ranges from 0.05 - 0.5 mg/L (Schullehner *et al*., 2017; Spiridon *et al*., 2018; Monson, 2022). Nitrite and ammonia values at the three observation stations showed <0.5 mg/L (Figure 5).

Total Phosphate & Phenol

Total Phosphate concentrations at three observation stations have not met the quality standards for classes I and II. At the phenol concentration, the value has not met the quality standards for classes I, II, and III, while at station III it has not met the quality standards for all four classes (Figure 6). The entry of phosphate into water bodies is heavily influenced by rainfall through water runoff (Rustiah *et al*., 2019; Wang

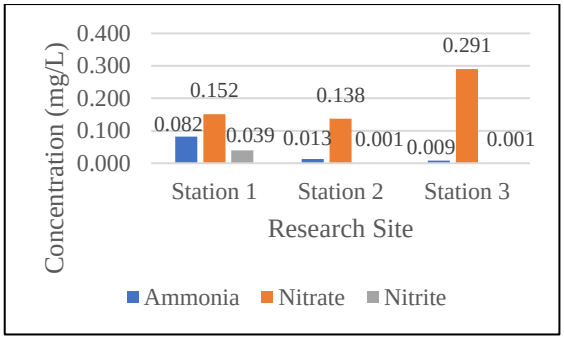

Figure 5. Ammonia, nitrate, and nitrite at three observation stations of lakes in Lati Petangis Forest Park

et al., 2022). Phosphate is one of the parameters that trigger eutrophication. The concentration of phosphate in sediments is higher than phosphate in surface waters (Rustiah *et al*., 2019; Li & Zuo, 2020). Phenol entering waters can be caused by natural sources such as the decomposition of dead plants. The nature of phenol in waters can persist for a long time and very reactive to form toxic substances (Anku *et al*., 2017).

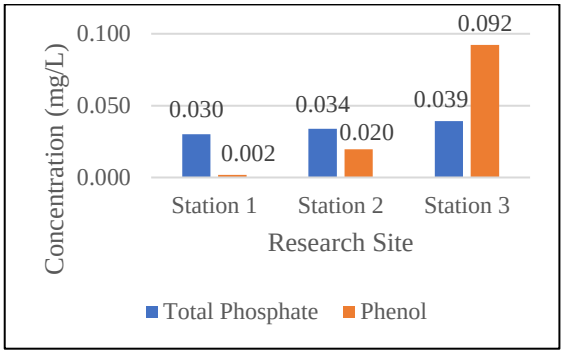

Figure 6. Total Phosphate and Phenol at three observation stations of lakes in Lati Petangis Forest Park

Dissolved Zinc & Dissolved Manganese

Dissolved Zinc (Zn) concentrations for station I and station II meet all four quality standard classes. While for station III only meets the quality standards of class IV. In addition, measurements of Dissolved Manganese (Mn) concentrations at three observation stations met all four classes (Figure 7). Excess concentration of zinc (Zn) produces toxic compounds that can accumulate in the body of aquatic biota. Zinc (Zn) enters the water generally due to anthropogenic activities (Noulas *et al*., 2018; Li *et al*., 2019). Manganese (Mn) entering waters generally comes from anthropogenic activities and natural processes. Manganese (Mn) concentration strongly influenced by dissolved

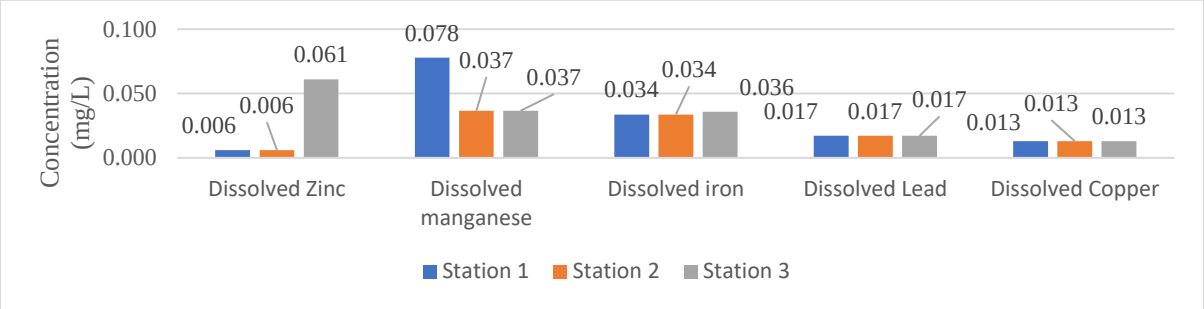

Figure 7. Dissolved Zinc, Dissolved Manganese, Dissolved Iron, Dissolved Lead, and Dissolved Copper at three observation stations of lakes in Lati Petangis Forest Park

oxygen, pH, sediment composition, and temperature (Neculita & Rosa, 2019; Kousa *et al*., 2021; Nkele *et al*., 2022).

Dissolved Iron, Dissolved Lead, & Dissolved Copper

Measurements of dissolved iron (Fe), dissolved lead (Pb), and dissolved copper (Cu) at three observation stations met all four quality standard classes (Figure 7). The entry of dissolved iron (Fe) into waters comes from mining and industrial activities, rock weathering, and input from groundwater (Xiao *et al*., 2022). High concentrations of iron in waters cause health problems for those who consume it (Kumar *et al*., 2017). Lead in water becomes toxic and contaminates aquatic biota through bioaccumulation and biomagnification mechanisms (Kołodyńska *et al*., 2018; Li *et al*., 2021). The toxicity level of lead (Pb) in waters is influenced by other water quality parameters, such as pH, temperature, dissolved organic matter content, and water hardness (Zheng *et al*., 2017). Copper (Cu) is mostly found in water bodies and surfaces rather than in the bottom. Copper concentration dynamics are related to binding with organic matter (Rader *et al*., 2019; Yusni & Ifanda, 2020).

Sulfide as H_2S & Sulfate

Measurements of sulfide concentrations as H_2S and sulfate at three observation stations met all four quality classes (Figure 8). Specific concentrations of organic matter decomposing into hydrogen sulfide are toxic in aquatic environments (Siang *et al*., 2017; Austigard *et al*., 2018). Sulfide as H_2S in waters comes from the decay of plants and animals from bacteria or the direct reduction process of sulfate (Austigard *et al*., 2018). H_2S as a gas in waters is observed to determine the potential for organic pollution of waters. High concentrations of sulfate are toxic and present serious risks to human health and ecological balance. Sulfate is widely sourced from industrial activities, agricultural runoff, rock weathering, and mining activities (Wang & Zhang, 2019; Zak *et al*., 2021).

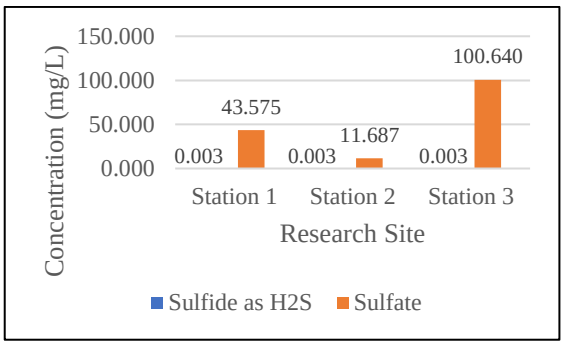

Figure 8. Sulfide as H_2S and Sulfate at three observation stations of lakes in Lati Petangis Forest Park

Water Quality Index

Based on Pollution Index (IP), station 1 meets the water quality standards for classes II, III, and IV, only class I is still lightly polluted. Station 2 is lightly polluted for water criteria classes I, II, and III. Only class IV has good condition criteria. Station 3 has moderate to lightly polluted criteria for all four water quality classes (Figure 9).

Physiochemical parameters used in STORET calculations were observed temporally. Time series data of pH, water temperature, Dissolved Oxygen (DO), Chemical Oxygen Demand (COD), Biological Oxygen Demand (BOD), Ammonia (NH3-N), Nitrate (NO3-N), Nitrite (NO2-N), Total Phosphate, Phenol, Dissolved Zinc (Zn), Dissolved Manganese (Mn), Dissolved Iron (Fe), Dissolved Lead (Pb),

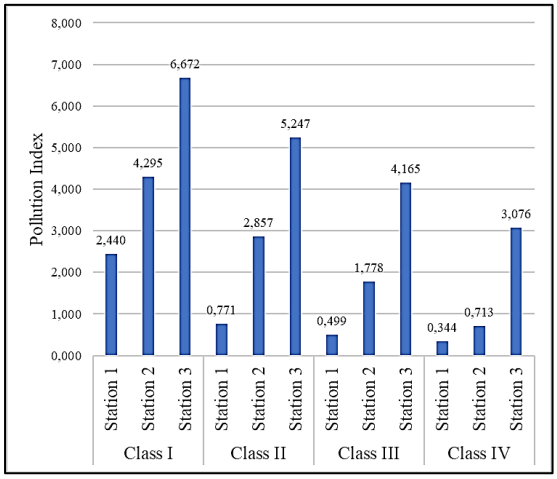

Figure 9. Pollution Index based on class categorized at each research station at Lati Petangis Forest Park

Dissolved Copper (Cu), Sulfide as (H_2S), and Sulfate of Lati Petangis Forest Park post-mining lake in 2017 (Sumargo, 2017) and 2020 (DLH Kab. Paser & FPIK UNMUL, 2020) combined with the data from this study showed that status of water lake at station 1 and station 2 only met the criteria for class IV. While the status of lake water at station 3 categorizes as heavily polluted for classes I and II, and moderately polluted for classes III and IV (Table 6).

Table 6. Water quality status of Lakes in Lati Petangis Forest Park based on STORET method

Parameter	Measurement Unit	Min.	Max.	Average	Score Class I	Score Class II	Score Class III	Score Class IV
Station 1 (Pit Lake I Saingprupuk Erai)								
Temperature	◦C	28,800	29,990	29,395	0	0	0	0
pH		7,310	8,210	7,760	0	0	0	0
Dissolved Oxygen (DO)	mg/L	3,470	4,800	4,135	-10	-2	0	0
Chemical Oxygen Demand (COD)	mg/L	8,000	11,890	9,945	-2	0	0	0
Biochemical Oxygen Demand (BOD)	mg/L	1,260	3,900	2,580	-8	-2	0	0
Ammonia (NH_3-N)	mg/L	0,057	0,082	0,069	-	-	-	-
Nitrate (NO_3-N)	mg/L	0,055	0,152	0,103	-	-	-	-
Nitrite (NO_2-N)	mg/L	0,039	0,087	0,063	-	-	-	-
Total Phosphate	mg/L	0,030	0,046	0,038	-10	-10	0	-
Phenol	mg/L	0,002	0,014	0,008	-8	-8	-2	0
Dissolved Zinc (Zn)	mg/L	0,001	0,006	0,003	0	0	0	0
Dissolved Manganese (Mn)	mg/L	0,001	0,078	0,039	0	0	0	0
Dissolved Iron (Fe)	mg/L	0,034	0,080	0,057	0	-	-	-
Dissolved Lead (Pb)	mg/L	-	-	-	-	-	-	-
Dissolved Copper (Cu)	mg/L	-	-	-	-	-	-	-
Sulfide as (H_2S)	mg/L	-	-	-	-	-	-	-
Sulfate	mg/L	-	-	-	-	-	-	-
STORET total score					-38	-22	-2	0

Parameter	Measurement Unit	Min.	Max.	Average	Score Class I	Score Class II	Score Class III	Score Class IV
Station 2 (Natural Lake Gentung Dayo)								
Temperature	◦C	29,600	29,880	29,740	0	0	0	0
pH		6,220	8,290	7,137	0	0	0	0
Dissolved Oxygen (DO)	mg/L	4,280	7,600	5,940	-4	0	0	0
Chemical Oxygen Demand (COD)	mg/L	8,000	19,830	12,963	-16	0	0	0
Biochemical Oxygen Demand (BOD)	mg/L	1,900	6,700	3,667	-16	-16	-4	0
Ammonia (NH_3-N)	mg/L	0,006	0,077	0,032	-	-	-	-
Nitrate (NO_3-N)	mg/L	0,017	0,138	0,064	-	-	-	-
Nitrite (NO_2-N)	mg/L	0,001	0,029	0,010	-	-	-	-
Total Phosphate	mg/L	0,034	0,086	0,059	-20	-20	0	-
Phenol	mg/L	0,008	0,020	0,014	-20	-20	-16	0
Dissolved Zinc (Zn)	mg/L	0,001	0,010	0,006	0	0	0	0
Dissolved Manganese (Mn)	mg/L	0,001	0,037	0,016	0	0	0	0
Dissolved Iron (Fe)	mg/L	0,034	0,204	0,104	0	-	-	-
Dissolved Lead (Pb)	mg/L	0,010	0,017	0,014	0	0	0	0
Dissolved Copper (Cu)	mg/L	0,007	0,013	0,010	0	0	0	0
Sulfide as (H_2S)	mg/L	0,003	0,003	0,003	-	-	-	-
Sulfate	mg/L	11,100	11,687	11,393	0	0	0	0
STORET total score					-76	-56	-20	0
Station 3 (Pit Lake II Saingprupuk Duo)								
Temperature	◦C	29,800	29,950	29,875	0	0	0	0
pH		6,520	7,980	7,157	0	0	0	0
Dissolved Oxygen (DO)	mg/L	3,860	5,100	4,480	-20	-16	0	0
Chemical Oxygen Demand (COD)	mg/L	10,530	28,000	20,303	-20	-4	0	0
Biochemical Oxygen Demand (BOD)	mg/L	2,047	4,200	2,812	-20	-4	0	0
Ammonia (NH_3-N)	mg/L	0,009	0,053	0,034	-	-	-	-
Nitrate (NO_3-N)	mg/L	0,043	0,291	0,179	-	-	-	-
Nitrite (NO_2-N)	mg/L	0,001	0,010	0,004	-	-	-	-
Total Phosphate	mg/L	0,039	0,131	0,092	-20	-20	-4	-
Phenol	mg/L	0,092	0,240	0,166	-20	-20	-20	-20

Parameter	Measurement Unit	Min.	Max.	Average	Score Class I	Score Class II	Score Class III	Score Class IV
Dissolved Zinc (Zn)	mg/L	0,001	0,061	0,025	-4	-4	-4	0
Dissolved Manganese (Mn)	mg/L	0,001	0,037	0,016	0	0	0	0
Dissolved Iron (Fe)	mg/L	0,016	0,481	0,178	-4	-	-	-
Dissolved Lead (Pb)	mg/L	0,010	0,017	0,014	0	0	0	0
Dissolved Copper (Cu)	mg/L	0,007	0,013	0,010	0	0	0	0
Sulfide as (H_2S)	mg/L	0,003	0,003	0,003	-	-	-	-
Sulfate	mg/L	49,233	100,640	74,937	0	0	0	0
STORET total score					-108	-68	-28	-20

Source: own study

The calculation and categorization of the water quality lakes status of Lati Petangis Forest Park using the Pollution Index (IP) and STORET showed differences. The STORET method shows more "polluted" than calculations using the Pollution Index (IP) method. The Pollution Index (IP) method bases the calculation on the maximum parameter value, which is obtained from the division of the most influential parameters against the quality standard. While the STORET method bases the assessment of all parameters used through the minimum value, maximum value, and average value. Determination of water quality status using the STORET method is able to see which parameters exceed or meet quality standards and more sensitive in describing the dynamic changes in water quality (Saraswati *et al*., 2014; Barokah *et al*., 2017).

Using the Pollution Index (IP) and STORET methods have their own advantages and disadvantages, as in the Pollution Index (IP), where the data source comes from a single observation (single sample), so it is only able to describe water quality in short moment. As for the STORET method, the data processed based on periodic development and time, so it is able to more fully and sensitively describe water quality. However, the STORET method needs to be careful in determining the water quality parameters, because the assessment is based on the accumulation of parameters that do not meet quality standards, so choosing the wrong water quality parameters can lead to errors in determining the conclusion of water quality status (Saraswati *et al*., 2014). Both the Pollution Index (IP) and STORET methods can be used in determining water quality status in Indonesia becauserecommended through the Decree of the Minister of Environment of Republic Indonesia No. 115/2003.

Based on measurements of water quality parameters, the source of pollution in three observed lakes is generally related to organic compounds in the waters, although in the station 3 there is an indicator of zinc (Zn) whose value exceeds the quality standard. The high concentration of zinc (Zn) in the waters can be attributed to the rock formations that make up the lake, which naturally through the process of erosion and sedimentation enter the waters (Rogozin & Gavrilkina, 2008). High organic compounds in the water are suspected to come from riparian vegetation through leaf litter and natural lake processes. Although this statement needs further study Meanwhile, the high organic compounds in the water are suspected to come from riparian vegetation through leaf litter and natural lake processes. Leaf litter will undergo decomposition, thus affecting the organic compounds of the waters (Mutshekwa *et al*., 2020). Although, this concern needs further research.

Indications of organic compound pollution at three research stations were supported by plankton data that was found in the research by DLH Kab. Paser & FPIK UNMUL (2020). Plankton can be used as bioindicators in determining water quality (Soeprobowati *et al*., 2021). Phytoplankton growth is influenced by nitrate and nitrite compounds (Idrus *et al*., 2017). Station 1 found many species of *Oscillatoria* sp. and *Navicula* sp. The presence of *Oscillatoria* sp. is associated with many organic compounds in the waters (Soetignya *et*

al., 2021) and the presence of *Navicula* sp. is a warning of deteriorating lake conditions (Yusuf, 2020). Station 2 found many species of *Navicula* sp. and *Nitzschia* sp. Both of species are found in water conditions with moderate to heavy pollution categories by nutrients or organic compounds (Heramza *et al*., 2021). Station 3 found many species of *Nitzschia* sp. and *Synedra ulna*. *Synedra ulna* indicates the status of eutrophic waters (Heramza *et al*., 2021).

The pollution pattern shown earlier has been observed in 2020. Concentrations of COD, total phosphate, phenol were always observed as sources of lake water pollution in the last 3 years. The source parameters of lake water pollution are known from the STORET calculation of the three observation stations. Therefore, more attention can be focused on reducing the concentration of COD, total phosphate, and phenol as organic pollutants.

Determination of water quality status using the Pollution Index and STORET can provide advice on the proper method to use as needed. STORET is recommended because it is more sensitive (Barokah *et al*., 2017). On the other sides, the Pollution Index can also be used to obtain a quick overview of water quality.

The importance of determining the water quality status of post-mining lakes is to determine the potential for lake development. For example, the pit lake at Collie in Australia has developed into an aquaculture site for crustaceans. Rassnitz Pit Lake, Paupitzsch Pit Lake and Gremmin Pit Lake in Germany have developed into part of protected areas for nature conservation (Blanchette & Lund, 2016; Sakellari *et al*., 2021). Monitoring the water quality status of the ex-mining lake in Lati Petangis Forest Park is necessary to develop the potential of the area, as contained in the water designation class through Government Regulation of the Republic of Indonesia No. 22/2021. Knowing the source of water pollutants can facilitate the focus of remediation to help formulating the usage of lake water as drinking water, water recreation facilities, aquaculture activities, or agricultural activities.

CONCLUSION

The determination of the water quality status at three observation stations based on the Pollution Index (PI) and STORET methods, shows that station 1 (Pit Lake I Saingprupuk Erai) and station 2 (Natural Lake Gentung Dayo) can only be used for agricultural or irrigation activities (class IV), while station 3 (Pit Lake II Saingprupuk Duo) cannot be used for the four classes based on the Government Regulation of the Republic of Indonesia No. 22/2021. The STORET methods shown more sensitive than Pollution Index. Furthermore, the pattern of pollution at three observation stations is related to water organic compounds, such as Chemical Oxygen Demand (COD), Biological Oxygen Demand (BOD), Total Phosphate, and Phenol. Thus, the value of Dissolved Oxygen (DO) is also affected. Comparison of the two methods of determining water quality status can provide advice on the suitable method according to their needs. Monitoring water quality can help determine the class of water designation.

ACKNOWLEDGEMENTS

This research was supported by the Paser Regency Environmental Service and the Laboratory of the Industrial Services Standardization and Services Center Samarinda. The authors would like to thank the staff of the Environmental Agency, the forest and land fire brigade of Lati Petangis Forest Park, and the laboratory technicians.

REFERENCES

Abdullahi, A.B., Siregar, A.R., Pakiding, W. & Mahyuddin. (2021). The analysis of BOD (Biological Oxygen Demand) and COD (Chemical Oxygen Demand) contents in the water of around laying chicken farm. *IOP Conference Series: Earth and Environmental Science,* 788(012155). DOI 10.1088/1755-1315/788/1/012155

Anku, W.W., Mamo, M.A., Mamo, M.A., Penny, P.W. & Govender, P.P. (2017). Phenolic Compounds Water: Sources, Reactivity, Toxicity, and Treatment Methods. Natural Sources, Importance and Applications. *Intech Open:* 419–443. DOI: 10.5772/66927

Austigard, Å.D., Svendsen, K. & Heldal, K.K. (2018). Hydrogen sulphide exposure in waste water treatment. *Journal of Occupational Medicine and Toxicology,* 13: 1–10. DOI: https://doi.org/10.1186/s12995-018-0191-z

Bappenas RI (Badan Perencanaan Pembangunan Nasional Republik Indonesia). (2021). *Air Bersih dan Sanitasi Layak (Tujuan Pembangunan Berkelanjutan SDGs*). Accessed in https://sdgs.bappenas.go.id/tujuan-6/ on 07 May 2023.

BPS Kab. Paser (Badan Pusat Statistik Kabupaten Paser). (2022). *Paser Regency in Numbers 2022 (Kabupaten Paser Dalam Angka 2022) pp. 341-347*. Tanah Grogot. CV Suvi Sejahtera.

Baker, J.A., Gilron, G., Chalmers, B.A. & Elphick, J.R. (2017). Evaluation of the effect of water type on the toxicity of nitrate to aquatic organisms. *Chemosphere,* 168: 435–440. DOI: https://doi.org/10.1016/j.chemosphere.2016.10.059

Barokah, G.R., Ariyani, F. & Siregar, T.H. (2017). Comparison Of Storet And Pollution Index Method To Assess The Environmental Pollution Status: A Case Study From Lampung Bay, Indonesia. *SQUALEN Bulletin of Marine and Fisheries Postharvest and Biotechnology,* 12(2): 67-74. DOI: https://doi.org/10.15578/squalen.287

Blanchette, M.L. & Lund, M.A. (2016). Pit lakes are a global legacy of mining: an integrated approach to achieving sustainable ecosystems and value for communities. *Current Opinion in Environmental Sustainability,* 23: 28–34. DOI: https://doi.org/10.1016/j.cosust.2016.11.012

Blanchette, M.L. & Lund, M.A. (2021). Aquatic ecosystems of the Anthropocene: Limnology and microbial ecology of mine pit lakes. *Microorganisms,* 9(6): 1207. DOI: https://doi.org/10.3390/microorganisms9061207

Carey, C.C. & Woelmer, W.M. (2020). Water Quality Assessment Procedures For Virginia: Dissolved Oxygen Assessment Of Lakes And Reservoirs. *2020 Report of the Academic Advisory Committee for Virginia Department of Environmental Quality, pp. 1-19*. Virginia Water Resources Research Center. Virginia.

Dan-Badjo, A.T., Ibrahim, O.Z., Guéro, Y., Morel, J.L., Feidt, C. & Echevarria, G. (2019). Impacts of artisanal gold mining on soil, water and plant contamination by trace elements at Komabangou, Western Niger. *Journal of Geochemical Exploration,* 205: 106328. DOI: https://doi.org/10.1016/j.gexplo.2019.06.010

Decree of the Minisiter of Environment of Republic Indonesia No.115/2003. (2003). *Keputusan Menteri Lingkungan Hidup Nomor 115 Tahun 2003 tentang Pedoman Penentuan Status Mutu Air*. Jakarta.

DLH Kab. Paser & FPIK UNMUL (Dinas Lingkungan Hidup Kabupaten Paser & Fakultas Perikanan dan Ilmu Kelautan Universitas Mulawarman). (2020). *Paser Regency Lati Petangis Forest Park Lake Fauna Study Report* (*Laporan Kajian Fauna Danau Taman Hutan Raya Lati Petangis Kabupaten Paser) pp. 1-21.* Tanah Grogot.

DLH Kab. Paser (Dinas Lingkungan Hidup Kabupaten Paser). (2017). *Potential Inventory of Lati Petangis Area (Inventarisasi Potensi Kawasan Tahura Lati Petangis) pp. 1-32*. Tanah Grogot.

Febiyanto, F. (2020). Effects of Temperature and Aeration on The Dissolved Oxygen (DO) Values in Freshwater Using Simple Water Bath Reactor: A Brief Report. *Walisongo Journal of Chemistry,* 3(1): 25. DOI: https://doi.org/10.21580/wjc.v3i1.6108

Gąsiorowski, M., Stienss, J., Sienkiewicz, E. & Sekudewicz, I. (2021). Geochemical Variability of Surface Sediment in Post-Mining Lakes Located in the Muskau Arch (Poland) and Its Relation to Water Chemistry. *Water, Air, & Soil Pollution,* 232: 108. DOI: https://doi.org/10.1007/s11270-021-05057-8

Gebrehiwot, S.G., Bewket, W., Mengistu, T., Nuredin, H., Ferrari, C.A. & Bishop, K. (2021). Monitoring and assessment of environmental resources in the changing landscape of Ethiopia: a focus on forests and water. *Environmental Monitoring and Assessment,* 193: 1–13. DOI: https://doi.org/10.1007/s10661-021-09421-3

Government Regulation of the Republic Indonesia No. 22/2021. (2021). *Peraturan Pemerintah (PP) Republik Indonesia Nomor 22 Tahun 2021 tentang Penyelenggaraan Perlindungan dan Pengelolaan Lingkungan Hidup*. Jakarta.

Handoko, M. & Sutrisno, A.J. (2021). Spatial and Temporal Analysis of Dissolved Oxygen (DO) and Biological Oxygen Demand (BOD) Concentrations in Rawa Pening Lake, Semarang Regency. *Jurnal Geografi Gea,* 21: 58–71. DOI: https://doi.org/10.17509/gea.v21i1.32330

Heramza, K., Barour, C., Djabourabi, A., Khati, W. & Bouallag, C. (2021). Environmental parameters and diversity of diatoms in the Aïn Dalia dam, Northeast of Algeria. *Biodiversitas* 22(9), 3633–3644. DOI: https://doi.org/10.13057/biodiv/d220901

Idrus, F. A., Chong, M. D., Abd Rahim, N. S., Mohd Basri, M. & & Musel, J. (2017). Physicochemical parameters of surface seawater in Malaysia exclusive economic zones off the Coast of Sarawak. *Borneo Journal of Resource Science and Technology,* 7(1): 1-10. DOI: https://doi.org/10.33736/bjrst.388.2017

Kołodyńska, D., Gęca, M., Skwarek, E. & Goncharuk, O. (2018). Titania-Coated Silica Alone and Modified by Sodium Alginate as Sorbents for Heavy Metal Ions. *Nanoscale Research Letters,* 13: 96. DOI: https://doi.org/10.1186/s11671-018-2512-7

Kousa, A., Komulainen, H., Hatakka, T., Backman, B. & Hartikainen, S. (2021). Variation in groundwater manganese in Finland. *Environmental Geochemistry and Health,* 43: 1193–1211. DOI: https://doi.org/10.1007/s10653-020-00643-x

Kumar, V., Bharti, P.K., Talwar, M., Tyagi, A.K. & Kumar, P. (2017). Studies on high iron content in water resources of Moradabad district (UP), India. *Water Science,* 31(1): 44–51. DOI: https://doi.org/10.1016/j.wsj.2017.02.003

Li, J. & Zuo, Q. (2020). Forms of nitrogen and phosphorus in suspended solids: A case study of Lihu Lake, China. *Sustainability,* 12(12): 5026. DOI: https://doi.org/10.3390/su12125026

Li, L., Sun, F., Liu, Q., Zhao, X. & Song, K. (2021). Development of regional water quality criteria of lead for protecting aquatic organism in Taihu Lake, China. *Ecotoxicology and Environmental Safety,* 222: 112479. DOI: https://doi.org/10.1016/j.ecoenv.2021.112479

Li, X.F., Wang, P.F., Feng, C.L., Liu, D.Q., Chen, J.K. & Wu, F.C. (2019). Acute Toxicity and Hazardous Concentrations of Zinc to Native Freshwater Organisms Under Different pH Values in China. *Bulletin of Environmental Contamination and Toxicology,* 103: 120–126. DOI: https://doi.org/10.1007/s00128-018-2441-2

Lund, M., van Etten, E., Polifka, J., Vasquez, M.Q., Ramessur, R., Yangzom, D. & Blanchette, M.L. (2020). The Importance of Catchments to Mine-pit Lakes: Implications for Closure. *Mine Water and the Environment,* 39: 572–588. DOI: https://doi.org/10.1007/s10230-020-00704-8

Mafuyai, G.M., Ayuba, M.S. & Zang, C.U. (2020). Physico-Chemical Characteristics of Tin Mining Pond Water Used for Irrigation in Plateau State, Central Nigeria. *Open Journal of Environmental Research,* 1(2): 9-35. DOI: https://doi.org/10.52417/ojer.v1i2.164

McJannet, D., Hawdon, A., Baker, B., Ahwang, K., Gallant, J., Henderson, S. & Hocking, A. (2019). Evaporation from coal mine pit lakes: Measurements and modelling. In AB Fourie & M Tibbet (eds). *Mine Closure 2019: Proceedings of the 13th International Conference on Mine Closure, Australian Centre for Geomechanics, Perth*, pp. 1391-1404.

Monson, P. (2022). *Aquatic Life Water Quality Standards Draft Technical Support Document for Nitrate*, pp. 1-19. Minnesota Pollution Control Agency. Minnesota.

Mutshekwa, T., Cuthbert, R.N., Wasserman, R.J., Murungweni, F.M. & Dalu, T. (2020). Nutrient Release Dynamics Associated with Native and Invasive Leaf Litter Decomposition: A Mesocosm Experiment. *Water*, 12(9): 2350. DOI: https://doi.org/10.3390/w12092350

Neculita, C.M. & Rosa, E. (2019). A review of the implications and challenges of manganese removal from mine drainage. *Chemosphere,* 214: 491–510. DOI: https://doi.org/10.1016/j.chemosphere.2018.09.106

Nizzoli, D., Welsh, D.T. & Viaroli, P. (2020). Denitrification and benthic metabolism in lowland pit lakes: The role of trophic conditions. *Science of The Total Environment,* 703: 134804. DOI:https://doi.org/10.1016/j.scitotenv.2019.134804

Nkele, K., Mpenyana-Monyatsi, L. & Masindi, V. (2022). Challenges, advances and sustainabilities on the removal and recovery of manganese from wastewater: A review. *Journal of Cleaner Production,* 377: 134152. DOI: https://doi.org/10.1016/j.jclepro.2022.134152

Noulas, C., Tziouvalekas, M. & Karyotis, T. (2018). Zinc In Soils, Water and Food Crops. *Journal of Trace Elements in Medicine and Biology,* 49: 252–260. DOI: https://doi.org/10.1016/j.jtemb.2018.02.009

Nyirenda, T.M., Zhou, J., Mapoma, H.W.T., Xie, L. & Li, Y. (2016). Hydrogeochemical Characteristics of Groundwater at the Xikuangshan Antimony Mine in South China. *Mine Water and the Environment,* 35: 86–93 DOI: https://doi.org/10.1007/s10230-015-0341-9

Oszkinis-Golon, M., Frankowski, M., Jerzak, L. & Pukacz, A. (2020). Physicochemical differentiation of the Muskau Arch pit lakes in the light of long-term changes. *Water*, 12(9): 2368. DOI: https://doi.org/10.3390/w12092368

Park, J.H., Edraki, M. & Baumgartl, T. (2017). A practical testing approach to predict the geochemical hazards of in-pit coal mine tailings and rejects. *Catena,* 148: 3–10. DOI: https://doi.org/10.1016/j.catena.2015.10.027

Peng, Z., Yang, K., Shang, C., Duan, H., Tang, L., Zhang, Y., Cao, Y. & Luo, Y. (2022). Attribution analysis of lake surface water temperature changing —taking China's six main lakes as example. *Ecological Indicators,* 145: 109651. DOI:https://doi.org/10.1016/j.ecolind.2022.109651

Pratiwi, Narendra, B.H., Siregar, C.A., Turjaman, M., Hidayat, A., Rachmat, H.H., Mulyanto, B., Suwardi, Iskandar, Maharani, R., Rayadin, Y., Prayudyaningsih, R., Yuwati, T.W., Prematuri, R. & Susilowati, A. (2021). Managing and reforesting degraded post-mining landscape in Indonesia: A review. *Land,* 10(6): 658. DOI: https://doi.org/10.3390/land10060658

Pukacz, A., Oszkinis-Golon, M. & Frankowski, M. (2020). The physico-chemical diversity of pit lakes of the Muskau Arch (Western Poland) in the context of their evolution and genesis. *Limnological Review*, 18(3): 115–126. DOI: https://doi.org/10.2478/limre-2018-0013

Punia, A., Bharti, R. & Kumar, P. (2021). Impact of mine pit lake on metal mobility in groundwater. *Environmental Earth Sciences,* 80(7): 245. DOI: https://doi.org/10.1007/s12665-021-09559-w

Qi, M., Han, Y., Zhao, Z. & Li, Y. (2021). Integrated determination of chemical oxygen demand and biochemical oxygen demand. *Polish Journal of Environmental Studies,* 30(2): 1785–1794. DOI: https://doi.org/10.15244/pjoes/122439

Qian, J., Jin, W., Hu, J., Wang, P., Wang, C., Lu, B., Li, K., He, X. & Tang, S. (2021). Stable isotope analyses of nitrogen source and preference for ammonium versus nitrate of riparian plants during the plant growing season in Taihu Lake Basin. *Science Total Environment,* 763: 143029. DOI:https://doi.org/10.1016/j.scitotenv.2020.143029

Rader, K.J., Carbonaro, R.F., van Hullebusch, E.D., Baken, S. & Delbeke, K. (2019). The Fate of Copper Added to Surface Water: Field, Laboratory, and Modeling Studies. *Environmental Toxicology and Chemistry,* 38(7): 1386–1399. DOI: https://doi.org/10.1002/etc.4440

Redondo-Vega, J.M., Melón-Nava, A., Peña-Pérez, S.A., Santos-González, J., Gómez-Villar, A. & González-Gutiérrez, R.B. (2021). Coal pit lakes in abandoned mining areas in León (NW Spain): characteristics and geoecological significance. *Environmental Earth Sciences,* 80: 1–14. DOI: https://doi.org/10.1007/s12665-021-10037-6

Risacher, F.F., Morris, P.K., Arriaga, D., Goad, C., Nelson, T.C., Slater, G.F. & Warren, L.A. (2018). The interplay of methane and ammonia as key oxygen consuming constituents in early stage development of Base Mine Lake, the first demonstration oil sands pit lake. *Applied Geochemistry Journal,* 93: 49–59. DOI: https://doi.org/10.1016/j.apgeochem.2018.03.013

Rogozin, A.G. & Gavrilkina, S. V. (2008). Causes for high concentration of copper and zinc in the water of some lakes in the Southern Urals. *Water Resources,* 35: 701–707. DOI: https://doi.org/10.1134/S0097807808060092

Roland, F.A.E., Darchambeau, F., Borges, A. V., Morana, C., De Brabandere, L., Thamdrup, B. & Crowe, S.A. (2018). Denitrification, anaerobic ammonium oxidation, and dissimilatory nitrate reduction to ammonium in an East African Great Lake (Lake Kivu). *Limnology and Oceanography*, 63(2): 687–701. DOI: https://doi.org/10.1002/lno.10660

Rustiah, W., Noor, A., Maming, Lukman, M., Baharuddin, A. & Fitriyah, T. (2019). Distribution Analysis of Nitrate and Phosphate in Coastal Area: Evidence from Pangkep River, South Sulawesi. *International Journal of Agriculture System,* 7(1): 9–17. DOI: 10.20956/ijas.v7i1.1835.

Sakellari, C., Roumpos, C., Louloudis, G. & Vasileiou, E. (2021). A Review about the Sustainability of Pit Lakes as a Rehabilitation Factor after Mine Closure. *Materials Proceedings*, 5(1): 52. DOI: https://doi.org/10.3390/materproc2021005052

Saraswati, S.P., Sunyoto, S., Kironoto, B.A. & Hadisusanto, S. (2014). Assessment of the Forms and Sensitivity of the Index Formula PI, STORET, CCME for the Determination of Water Quality Status. *Jurnal Manusia dan Lingkungan,* 21(2), 129-142. DOI: https://doi.org/10.22146/jml.18536

Schullehner, J., Stayner, L. & Hansen, B. (2017). Nitrate, nitrite, and ammonium variability in drinking water distribution systems. *International Journal of Environmental Research and Public*

Health, 14(3): 276. DOI: https://doi.org/10.3390/ijerph14030276

Siang, H.Y., Tahir, N.M., Malek, A. & Isa, M.A.M. (2017). Breakdown Of Hydrogen Sulfide In Seawater Under Different Ratio Of Dissolved Oxygen / Hydrogen Sulfide. *Malaysian Journal of Analytical Sciences,* 21(5): 1016–1027. DOI: https://doi.org/10.17576/mjas-2017-2105-03

Soeprobowati, T.R., Addadiyah, N.L., Hariyati, R. & Jumari, J. (2021). Physico-chemical and biological water quality of Warna and Pengilon Lakes, Dieng, Central Java. *Journal Of Water And Land Development,* 51(10-12): 38–49. DOI: 10.24425/jwld.2021.139013

Soetignya, W.P., Marniati, P., Adijaya, M. & Anzani, Y.M. (2021). The diversity of plankton as bioindicators in Kakap River Estuary, West Kalimantan. *Depik Jurnal Ilmu-Ilmu Perairan, Pesisir dan Perikanan,* 10(2): 174-179. DOI:https://doi.org/10.13170/depik.10.2.21303

Soni, A., Mishra, B. & Singh, S. (2014). Pit lakes as an end use of mining: A review. *Journal of Mining and Environment,* 5(2): 99–111. DOI: https://doi.org/10.22044/jme.2014.326

Spiridon, C., Teodorof, L., Burada, A., Despina, C., Seceleanu-Odor, D., Tudor, I.M., Ibram, O., Georgescu, L.P., Ţopa, C.M., Negrea, B.M. & Tudor, M. (2018). Seasonal variations of nutrients concentration in aquatic ecosystems from danube delta biosphere reserve. *AACL Bioflux,* 11(6): 1882–1891.

Sumargo. (2017). Water Quality Analysis of Lake Former Coal Mine Excavation in Lati Petangis Forest Park, Batu Engau District, Paser Regency (Analisis Kualitas Air Danau Bekas Galian Tambang Batu Bara di Tahura Lati Petangis Kecamatan Batu Engau Kabupaten Paser). *Thesis Master*. Mulawarman University, Samarinda.

Suriadikusumah, A., Mulyani, O., Sudirja, R., Sofyan, E.T., Maulana, M.H.R. & Mulyono, A. (2021). Analysis of the water quality at Cipeusing river, Indonesia using the pollution index method. *Acta Ecologica Sinica,* 41(3): 177–182. DOI: https://doi.org/10.1016/j.chnaes.2020.08.001

Thakur, T.K., Dutta, J., Upadhyay, P., Patel, D.K., Thakur, A., Kumar, M. & Kumar, A. (2022). Assessment of land degradation and restoration in coal mines of central India: A time series analysis. *Ecological Engineering,* 175: 106493. DOI: https://doi.org/10.1016/j.ecoleng.2021.106493

Tyas, D.S., Soeprobowati, T.R. & Jumari, J. (2021). Water Quality of Gatal Lake, Kotawaringin Lama, Central Kalimantan. *Journal of Ecological Engineering,* 22(3): 99–110. DOI: https://doi.org/10.12911/22998993/132427

UNDP (United Nations Development Programme). (2015). *Sustainable Development Goals*. Accessed in https://www.undp.org/sustainable-development-goals on 07 May 2023.

Verma, S., Mukherjee, A., Mahanta, C., Choudhury, R., Badoni, R.P. & Joshi, G. (2019). Arsenic fate in the Brahmaputra river basin aquifers: Controls of geogenic processes, provenance and water-rock interactions. *Applied Geochemistry,* 107: 171-186. DOI: https://doi.org/10.1016/j.apgeochem.2019.06.004

Wang, H. & Zhang, Q. (2019). Research advances in identifying sulfate contamination sources of water environment by using stable isotopes. *International Journal of Environmental Research and Public Health,* 16(11): 1914. DOI: https://doi.org/10.3390/ijerph16111914

Wang, R., Cai, C., Zhang, J., Sun, S. & Zhang, H. (2022). Study on phosphorus loss and influencing factors in the water source area. *International Soil and Water Conservation Research,* 10(2): 324–334. DOI: https://doi.org/10.1016/j.iswcr.2021.07.002

Wilson, P.C. (2010). *Water Quality Notes: Dissolved Oxygen,* pp. 1-9. Soil and Water Science Department, Florida Cooperative Extension Service, Institute of Food and Agricultural Sciences, University of Florida. Florida. http://edis.ifas.ufl.edu.

Xiao, X., Han, G., Zeng, J., Liu, M. & Li, X. (2022). Geochemical and Seasonal Characteristics of Dissolved Iron Isotopes in the Mun River, Northeast Thailand. *Water,* 14(13): 2038. DOI: https://doi.org/10.3390/w14132038

Yusni, E. & Ifanda, D. (2020). Analysis of heavy metal of copper (Cu) and lead (Pb) at Siombak Lake North Sumatera Province. *IOP Conference Series: Earth and Environmental Science* 454(012129). DOI: 10.1088/1755-1315/454/1/012129

Yusuf, Z.H. (2020). Phytoplankton as bioindicators of water quality in nasarawa reservoir, Katsina State Nigeria. *Acta Limnologica Brasiliensia*, 32(4): 1-11. DOI: 10.1590/s2179-975x3319

Zak, D., Hupfer, M., Cabezas, A., Jurasinski, G., Audet, J., Kleeberg, A., McInnes, R., Kristiansen, S.M., Petersen, R.J., Liu, H. & Goldhammer, T. (2021). Sulphate in freshwater ecosystems: A review of sources, biogeochemical cycles, ecotoxicological effects and bioremediation. *Earth-Science Reviews,* 212: 103446. DOI: https://doi.org/10.1016/j.earscirev.2020.103446

Zhang, D., Li, M., Yang, Y., Yu, H., Xiao, F., Mao, C., Huang, J., Yu, Y., Wang, Y., Wu, B., Wang, C., Shu, L., He, Z. & Yan, Q. (2022). Nitrite and nitrate reduction drive sediment microbial nitrogen cycling in a eutrophic lake. *Water Research,* 220: 118637. DOI: https://doi.org/10.1016/j.watres.2022.118637\

Zhao, S., Zhang, B., Sun, X. & Yang, L. (2021). Hot spots and hot moments of nitrogen removal from hyporheic and riparian zones: A review. *Science of The Total Environment,* 762: 144168. DOI: https://doi.org/10.1016/j.scitotenv.2020.144168

Zheng, L., Liu, Z., Yan, Z., Zhang, Y., Yi, X., Zhang, J., Zheng, X., Zhou, J. & Zhu, Y. (2017). pH-dependent ecological risk assessment of pentachlorophenol in Taihu Lake and Liaohe River. *Ecotoxicology and Environmental Safety,* 135: 216–224. DOI: https://doi.org/10.1016/j.ecoenv.2016.09.023

Zhou, M., Li, X., Zhang, M., Liu, B., Zhang, Y., Gao, Y., Ullah, H., Peng, L., He, A. & Yu, H. (2020). Water quality in a worldwide coal mining city: A scenario in water chemistry and health risks exploration. *Journal of Geochemical Exploration,* 213: 106513. DOI: https://doi.org/10.1016/j.gexplo.2020.106513

Zhu, G., Wu, X., Ge, J., Liu, F., Zhao, W. & Wu, C. (2020). Influence of mining activities on groundwater hydrochemistry and heavy metal migration using a self-organizing map (SOM). *Journal of Cleaner Production,* 257: 120664. DOI:https://doi.org/10.1016/j.jclepro.2020.120664

Borneo Journal of Resource Science and Technology (2024), 14(1): 18-29
DOI: https:doi.org/10.33736/bjrst.5849.2024

Ethnoichthyology of the First Record of Spine Bahaba (*Bahaba polykladiskos*) from Muar, Johor, Malaysia

ILHAM-NORHAKIM MOHD LOKMAN[1,2,3], NAJMUDDIN MOHD FAUDZIR[1], HARIS HIDAYAH[1], OTHMAN NURSYUHADA[1], RAMLI FARAH FARHANA[1], SARIYATI NUR HARTINI[1], HALIM MUHAMMAD RASUL ABDULLAH[4], ABDULLAH-FAUZI NURFATIHA AKMAL FAWWAZAH[1] & ABDUL-LATIFF MUHAMMAD ABU BAKAR[*1]

[1]Environmental Management and Conservation Research Unit (eNCORe), Faculty of Applied Sciences and Technology, Universiti Tun Hussein Onn Malaysia, (Pagoh Campus) 84600 Muar, Johor, Malaysia; [2]Kim Ichthyologist Centre, Kampung Parit Samsu, Jalan Temenggong Ahmad, 84150 Parit Jawa Muar, Johor, Malaysia; [3]Naturetech Resources Enterprise TL MRBP F32/A, Jalan Temenggong Ahmad, 84150, Parit Jawa, Muar Johor; [4]Tropical Infectious Diseases Research & Education Centre (TIDREC), Universiti Malaya, 50603, Kuala Lumpur
*Corresponding author: latiff@uthm.edu.my
Received: 11 July 2023 Accepted: 23 January 2024 Published: 30 June 2024

ABSTRACT

The Spine Bahaba (*Bahaba polykladiskos*), locally known as 'Gelama Tirusan,' is a member of the Sciaenidae fish family that is distributed across Southeast Asia, reaching as far as North Australia. This species is renowned for its swim bladder, which produces a distinctive loud sound. Despite its distribution in Southeast Asia, no previous studies have reported the presence of the Spine Bahaba in Peninsular Malaysia. This research aims to document the first-ever record of *B. polykladiskos* in Muar River, Johor, and provide ethnoichthyological insights regarding this species. The ethnoichthyological data were collected using a convenience snowball sampling technique, involving the collection of information from communities residing in the Muar area. In total, 47 respondents participated in the study. The results indicate that a majority of the respondents were familiar with (98%) and had encountered (94%) *B. polykladiskos* in both the Muar River and the local fish market. The study also documented the demand and trade associated with *B. polykladiskos* in Muar, with recorded prices ranging from RM 20 to RM 11,500 per fish. Furthermore, this research provides an introductory description of the uses and perceived benefits of *B. polykladiskos* in traditional medicine, particularly in relation to sexual prowess among male respondents. The study successfully establishes a baseline information for *B. polykladiskos* in Peninsular Malaysia using an ethnoichthyological approach, thus extending the known geographical distribution of this distinctive species.

Keywords: Gelama Tirusan, Peninsular Malaysia, Sciaenidae, traditional medicine

INTRODUCTION

Spine Bahaba, *Bahaba polykladiskos* (Bleeker, 1852), known locally as 'Gelama Tirusan' in Malaysia, was originally described from Banjarmasin, Borneo, Indonesia. This species is highly targeted due to the lucrative value of its swim bladder. However, the taxonomic classification of *B. polykladiskos* remains problematic. Chao *et al.* (2020) suggest that it should be reclassified under the genus *Boesemania*, (Trewavas, 1977). Nevertheless, pending the completion of additional studies, it has been decided to maintain the name *B. polykladiskos* (Bleeker, 1852) as suggested by Parenti (2020). Belonging to the family Sciaenidae, fish in this family are commonly referred to as croakers or drums. The Sciaenidae family is one of the largest perciform fish families and comprises several economically significant species (Nelson, 2006; Lo *et al.*, 2017). The name "croakers" or "drums" stems from their unique ability to produce sound by utilising their swim bladder as a resonating chamber (Nelson, 2006; Ramcharitar *et al.*, 2006). The Spine Bahaba can reach a maximum size of 200 cm in standard length (Nurhayati *et al.*, 2016). Its head and body are entirely covered by scales, with the complete lateral-line scales. The species possesses a long and continuous dorsal fin, with a noticeable notch between the anterior dorsal spines and the posterior soft rays. The anal fin consists of two spines, with the second spine being enlarged (Sasaki, 2001). The

caudal fin of the Spine Bahaba is typically emarginate. The body coloration of the species displays significant variation, ranging from silvery to dark brown (Figure 1).

Similar to other sciaenids, the Spine Bahaba typically exhibits demersal behavior and occupies habitats characterised by sandy or muddy substrates (Robins *et al*., 1986; Murdy *et al.*, 1997). It is predominantly found in shallow coastal waters and estuaries, often in close proximity to continental regions. In certain instances, it has been known to venture into freshwater environments (Nurhayati *et al.*, 2016). The species can be found in a depth range of 10 to 35 m (Nelson, 2006; Chao *et al.*, 2020). Records of the Spine Bahaba's distribution include the Gulf of Thailand (Yoshida *et al.*, 2013), the Mekong drainage (Kottelat, 1989; Rainboth *et al*., 2012; Huan *et al.*, 2016; Tám *et al.*, 2019), South Sumatra (Nurhayati *et al.*, 2016; Ridho & Patriono, 2017), the South China Sea (Randall & Lim, 2000), and extending westward to south Borneo (Kottelat, 2013; Chao *et al.*, 2020; Parenti, 2020) (Figure 2). However, there is a notable absence of official reports documenting the presence of this species in the waters of Peninsular Malaysia within the existing literature.

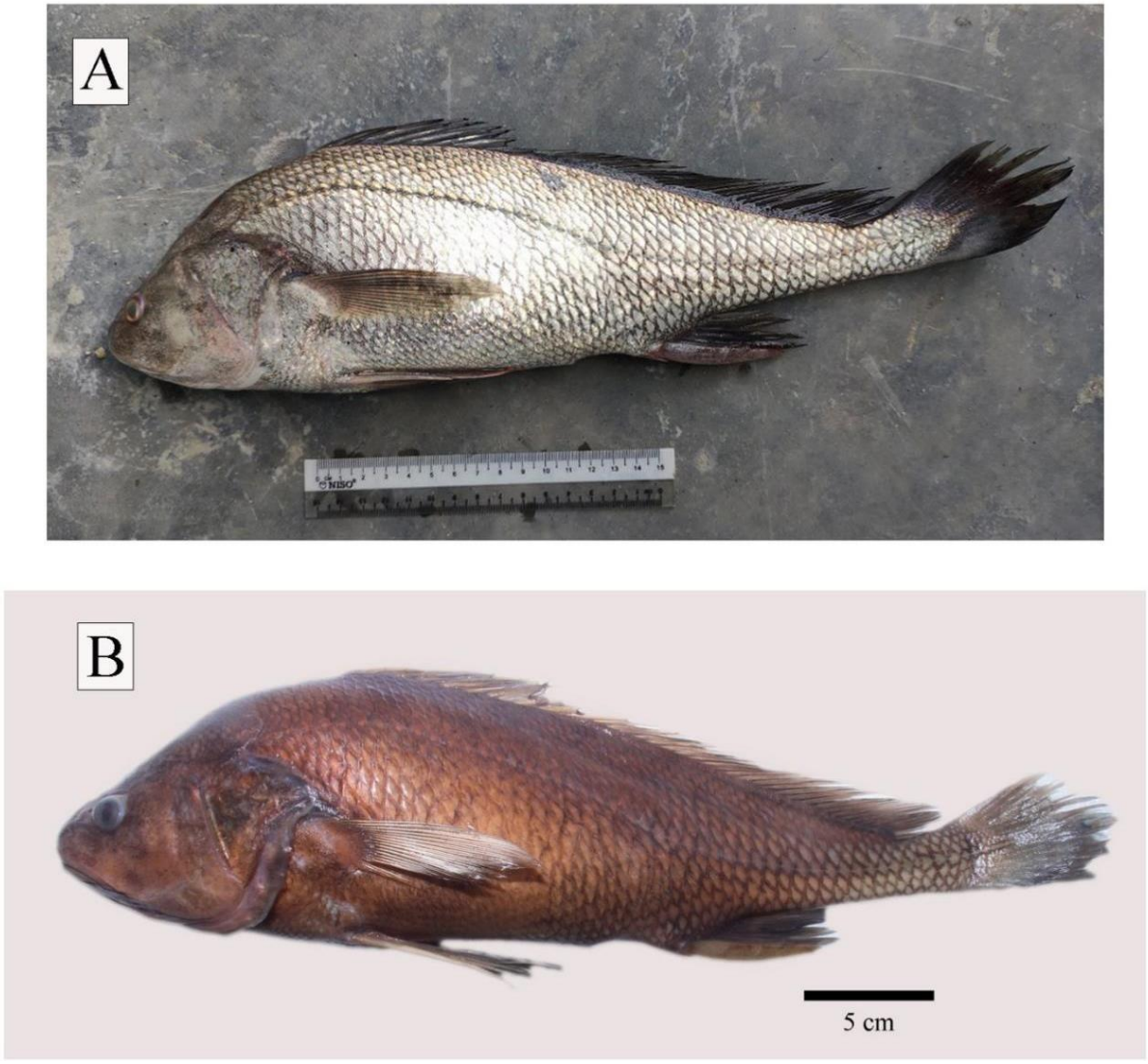

Figure 1. Specimen of Spiny Bahaba UMKL 12883 collected in Muar, Johor. A) Freshly caught specimen. B) Preserved specimen

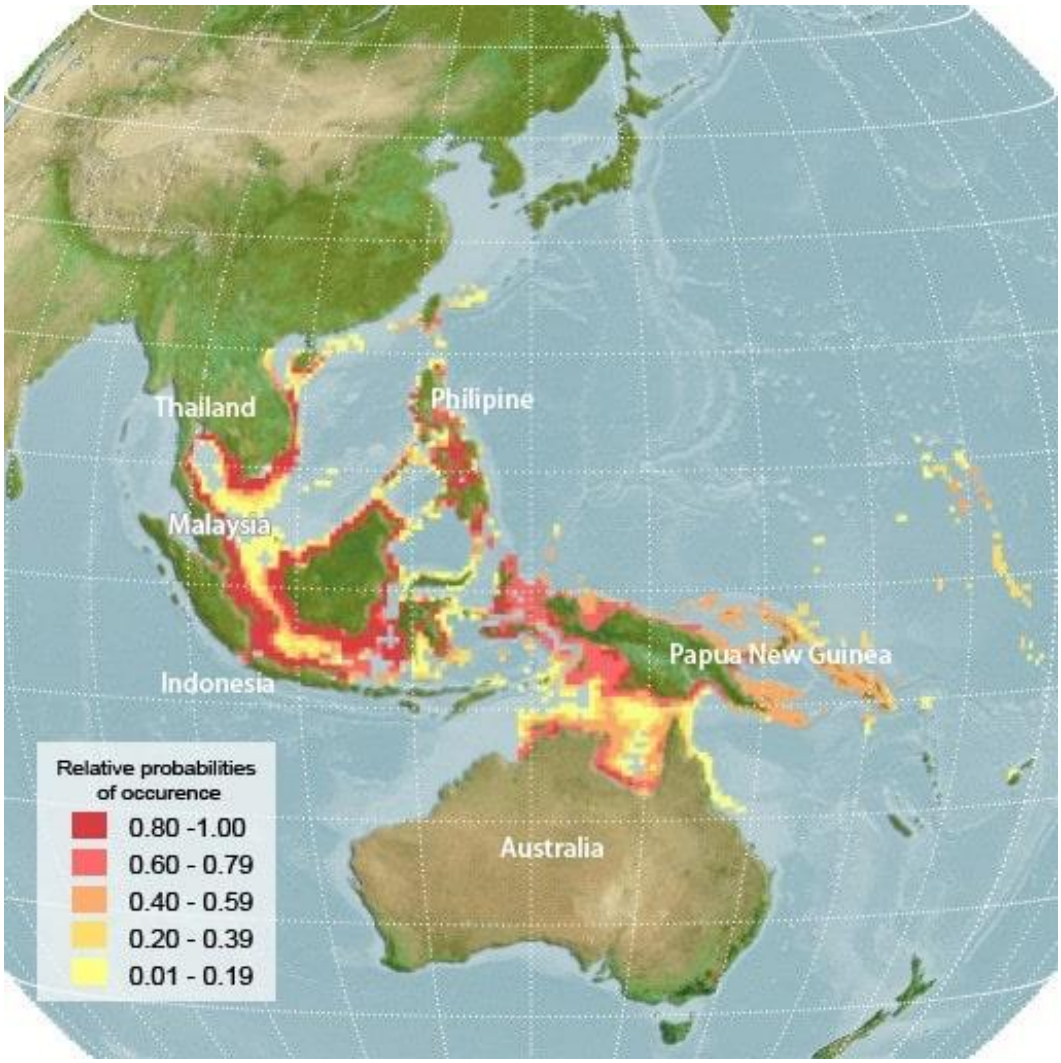

Figure 2. Computer generated native distribution of *B. polykladiskos*. (AquaMaps 2019)

Ethnoichthyology, as a branch of ethnobiology, focuses on exploring the intricate relationships between humans and fish (Oishi, 2016; Svanberg & Locker, 2020). The local fishing communities possess valuable traditional ecological knowledge that can serve as a significant source of information, particularly regarding fish behavior, abundance and distribution, owing to their extensive expertise in fish biology and classification (Djidohokpin *et al.*, 2020). However, despite their wealth of knowledge, the local information derived from fishing communities has yet to be formally integrated into fisheries management practices. By bridging the gap between scientists and decision-makers, it becomes possible to interpret and supplement the local fishing community's knowledge with scientific information, thereby enhancing the development of effective management strategies for small-scale fisheries (Berkes *et al.*, 2001). Therefore, a comprehensive understanding of ethnoichthyology is crucial, as it not only enhances our comprehension of marine ecosystem dynamics and fishing activities but also contributes to improving the community's livelihoods, especially when it involves medicinal purposes or subsistence practices (Djidohokpin *et al.*, 2020). The potential of ethnoichthyological studies to serve as valuable management tools is significant, as they shed light on critical information that can provide essential guidelines for biological research, particularly within the context of the Muar fishers community.

The documentation of fish utilisation, particularly for medicinal purposes, requires immediate attention. It is essential to preserve and document this knowledge, as it currently remains unavailable for further study and future reference. Given the escalating anthropogenic activities, the alarming rate of biodiversity loss, and the degradation of natural habitats, the

invaluable knowledge and insights related to fish are at risk of extinction, rapidly disappearing if not adequately documented. Therefore, the present study aimed to document the occurrence of *B. polykladiskos* in the Muar River, while also collecting ethnoichthyological information from the local communities.

MATERIALS & METHODS

Study Area

The study area encompasses the Muar River, as depicted in Figure 3. Serving as the main artery of the Muar River Basin, the river spans an estimated width of 150 to 300 m. Its origin lies within the longitudes 102°14'00" East to 103°04'00" East and latitudes 1°52'00" North to 2°54'00" North. Flowing across three states in South Peninsular Malaysia—Negeri Sembilan, Pahang, and Johor—the river stretches a total length of 329 km (Bahaman *et al.*, 2011; Ching *et al.*, 2015; Idris *et al.*, 2016). The Muar River is situated in a region characterised by distinct seasons: the Southwest Monsoon prevails from April to September, while the Northeast Monsoon dominates from October to March. Over the period from 1991 to 2021, the average annual rainfall in the Muar River region was recorded at 2470 mm, accompanied by a mean air temperature of 25.6 °C (Muar Climate, 2023). The local topography ranges from 253 m to 1 m above sea level. The land cover in the water catchment areas consists of 1.6% wetlands, 8.2% urban areas, 40.8% agricultural land, and 49.4% forested areas (Ching *et al.*, 2013). Historically, the Muar River served as a vital trade route for merchants accessing the East Coast of Peninsular Malaysia (Idris *et al.*, 2016). Presently, the river is primarily utilised for recreational activities, such as fishing and camping, by local residents (Samah *et al.*, 2011). The distinct landscape of the Muar River has also attracted attention from sociological studies (Samah *et al.*, 2011), providing an exciting opportunity for ethnoichthyological research. The local population relies on the Muar River for various socio-economic activities, including fishing, aquaculture, recreation, tourism, and sports (Samah *et al.*, 2011). The lower section of the Muar River was selected as the study site due to the presence of several fish markets, which offer a wide range of potential respondents with knowledge and experience related to *B. polykladiskos*.

Figure 3. The area of sampling for respondents in Muar City

Data Collection and Analysis

The fish specimen from Muar River, Johor was caught using a gill net. The specimen was fixed in 10% formalin and later transferred into 70% ethanol for long term preservation. The preserved fish was deposited in the Muzium Zoologi Universiti Malaya, Kuala Lumpur (UMKL). Methods of counting and measuring generally followed Hubbs & Lagler (1964). The measurements were taken to the nearest 0.1 mm with digital calipers on the left side of the fish and measurements of the body parts were recorded as proportion of standard length (SL). Fish specimen was identified following Sasaki (2001) and Yoshida *et al*. (2013).

Data on ethnoichthyological knowledge associated with *B. polykladiskos* were obtained through the distribution of questionnaires among local communities in Muar. These questionnaires, derived from the EthnoKIT©, were specifically designed for an exploratory study, as this research represents the first documentation of *B. polykladiskos* in the area. The questionnaires were structured into two sections: a demographic questionnaire and an ethnoichthyological assessment, mirroring the format of EthnoKIT©, which also comprises two sections. To ensure the acquisition of relevant data, an exponential non-discriminative snowball sampling method was employed, utilising the Google Forms platform. This approach allowed us to effectively target respondents within the fisheries-related community. The survey was conducted over the course of one month in June 2021. Subsequently, all collected data were meticulously cleaned and analysed using Microsoft Excel and SPSS software (version 22). Descriptive and inferential analyses were conducted to examine the data, employing appropriate statistical techniques to derive meaningful insights.

RESULTS

Species Account

Class Actinopterygii
Order Perciformes
Family Sciaenidae
Bahaba polykladiskos (Bleeker, 1852)
Table 1; Figure 1

New record. UMKL 12883, 1 ex., 340 mm SL; Malaysia: Johor: Muar River estuary (2° 2.9974 N, 102° 33.9468 E); coll. Mohd Ilham Norhakim Lokman, 20 February 2021.

Description. Body relatively elongated with a standard length 340 mm. Caudal peduncle slender (7.0% of SL), dorsal fin continuous with a deep notch (XI, 28), lateral line scales extending onto caudal fin (46+9), anal fin with two spines and 7 soft rays (II, 7) with the second spine largest and stout. Freshly caught fish silvery color (Figure 1). Detailed morphometric measurements and meristic counts are provided in Table 1.

Table 1. Morphometric and meristic data of *Bahaba polyklasdiskos* UMKL 12883 in present study. Measurements in millimeter (mm)

Measurements (mm)	
Standard length (SL)	340
Measurements in % of SL	
Head length	33.5
Eye diameter	4.3
Snout to anal-fin origin	66.2
Snout to dorsal-fin origin	34.1
Snout to pelvic-fin insertion	33.7
Pectoral-fin length	23.8
Pelvic-fin length	23.4
Body depth	28.4
Body width	18.3
Dorsal-fin base length	68.2
Longest dorsal spine length	15.2
Anal-fin base length	10.5
Longest anal spine length	17.7
Caudal peduncle depth	7.00
Meristics	
Dorsal-fin rays	XI, 28
Anal-fin rays	II, 7
Pectoral-fin rays	18
Pored lateral line scales	46+9
Scales above lateral line	7
Scales below lateral line	7
Circumpeduncular scales	15

Ethnoichthyological Study

A total of 47 local individuals residing in the vicinity of the Muar River participated in the

questionnaire concerning *B. polykladiskos* during the month of June 2021. Table 2 presents the socio-demographic characteristics of the study respondents. The majority of the respondents were male, accounting for 96% (n=45) of the total, while females constituted only 4% (n=2). In terms of age distribution, 21% (n=10) fell within the range of 18-30 years, followed by 38% (n=18) in the 31 - 40 age group, and 40% (n=19) were 41 years old or older. The respondents included individuals from the Malay community (77%) as well as the Chinese community (23%). Regarding educational background, the highest proportion of respondents completed O-level or SPM (70%), followed by those with a Diploma (23%), and a bachelor's degree (4%). The survey revealed that approximately 32% of the respondents were self-employed, 30% worked in the private sector, 17% were engaged in fishing activities, 13% worked as fishmongers, while the remaining individuals consisted of business owners (4%) and government sector employees (4%). In terms of income, the majority of respondents reported earning between RM 1000 - 2,999 per month (40%), followed by those earning between RM 3000-4999 per month (30%), above RM 5000 per month (21%), and below RM 1000 per month (9%).

Table 2. Demography of respondents

Demography	Frequency	Percentage (%)
Gender		
Male	45	96
Female	2	4
Age		
18-30 years old	10	21
31-40 years old	18	38
41 years old and above	19	40
Race		
Malay	36	77
Chinese	11	23
Education		
Diploma/Matrik/STPM	11	23
Degree	2	4
Malaysian Skill Certificate	1	2
UPSR/PMR/SPM	33	70
Occupation		
Business owner	2	4
Fishermen	8	17
Fishmonger	6	13
government	2	4
Private	14	30
Self-employed	15	32
Income range per month		
under RM 1000	4	9
RM 1,000-2,999	19	40
RM 3,000-4,999	14	30
above RM 5,000	10	21

Knowledge and Demand of *B. polykladiskos*

In relation to personal experiences of the respondents with *B. polykladiskos*, a noteworthy 98% of the respondents demonstrated recognition of the species, with 94% having actually observed it (Table 3). When queried about the sources from which they acquired

information about the species, 41% of the respondents cited firsthand encounters through netting the fish, followed by anglers at 20%, and gaining knowledge through the process of buying and selling at 13%. Additionally, 13% mentioned learning about the species through acquaintances. Other sources of information were each mentioned by less than 10% of the respondents, including the internet (7%), consumption as a luxury food item (2%), information obtained from magazines (2%), and personal discovery (2%). The survey also revealed that the respondents primarily encountered this species in the Muar River (74%) and in market areas (21%). To gauge the demand for *B. polykladiskos*, respondents were asked about their experiences with purchasing and selling this species (Figure 4). The results indicate that 79% of the respondents stated that they would not buy the fish, while only 21% expressed willingness to purchase it. Correspondingly, 81% of the respondents had never bought the fish. However, with regard to selling the species, 70% of the respondents reported having experience in selling *B. polykladiskos*. This is reflected in their responses regarding the price of *B. polykladiskos*, with the maximum recorded price reaching RM 11,500 and a mean price of RM 2,238.22 per fish. It is

Table 3. Knowledge and experience of Muar communities with *B. polykladiskos*

Knowledge and experience with *B. polykladiskos*	Yes (%)
Personal experience	
Recognize *B.polykladiskos*	98
Have seen *B. polykladiskos*	94
Source of information	
Angler	20
Buyer & seller	13
Fisherman (netting)	41
Friends	13
Internet	7
Luxury food	2
Magazine	2
Self-discovery	2
Location of *B. polykladiskos*	
Market	21
Muar river	74
Never seen	5

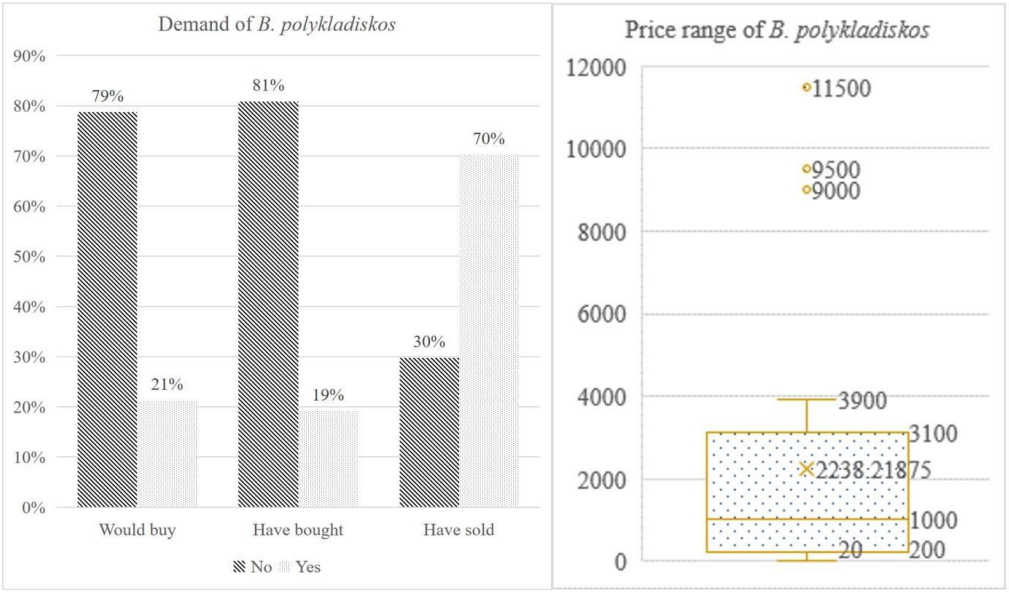

Figure 4. Demand and price range of *B. polykladiskos* in Muar

worth noting that the price range for this species is quite disparate, as the lowest recorded price stood at only RM 20. This disparity in price was initially determined by its gender with male has higher price than female. Then, the price was determined by its weight whether it exceed 2 kg. Lower than 2 kg would definitely has lower price. The price only plummeted after the weight exceeds 5 kg as based on the weight, the swim bladder would logically be bigger and highly sought for traditional medicine.

Activities Involving *B. polykladiskos*

Subsequently, we aimed to evaluate the level of involvement of each respondent in catching *B. polykladiskos*. Notably, a considerable 66% of the respondents reported having participated in the capture of *B. polykladiskos*, while the remaining 34% had not engaged in such activities. Among those involved in catching *B. polykladiskos*, diverse opinions were expressed regarding the optimal timing for catching the fish (Figure 5). The most frequently cited response was during periods of brackish water (39%), primarily in the vicinity of the Muar River. This was followed by preferences for capturing the fish during the rainy season (20%) and at night-time (20%). Additional responses falling under the category of "Others" included catching *B. polykladiskos* during the early part of the year (6%), towards the end of the year (7%), during daytime, and during neap tide (2%).

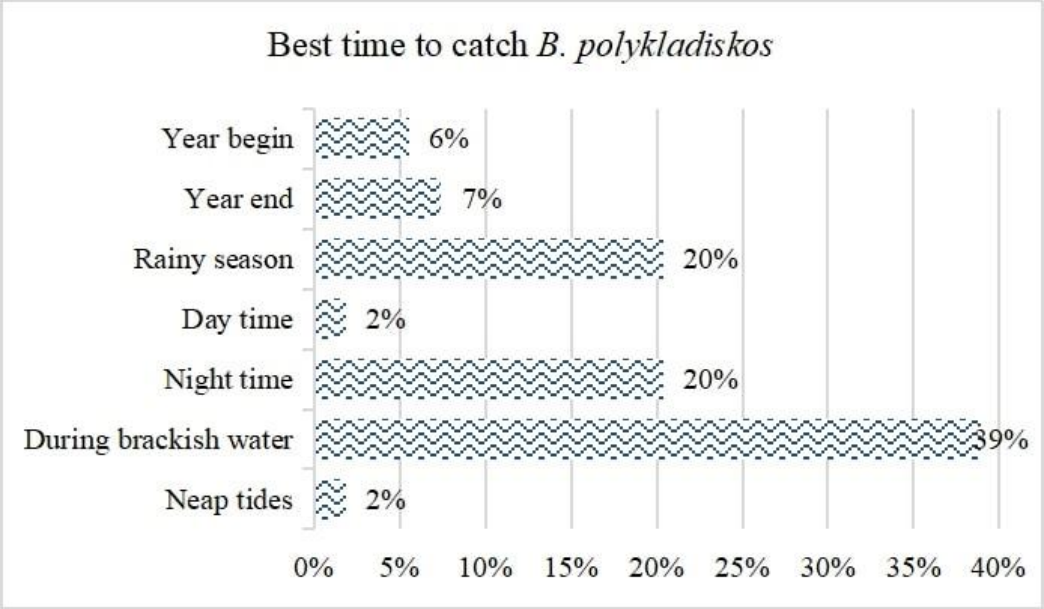

Figure 5. Best time to catch *B. polykladiskos* in Muar

Belief and Uses of *B. polykladiskos*

Table 4 illustrates the diverse uses and associated benefits of consuming *B. polykladiskos* as reported by the respondents. Among the participants, 60% attributed the use of this species to beliefs and folklore, while 30% acknowledged its utilisation as a food source. Additionally, 17% recognized *B. polykladiskos* for its traditional medicinal properties. Interestingly, a smaller proportion (6%) mentioned its application in surgical sutures. When examining the perceived benefits of consuming *B. polykladiskos*, the respondents highlighted its contribution to general health (66%), maintenance of internal organ health (60%), enhancement of sexual prowess (40%), and potential longevity effects (15%). On additional information of the use of *B. polykladiskos* is the use in making traditional cuisine. The Spine Bahaba species, known for its mild taste and affordability (typically priced at RM 10 or below), finds a unique utility in local culinary practices. The swim bladder, commonly referred to as 'gelembung ikan,' is skillfully transformed by the community into bite-sized crispy snacks through deep frying. These crispy morsels are then incorporated into herbal soups, where they serve as a traditional remedy in local folk medicine. Apart from that, *B. polykladiskos* also known as the symbol of grandeur, as it is frequently utilized by locals as a collector's item.

Table 4. Uses and benefits *B. polykladiskos*

Uses of *B. polykladiskos*	Answered yes (%)
Food	30
Traditional medicine	17
Folklore & believe	60
Surgical suture	6
Believed benefit of *B. polykladiskos*	
Longevity	15
Sexual Prowess	40
Internal organ health	60
General health	66

DISCUSSION

This study represents the first documented occurrence of *B. polykladiskos* in Peninsular Malaysia, specifically within the Muar River in Johor, Malaysia. The conservation status of *B. polykladiskos* is currently classified as data deficient (DD) in the IUCN Red List of Threatened Species due to the scarcity of information regarding its population and life history (Chao *et al.*, 2020). Habitat degradation poses a significant threat to this species, as unprotected spawning habitats in estuaries can adversely affect the larvae and juveniles of *B. polykladiskos* (Chao *et al.*, 2020). A clear example of the impact of such threats can be observed in the case of its sister species, *Bahaba taipingensis*, which is endemic to China. The intensive use of bottom trawling has resulted in high juvenile mortality and has ultimately led to the commercial extinction of *B. taipingensis*, warranting its listing as critically endangered (CR) on the IUCN Red List of Threatened Species (Sadovy & Cheung, 2003; Moore, 2012; Liu, 2020).

In comparison to previous studies, the application of the ethnoichthyology method in this research extends beyond the mere taxonomic identification of fish based on local names. It also encompasses aspects such as fish morphology, ecology, behavior, and medicinal uses (Djidohokpin *et al.*, 2020). Although the ethnoichthyological information collected in this study remains limited to the basic knowledge held by local communities, it serves as a valuable resource for researchers, laying the groundwork for future investigations, given that this represents the first-ever report of *B. polykladiskos* in Peninsular Malaysia.

The fish maw derived from *Bahaba* species holds significant value in traditional Chinese medicine, as it is believed to possess various health benefits, including anti-fatigue properties (Zhao *et al.*, 2016), immune-boosting effects (Wen *et al.*, 2015), and anti-aging properties (He *et al.*, 2021). Consequently, fish maw can be sold at high prices. Our findings reveal a wide price range for *B. polykladiskos*, dependent on the size and quality of the fish. While the maximum price recorded reached RM11,500, it remains lower than the reported price in Sarawak, East Malaysia, where *B. polykladiskos* fish maw was sold for RM60,000 per kg (Latip, 2019). The fish maw trade holds considerable global market value, with Hong Kong serving as a major trade hub. Import data from Hong Kong for the years 2015 to 2018 indicate declared import values ranging from 264 to 394 million USD (de Mitcheson *et al.*, 2019). Given the significant conservation implications, such as high demand (Ben-Hasan *et al.*, 2021), the uncertain IUCN status, and evidence of trade activity, it is crucial to establish specific regulations and conduct further research on this species in the future.

CONCLUSION

This study presents the initial documentation of Gelama Tirusan (*B. polykladiskos*) in Peninsular Malaysia, specifically within the Muar River of Johor. Through the application of the ethnoichthyology approach, the investigation successfully elucidates the trade activity, uses, and perceived benefits of this species among local communities. As a next step, we strongly recommend the conduction of further research to ascertain the species' distribution and population size, as well as to gain a comprehensive

understanding of its biology and ethnoichthyology within the Malaysian context. Such studies would significantly contribute to the knowledge base surrounding Gelama Tirusan and its conservation in Malaysia.

ACKNOWLEDGEMENTS

This project is funded by the Ministry of Higher Education Malaysia (MOHE) through the Fundamental Research Grant Scheme FRGS/1/2022/WAB11/UTHM/02/2 and UTHM-GPPS-H553 postgraduate grant by Universiti Tun Hussein Onn Malaysia. We are deeply indebted to Mr. Lokman Ali and Mr. Saiful Azad Lokman for their assistance in this study. The authors acknowledge the Ministry of Higher Education Malaysia and Universiti Tun Hussein Onn Malaysia for providing the necessary funding, facilities, and assistance.

REFERENCES

Bahaman, A.S., Sulaiman, M., Hayrol, A., Mohd, S.O., Asnarulkhadi, A.S. & Siti, A.R. (2011). Relationship to the river: the case of the Muar River community. *American Journal of Environmental Sciences*, 7(4): 362-369. DOI:10.3844/ajessp.2011.362.369

Ben-Hasan, A., de-Mitcheson, Y.S., Cisneros-Mata, M.A., Jimenez, É.A., Daliri, M., Cisneros-Montemayor, A.M., Nair, R.J., Thankappan, S.A., Walters, C.J. & Christensen, V. (2021). China's fish maw demand and its implications for fisheries in source countries. *Marine Policy*, 132: 104696. DOI:10.1016/j.marpol.2021.104696

Berkes, F., Mahon, R., McConney, P., Ponnac, P. & Pomeroy, R. (2001). *Managing Small-scale Fisheries: Alternative Directions and Methods*. International Development Research Centre Press.

Bleeker, P. (1852). Zesde bijdrage tot de kennis der ichthyologische fauna van Borneo. Visschen van Pamangkat, Bandjermassing, Praboekarta en Sampit. *Natuurkundig Tijdschrift voor Nederlandsch Indië*, 3: 407-442.

Chao, L., Vidthayanon, C., Janekikarn, S., Seah, Y.G., Wong, L., Loh, K.H., Hadiaty, R.K., Suharti, S., Russell, B., Larson, H. & Shah, N.H.A. (2020). *Bahaba polykladiskos* (errata version published in 2021). *The IUCN Red List of Threatened Species* 2020: e.T49169667A196840480.

Ching, Y.C., Baharudin, Y., Mohd-Ekhwan, T., Lee, Y.H., Maimon, A. & Salmijah, S. (2013). Impact of climate change on flood risk in the Muar River basin of Malaysia. *Disaster Advances*, 6(10): 11-17.

Ching, Y.C., Lee, Y.H., Toriman, M.E., Abdullah, M. & Yatim, B.B. (2015). Effect of the big flood events on the water quality of the Muar River, Malaysia. *Sustainable Water Resources Management*, 1(2): 97-110. DOI:10.1007/s40899-015-0009-4

de Mitcheson, Y.S., To, A.W.L., Wong, N.W., Kwan, H.Y. & Bud, W.S. (2019). Emerging from the murk: threats, challenges and opportunities for the global swim bladder trade. *Reviews in Fish Biology and Fisheries*, 29(4): 809-835. DOI:10.1007/s11160-019-09585-9

Djidohokpin, G., Sossoukpè, E., Adandé, R., Voudounnou, J.V., Fiogbé, E.D. & Haour, A. (2020). Ethnoichthyology of fishing communities in the Lower Valley of Ouémé in Benin, West Africa. *Ethnobiology Letters*, 11(1): 137-151. DOI:10.14237/ebl.11.1.2020.1686

He, X., Xie, L., Zhang, X., Lin, F., Wen, X. & Teng, B. (2021). The structural characteristics of collagen in swim bladders with 25-year sequence aging: The impact of age. *Applied Science*, 11(10): 4578. DOI:10.3390/app11104578

Huan, N.X., Duyen, N.T. & Nam, N.T. (2016). Fish species composition in the Dinh an estuary, Tra Vinh Province. *VNU Journal of Science: Natural Science and Technology*, 32(1S): 69-76.

Hubbs, C.L. & Lagler, K.F. (1964). *Fishes of the Great Lake Region*. The University of Michigan Press, Ann Arbor, Michigan, 213 pp.

Idris, K., Mohamed-Shaffril, H.A., Md-Yassin, S., Abu-Samah, A., Hamzah, A. & Abu-Samah, B. (2016). Quality of life in rural communities: Residents living near to Tembeling, Pahang and Muar Rivers, Malaysia. *PloS one,* 11(3): e0150741. DOI:10.1371/journal.pone.0150741

Kottelat, M. (1989). Zoogeography of the fishes from Indochinese inland waters with an annotated check-list. *Bulletin Zoologisch Museum,* 12(1): 1-55.

Kottelat, M. (2013). The fishes of the inland waters of Southeast Asia: a catalogue and core bibliography of the fishes known to occur in freshwaters, mangroves, and estuaries. *Raffles Bulletin of Zoology* Supplement 27: 1-663.

Latip K. (2019, Januari 31). Limpa ikan terusan dijual RM60,000 sekilogram, *Berita Harian*. https://www.bharian.com.my/amp/berita/wilayah/2019/01/526196/limpa-ikan-terusan-dijual-rm60000-sekilogram.

Liu, M. (2020). *Bahaba taipingensis*. *The IUCN Red List of Threatened Species* 2020. DOI:10.2305/IUCN.UK.2020-2.RLTS.T61334A130105307.en. Accessed on 29 October 2021.

Lo, P.C., Liu, S.H., Nor, S.A.M. & Chen, W.J. (2017). Molecular exploration of hidden diversity in the Indo-West Pacific sciaenid clade. *PLoS ONE,* 12(4): e0176623. DOI:10.1371/journal.pone.0181511

Moore, M. (2012, August 21). Chinese fisherman hooks £300,000 fish, *The Daily Telegraph*. https://www.telegraph.co.uk/news/worldnews/asia/china/9489137/Chinese-fisherman-hooks-300000-fish.html.

Muar climate: Average temperature, weather by month, Muar water temperature - Climate-Data.org. (2023). En.climate-Data.org. https://en.climate-data.org/asia/malaysia/johor/muar-25944/.

Murdy, E.O., Birdsong R.S. & Musick, J.A. (1997). *Fishes of the Chesapeake Bay*. Smithsonian Institution Press.

Nelson, J.S. (2006). *Fishes of the World*. 4th Edition. John Wiley and Sons.

Nurhayati, N., Fauziyah, F. & Bernas, S.M. (2016). Relationship of length-weight and growth pattern of fish in Musi River estuary Banyuasin regency South Sumatra. *Maspari Journal*, 8(2): 111-118.

Oishi, T. (2016). Ethnoecology and ethnomedicinal use of fish among the Bakwele of southeastern Cameroon. *Revue d'ethnoécologie,* 10(10): 1-38. DOI:10.4000/ethnoecologie.2893

Parenti, P. (2020). An annotated checklist of fishes of the family Sciaenidae, *Journal of Animal Diversity*, 2(1): 1-92. DOI:10.29252/JAD.2020.2.1.1

Rainboth, W.J., Vidthayanon, C. & Yen, M.D. (2012). *Fishes of the greater Mekong ecosystem with species list and photographic atlas*. Miscellaneous Publications Museum of Zoology.

Ramcharitar, J., Gannon, D.P. & Popper, A.N. (2006). Bioacoustics of fishes of the Family Sciaenidae (Croakers and Drums). *Transactions of the American Fisheries Society*, 135(5): 1409-1431. DOI:10.1577/T05-207.1

Randall, J.E. & Lim, K.K.P. (2000). A checklist of the fishes of the South China Sea. *The Raffles Bulletin of Zoology* 8: 569-667.

Ridho, M.R. & Patriono, E. (2017). Keanekaragaman jenis ikan di Estuaria Sungai Musi, Pesisir Kabupaten Banyuasin, Provinsi Sumatra Selatan. *Jurnal Penelitian Sains*, 19(1): 19106-32-19106-37

Robins, C.R., Ray, G.C. & Douglas, J. (1986). *Atlantic coast fishes*. Houghton Mifflin.

Sadovy, Y. & Cheung, W.L. (2003). Near extinction of a highly fecund fish: the one that nearly got away. *Fish and Fisheries,* 4(1): 86-99. DOI:10.1046/j.1467-2979.2003.00104.x

Samah, B.A., Yassin, S.M., Shaffril, H.A.M., Hassan, M.D., Othman, M.S., Abu-Samah, A. & Ramli, S.A. (2011). Relationship to the river: The case of the Muar River community.

American Journal of Environmental Science, 7(4): 362-369. DOI:10.3844/ajessp.2011.362.369

Sasaki, K. (2001). Sciaenidae. Croakers (drums). In: K.E. Carpenter & V.H. Niem (Ed.). *The Living Marine Resources of the Western Central Pacific* (pp.3117-3174). FAO, Rome.

Svanberg, I. & Locker, A. (2020). Ethnoichthyology of freshwater fish in Europe: a review of vanishing traditional fisheries and their cultural significance in changing landscapes from the later medieval period with a focus on northern Europe. *Journal of Ethnobiology and Ethnomedicine*, 16(1): 1-29. DOI:10.1186/s13002-020-00410-3

Tám, T.X., Phi, Đ.T.Á. & Như, N.Á. (2019). Nghiên Cứu Thành Phần Loài Và Sự Phân Bố Của Các Loài Cá Ở Sông Tiền, Đoạn Qua Tỉnh Tiền Giang. *Ho Chi Minh City University of Education – Journal of Science*, 16(6): 115-132.

Trewavas, E. (1977). The sciaenid fishes (croakers or drums) of the Indo-West-Pacific. *Trancsactions of the Zoological Society of London*, *33*, 253-541.

Wen, J., Zeng, L., Sun, Y., Chen, D., Xu, Y., Luo, P., Zhao, Z., Yu, Z. & Fan, S. (2015). Authentication and traceability of fish maw products from the market using DNA sequencing. *Food Control*, 55(1): 185-189. DOI:10.1016/j.foodcont.2015.02.033

Yoshida, T., Motomura, H., Musikasinthorn, P. & Matsuura, K. (2013). *Fishes of northern Gulf of Thailand*. National Museum of Nature and Science, Tsukuba, Research Institute for Humanity and Nature.

Zhao, Y.Q., Zeng, L., Yang, Z.S., Huang, F.F., Ding, G.F. & Wang, B. (2016). Anti-Fatigue effect by peptide fraction from protein hydrolysate of Croceine Croaker (*Pseudosciaena crocea*) swim bladder through inhibiting the oxidative reactions including DNA damage. *Marine Drugs*, 14(2): 221. DOI:10.3390/md14120221.

Borneo Journal of Resource Science and Technology (2024), 14(1):30-53
DOI: https:doi.org/10.33736/bjrst.6077.2024

Computational Analysis of Epstein-Barr Virus *Bam*HI A Rightward Transcript (BART) MicroRNAs (miRNAs) Regulation on Messenger RNAs and Long Non-Coding RNAs in Nasopharyngeal Cancer

DAPHNE OLIVIA JAWAI ANAK SADAI & EDMUND UI HANG SIM*

Faculty of Resource Science and Technology, Universiti Malaysia Sarawak, 94300 Kota Samarahan, Sarawak, Malaysia
*Corresponding author: uhsim@unimas.my
Received: 13 September 2023 Accepted: 15 April 2024 Published: 30 June 2024

ABSTRACT

To date, the regulatory framework mediated by Epstein-Barr virus (EBV) *Bam*HI A rightward transcript (BART) microRNAs (miRNAs) via their interaction with long non-coding RNAs (lncRNAs) in the context of nasopharyngeal cancer (NPC) pathogenesis remains partially understood. To derive a more complete insight into this phenomenon, we embarked on a computational study to identify BART miRNAs, mRNAs, lncRNAs, and all associated factors relevant to NPC tumourigenesis and to characterise their interactions. *In silico* integration of multi-level RNA expression and construction of regulatory networks were performed. We found six EBV BART miRNAs (ebv-miR-BART21-3p, ebv-miR-BART19-3p, ebv-miR-BART15, ebv-miR-BART2-5p, ebv-miR-BART20-3p and ebv-miR-BART11-5p) that could interact with four mRNAs (EYA4, EYA1, EBF1 and MACROD2) associated with NPC pathogenesis. These mRNAs can interact with six non-EBV miRNAs (hsa-miR-1246, hsa-miR-93-5p, hsa-miR-16-5p, hsa-miR-135b-5p, hsa-miR-211-5p and hsa-miR-1305), which in turn, could interact with three lncRNAs (CASC2, TPTE2P1 and ARHGEF26-AS1). These findings could shed light on the roles of dysregulated competing endogenous RNA (ceRNA) network in NPC oncogenesis. In addition, we have also predicted the oncogenic and tumour suppressive functions of BART miRNAs and lncRNAs, and more precisely, the involvement of BART miRNAs in DNA repair regulation and apoptosis.

Keywords: BART miRNAs, bioinformatics, EBV, lncRNA, nasopharyngeal cancer

INTRODUCTION

Nasopharyngeal cancer (NPC) is a rare head and neck cancer on a global scale, yet it disproportionately affects populations in southern China and Southeast Asia, including Malaysia (Chang & Adami, 2006). Originating from the fossa of Rosenmüller and lining the nasopharynx epithelial (Tabuchi *et al.,* 2011), NPC is ranked as the sixth most common cancer in Malaysia, where Malaysian males are primarily affected by it, ranking fifth most common cancer affecting males in Malaysia (Global Cancer Observatory, 2022). The correlation of NPC with Epstein-Barr virus (EBV) infection has been well-documented, leading to aberrant RNA regulation within the host (Nakanishi *et al.,* 2017; Tsao *et al.,* 2017). This association is particularly prominent in type II (differentiated non-keratinizing carcinoma) and type III (undifferentiated non-keratinizing carcinoma) NPC (Su *et al.,* 2023), prevalent among Asian populations (Wang *et al.,* 2013).

Epstein-Barr virus (EBV) is a linear, double-stranded DNA virus classified in the family of *Herpesviridae*, a subfamily of *Gammaherpesviridae* (Sarwari *et al.,* 2016). The EBV genome is capable of expressing miRNAs that act similarly to mammalian miRNAs by binding to the 3'UTR of host mRNAs, albeit via imperfect complementary binding mediated at the 5' seed region of EBV miRNAs (Skalsky & Cullen, 2010). The miRNAs clusters encoded by EBV are the *Bam*HI A rightward transcript (BARTs) and *Bam*HI H rightward open reading frame 1 (BHRF1) clusters (Cai *et al.*, 2006).

In terms of disease association, EBV infection has been correlated with NPC pathogenesis (Nakanishi *et al.,* 2017; Tsao *et al.,* 2017). The post-infection period involving latency pattern type II is characterised by the presence of the BART cluster and the absence of the BHRF1 cluster, where the BART miRNAs function as oncogenes via down-regulating the apoptotic host mRNAs by binding to their

3'UTR (Kang *et al.,* 2015). Incidentally, lncRNA levels are also affected during EBV infection (Zhang *et al.,* 2020), with a significant negative correlation between lncRNAs and BART miRNAs levels as observed in the down-regulation of LOC553103 following the up-regulation of EBV-miR-BART6-3p (He *et al.,* 2016). Thus far, the intricacies underlying the regulatory network concerning BART miRNAs and lncRNAs in NPC pathogenesis have not been fully and definitively established, although it is apparent that the dysregulation of lncRNAs (He *et al.,* 2017) and the competing endogenous RNAs (ceRNA) network (Xu *et al.,* 2020) may play a role in the disease.

The exploration and understanding of regulatory mechanisms between BART miRNAs and the ceRNA network could unveil potential biomarkers on a preliminary level for early diagnosis, improve survival rates, and develop therapeutic targets for highly metastatic EBV-positive NPC. The deep-seated location of the nasopharynx, coupled with the absence of noticeable clinical symptoms in the early stage, contributes to the high mortality in NPC owing to its invasive and metastatic nature (Tabuchi *et al.,* 2011; Wang *et al.,* 2017; Dwijayanti *et al.,* 2020; Tan *et al.,* 2022).The ceRNA regulatory network involves the binding of miRNAs to both mRNAs and lncRNAs and is based on the hypothesis that lncRNA and mRNAs regulate each other by competing for binding sites on shared miRNAs through partially complementary sequences known as the miRNA recognition elements (MREs) (Salmena *et al.,* 2011). Anomalies in this regulatory network are commonly linked to tumorigenesis (Lee & Young, 2013).

To unravel the interaction among EBV-BART miRNAs, mRNAs, and lncRNAs in NPC pathogenesis, we performed a computational analysis involving constructing and analysing a regulatory network that combines the ceRNA and EBV-miRNAs-mRNAs networks. The outcomes were complemented by the curative and integrative analysis of the expression data of lncRNA, miRNA and mRNA extracted from the Gene Expression Omnibus (GEO) database. Our findings reveal novel conceptual insights into the regulation of lncRNAs by EBV-BART miRNAs with the uncovering of potential biomarkers for therapeutic design and the plausible effects on the modulation of DNA repair and apoptosis in the context of NPC pathogenesis.

MATERIALS AND METHODS

Retrieval of Microarray Data Pertaining to MicroRNAs (miRNAs), Long Non-Coding RNAs (lncRNAs) and Messenger RNAs (mRNAs)

The microarray gene expression profiles of messenger RNAs (mRNAs), microRNAs (miRNAs) and long non-coding RNAs (lncRNAs) from nasopharyngeal cancer (NPC) were retrieved from the Gene Expression Omnibus (GEO) database hosted on the National Centre for Biotechnology Information (NCBI) website (Karagkouni *et al.,* 2020). Specifically, the access year of the datasets was between 2020 and 2023. The keyword "nasopharyngeal carcinoma" was used, and the organism filter was set to *Homo sapiens*. Excluded datasets were from those that are: (i) of cell line samples, (ii) without normal nasopharyngeal controls, and (iii) those submitted before 2014. This filtering is to ensure that the expression datasets follow updated microarray guidelines and protocols. Subsequently, all the datasets were checked for quantile normalization, and quantile normalization was done using an R software called Limma R package in R studio (version 4.0.1).

Identification of Differentially Expressed mRNA (DEmRNA), Differentially Expressed lncRNA (DElncRNA), and Differentially Expressed miRNA (DEmiRNA)

The DEmRNAs, DEmiRNAs, and DElncRNAs were identified using GEO2R (Chen *et al.,* 2015). The cut-off criteria were p-value < 0.05 (Ye *et al.,* 2015) and $|\log2 \text{ fold-change}| \geq 1$ (Liu *et al.,* 2019) to ensure statistically significant. Subsequently, the overlaps of differentially expressed RNAs between two or more datasets were identified and visualised using Venn diagrams via the Venny Tool resource.

Identification of DEmiRNA-Target mRNA Interaction

Gene targets of DEmiRNAs were identified following inverse expression correlation using computationally-predicted functions in miRwalk 2.0 and an experimentally validated database of miRTarBase (Zhu *et al.,* 2020). For miRWalk 2.0,

the cut-off criteria were p-value < 0.05, and those are common in at least five databases integrated into miRWalk 2.0, while for miRTarBase, the predicted target mRNAs with both "less strong" and "strong evidence" validation methods were selected. Then, all the target mRNAs from all the databases were combined. The overlapping datasets of predicted target mRNAs and DEmRNAs were examined and visualised using Venn diagrams.

Identification of DEmiRNA-Target lncRNA Interaction

The lncRNAs targeted by DEmiRNAs were identified using experimentally supported interaction databases, namely DIANA-LncBase V3 and StarBase V2 (Hu *et al.,* 2020). The parameters for DIANA-LncBase V3 were set to *Homo sapiens* for species and high miRNA confidence level to ensure accuracy. Meanwhile, for StarBase V2, the parameters were set to strict stringency (>=5) for the CLIP Data and low stringency (>=1) for the Degradome Data parameter (Liang & Sun, 2019). For the computational prediction, miRcode and DIANA-LncBase V2 databases were utilized. The parameters for miRcode were set as gene class for all lncRNAs, site conservation for most mammals, and transcript region for any/ncRNA. Conversely, the parameter for the DIANA-LncBase V2 database was set to a default threshold ≥ 0.07 for high sensitivity and precision (Liang & Sun, 2019). All the target lncRNAs from all the databases were combined. The comparison of predicted target lncRNAs with DElncRNAs was examined and visualised using Venn diagrams.

Construction of mRNA-miRNA-lncRNA ceRNA Network

The mRNA-miRNA-lncRNA competing endogenous RNA (ceRNA) network was constructed using Cytoscape software (Version 3.8.2) (Yang *et al.,* 2011) to merely visualize mRNA-miRNA-lncRNA interaction according to the parameters mentioned during the curation of target mRNAs and lncRNAs for DEmiRNAs. Within the network, the lncRNAs served as the target lncRNAs of DEmiRNA, while the mRNAs acted as the target genes for DEmiRNAs. The mRNAs and lncRNAs, regulated by common miRNAs, were selected for constructing the ceRNA network by merging DEmiRNA-target mRNA and DEmiRNA-target lncRNA interactions.

Construction of EBV miRNA-mRNA Interaction Network

The predicted EBV miRNAs-mRNAs interaction was identified by using ViRBase (Zhou *et al.,* 2019), and the keyword search for Virus Type was set to *Human gammaherpesvirus 4* (Jing *et al.,* 2018). The cut-off criterion was set to a confidence score of 0.5 to 1.00. Only EBV miRNAs from the *Bam*H1 fragment A transcript (BART) cluster were selected due to its overexpression in NPC tumor samples and cell lines (Zhang *et al.,* 2022). Next, the mRNAs interacting with the EBV miRNAs overlapped with the ceRNA DEmRNA using a Venn diagram. Subsequently, the EBV miRNA-mRNA interaction network was constructed and visualised using Cytoscape (Zhou *et al.,* 2019).

Construction of Protein-Protein Interaction (PPI) Network

The physical protein-protein interaction (PPI) among the expressed proteins of DEmRNAs was identified using the Search Tool for the Retrieval of Interacting Gene (STRING) database (Jing *et al.,* 2018) to visualise the indirect and direct interaction types of the PPI**.** A cut-off criterion of a combined score > 0.4, representing a medium or high confidence level, was applied (Tang *et al.,* 2018). Then, the PPI network was constructed, visualised and analysed in Cytoscape software using the STRING database plug-in; with a combined score of more than 0.55, a medium or high confidence was set for stronger interaction evidence. Following this, the cytoHubba plug-in of the Cytoscape was used to filter out the top 20 hub genes, which are strongly connected to each other, using the degree algorithm (Xu *et al.,* 2020). Here, the hub genes refer to the genes expressing the proteins in the PPI network. Additionally, the Network Analyzer plug-in of the Cytoscape was utilised to further filter out hub genes among the top 20 hub genes by calculating the node degree (Karagkouni *et al.*, 2020). An undirected network parameter was applied to further filter out the hub genes. Genes with a connectivity degree greater than five were considered hub genes level genes due to being deemed as contributor causes of biological processes (Han *et al.,* 2004; Ye *et al.,* 2018). Lastly, the

Molecular Complex Detection (MCODE) plug-in of the Cytoscape was used to analyse and screen for the gene modules of the PPI network (Chen *et al.,* 2015). The parameters used were degree cut-off = 2 for network scoring, a node score cut-off = 0.2 for cluster finding, k-core = 2, and max. Depth = 100 (Yan *et al.,* 2019). Self-edges nodes were excluded by turning off Loops, the Haircut option was included to remove singly connected nodes from clusters, and the Fluff option was excluded to prevent the expansion of the cluster core (Bader *et al.,* 2020). The gene modules with scores ≥ 4 and nodes ≥ 4 were considered significant.

Construction of Transcription Factors (TF)-mRNAs Network

The predicted transcription factors (TFs) among the DEmRNAs were identified using the TFcheckpoint database (Zhong *et al.,* 2019), focusing solely on TFs supported by experimental evidence. A comparison of TFs with the DEmRNAs was made using Venn diagrams. Subsequently, the TFs-DEmRNAs network was constructed and visualized using Cytoscape (Zhou *et al.,* 2019). Any of the TFs observed as hub genes in the PPI network were considered as hub TFs (Jing *et al.,* 2018).

Construction of Cross-Regulatory Networks (Transcription Factor (TF)-DmRNAs, Competing Endogenous Network (ceRNA), EBV miRNAs-DEmRNAs)

All three networks (TF-DEmRNAs, ceRNA, EBV miRNAs-DEmRNAs) were examined using Cytoscape to identify overlapping RNAs. These shared RNAs were then used to construct a cross-regulatory network to visualise the regulatory interactions between the RNAs with EBV BART miRNAs using Cytoscape (Zhou *et al.,* 2019).

Functional and Pathway Enrichment Analysis of DEmRNAs Affected by EBV miRNAs

Database for Annotation, Visualisation and Integrated Discovery (DAVID) database was utilised to identify the cellular functions and pathways affected by EBV BART miRNAs in NPC tumorigenesis (Yan *et al.,* 2019). The database provides Gene Ontology (GO) terms, including Biological Processes (BP), Molecular Function (MF) and Cellular Component (CC), to dissect the affected cellular functions of the DEmRNAs targeted by EBV BART miRNAs (Zhang *et al.,* 2019). Besides this, DAVID provided KEGG pathway enrichment analysis used to explore the affected pathway by EBV BART miRNAs (Yang *et al.,* 2019). Both GO and KEGG pathway analyses were subjected to a cut-off criterion of p-value < 0.05 (Zhou *et al.,* 2019). The results of the enrichment analyses were visually represented using bubble plots in GraphPad Prism (Version 9.1.0).

Statistical Analysis and Network Visualization

The differentially expressed RNAs between groups in this study were estimated by using a student t-test generated by the GEO2R, while the Benjamini–Hochberg false discovery rate was used to generate p-value adjustment to minimise false positive results (National Center for Biotechnology Information, 2024). For Gene Ontology (GO) enrichment analysis, DAVID utilises Fisher's exact test to avoid counting duplicated genes (DAVID Bioinformatics Resources, 2021). Notably no statistical analysis was done on all the networks constructed using Cytoscape software, as its primary function is only to link and visualise interactions between EBV BART miRNAs and all the RNAs. The interactions between the EBV BART miRNAs and RNAs retrieved from the databases used were identified by using algorithms tailored to each database, especially computationally predicted.

RESULTS

Microarray Data of MicroRNAs (miRNAs), Long Non-Coding RNAs (lncRNAs) and Messenger RNAs (mRNAs)

Five datasets were extracted from the microarray gene expression profiles curated from Gene Expression Omnibus (GEO) database. These include one dataset for miRNAs (GSE70970), three datasets for lncRNA (GSE95166, GSE126683 and GSE61218), and two datasets for mRNA (GSE64634 and GSE126683). The information about these datasets is provided in Supplementary Table 1. GSE126683 and GSE61218 each contain a combination of lncRNA and mRNA expression data.

Identification of Differentially Expressed mRNA (DEmRNA), miRNA (DEmiRNA) and lncRNA (DElncRNA)

The DEmRNA, DEmiRNA and DElncRNA data, assayed via Gene Expression Omnibus 2 R (GEO2R), is provided in Supplementary Table 2. Comparative analysis of each type of differentially expressed RNAs is illustrated in Supplementary Figures 1 and 2. Regarding the lncRNA datasets from GSE95166, GSE126683 and GSE61218, no overlap was observed among the up-regulated lncRNAs (Supplementary Figure 1a). However, for down-regulated lncRNAs, overlapping data showing three common/shared lncRNAs among the datasets was evident (Supplementary Figure 1b). These were Cancer Susceptibility Candidate 2 (CASC2), Transmembrane Phosphoinositide 3-phosphatase and Tensin homolog 2 pseudogene 1 (TPTE2P1), and Rho Guanine Nucleotide Exchange Factor 26 Antisense RNA 1 (ARHGEF26-AS1). For the overlapping data of the three mRNA datasets of GSE64634, GSE126683 and GSE61218 they revealed 65 commonly up-regulated (Supplementary Figure 2a) and 123 down-regulated mRNAs (Supplementary Figure 2b). No comparison was made for the miRNA dataset (GSE70970) because only one such dataset was available from 2014 onwards until 2023.

Identification of Interaction Between DEmiRNA and mRNA or lncRNA

The target mRNAs interacting with DEmiRNAs (in the GSE70970 dataset) were obtained from miRwalk 2.0 and miRTarBase databases. The results of the target mRNAs for both up-regulated and down-regulated miRNAs from the combined databases were compared with the DEmRNAs and illustrated using a Venn diagram (Supplementary Figure 3 and 4, Supplementary Tables 3 and 4). Specifically, the Venn diagram illustrates the number of target mRNAs of the up-regulated miRNAs when overlapped with the 123 down-regulated DEmRNAs. For the target lncRNAs interacting with the DEmiRNAs, they were obtained from the DIANA-LncBase V3, StarBase V2, miRcode and DIANA-LncBase V2 databases. Results of the target lncRNAs for the up-regulated miRNAs from the combined databases were compared with the DElncRNAs and illustrated using a Venn diagram (Supplementary Figure 5 and Supplementary Table 5). The Venn diagram demonstrates the target lncRNAs of the up-regulated miRNAs when they overlapped with the three down-regulated lncRNAs.

lncRNA-miRNA-mRNA ceRNA Competing Endogenous RNA (ceRNA) Network Construction

The constructed lncRNA-miRNA-mRNA competing endogenous RNA **(**ceRNA) network comprises of 17 up-regulated DEmiRNAs, interacting with 58 down-regulated DEmRNAs, and 3 down-regulated DElncRNAs (Figure 1 and Supplementary Table 6). The ceRNA network illustrates the intricate interactions and interplay among all the RNAs, both directly and indirectly, shedding light on how the dysregulation of one RNA could affect the expression level of other RNAs in the context of NPC tumorigenesis. However, it is worth noting that only one ceRNA was constructed due to no common up-regulated lncRNAs in the three GEO datasets (GSE95155, GSE126683 and GSE61218).

EBV miRNA-mRNA Interaction Network Construction

Utilising the ViRBase database, it revealed 5,411 interactions between Epstein-Barr Virus (EBV) *Bam*H1 A transcript (BART) miRNA and mRNA. Results of overlapping this data with the down-regulated DEmRNAs in the competing endogenous RNA **(**ceRNA) network using the Venn diagram and Cytoscape revealed four common down-regulated DEmRNAs, namely Early B-cell factor transcription factor 1 (EBF1), Mono-ADP Ribosylhydrolase 2 (MACROD2), Eye Absent transcriptional coactivator And phosphatase 1 (EYA1) and Eye Absent transcriptional coactivator And phosphatase 4 (EYA4) (Supplementary Figure 6 and Figure 2). These DEmRNAs were used to construct the EBV BART miRNA-mRNA network and visualised using Cytoscape (Figure 3). We demonstrated the regulatory relationship between the EBV BART miRNA and the DEmRNAs, whereby the former could down-regulate the latter. Specifically, we inferred that EYA4 interacts with ebv-miR-BART19-3p and ebv-miR-BART15; EYA1 interacts with ebv-miR-BART21-3p and ebv-miR-BART12-5p; MACROD2 interacts with ebv-miR-BART20-3p; and EBF1 interacts with ebv-miR-BART11-5p (Figure 3).

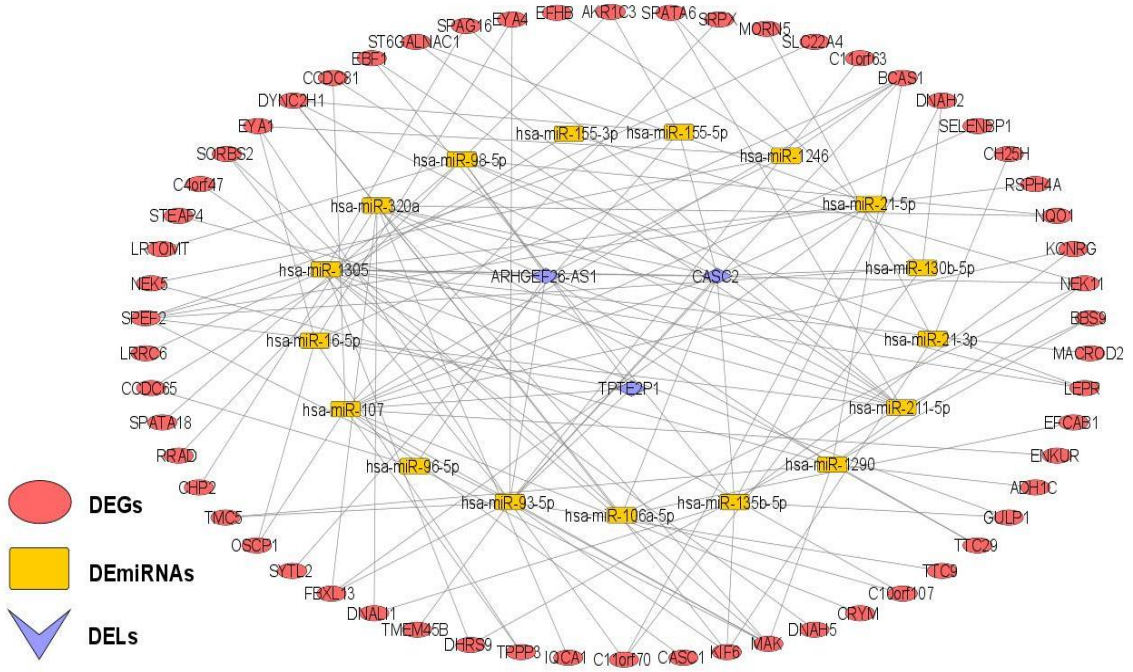

Figure 1. The lncRNA-miRNA-mRNA ceRNA network with 17 up-regulated DEmiRNAs (yellow rectangle), interacting with 58 down-regulated DEGs (red eclipse), and- 3 down-regulated DELs (purple diamond)

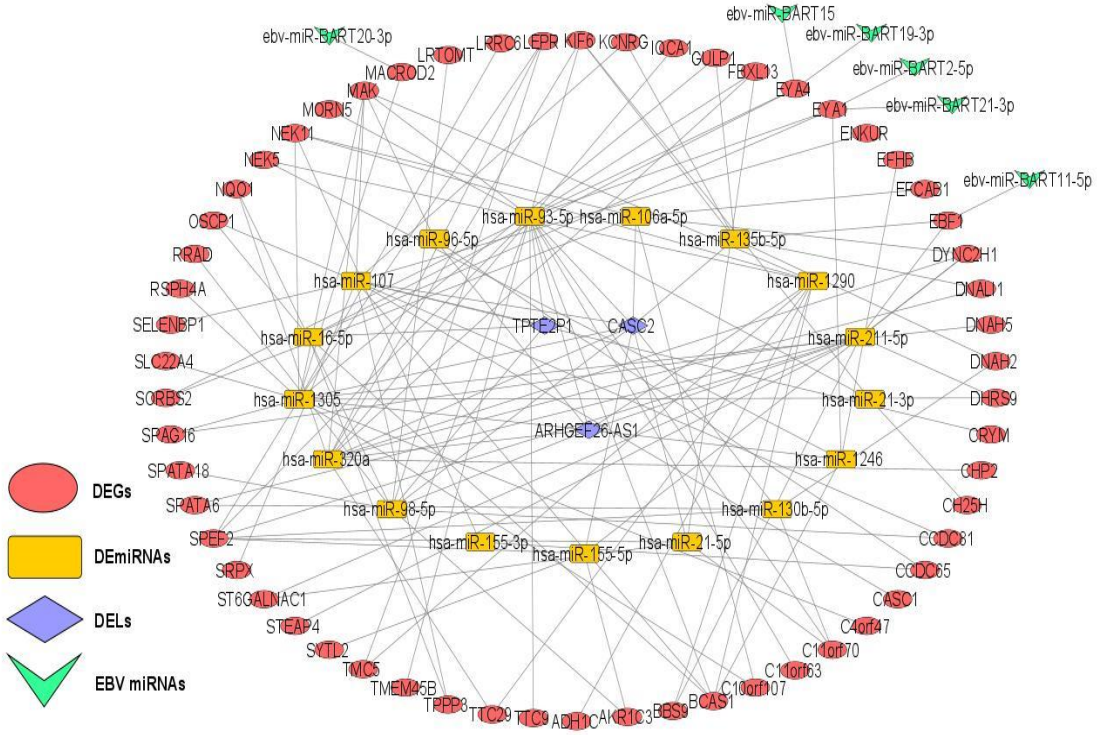

Figure 2. Overlapped down-regulated DEmRNAs in the ceRNA network with target mRNAs for BART miRNAs in Cytoscape revealed 4 common down-regulated DEmRNAs, namely EBF1, MACROD2, EYA1 and EYA4. The EBV BART miRNAs are in green V

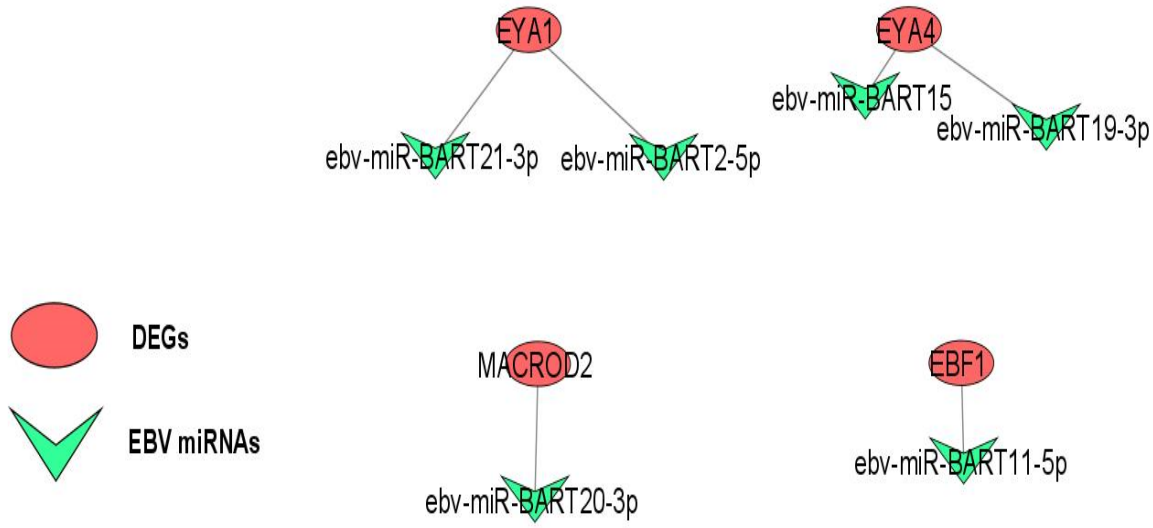

Figure 3. The EBV miRNAs-mRNAs network illustrating the interactions of the four down-regulated ceRNA DEGs (red eclipse) with six EBV BART miRNAs (green V)

Protein-Protein Interaction (PPI) Network Construction

As indicated by the Search Tool for the Retrieval of Interacting Gene (STRING) database of the Cytoscape plug-in, the protein-protein interaction (PPI) network of the down-regulated common mRNAs in three of the GEO datasets (GSE64634, GSE126683 and GSE61218) exhibited 123 nodes and 179 edges. Notably, seventy-seven of the proteins expressed interacted with each other (Figure 4), hinting at shared similar biological functions. Following CytoHubba filtration of the top 20 DEmRNAs, DNAH5 was ranked first with 21 degrees of connectivity, while DNAAF1 exhibited the lowest connectivity degree with 7 degrees (Figure 5). Subsequently, eighteen of the DEmRNAs have a connectivity degree of greater than five based on Network Analyzer analysis. Among them, DNAH5 interacted with 18 DEmRNAs, exhibiting the highest connectivity degree whereas both DNAAF1 and TEKT1 exhibited the lowest connectivity by interacting with 6 DEmRNAs (Figure 6, Supplementary Table 7). These DEmRNAs are considered hub genes and potential tumour suppressors due to their ability to control the expression of other multiple genes. Furthermore, 2 gene modules or protein sets in the PPI network (Module 1 and 2) were generated via MCODE (Table 1, Figure 7). The genes in Module 1 consisted of hub genes, unlike Module 2. Notably, the genes within both modules are neighbouring genes packed closely together in the PPI network and are highly interconnected with each other compared to other genes in the PPI network. Meaning these DEmRNAs or proteins are closely related and functionally similar in each module. The functions primarily influence proper cilia functions and motility. This suggests that the down-regulation of genes in these modules may cause nasopharyngeal carcinoma (NPC) by affecting the nasal ciliary motor's function, impairing fluid and particle clearance in the nasopharynx (Ringers *et al*., 2020).

Construction of Transcription Factors (TF)-mRNAs Network

The TFcheckpoint database yielded 1,021 transcription factors (TFs), of which two, EBF1 and NR2F2, were found to overlap with the down-regulated DEmRNAs identified in the three GEO datasets (GSE64634, GSE126683 and GSE61218) by using Venn diagram (Supplementary Figure 7). However, upon visualization in Cytoscape, neither of these TFs showed links with other DEmRNAs in the protein-protein interaction (PPI) network (Figure 8). As such, no TF-mRNAs network was constructed.

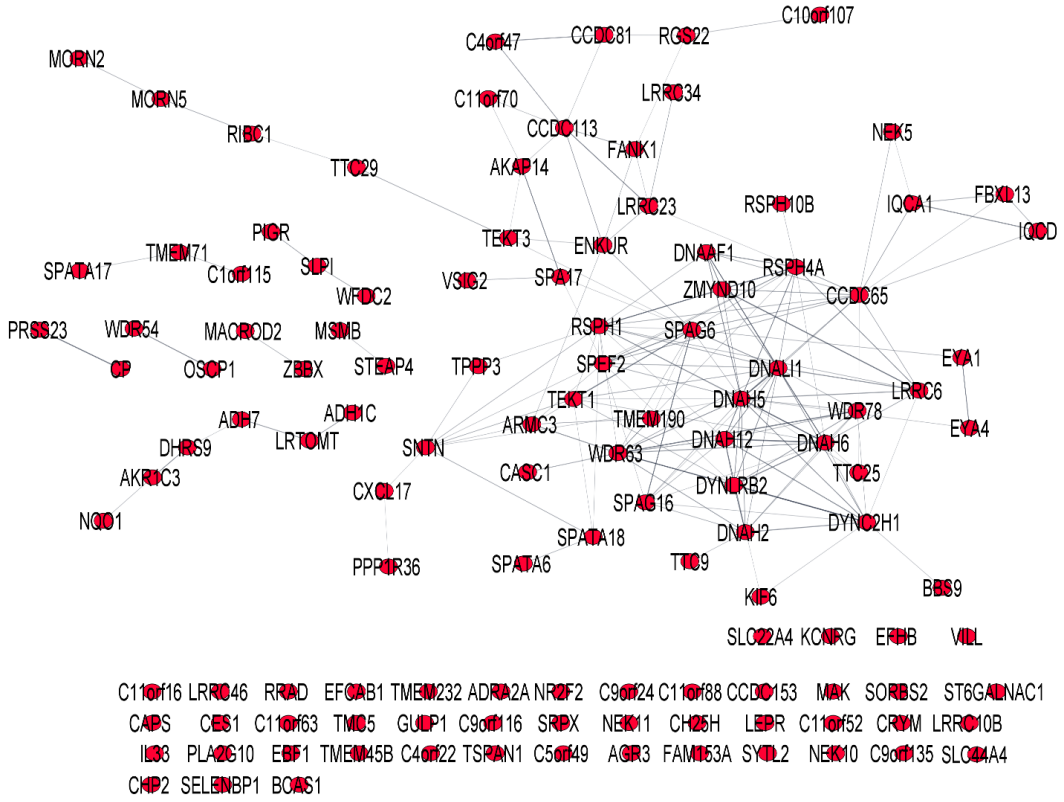

Figure 4. The protein-protein interaction (PPI) between all the down-regulated DEGs retrieved from the STRING database shows 123 nodes and 179 edges, with 77 of the DEGs interacting with each other out of all the 123 DEGs

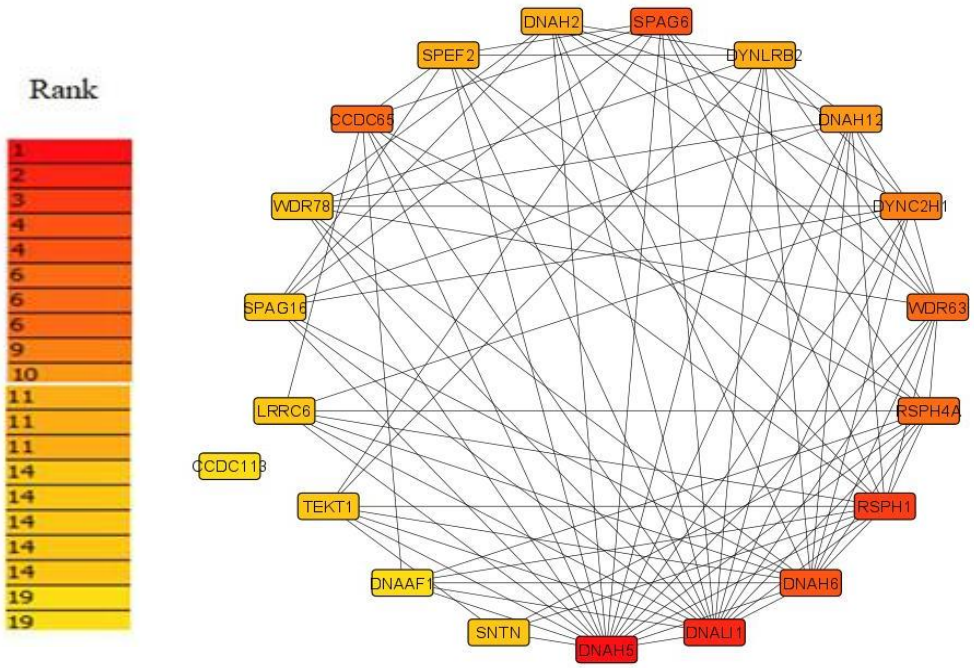

Figure 5. The top 20 DEGs from the PPI ranked according to connectivity degree. Red represents DEG with high connectivity degree and the colour scheme changes to orange and yellow as the connectivity degree decreases. The yellow represents the lowest connectivity degree

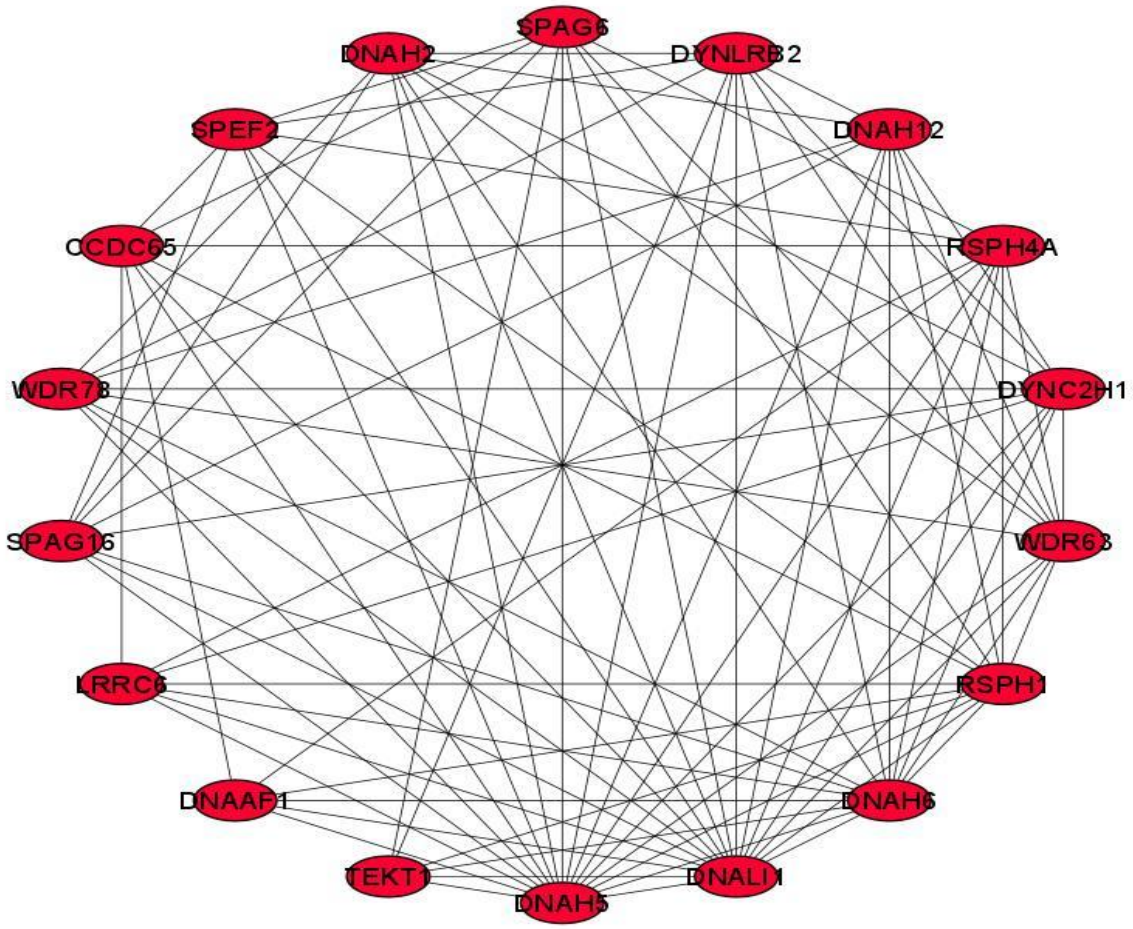

Figure 6. Eighteen hub genes or proteins with connectivity degree greater than 5 among the top 20 hub genes analysed using Network Analyzer analysis. DNAH5 has the highest connectivity degree where it interacts with 18 other DEGs and, gradually the interaction decreases in a counterclockwise from DNAH5 to TEKT1, that has the lowest connectivity degrees, similar to DNAAF1 where they interact with 6 other DEGs among themselves

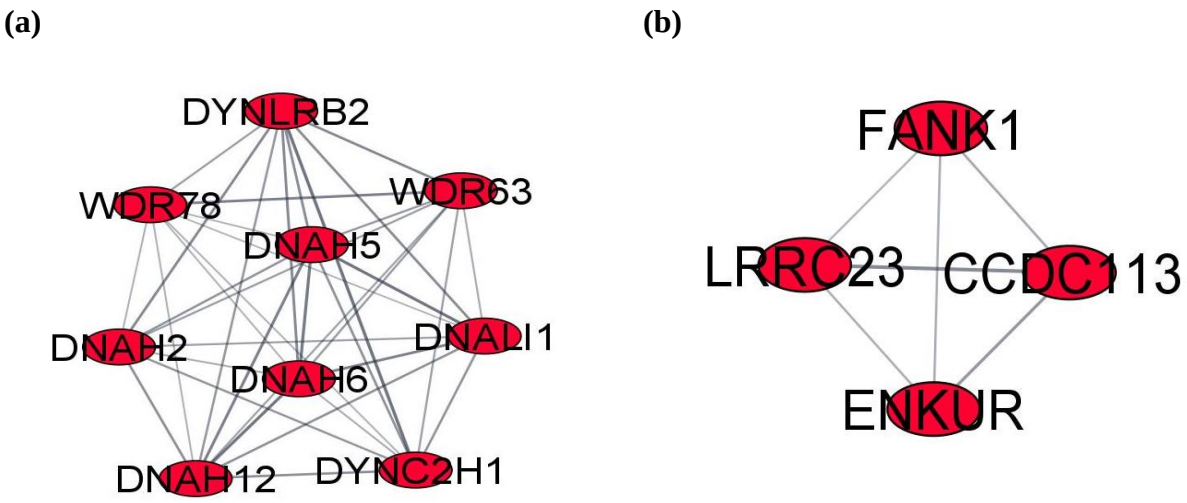

Figure 7. The two modules in the protein-protein interaction (PPI) network with scores ≥ 4 and nodes ≥ 4. Module 1 (a) consisting of all DEGs hub genes, and Module 2 (b) consisting of other DEGs in the PPI. Both modules are essential in proper cilia functions and motility

Table 1. The genes or expressed proteins by the genes consisted in gene modules 1 and 2 extracted from the protein-protein interaction (PPI) network.

Module	Score	Nodes	Edges	DEmRNAs or Proteins
1	9.000	9	36	WDR78, DNAH2, DNAH12, DYNLRB2, DNAH6, DNAH5, WDR63, DNALI1, DYNC2H1
2	4.000	4	6	FANK1, LRRC23, CCDC113, ENKUR

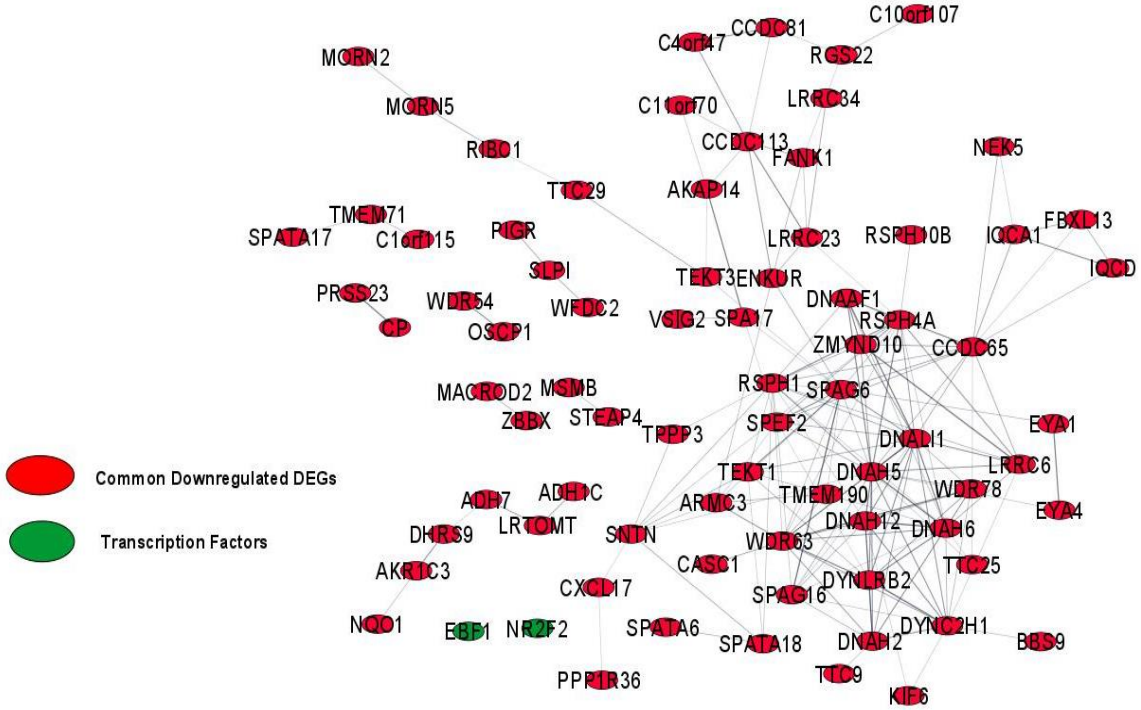

Figure 8. The transcription factors (TF)-mRNAs network model showing the two TFs, EBF1 and NR2F2 (green eclipse), that are not connected to the other down-regulated DEGs (red eclipse) in the protein-protein interaction (PPI) network

Construction of Cross-Regulatory Networks (Competing Endogenous RNA (ceRNA) and Epstein-Barr virus (EBV) *Bam*HI A rightward transcript (BART) miRNAs-DEmRNAs network)

The cross-regulatory network was constructed by merging the two networks, the competing endogenous RNA (ceRNA) network and Epstein-Barr virus (EBV) *Bam*HI A rightward transcript (BART) miRNAs-DEmRNAs network in Cytoscape. It unveils interactions among six EBV miRNAs (ebv-miR-BART21-3p, ebv-miR-BART19-3p, ebv-miR-BART15, ebv-miR-BART2-5p, ebv-miR-BART20-3p and ebv-miR-BART11-5p), four DEmRNAs (EYA4, EYA1, EBF1 and MACROD2), and six DEmiRNAs (hsa-miR-1246, hsa-miR-93-5p, hsa-miR-16-5p, hsa-miR-135b-5p, hsa-miR-211-5p and hsa-miR-1305). In addition, three DElncRNAs (CASC2, TPTE2P1 and ARHGEF26-AS1) are interacting with six of these DEmiRNAs (Figure 9 and Table 2). The cross-regulatory network reveals that EBV BART miRNAs down-regulate the four DEmRNAs, leading to the up-regulation of the six host miRNAs. This occurs due to the limited availability of DEmRNAs for repression of degradation, resulting in the down-regulation of the three DElncRNAs because no miRNA was sponged in EBV-positive nasopharyngeal cancer (NPC). Notably, the cross-regulatory network illustrates the interaction of the TF EBF1 with ebv-miR-BART11-5p. Nevertheless, EBF1 was not interacting with any other DEmRNAs in the network. Moreover, no hub genes are shown to interact with any of the EBV BART miRNAs.

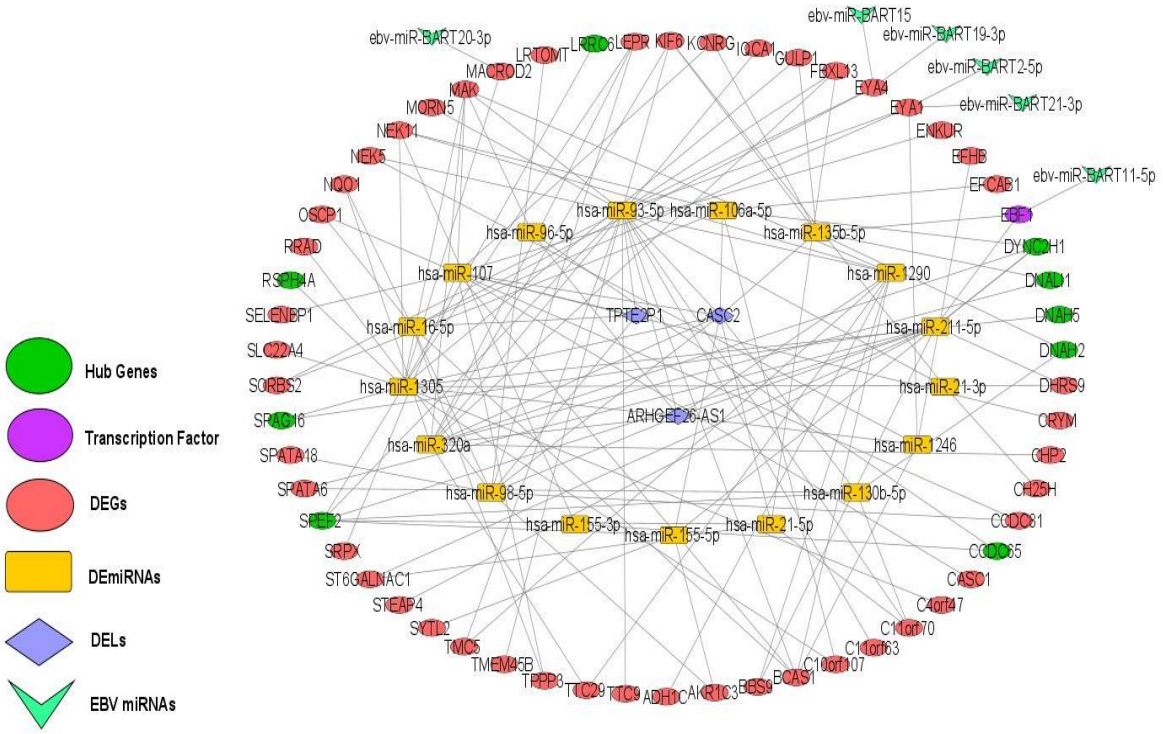

Figure 9. The cross-regulatory network for the DEL-DEmiRNAs-DEGs and EBV miRNAs-DEGs networks, showing four of the EBV miRNAs (ebv-miR-BART21-3p, ebv-miR-BART19-3p, ebv-miR-BART15, ebv-miR-BART2-5p, ebv-miR-BART20-3p and ebv-miR-BART11-5p) interacting with four of the DEGs (EYA4, EYA1, EBF1 and MACROD2). Moreover, these DEGs were interacting with six miRNAs (hsa-miR-1246, hsa-miR-93-5p, hsa-miR-16-5p, hsa-miR-135b-5p, hsa-miR-211-5p and hsa-miR-1305), and these miRNAs are interacting with three lncRNAs (CASC2, TPTE2P1 and ARHGEF26-AS1)

Table 2. The intricate interactions between Epstein-Barr virus (EBV) *Bam*HI A rightward transcript (BART) miRNAs, DEmRNAs, DEmiRNAs and DElncRNAs in the cross-regulatory network

Up-regulated EBV BART miRNAs	Down-regulated DEmRNAs	Up-regulated DEmiRNAs	Down-regulated DElncRNAs
EBV-miR-BART11-5p	EBF1	hsa-miR-211-5p	ARHGEF26-AS1
		hsa-miR-135b-5p	CASC2
EBV-miR-BART20-3p	MACROD2	hsa-miR-1305	CASC2 and ARHGEF26-AS1
EBV-miR-BART21-3p and EBV-miR-BART2-5p	EYA1	hsa-miR-1246	ARHGEF26-AS1
		hsa-miR-93-5p	ARHGEF26-AS1, CASC2 and TPTE2P1
EBV-miR-BART15 and EBV-miR-BART19-3p	EYA4	hsa-miR-93-5p	ARHGEF26-AS1, CASC2 and TPTE2P1
		hsa-miR-16-5p	TPTE2P1

Functional and Pathway Enrichment Analysis of DEmRNAs

The Gene Ontology (GO) enrichment results (from DAVID analysis), for the four DEmRNAs (EYA1, EYA4, EBF1 and MACROD2) targeted by the six Epstein-Barr virus (EBV) *Bam*HI A rightward transcript (BART) miRNAs (ebv-miR-BART21-3p, ebv-miR-BART19-3p, ebv-miR- BART15, ebv-miR-BART2-5p, ebv-miR-BART20-3p and ebv-miR-BART11-5p) in the cross-regulatory network revealed enrichment in eleven GO terms at the cut-off P-value < 0.05. These were eight GO terms for Biological Processes (BP), two GO terms in Molecular Function (BF) and one GO term for Cellular

Component (CC) (Figure 10). The Biological Processes (BP) revealed the involvement of the DEmRNAs in regulating DNA repair and apoptosis. Due to down-regulation by EBV BART miRNAs, these DEmRNAs were predicted to be unable to perform their functions, potentially leading to tumour cell proliferation and NPC tumorgenesis. Besides, the Molecular Function (BF) analysis exhibited that the proteins encoded by these DEmRNAs require metal ion binding for DNA repair and immune systems surveillance. Additionally, all these DEmRNAs were presumed to be located in the nucleus of the cells when targeted by EBV BART miRNAs, as indicated by the Cellular Component (CC) term. However, the KEGG pathway enrichment analysis for the four DEmRNAs targeted by the six EBV BART miRNAs in the cross-regulatory network did not yield any significant results.

DISCUSSION

In the present study, we constructed a comprehensive cross-regulatory network by integrating the competing endogenous RNA (ceRNA) regulatory and EBV miRNA-mRNA interaction networks to unravel the intricate molecular mechanisms mediated by EBV BART miRNAs during NPC tumorigenesis. We demonstrated that EBV BART miRNAs target and dysregulate mRNA expression, thereby disrupting the intricate balance of gene regulation. This dysregulation extends to microRNAs (miRNAs) and long non-coding RNAs (lncRNAs), leading to the oncogenesis of NPC. We also infer that the candidate EBV BART miRNAs and lncRNAs could potentially have oncogenic and tumour-suppressive functions. These insights shed light on the complex interplay between EBV BART miRNAs, mRNAs, miRNAs and lncRNAs, providing an understanding of NPC tumorgenesis and the development of novel therapeutic strategies.

The competing endogenous RNA (ceRNA) network exhibits 58 mRNAs that are indirectly dysregulated by 3 lncRNAs. This is through 18 miRNAs sponged/targeted by the 3 lncRNAs. The lncRNAs are suggested to be down-regulated, which consequently caused the down-regulation of the mRNAs, independent of the presence of EBV BART miRNAs. In a previous study, a ceRNA network showed 2,654 mRNAs were regulated by 132 lncRNAs via 565 corresponding miRNAs in NPC using datasets that were submitted even before 2014 (Xu *et al.,* 2020). When considering the presence of EBV BART miRNAs, the four DEmRNAs targeted by BART miRNAs are assumed to be down-regulated by these EBV BART miRNAs. This causes the up-regulation of host miRNAs and subsequent down-regulation of the lncRNAs. In this scenario, the BART miRNAs mimic the function of the host's miRNAs, sponging/targeting the host's mRNAs. In other words, the BART miRNAs competing with the host's miRNAs for mRNAs and incidentally down-regulated the lncRNAs. This intricate interplay is believed to contribute to the development of EBV-associated NPC.

In this study, we uncovered 14 up-regulated miRNAs similar to those in a previous study (Xu *et al.,* 2020), but this is not the case for lncRNAs and mRNAs, which are novel discoveries. Therefore, 58 mRNA, 17 miRNA and 3 lncRNA are new non-coding RNAs potentially associated with NPC tumorigenesis. For the cross-regulatory network, six of the miRNAs are up-regulated in NPC tumour samples, cell lines and serum, excluding hsa-miR-211-5p and hsa-miR-16-5p (Zhu *et al.,* 2009; Plieskatt *et al.,* 2014; Tang *et al.,* 2014), and our results here are the first to connect them with the tumorigenesis of NPC. Interestingly, hsa-miR-16-5p, hsa-miR-211-5p and hsa-miR-1305 are observed to demonstrate opposite effects in various cancers, including non-small cell lung cancer (NSCLC) and hepatocellular carcinoma (HCC), where they are down-regulated and elicit the up-regulation of their target mRNAs, including XIST, MDM2 and ACSL4 (Cai *et al.,* 2019; Qin *et al.,* 2020; Du *et al.,* 2021).

In addition, to identify interactive relationships among down-regulated mRNAs, the protein-protein interaction (PPI) network was constructed (Tang *et al.,* 2018) and it unveils 18 hub genes with connectivity degree greater than 5. These genes, interacting with more than 5 other genes in the PPI network, possess the capacity to regulate the expression of other multiple genes. Notably, these hub genes are potential new candidate NPC-associated hub genes compared to a previous study by Xu *et al.* (2020). However, the cross-regulatory network analysis did not reveal the targeting of these hub genes by six of the BART miRNAs

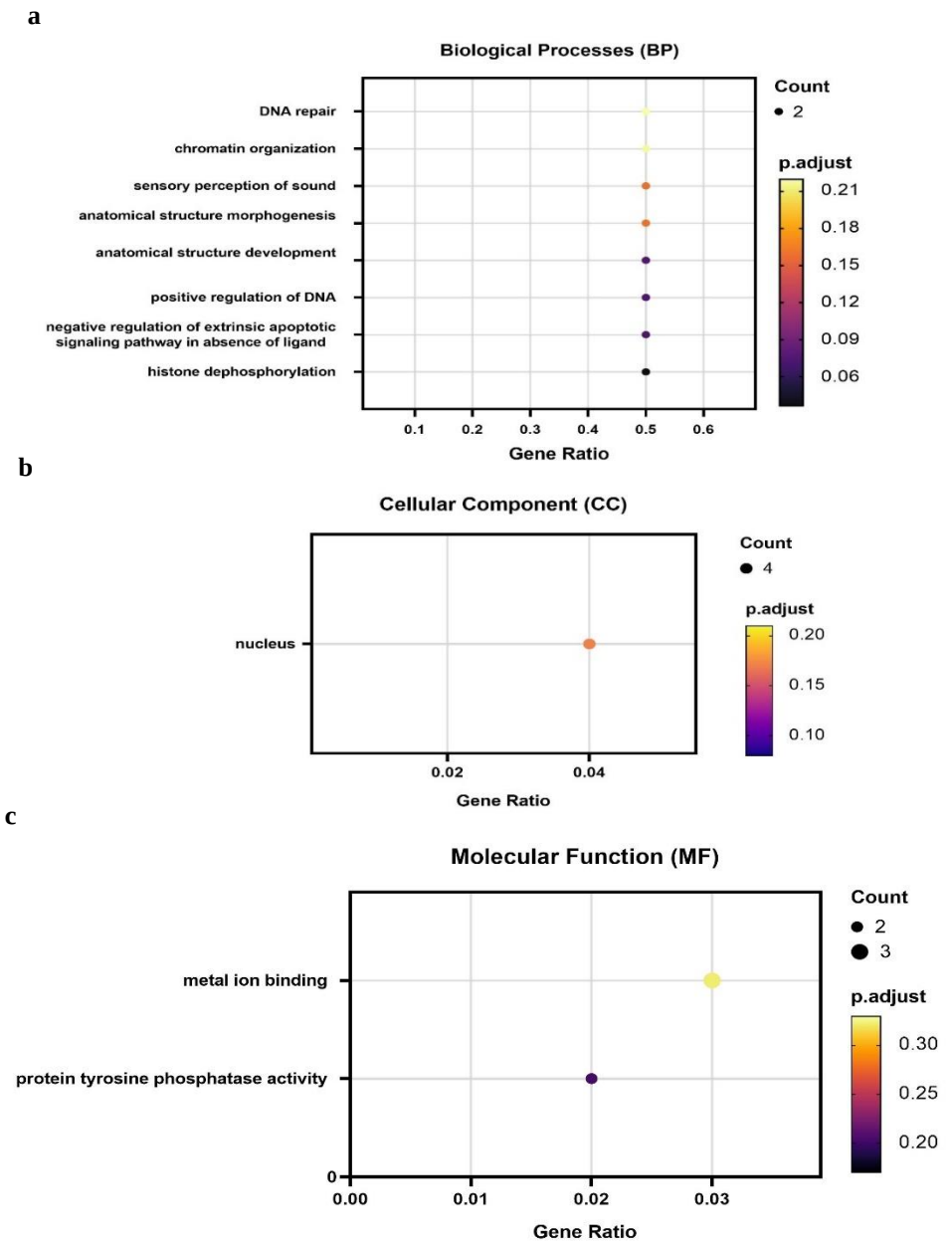

Figure 10. The Gene Ontology (GO) enrichment results for the DEGs targeted by EBV BART miRNAs in the cross-regulatory network showing (a) 8 GO terms for Biological Processes (BP), (b) one GO term for Cellular Component (CC), and (c) one GO terms for Molecular Function (BF)

Furthermore, these dysregulated hub genes co-expressed together in a module, termed module 1, affecting similar biological functions essential for healthy nasopharynx functions. Both module 1 and module 2, are pivotal for normal motile cilia functions (Rashid *et al.,* 2006; Johnson *et al.,* 2018; Zhu *et al.,* 2019; Vig *et al.,* 2020; Bazan *et al.,* 2021; Braschi *et al.,* 2022). Thus, hypothetically the down-regulation of these modules genes contributes to NPC by affecting the nasal ciliary motor. Motile cilia lining the nasopharynx is crucial for coordinated beating, facilitating proper flow and clearance of fluids and particles (Ringers *et al.,* 2020; Lee *et al.,* 2021).

Therefore, when EBV infection occurs, individuals with mucociliary clearance defect are predisposed to EBV-positive NPC tumorigenesis resulting from the ineffective sweeping of mucus covering the nasal epithelium towards the nasopharynx by coughing, impeding the removal of particles and pathogens from the respiratory tract (Marttin *et al.,* 1997; Gizurarson, 2015; Kamiya *et al.,* 2020). Consequently, EBV gains the opportunity to colonize epithelial cells and B-cells in the nasopharynx. Our data from the analysis of this

cross-regulatory network highlights the interaction between six EBV miRNAs (ebv-miR-BART21-3p, ebv-miR-BART19-3p, ebv-miR-BART15, ebv-miR-BART2-5p, ebv-miR-BART20-3p and ebv-miR-BART11-5p) and four DEmRNAs (EYA4, EYA1, EBF1 and MACROD2), resulting in their down-regulation. Subsequently, this causes the up-regulation of six miRNAs (hsa-miR-1246, hsa-miR-93-5p, hsa-miR-16-5p, hsa-miR-135b-5p, hsa-miR-211-5p, and hsa-miR-1305), leading to the up-regulation of three lncRNAs (CASC2, TPTE2P1, and ARHGEF26-AS1). Based on this, the association of EBV with NPC can be deduced through the regulatory mechanisms of EBV BART miRNAs targeting the host's mRNAs, thereby affecting both miRNAs and lncRNAs that interact with them. Currently, the interplay interactions between EBV miRNAs and lncRNAs in NPC have not yet been updated, apart from our study, as the interest has shifted towards understanding the regulatory mechanisms of EBV miRNA/lncRNA on circular RNA (circRNA) in NPC.

Previous studies have consistently reported high expression levels of all six BART miRNAs in NPC tissue samples, cell lines and serum samples (Cosmopoulos *et al.,* 2009; Song *et al.,* 2016; Lung *et al.,* 2018; Jiang *et al.,* 2020; Zhou *et al.,* 2022). However, conflicting findings were noted for BART15 expression in NPC cell lines, with Amoroso *et al.* (2011) revealing it was barely expressed, and Lung *et al.* (2018) revealing it is undetected, while Cosmopoulos *et al.* (2009) observed it is highly expressed in both NPC cell line and tumour biopsy. In terms of the interaction of these six BART miRNAs in NPC, only BART2-5p was found to down-regulate the gene RND3 expressions in NPC pathogenesis (Jiang *et al.,* 2020). In other cancers, only BART11-5p was observed interacting with EBF1 in the EBV-transformed lymphoblastoid cell line (LCL) (Ross *et al.*, 2013), which is consistent with our result. However, the information regarding the interactions of BART19-3p, BART15, BART21-3p, and BART20 in cancer is currently unavailable.

With reference to the Biological Processes (BP) from the Gene Ontology (GO) term, two of the DEmRNAs targeted by the BART miRNAs, which are EYA1 and EYA4, are associated with DNA repair, chromatin organization, histone dephosphorylation, apoptosis, anatomical structure morphogenesis and development and sensory perception of sound. These DEmRNAs are also metalloproteins based on the Molecular Function (MF) of the GO term as metal ion binding (MIB). Our cross-regulatory network data revealed that EYA1 is down-regulated by ebv-miR-BART21-3p and ebv-miR-BART2-5p, while EYA4 is down-regulated by ebv-miR-BART19-3p and ebv-miR-BART15. Despite this finding, there is no information on these interactions in NPC to our knowledge.

The *EYA* gene family encodes proteins tyrosine phosphatase that respond to DNA damage when bound by Mg^{2+} ion, based on the Molecular Function (MF) of the GO term as metal ion binding (MIB) **(**Tadjuidje *et al.,* 2012; Sadatomi *et al.,* 2013; Lung *et al.*, 2018). This protein works in combination with the protein tyrosine kinases, and their structural/functional aberrancies usually lead to no chromatin organization and histone dephosphorylation, consequently inhibiting DNA repair and eventually diseases, including cancers (Tadjuidje *et al*., 2012; Sadatomi *et al*., 2013; Kong *et al.,* 2019). In fact, EYA4 is known to be involved in the promotion of DNA repair and inhibition of apoptosis in oesophagal squamous cell carcinoma (Xu & Fisher, 2012), while EYA1 is down-regulated in gastric cancer tissues and correlated with tumour size and metastasis (Nikpour *et al*., 2014). We suspected that, in NPC tumorigenesis, EBV utilizes its BART21-3p, BART2-5p, BART19-3p, and BART15 miRNAs to hijack these biological processes by down-regulating EYA1 and EYA4.

Similarly, we suspected that EBV utilizes these BART miRNAs to inhibit apoptosis. Typically, when histone dephosphorylation is defective during DNA damage, JNK (c-Jun N-terminal protein kinase) is recruited for extrinsic apoptosis pathway activation (Dhanasekaran & Reddy, 2008; Nowsheen *et al.,* 2018). The suggestion of EBV using BART21-3p, BART2-5p, BART19-3p and BART15 miRNAs in down-regulating the major histocompatibility complex class I chain-related peptide A (MICA) and peptide B (MICB) ligands, expressed upon viral infection and DNA damage by targeting EYA1 and EYA4 (Zingoni *et al.,* 2018; Png *et al.,* 2021), is plausible**.** The absence of these ligands facilitates EBV to escape natural killer (NK) cell-mediated immune surveillance by inhibiting JNK signalling pathway activation and avoiding

apoptosis (Wong *et al.,* 2018).

Without apoptosis, infected cells proliferate uncontrollably, leading to anatomical structure morphogenesis and development, including angiogenesis and vasculogenic mimicry (VM), commonly observed in cancerous cells, including NPC (Luo *et al.,* 2021; Tian *et al.,* 2021). The proliferation and growth of the tumour tissues and cells require more oxygen and nutrients in the tumour microenvironment, thus the formation of angiogenesis and VM to sustain the tumour growth (Zuazo-Gaztelu & Casanovas, 2018; Xiang *et al.,* 2018; Fernández-Cortés *et al.,* 2019; Teleanu *et al.,* 2019). As the size of tumour cells increases, it covers and impairs the adjacent Eustachian tube, causing middle ear effusion or Otitis media with effusion (OME), tinnitus, and consequently, hearing loss (Utama *et al.,* 2022). Interestingly, OME, tinnitus, and hearing loss are the symptoms of NPC (Ho *et al.,* 2008; Tsunoda *et al.,* 2021), where a history of OME is prevalent among NPC patients (Huang *et al.,* 2012).

The buildup of fluid in the middle ear, known as middle ear effusion or OME, puts pressure on the tympanic membrane and impedes its proper vibration, leading to hearing loss (Searight *et al.,* 2022). A decrease in the cilia density of the mucociliary epithelium and the increase in goblet cells lining the Eustachian tube obstructs the ear secretion drainage from the middle ear into the nasopharynx (Matsune *et al.,* 1992; Depreux *et al.,* 2008; Casale *et al.,* 2023). From this, tinnitus occurs subsequently, combined with an increase in the size of tumour cells covering the Eustachian tube, stems from negative pressure in the middle ear due to no pressure equalization in the middle ear with atmospheric pressure (Bal & Deshmukh, 2022; Mayo Clinic, 2022; Casale *et al.,* 2023). Middle ear ventilation is essential for proper eardrum vibration and sound transmission (Casale *et al.,* 2023). Our findings have provided molecular insights into the causes of hearing impairment among NPC patients, mediated by non-coding EBV RNAs (BART miRNAs) and EYA genes. The verification and detailed mechanisms for this must be further investigated via relevant functional studies.

We have observed BART11-5p targeting the transcription factor (TF) EBF1 in the cross-regulatory network. EBF1 is a transcription factor that works with E2A and PAX5 in B cell development (Poh *et al.,* 2016). However, our results did not reveal EBF1 interacting with the DEmRNAs in the ceRNA network; thus, no TF-mRNA network was constructed. We attribute this to the limited NPC microarray dataset available in the time frame chosen for our study. Based on the literature, EBF1 requires metal ion binding (MIB) for structural conformational, regulatory, and enzymatic activity, specifically divalent zinc ion (Zn^{2+}) (Hagman *et al.,* 2011; Vilagos *et al.,* 2012). This is also shown by the Molecular Function (MF) of the GO term. It has been shown that the targeting of EBF1 by BART11-5p causes abnormal germinal centre reactions in the lymphoid tissues, thereby inhibiting mature B-cells development (Permyakov, 2021). We suspect that when BART11-5p targets EBF1, it inhibits MIB-EBF1 interaction, leading to the deterioration of B-cell production. This hypothesis is yet to be experimentally tested. More importantly, this could be one of the mechanisms EBV uses for immune evasion in the context of EBV-related carcinogenesis, including NPC – a research prospect that warrants exploration.

The final DEmRNA targeted by BART miRNA in our data is MACROD2, which is targeted by ebv-miR-BART20-3p. MACROD2 plays a crucial role in reversible ADP-ribosylation, acting as a hydrolase (Žaja *et al.,* 2020), and is associated with critical cellular pathways of DNA repair and apoptosis in eukaryotes (Golia *et al.,* 2017). It acts as a negative feedback loop and restricts the recruitment repair factors and effector proteins to the DNA break site when phosphorylates by ATM and exported out of the nucleus (Golia *et al.,* 2017). Following DNA repair, MACROD2 facilitates the removal of terminal autoinhibitory mono-ADP-ribose from the transferase Poly(ADP-ribose) polymerases 1 (PARP1), a process known as dePARylation or histone dephosphorylation to prevent entrapment of proteins involved in DNA repair at the damage site and causing hypersensitivity to DNA damage (Sakthianandeswaren *et al.,* 2018; Kassab *et al.,* 2020). Its dysregulation is associated with various cancers (Linnebacher *et al.,* 2013; Mohseni *et al.,* 2014; Briffa *et al.,* 2015; van den Broek *et al.,* 2015; Hu *et al.,* 2016; Cohen & Chang, 2018). In fact, its down-regulation in colorectal cancer has been linked to the increase in PARP1 mono-ADP-ribosylation

that reduces its transferase activity, leading to DNA repair impairment while heightening sensitivity to DNA damage (Hu *et al.,* 2016). Prior to our findings, the link between non-coding EBV RNAs (BART miRNA per se) and MACROD2 with respect to NPC oncogenesis has never been implied. As such, the ebv-miR-BART20-3p/MACROD2 regulatory network is an important and potent mechanism for deeper investigation.

In our current study, we have elucidated the interaction of three lncRNAs (CASC2, TPTE2P1, and ARHGEF26-AS1) with six miRNAs (hsa-miR-1246, hsa-miR-93-5p, hsa-miR-16-5p, hsa-miR-135b-5p, hsa-miR-211-5p, and hsa-miR-1305). Our data also showed that the three lncRNAs were down-regulated, thus implying their roles as tumour suppressors. Indeed, it is not uncommon for lncRNAs to act as tumour suppressors (Sakthianandeswaren *et al.,* 2018). However, only CASC2 and ARHGEF26-AS1 were hinted by previous studies could act as tumor suppressors. Specifically, in the context of nasopharyngeal carcinoma (NPC), only CASC2 was observed to be down-regulated in NPC tissue samples and cell lines, where it promotes cell proliferation and inhibits apoptosis by down-regulating RBBP8 through up-regulation of miR-18a-5p (Miao *et al.,* 2019). Nevertheless, studies on the down-regulation of CASC2 in EBV-positive NPC remain limited.

Our findings on the down-regulation of CASC2 and ARHGEF26-AS1 in NPC are consistent with previous studies in cancers, such as lung adenocarcinoma (LUAD) and esophageal carcinoma (Chen *et al.,* 2021; Yao *et al.,* 2021), but not for TPTE2P1. Based on previous studies, TPTE2P1 is typically up-regulated in other cancers, including colorectal, gallbladder, and hepatocellular carcinomas (Liu *et al.,* 2019), suggesting its potential dual role as both a tumour suppressor and an oncogene. Nevertheless, there are limited studies conducted on TPTE2P1 and ARHGEF26-AS1 expression in NPC, particularly in EBV-positive NPC. Moreover, we are the first ones to demonstrate the interaction of ARHGEF26-AS1 and CASC2 with six of the miRNAs, as well as the interaction of TPTE2P1 with four of the miRNAs in NPC. Notably, the interaction of these lncRNAs with the miRNAs is also limited in other cancer contexts. One limitation of our study is its reliance on curated microarray datasets rather than RNA sequencing datasets. Consequently, the limited dataset, especially for the miRNA dataset, is not amenable for deriving pathway(s) affected by EBV miRNAs.

In addition, the exclusion of constructing an EBV-negative ceRNA counterpart to compare to the result may introduce the potential for false positives. However, it is noteworthy that the mRNA and lncRNA microarray datasets curated for this study comprise samples from NPC patients residing in endemic regions, including China and Hong Kong, which are highly associated with EBV-positive NPC. This context increases the credibility of our results, reducing the likelihood of false positives. Although this rationale may not apply to the miRNA dataset, the presence of some significantly up-regulated EBV BART miRNAs, with p-value < 0.05, insinuating that all the NPC patients within this dataset might be EBV-positive NPC.

Moreover, the mRNA and lncRNA targeted by miRNAs, as well as the EBV miRNAs targeting the mRNAs, are curated from up-to-date databases that amalgamate experimental evidence with computational prediction. For example, the miRTarBase uses high-throughput techniques, including cross-linking and immunoprecipitation and high-throughput sequencing (CLIP-seq), cross-linking, ligation, and sequencing of hybrids (CLASH-seq) and DEmRNA radome-seq which are validated by using the miRNA-target gene expression profiles sourced from prominent repositories such as GEO and The Cancer Genome Atlas (TCGA) databases, for identification of miRNA-target mRNA (Moore *et al.,* 2015; Miao *et al.,* 2019).

Likewise, the DIANA-LncBase V3 and StarBase V2 also curate interactions between miRNA and target lncRNA that are validated by using CLIP-seq, including HITS-CLIP (high-throughput sequencing of RNA isolated by crosslinking immunoprecipitation), PAR-CLIP (photoactivatable-ribonucleoside-enhanced crosslinking and immunoprecipitation) and CLEAR-CLIP (covalent ligation and endogenous Argonaute-bound RNA) which enable the identification of Argonaute (AGO):miRNA binding sites on targeted RNAs (Huang *et al.,* 2020). Next, the EBV BART interactions with target mRNAs curated from VirBase undergo experimental validation using CLIP-seq, quantitative real-time PCR, Western

Blot and immunohistochemistry analysis techniques. A high confidence score was set to curate EBV miRNAs-mRNAs interactions as this is commensurate to more evidence resources supporting these interactions. Nevertheless, the results of this study need to be validated experimentally in the future.

A comprehensive study in the future would necessitate the incorporation of RNA-sequence datasets as microarray datasets have become less favored in recent years, contributing to the limited datasets in our study. The preference for RNA-sequencing stems from its ability to provide extensive quantification through whole transcriptome sequencing, enabling the detection of more differentially expressed genes with higher fold changes, thereby enhancing result accuracy. Regardless, data processing and analysis are standardized and well-established for microarray datasets compared to RNA-sequence datasets (Rao *et al.,* 2019). From this arises the complexity of data processing and analysis due to the multitude of tool options available, which may overwhelm beginners and potentially lead to false positives compared to microarray datasets (Corchete *et al.,* 2020). Besides, different expression analysis methods in RNA-seq may result in under- or overestimated read counts, introducing variability in the data interpretation process (Christelle & Watson, 2015). Furthermore, the physiological veracity of our findings will require molecular experimentations that include quantitative real-time PCR, Western Blot, and immunohistochemistry analyses. These experiments will enable the verification of EBV miRNA mechanisms in NPC pathogenesis through expression level and the roles of the predicted DEmRNAs targeted by the EBV miRNAs.

CONCLUSION

Our constructed cross-regulatory network has uncovered novel insights into the interplay between EBV miRNAs and lncRNAs presumptively associated with NPC pathogenesis. The cross-regulatory network illuminates the intricate interactions and the muti-level regulation between EBV BART miRNAs, mRNA, lncRNA, and miRNAs further upon EBV infection. We identified that BART miRNAs shift the ceRNA activity by indirectly regulating lncRNAs in EBV-associated NPC. Furthermore, from the cross-regulatory network, the biological, cellular, and molecular processes caused by the dysregulation of the four DEmRNAs, namely EYA1, EYA4, MACROD2, and EBF1, targeted by the BART miRNAs, were also inferred. These four DEmRNAs involve those responsible for DNA repair regulation and apoptosis induced by DNA damage. Additionally, we provided hypothetical scenarios wherein lncRNAs were indirectly targeted by BART miRNAs and implied both factors as potential prognostic biomarkers and therapeutic targets of NPC to mitigate the adverse effects of current treatments. Lastly, our analysis hints at a potential tumor suppressor-like role of BART miRNAs and lncRNAs linked to specific DEmRNAs, albeit in a preliminary capacity, as inferred from the cross-regulatory network.

ACKNOWLEDGEMENTS

The authors acknowledge the support given by Universiti Malaysia Sarawak in the conduct, reporting, and publication of this study.

REFERENCES

Amoroso, R., Fitzsimmons, L., Thomas, W.A., Kelly, G.L., Rowe, M. & Bell, A.I. (2011). Quantitative studies of Epstein-Barr virus-encoded microRNAs provide novel insights into their regulation. *Journal of Virology,* 85(2): 996-1010. DOI: 10.1128/jvi.01528-10

Bader, G., Pavlovic, V. & Lopes, C. (2020). *MCODE Documentation Release 2.0.0.* [online] Available at: chrome-extension://efaidnbmnnnibpcajpcglclefindmkaj/https://mcode.readthedocs.io/_/downloads/en/latest/pdf/ [Accessed on 23 March 2021].

Bal, R. & Deshmukh, P. (2022). Management of eustachian tube dysfunction: A Review. *Cureus,* 14(11). DOI: 10.7759/cureus.31432

Bazan, R., Schröfel, A., Joachimiak, E., Poprzeczko, M., Pigino, G. & Wloga, D. (2021). Ccdc113/Ccdc96 complex, a novel regulator of ciliary beating that connects radial spoke 3 to dynein g and the nexin link. *PLoS Genetics,* 17(3): e1009388. DOI: 10.1371/journal.pgen.1009388

Braschi, B., Omran, H., Witman, G.B., Pazour, G.J., Pfister, K.K., Bruford, E.A. & King, S.M. (2022). Consensus nomenclature for dyneins and associated assembly factors. *Journal of Cell Biology,* 221(2): e202109014. DOI: 10.1083/jcb.202109014

Briffa, R., Um, I., Faratian, D., Zhou, Y., Turnbull, A. K., Langdon, S.P. & Harrison, D.J. (2015). Multi-Scale genomic, transcriptomic and proteomic analysis of colorectal cancer cell lines to identify novel biomarkers. *PLoS One,* 10(12): e0144708. DOI: 10.1371/journal.pone.0144708

Cai, X., Schäfer, A., Lu, S., Bilello, J.P., Desrosiers, R.C., Edwards, R., Raab-Traub, N. & Cullen, B. R. (2006). Epstein–Barr virus microRNAs are evolutionarily conserved and differentially expressed. *PLoS Pathogens,* 2(3): e23. DOI: 10.1371/journal.ppat.0020023

Cai, Y., Hao, Y., Ren, H., Dang, Z., Xu, H., Xue, X. & Gao, Y. (2019). miR-1305 inhibits the progression of non-small cell lung cancer by regulating MDM2. *Cancer Management and Research*, 11: 9529. DOI: 10.2147/CMAR.S220568

Casale, J., Shumway, K.R. & Hatcher, J.D. (2023). *Physiology, eustachian tube function*. [e-book] Treasure Island: StatPearls Publishing. Available through: https://www.ncbi.nlm.nih.gov/books/NBK532284/ [Accessed on 27 May 2023].

Chang, E.T. & Adami, H.O. (2006). The enigmatic epidemiology of nasopharyngeal carcinoma. *Cancer Epidemiology and Prevention Biomarkers*, 15(10): 1765-1777. DOI: 10.1158/1055-9965.EPI-06-0353

Chen, C., Zhao, J., Liu, J.N. & Sun, C. (2021). Mechanism and Role of the Neuropeptide LGI1 Receptor ADAM23 in Regulating Biomarkers of Ferroptosis and Progression of Esophageal Cancer. *Disease Markers,* 2021: 227897. DOI: 10.1155/2021/9227897

Chen, J., Yang, R., Zhang, W. & Wang, Y. (2015). Candidate pathways and genes for nasopharyngeal carcinoma based on bioinformatics study. *International Journal of Clinical and Experimental Pathology,* 8(2): 2026-2032.

Cohen, M.S. & Chang, P. (2018). Insights into the biogenesis, function, and regulation of ADP-ribosylation. *Nature Chemical Biology,* 14: 236-243. DOI: 10.1038/nchembio.2568

Corchete, L.A., Rojas, E.A., Alonso-López, D., De Las Rivas, J., Gutiérrez, N.C. & Burguillo, F.J. (2020). Systematic comparison and assessment of RNA-seq procedures for gene expression quantitative analysis. *Scientific Reports*, 10(1): 19737. DOI: 10.1038/s41598-020-76881-x

Cosmopoulos, K., Pegtel, M., Hawkins, J., Moffett, H., Novina, C., Middeldorp, J. & Thorley-Lawson, D.A. (2009). Comprehensive profiling of Epstein-Barr virus microRNAs in nasopharyngeal carcinoma. *Journal of Virology,* 83(5): 2357-2367. DOI: 10.1128/jvi.02104-08

Christelle, R. & Watson, M. (2015). Errors in RNA-Seq quantification affect genes of relevance to human disease. *Genome Biology*, 177: 16. DOI: 10.1186/s13059-015-0734-x

DAVID Bioinformatics Resources. (2021). *Functional annotation tool.* [online] Available at: https://david.ncifcrf.gov/helps/functional_annotation.html#E3 [Accessed on 25 May 2023].

Depreux, F.F., Darrow, K., Conner, D.A., Eavey, R. D., Liberman, M.C., Seidman, C.E. & Seidman, J.G. (2008). Eya4-deficient mice are a model for heritable otitis media. *The Journal of Clinical Investigation,* 118(2): 651-658. DOI: 10.1172/JCI32899

Dhanasekaran, D.N. & Reddy, E.P. (2008). JNK signaling in apoptosis. *Oncogene, 27*(48): 6245-6251. DOI: 10.1038/onc.2008.301

Du, R., Jiang, F., Yin, Y., Xu, J., Li, X., Hu, L. & Wang, X. (2021). Knockdown of lncRNA X inactive specific transcript (XIST) radiosensitizes non-small cell lung cancer (NSCLC) cells through regulation of miR-16-5p/WEE1 G2 checkpoint kinase (WEE1) axis. *International Journal of Immunopathology and Pharmacology,* 35. DOI: 10.1177/205873842096608

Dwijayanti, F., Prabawa, A., Besral & Herawati, C. (2020). The five-year survival rate of patients with nasopharyngeal carcinoma based on tumor response after receiving neoadjuvant chemotherapy, followed by chemoradiation, in Indonesia: a retrospective study. *Oncology,* 98(3): 154-160. DOI: 10.1159/000504449

Fernández-Cortés, M., Delgado-Bellido, D. & Oliver, F. J. (2019). Vasculogenic mimicry: become an endothelial cell "but not so much". *Frontiers in Oncology,* 9: 803. DOI: 10.3389/fonc.2019.00803

Gizurarson, S. (2015). The effect of cilia and the mucociliary clearance on successful drug delivery. *Biological and Pharmaceutical Bulletin,* 38(4): 497-506. DOI: 10.1248/bpb.b14-00398

Global Cancer Observatory. (2022). *Malaysia Fact Sheet.* [online] Available at: https://gco.iarc.who.int/media/globocan/factsheets/populations/458-malaysia-fact-sheet.pdf [Accessed on 25 May 2023].

Golia, B., Moeller, G.K., Jankevicius, G., Schmidt, A., Hegele, A., Preißer, J., Tran, M.L., Imhof, A. & Timinszky, G. (2017). ATM induces MacroD2 nuclear export upon DNA damage. *Nucleic Acids Research,* 45(1): 244-254.

Hagman, J., Ramírez, J. & Lukin, K. (2011). B lymphocyte lineage specification, commitment and epigenetic control of transcription by early B cell factor 1. *Epigenetic Regulation of Lymphocyte Development*, 356: 17-38. DOI: 10.1007/82_2011_139

Han, J.D.J., Bertin, N., Hao, T., Goldberg, D.S., Berriz, G.F., Zhang, L.V., Dupuy, D., Walhout, A. J.M., Cusick, M.E., Roth, F.P. & Vidal, M. (2004). Evidence for dynamically organized modularity in the yeast protein–protein interaction network. *Nature*, 430(6995): 88-93. DOI: 10.1038/nature02555

He, B., Li, W., Wu, Y., Wei, F., Gong, Z., Bo, H., Wang, Y., Li, X., Xiang, B., Guo, C., Liao, Q., Chen, P., Zu, X., Zhou, M., Ma, J., Li, X., Li, Y., Li, G., Xiong, W. & Zeng, Z. (2016). Epstein-Barr virus-encoded miR-BART6-3p inhibits cancer cell metastasis and invasion by targeting long non-coding RNA LOC553103. *Cell Death and Disease,* 7(9): e2353-e235. DOI: 10.1038/cddis.2016.253

He, R., Hu, Z., Wang, Q., Luo, W., Li, J., Duan, L., Zhu, Y.S. & Luo, D.X. (2017). The role of long non-coding RNAs in nasopharyngeal carcinoma: As systemic review. *Oncotarget,* 8(9): 16075-16083. DOI: 10.18632/oncotarget.14211

Ho, K.Y., Lee, K.W., Chai, C.Y., Kuo, W.R., Wang, H.M. & Chien, C.Y. (2008*).* Early recognition of nasopharyngeal cancer in adults with only otitis media with effusion. *Journal of Otolaryngology--Head & Neck Surgery,* 37(3): 362-365. DOI: 10.2310/7070.2008.0071

Hu, N., Kadota, M., Liu, H., Abnet, C.C., Su, H., Wu, H., Freedman, N.D., Yang, H.H., Wang, C., Yan, C., Wang, L., Gere, S., Hutchinson, A., Song, G., Wang, Y., Ding, T., Qiao, Y.L., Koshiol, J., Dawsey, S.M., Giffen, C., Goldstein, A.M., Taylor, P.R. & Lee, M.P. (2016). Genomic landscape of somatic alterations in esophageal squamous cell carcinoma and gastric cancer. *Cancer Research,* 76: 1714-1723. DOI: 10.1158/0008-5472.CAN-15-0338

Hu, W., Xie, Q., Xu, Y., Tang, X. & Zhao, H. (2020). Integrated bioinformatics analysis reveals function and regulatory network of miR-200b-3p in endometriosis. *BioMed Research International*, 2020: 962953. DOI: 10.1155/2020/3962953

Huang, H.Y., Lin, Y.C.D., Li, J., Huang, K.Y., Shrestha, S., Hong, H.C., Tang, Y., Chen, Y.G., Jin, C.N., Yu, Y., Xu, J.T., Li, Y.M., Cai, X.X., Zhou, Z.Y., Chen, X.H., Pei, Y.Y., Hu, L., Su, J. J., Cui, S.D., Wang, F. Xie, Y.Y., Ding, S.Y., Luo, M.F., Chou, C.H., Chang, N.W., Chen, K.W., Cheng, Y.H., Wan, X.H., Hsu, W.L., Lee, T.Y., We, F.X. & Huang, H.D. (2020). miRTarBase 2020: updates to the experimentally validated microRNA–target interaction database. *Nucleic Acids Research*, 48(D1): D148-D154. DOI: 10.1093/nar/gkz896

Huang, W.Y., Lin, C.C., Jen, Y.M., Lin, K.T., Yang, M.H., Chen, C.M., Chang, Y.N., Sung, F.C. & Kao, C.H. (2012). Association between adult otitis media and nasopharyngeal cancer: a nationwide population-based cohort study. *Radiotherapy and Oncology*, 104(3): 338-342. DOI: 10.1016/j.radonc.2012.08.015

Jiang, C., Li, L., Xiang, Y.Q., Lung, M.L., Zeng, T., Lu, J., Tsao, S.W., Zeng, M.S., Yun, J.P., Kwong, D.L.W. & Guan, X. Y. (2020). Epstein–Barr Virus miRNA BART2-5p Promotes Metastasis of Nasopharyngeal Carcinoma by Suppressing RND3BART2-5p Promotes Metastasis of Nasopharyngeal Carcinoma. *Cancer Research*, 80(10): 1957-1969. DOI: 10.1158/0008-5472.CAN-19-0334

Jing, J.J., Wang, Z.Y., Li, H., Sun, L.P. & Yuan, Y. (2018). Key elements involved in Epstein–Barr virus-associated gastric cancer and their network regulation. *Cancer Cell International*, 18(1): 1-12. DOI: 10.1186/s12935-018-0637-5

Johnson, J.A., Watson, J.K., Nikolić, M.Z. & Rawlins, E.L. (2018). Fank1 and Jazf1 promote multiciliated cell differentiation in the mouse airway epithelium. *Biology Open*, 7(4): bio033944. DOI: 10.1242/bio.033944

Kamiya, Y., Fujisawa, T., Katsumata, M., Yasui, H., Suzuki, Y., Karayama, M., Hozumi, H., Furuhashi, K., Enomoto, N., Nakamura, Y., Inui, N., Setou, M., Itom M., Suzuki, T., Koji, I. & Suda, T. (2020). Influenza A virus enhances ciliary activity and mucociliary clearance via TLR3 in airway epithelium. *Respiratory Research*, 21(1): 1-13. DOI: 10.1186/s12931-020-01555-1

Kang, D., Skalsky, R.L. & Cullen, B.R. (2015). EBV BART microRNAs target multiple pro-apoptotic cellular genes to promote epithelial cell survival. *PLoS Pathogens,* 11(6): e1004979. DOI: 10.1371/journal.ppat.1004979

Karagkouni, D., Paraskevopoulou, M.D., Tastsoglou, S., Skoufos, G., Karavangeli, A., Pierros, V., Zacharopoulou, E. & Hatzigeorgiou, A.G. (2020). DIANA-LncBase v3: Indexing experimentally supported miRNA targets on non-coding transcripts. *Nucleic Acids Research*, 48(D1): D101-D110. DOI: 10.1093/nar/gkz1036

Kassab, M.A., Yu, L.L. & Yu, X. (2020). Targeting dePARylation for cancer therapy. *Cell and Bioscience*, 10(1): 1-9. DOI: 10.1186/s13578-020-0375-y

Kong, D., Ma, W., Zhang, D., Cui, Q., Wang, K., Tang, J., Liu, Z. & Wu, G. (2019). EYA1 promotes cell migration and tumor metastasis in hepatocellular carcinoma. *American Journal of Translational Research*, 11(4), 2328-2338.

Lee, L. & Ostrowski, L.E. (2021). Motile cilia genetics and cell biology: Big results from little mice. *Cellular and Molecular Life Sciences*, 78(3): 769-797. DOI: 10.1007/s00018-020-03633-510.1016/j.yexcr.2018.02.028

Lee, T.I. & Young, R.A. (2013). Transcriptional regulation and its misregulation in disease. *Cell*, 152(6): 1237-1251. DOI: 10.1016/j.cell.2013.02.014

Liang, W. & Sun, F. (2019). Identification of pivotal lncRNAs in papillary thyroid cancer using lncRNA–mRNA–miRNA ceRNA network analysis. *PeerJ*, 7: e7441. DOI: 10.7717/peerj.7441

Linnebacher, M., Ostwald, C., Koczan, D., Salem, T., Schneider, B., Krohn, M., Ernst, M. & Prall, F. (2013). Single nucleotide polymorphism array analysis of microsatellite-stable, diploid/near-diploid colorectal carcinomas without the CpG island methylator phenotype. *Oncology Letters*, 5: 173-178. DOI: 10.3892/ol.2012.1006

Liu, K., Kang, M., Zhou, Z., Qin, W. & Wang, R. (2019). Bioinformatics analysis identifies hub genes and pathways in nasopharyngeal carcinoma. *Oncology letters*, 18(4): 3637-3645. DOI: 10.3892/ol.2019.10707

Lung, R.W.M., Hau, P.M., Yu, K.H.O., Yip, K.Y., Tong, J.H.M., Chak, W.P., Chan, A.W., Lam, K.H., Lo, A.K., Tin, E.K., Chau, S.L., Pang, J.C., Kwan, J.S., Busson, P., Young, L.S., Yap, L.F., Tsao, S.W., To, K.F. & Lo, K.W. (2018). EBV-encoded miRNAs target ATM-mediated response in nasopharyngeal carcinoma. *The Journal of Pathology*, 244(4): 394-407. DOI: 10.1002/path.5018

Luo, Y., Wang, J., Wang, F., Liu, X., Lu, J., Yu, X., Ma, X., Peng, X. & Li, X. (2021). Foxq1 promotes metastasis of nasopharyngeal carcinoma by inducing vasculogenic mimicry via the EGFR signaling pathway. *Cell Death & Disease*, 12(5): 411. DOI: 10.1038/s41419-021-03674-z

Marttin, E., Schipper, N.G., Verhoef, J.C. & Merkus, F.W. (1998). Nasal mucociliary clearance as a factor in nasal drug delivery. *Advanced Drug Delivery Reviews*, 29(1-2): 13-38. DOI: 10.1016/S0169-409X(97)00059-8

Matsune, S., Sando, I. & Takahashi, H. (1992). Distributions of eustachian tube goblet cells and glands in children with and without otitis media. *Annals of Otology, Rhinology & Laryngology*, 101(9): 750-754. DOI: 10.1177/000348949210100

Mayo Clinic. (2022). *Tinnitus*. [online] Available at: https://www.mayoclinic.org/diseases-conditions/tinnitus/symptoms_causes/syc_20350156#:~:text=Your%20ear%20canals%20can%20become,brain%20function%20linked%20to%20hearing. [Accessed on 27 May 2023].

Miao, W.J., Yuan, D.J., Zhang, G.Z., Liu, Q., Ma, H.M. & Jin, Q.Q. (2019). lncRNA CASC2/miR-18a-5p axis regulates the malignant potential of nasopharyngeal carcinoma by targeting RBBP8. *Oncology Reports*, 41(3): 1797-1806. DOI: 10.3892/or.2018.6941

Mohseni, M., Cidado, J., Croessmann, S., Cravero, K., Cimino-Mathews, A., Wong, H.Y., Scharpf, R., Zabransky, D.J., Abukhdeir, A.M., Garay, J.P., Wang, G.M., Beaver, J.A., Cochran, R.L., Blair, B.G., Rosen, D.M., Erlanger, B., Argani, P., Hurley, P.J., Lauring, J. & Park, B.H. (2014). MACROD2 overexpression mediates estrogen independent growth and tamoxifen resistance in breast cancers. *Proceedings of the National Academy of Science U.S.A*, 111: 17606-17611. DOI: 10.1073/pnas.1408650111

Moore, A.C., Winkjer, J.S. & Tseng, T.T. (2015). Bioinformatics resources for microRNA discovery. *Biomarker Insights*, 10(Suppl 4): 53-58. DOI: 10.4137/BMI.S29513

Nakanishi, Y., Wakisaka, N., Kondo, S., Endo, K., Sugimoto, H., Hatano, M., Ueno, T., Ishikawa, K. & Yoshizaki, T. (2017). Progression of understanding for the role of Epstein-Barr virus and management of nasopharyngeal carcinoma. *Cancer Metastasis Review*, 36(3): 435–447. DOI: 10.1007/s10555-017-9693-x

National Center for Biotechnology Information. (2024). *About GEO2R.* [online] Available at: https://www.ncbi.nlm.nih.gov/geo/info/geo2r.html#:~:text=Summary%20statistics,-RNA%2Dseq%3A&text=GEO2R%20uses%20the%20Wald%20test,or%20more%20groups%20of%20Samples.&text=P%2Dvalue%20after%20adjustment%20for,by%20which%20to%20interpret%20results. [Accessed on 25 May 2023].

Nikpour, P., Emadi-Baygi, M., Emadi-Andani, E. & Rahmati, S. (2014). EYA1 expression in gastric carcinoma and its association with clinicopathological characteristics: a pilot study. *Medical Oncology*, 31(5): 1-5. DOI: 10.1007/s12032-014-0955-y

Nowsheen, S., Aziz, K., Luo, K., Deng, M., Qin, B., Yuan, J., Jeganathan, K.B., Yu, J., Zhang, H., Ding, W., van Deursen, J.M. & Lou, Z. (2018). ZNF506-dependent positive feedback loop regulates H2AX signaling after DNA damage. *Nature Communications*, 9(1): 1-11. DOI: 10.1038/s41467-018-05161-0

Permyakov, E.A. (2021). Metal binding proteins. *Encyclopedia*, 1(1): 261-292. DOI: 10.3390/encyclopedia1010024

Png, Y.T., Yang, A.Z.Y., Lee, M.Y., Chua, M.J.M. & Lim, C.M. (2021). The role of NK cells in EBV infection and EBV-associated NPC. *Viruses*, 13(2): 300. DOI: 10.3390/v13020300

Plieskatt, J.L., Rinaldi, G., Feng, Y., Levine, P.H., Easley, S., Martinez, E., Hashmi, S., Sadeghi, N., Brindley, P.J., Bethony, J.M. & Mulvenna, J.P. (2014). Methods and matrices: approaches to identifying miRNAs for Nasopharyngeal carcinoma. *Journal of Translational Medicine*, 12(1): 1-20. DOI: 10.1186/1479-5876-12-3

Poh, S.S., Chua, M.L.K. & Wee, J.T. (2016). Carcinogenesis of nasopharyngeal carcinoma: an alternate hypothetical mechanism. *Chinese Journal of Cancer*, 35(1): 1-9. DOI: 10.1186/s40880-015-0068-9

Qin, X., Zhang, J., Lin, Y., Sun, X.M., Zhang, J.N. & Cheng, Z.Q. (2020). Identification of MiR-211-5p as a tumor suppressor by targeting ACSL4 in Hepatocellular Carcinoma. *Journal of Translational Medicine*, 18: 1-13. DOI: 10.1186/s12967-020-02494-7

Rao, M.S., Van Vleet, T.R., Ciurlionis, R. & Blomme, E.A. (2019). Comparison of RNA-Seq and microarray gene expression platforms for the toxicogenomic evaluation of liver from short-term rat toxicity studies. *Frontiers in Genetics*, 9: 425202. DOI: 10.3389/fgene.2018.00636

Rashid, S., Breckle, R., Hupe, M., Geisler, S., Doerwald, N. & Neesen, J. (2006). The murine Dnali1 gene encodes a flagellar protein that interacts with the cytoplasmic dynein heavy chain 1. *Molecular Reproduction and Development: Incorporating Gamete Research*, 73(6): 784-794. DOI: 10.1002/mrd.20475

Ringers, C., Olstad, E.W. & Jurisch-Yaksi, N. (2020). The role of motile cilia in the development and physiology of the nervous system. *Philosophical Transactions of the Royal Society B*, 375(1792): 20190156. DOI: 10.1098/rstb.2019.0156

Ross, N., Gandhi, M.K. & Nourse, J.P. (2013). The Epstein-Barr virus microRNA BART11-5p targets the early B-cell transcription factor EBF1. *American Journal of Blood Research*, 3(3): 210-224.

Sadatomi, D., Tanimura, S., Ozaki, K.I. & Takeda, K. (2013). Atypical protein phosphatases: emerging players in cellular signaling. *International Journal of Molecular Sciences*, 14(3): 4596-4612. DOI: 10.3390/ijms14034596

Sakthianandeswaren, A., Parsons, M.J., Mouradov, D., Mackinnon, R.N., Catimel, B., Liu, S., Palmieri, M., Love, C., Jorissen, R.N., Li, S., Whitehead, L., Putoczki, T.L., Preaudet, A., Tsui, C., Nowell, C.J., Ward, R.L., Hawkins, N.J., Desai, J., Gibbs, P., Ernst, M., Street, I., Buchert, M. & Sieber, O. M. (2018). Macrod2 haploin sufficiency impairs catalytic activity of PARP1 and Promotes chromosome instability and growth of intestinal tumors. *Cancer Discovery*, 8: 988-1005. DOI: 10.1158/2159-8290.CD-17-0909

Salmena, L., Poliseno, L., Tay, Y., Kats, L. & Pandolfi, P.P.A (2011). ceRNA hypothesis: The Rosetta Stone of a hidden RNA language? *Cell*, 146(3): 353-358. DOI: 10.1016/j.cell.2011.07.014

Sarwari, N.M., Khoury, J.D. & Hernandez, C.M.R. (2016). Chronic Epstein Barr virus infection leading to classical Hodgkin lymphoma. *BMC Hematology*, 16(1): 1-6. DOI: 10.1186/s12878-016-0059-3

Searight, F.T., Singh, R. & Peterson, D.C. (2022). *Otitis Media with Effusion.* [e-book] Treasure Island: StatPearls Publishing. Available through: https://www.ncbi.nlm.nih.gov/books/NBK538293/ [Accessed on 27 May 2023].

Skalsky, R.L. & Cullen, B.R. (2010). Viruses, microRNAs, and host interactions. *Annual Review*

Microbiology, 64: 123-141. DOI: 10.1146/annurev.micro.112408.134243

Song, M.H., Kwon, T.J., Kim, H.R., Jeon, J.H., Baek, J.I., Lee, W.S., Kim, U.K. & Choi, J. Y. (2013). Mutational analysis of EYA1, SIX1 and SIX5 genes and strategies for management of hearing loss in patients with BOR/BO syndrome. *PLoS One,* 8(6): e67236. DOI: 10.1371/journal.pone.0067236

Song, Y., Li, X., Zeng, Z., Li, Q., Gong, Z., Liao, Q., Li, X., Chen, P., Xiang, B., Zhang, W., Xiong, F., Zhou, Y., Zhou, M., Ma, J., Li, Y., Chen, X., Li, G. & Xiong, W. (2016). Epstein-Barr virus encoded miR-BART11 promotes inflammation-induced carcinogenesis by targeting FOXP1. *Oncotarget,* 7(24): 36783. DOI: 10.18632/oncotarget.9170

Su, Z.Y., Siak, P.Y., Leong, C.O. & Cheah, S.C. (2023). The role of Epstein–Barr virus in nasopharyngeal carcinoma. *Frontiers in Microbiology,* 14: 1116143. DOI: 10.3389/fmicb.2023.1116143

Tan, Y., Jiang, C., Jia, Q., Wang, J., Huang, G. & Tang, F. (2022). A novel oncogenic seRNA promotes nasopharyngeal carcinoma metastasis. *Cell Death & Disease*, 13(4): 401. DOI: 10.1038/s41419-022-04846-1

Tabuchi, K., Nakayama, M., Nishimura, B., Hayashi, K. & Hara, A. (2011). Early detection of nasopharyngeal carcinoma. *International Journal of Otolaryngology,* 2011: 638058. DOI: 10.1155/2011/638058

Tadjuidje, E., Wang, T.S., Pandey, R.N., Sumanas, S., Lang, R.A. & Hegde, R.S. (2012). The EYA tyrosine phosphatase activity is pro-angiogenic and is inhibited by benzbromarone. *PLoS One*, 7(4): e34806. DOI: 10.1371/journal.pone.0034806

Tang, J., Kong, D., Cui, Q., Wang, K., Zhang, D., Yuan, Q., Liao, X., Gong, Y. & Wu, G. (2018). Bioinformatic analysis and identification of potential prognostic microRNAs and mRNAs in thyroid cancer. *PeerJ,* 6: e4674. DOI: 10.7717/peerj.4674

Tang, J.F., Yu, Z.H., Liu, T., Lin, Z.Y., Wang, Y.H., Yang, L.W., He, H.J., Huang, H.L. & Liu, G. (2014). Five miRNAs as novel diagnostic biomarker candidates for primary nasopharyngeal carcinoma. *Asian Pacific Journal of Cancer Prevention,* 15(18): 7575-7581. DOI: 10.7314/apjcp.2014.15.18.7575

Teleanu, R.I., Chircov, C., Grumezescu, A.M. & Teleanu, D.M. (2019). Tumor angiogenesis and anti-angiogenic strategies for cancer treatment. *Journal of Clinical Medicine,* 9(1): 84. DOI:doi.org/10.3390/jcm9010084

Tian, X., Liu, Y., Wang, Z. & Wu, S. (2021). miR-144 delivered by nasopharyngeal carcinoma-derived EVs stimulates angiogenesis through the FBXW7/HIF-1α/VEGF-A axis. *Molecular Therapy-Nucleic Acids,* 24: 1000-1011. DOI: 10.1016/j.omtn.2021.03.016

Tsao, S.W., Tsang, C.M. & Lo, K.W. (2017). Epstein-Barr virus infection and nasopharyngeal carcinoma. *Philosophical Transactions of the Royal Society B: Biological Sciences,* 372(1732): 20160270. DOI: 10.1098/rstb.2016.0270

Tsunoda, A., Suzuki, M., Kishimoto, S., Anzai, T., Matsumoto, F., Ikeda, K. & Terasaki, O. (2021). Otitis media with effusion caused by a parapharyngeal tumor showing normal nasopharyngeal findings. *Ear, Nose & Throat Journal,* 100(7): 543-545. DOI: 10.1177/0145561319881513

Utama, D.S., Ralahayu, P. & Bahar, E. (2022). Relationship between primary tumors of nasopharyngeal carcinoma with the degree of conductive hearing loss in Dr. Mohammad Hoesin Hospital Palembang. *Bioscientia Medicina: Journal of Biomedicine and Translational Research,* 6(3): 1423-1434. DOI: 10.37275/bsm.v6i3.453

Wang, K.H., Austin, S.A., Chen, S.H., Sonne, D.C. & Gurushanthaiah, D. (2017). Nasopharyngeal carcinoma diagnostic challenge in a nonendemic setting: Our experience with 101 patients. *Permanente Journal,* 21(3): 16-180. DOI: 10.7812/TPP/16-180

Wang, Y., Zhang, Y. & Ma, S. (2013). Racial differences in nasopharyngeal carcinoma in the United States. *Cancer Epidemiology,* 37(6): 793-802. DOI: 10.1016/j.canep.2013.08.008

Wong, T.S., Chen, S., Zhang, M.J., Chan, J.Y.W. & Gao, W. (2018). Epstein-Barr virus-encoded microRNA BART7 downregulates major histocompatibility complex class I chain-related peptide A and reduces the cytotoxicity of natural killer cells to nasopharyngeal carcinoma. *Oncology Letters,* 16(3): 2887-2892. DOI: 10.3892/ol.2018.9041

van den Broek, E., Dijkstra, M.J., Krijgsman, O., Sie, D., Haan, J.C., Traets, J.J., van de Wiel, M.A., Nagtegaal, I.D., Punt, C.J., Carvalho, B., Ylstra,

B., Abeln, S., Meijer, G.A. & Fijneman, R.J. (2015). High prevalence and clinical relevance of genes affected by chromosomal breaks in colorectal cancer. *PLoS One,* 10(9): e0138141. DOI: 10.1371/journal.pone.0138141

Vig, A., Poulter, J.A., Ottaviani, D., Tavares, E., Toropova, K., Tracewska, A.M., Mollica, A., Kang, J., Kehelwathugoda, O., Paton, T., Maynes, J.T., Wheway, G., Arno, G., Khan, K.N., McKibbin, M., Toomes, C., Ali, M., Scipio, M.D., Li, S., Ellingford, J., Black, G., Webster, A., Rydzanicz, M., Stawiński, P., Ploski, R., Vincent, A., Cheetham, M.E., Inglehearn, C.F., Roberts, A. & Heon, E. (2020). DYNC2H1 hypomorphic or retina-predominant variants cause nonsyndromic retinal degeneration. *Genetics in Medicine,* 22(12), 2041-2051. DOI: 10.1038/s41436-020-0915-1

Vilagos, B., Hoffmann, M., Souabni, A., Sun, Q., Werner, B., Medvedovic, J., Bilic, I., Minnich, M., Axelsson, E., Jaritz, M. & Busslinger, M. (2012). Essential role of EBF1 in the generation and function of distinct mature B cell types. *Journal of Experimental Medicine,* 209(4): 775-792. DOI: 10.1084/jem.20112422

Xing, B., Qiao, X.F., Qiu, Y.H. & Li, X. (2021). TMPO-AS1 regulates the aggressiveness-associated traits of nasopharyngeal carcinoma cells through sponging miR-320a. *Cancer Management and Research,* 13: 415-425. DOI: 10.2147/CMAR.S285113

Xu, Y. & Fisher, G.J. (2012). Receptor type protein tyrosine phosphatases (RPTPs)–roles in signal transduction and human disease. *Journal of Cell Communication and Signaling,* 6(3): 125-138. DOI: 10.1007/s12079-012-0171-5

Xu, Y., Huang, X., Ye, W., Zhang, Y., Li, C., Bai, P., Lin, Z. & Chen, C. (2020). Comprehensive analysis of key genes associated with ceRNA networks in nasopharyngeal carcinoma based on bioinformatics analysis. *Cancer Cell International,* 20: 408. DOI: 10.1186/s12935-020-01507-1

Yan, X., Liu, X.P., Guo, Z.X., Liu, T.Z. & Li, S. (2019). Identification of hub genes associated with progression and prognosis in patients with bladder cancer. *Frontiers in Genetics,* 10: 408. DOI: 10.3389/fgene.2019.00408

Yang, J.H., Li, J.H., Shao, P., Zhou, H., Chen, Y.Q. & Qu, L.H. (2011). starBase: a database for exploring microRNA–mRNA interaction maps from Argonaute CLIP-Seq and Degradome-Seq data. *Nucleic Acids Research,* 39(suppl_1): D202-D209. DOI: 10.1093/nar/gkq105

Yang, Y., Liu, W., Zhang, Y., Wu, S. & Luo, B. (2019). Integrated analysis of the miRNA-mRNA network associated with LMP1 gene in nasopharyngeal carcinoma. *bioRxiv,* 615237. DOI: 10.1101/615237

Yao, J., Chen, X., Liu, X., Li, R., Zhou, X., & Qu, Y. (2021). Characterization of a ferroptosis and iron-metabolism related lncRNA signature in lung adenocarcinoma. *Cancer Cell International,* 21(1): 1-14. DOI: 10.1186/s12935-021-02027-2

Ye, Z., Wang, F., Yan, F., Wang, L., Li, B., Liu, T., Hu, F., Jiang, M., Li, W. & Fu, Z. (2019). Bioinformatic identification of candidate biomarkers and related transcription factors in nasopharyngeal carcinoma. *World Journal of Surgical Oncology,* 17(1): 1-10. DOI: 10.1186/s12957-019-1605-9

Žaja, R., Aydin, G., Lippok, B.E., Feederle, R., Lüscher, B. & Feijs, K.L.H. (2020). Comparative analysis of MACROD1, MACROD2 and TARG1 expression, localisation and interactome. *Scientific Reports,* 10(1): 8286. DOI: 10.1038/s41598-020-64623-y

Zhang, T., Chen, Z., Deng, J., Xu, K., Che, D., Lin, J., Jiang, P., Gu, X. & Xu, B. (2022). Epstein–Barr virus-encoded microRNA BART22 serves as novel biomarkers and drives malignant transformation of nasopharyngeal carcinoma. *Cell Death & Disease,* 13(7): 1-14. DOI: 10.1038/s41419-022-05107-x

Zhang, Q., Luo, D., Xie, Z., He, H. & Duan, Z. (2020). The oncogenic role of miR-BART19-3p in Epstein-Barr virus-associated Diseases. *BioMed Research International,* 2020: 5217039. DOI: 10.1155/2020/5217039

Zhang, S., Yue, W., Xie, Y., Liu, L., Li, S., Dang, W., Xin, S., Yang, L., Zhai, X., Cao, P. & Lu, J. (2019). The four-microRNA signature identified by bioinformatics analysis predicts the prognosis of nasopharyngeal carcinoma patients. *Oncology Reports,* 42(5): 1767-1780. DOI: 10.3892/or.2019.7316

Zhong, Y., Zhu, Y., Dong, J., Zhou, W., Xiong, C., Xue, M., Shi, M. & Chen, H. (2019). Identification of key transcription factors AP-1 and AP-1-Dependent miRNAs forming a co-regulatory network controlling PTEN in liver ischemia/reperfusion injury. *BioMed Research International*, 2019: 962682. DOI: 10.1155/2019/8962682

Zhou, R.S., Zhang, E.X., Sun, Q.F., Ye, Z.J., Liu, J.W., Zhou, D.H. & Tang, Y. (2019). Integrated analysis of lncRNA-miRNA-mRNA ceRNA

network in squamous cell carcinoma of tongue. *BMC Cancer*, 19(1): 1-10. DOI: 10.1186/s12885-019-5983-8

Zhou, J., Zhang, B., Zhang, X., Wang, C. & Xu, Y. (2022). Identification of a 3-miRNA signature associated with the prediction of prognosis in nasopharyngeal carcinoma. *Frontiers in Oncology*, 11: 5969. DOI: 10.3389/fonc.2021.823603

Zhu, X., Jiang, L., Yang, H., Chen, T., Wu, X. & Lv, K. (2020). Analyzing the lncRNA, miRNA, and mRNA-associated ceRNA networks to reveal potential prognostic biomarkers for glioblastoma multiforme. *Cancer Cell International*, 20(1): 1-12. DOI: 10.1186/s12935-020-01488-1

Zhu, J.Y., Pfuhl, T., Motsch, N., Barth, S., Nicholls, J., Grässer, F. & Meister, G. (2009). Identification of novel Epstein-Barr virus microRNA genes from nasopharyngeal carcinomas. *Journal of Virology*, 83(7): 3333-3341. DOI: 10.1128/JVI.01689-08

Zingoni, A., Molfetta, R., Fionda, C., Soriani, A., Paolini, R., Cippitelli, M., Cerboni, C. & Santoni, A. (2018). NKG2D and its ligands: "One for all, all for one". *Frontiers in Immunology*, 9: 476. DOI: 10.3389/fimmu.2018.00476

Zuazo-Gaztelu, I. & Casanovas, O. (2018). Unraveling the role of angiogenesis in cancer ecosystems. *Frontiers in Oncology*, 8: 248. DOI: 10.3389/fonc.2018.00248

Borneo Journal of Resource Science and Technology (2024), 14(1): 54-68
DOI: https:doi.org/10.33736/bjrst.6108.2024

Physicochemical Investigation and Analysis of Nypa Sap (*Nypa fruticans* Wurmb) using a Novel Collecting Device

ANA SAKURA ZAINAL ABIDIN[1], HANIF MOHD TEDDY[2], MOHD RAZIP ASARUDDIN[2], MOHD ZULHATTA KIFLI[1], RASLI MUSLIMEN[1], MARINI SAWAWI[1], ABANG AHMAD DZULFAKHRI[1], KASYFUL AZHIM YUSSOF[1], FREDY MUHAMAD FIRDAUS[1], & KHAIRUL FIKRI TAMRIN[1*]

[1]Faculty of Engineering, Universiti Malaysia Sarawak, 94300 Kota Samarahan, Sarawak, Malaysia, [2]Faculty of Resource Science and Technology, Universiti Malaysia Sarawak, 94300 Kota Samarahan, Sarawak, Malaysia
*Corresponding author: tkfikri@unimas.my
Received: 2 October 2023 Accepted: 29 April 2024 Published: 30 June 2024

ABSTRACT

A sweetener from *Nypa fruticans* Wurmb offers significant health benefits. The traditional process of sap tapping requires careful attention to enhance cleanliness. In this research, a nypa sap harvesting device has been developed, and a time study for its installation has been conducted. The physicochemical properties of the sap gathered from the device were evaluated and compared with the traditional method in terms of total soluble solids(TSS) reading, pH level, total dissolved solid (TDS) and electrical conductivity (EC) value, and glucose content. Both methods showed no significant difference, with an average TSS reading of 14 to 15 °brix, pH of 3.57-3.97, glucose content of 25.9 to 32.4, TDS of 2340-2726 ppm, and EC reading of 4679-5472 µs/cm. Slight differences in physicochemical properties were observed due to the random selection of trees for the experiment. The use of the device was found to improve the physical cleanliness of the sap by 97% and chemical purity by 7% to 11%. The colour of the sap collected with the device was milky white compared to the traditional bamboo method, resulting in a yellowish-white sap. The time study showed a 40% improvement compared to the first trial, indicating the practicality of the device, which can be easily installed by the operator. The physicochemical properties of the sap collected using the device can be further improved with the addition of preservatives. The findings are expected to enhance sap harvesting hygiene and the quality of sap, directly affecting the quality and benefits of the derived products.

Keywords: Agrotechnology, collecting device, nypa sap, physicochemical

INTRODUCTION

Sugar is a primary ingredient in most food and beverages. However, diets high in sugar can contribute to chronic, long-term health conditions that can lead to diabetes and obesity. As consumer awareness about health increases, there is a growing demand for healthier and organic sweeteners as an alternative to commercial table sugar (Reed & McDaniel, 2006. In particular, the European market is willing to pay a premium price for such sweeteners. However, entry into the European market is not easy, as all products must meet the food production standards imposed by the European Commission (Somorin *et al*., 2021).

Nypa fruticans Wurmb is a type of palm tree that can be found abundantly in muddy soils along rivers. It forms extensive stands in brackish to tidal freshwater, demonstrating wide ecological tolerance. In terms of chemical composition, nypa sugar contains less reducing sugar than table sugar (Radam *et al*., 2014). The presence of sugar in nypa sap can have an adverse effect due to the hydrolysis of sucrose into glucose and alkaline invertase enzymes that consequently ferment and deteriorate the sap and its derived products (Tamunaidu & Saka, 2012; Sainz-Polo *et al*., 2013). Nypa sugar, made from nypa sap, is the main source of income for communities in Kampung Tambirat Kota Samarahan, Sarawak, Malaysia. In Sarawak, the community still produces the sweetener using a traditional method by which the sap is extracted through a tapping process by chopping off the thin palm inflorescence. A traditional bamboo container, as shown in Figure 1, is used to store the nypa sap during the overnight collection process. However, this method is deemed

unclean as the collected sap is exposed to foreign particles such as insects, rodents, dust, pollen, rainwater and other debris that can contaminate the sap (Madigal, 2020).

Figure 1. Nypa sap collection vessel using a traditional bamboo container

In order to meet the premium market requirements, such as those in Europe, traditional sugar producers in Sarawak would need to improve the cleanliness standards of the nypa palm production process. The sap harvesting process is particularly critical in production. Therefore, a device has been developed to enhance the cleanliness level while maintaining the sap quality.

Experiments and a series of analyses have been conducted to validate the performance of the developed nypa sap collecting device. Due to the nature of nypa sap, which hydrolyses immediately after collection, on-site total sugar determination is essential. On-site sugar analysis by brix and inverted sugar measurement using a portable refractometer and glucometer was established in this study as a quick and simple analytical on-site method based on the settings by Tamunaidu & Saka (2012).

MATERIALS AND METHODS:

The development of the collecting device involved basic studies of nypa plant anatomy and physiology. The study focused on nypa trees located at Kampung Tambirat, Sarawak, Malaysia (Coordinate: 1.551554 DD, 110.509297 DD). Accuracy was crucial to ensure the device fit perfectly, preventing any foreign substances from contaminating the sap. The dimensions of the nypa stalk diameter were measured at three positions – the tip, middle and end of the stalk (within its sap-producing capacity) using a Vernier caliper, as illustrated in Figure 2.

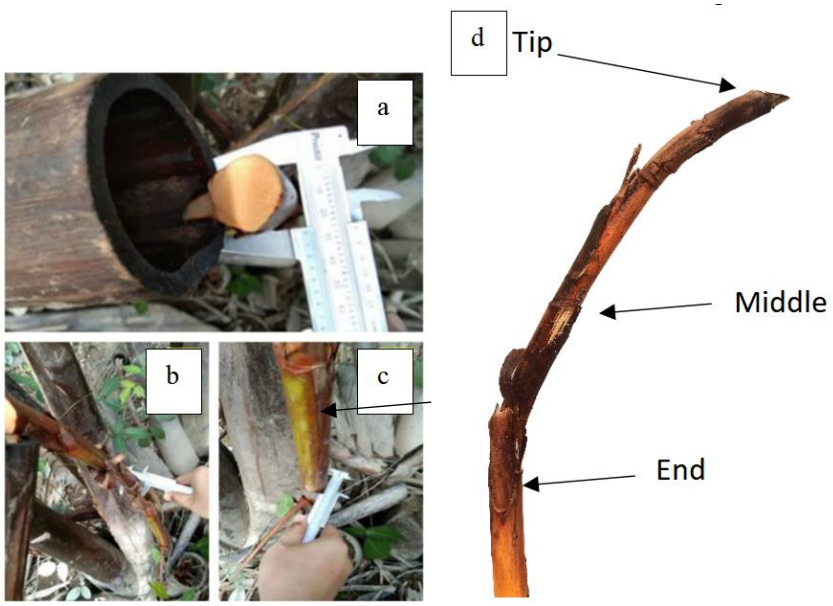

Figure 2. Diameter measurement of the tip (a), middle (b), and end (c) parts of the nypa palm stalk, along with a schematic diagram of the measurement process (d)

On-site experiments were conducted to verify the functionality of the developed nypa sap collecting device. The experiments were carried out at Kampung Tambirat in Kota Samarahan, Sarawak, Malaysia, on three different dates: 15th April 2022 (Time: 1700 hrs, Atmospheric Condition: Cloudy, Temperature: 30 ℃, Humidity: 85%, Wind Speed (mph): 5.6NW), 18th May 2022 (Time: 1700 hrs, Atmospheric Condition: Cloudy, Temperature: 30 ℃, Humidity: 77%, Wind Speed (mph): 5.8E), and 24th May 2022 (Time: 1700 hrs, Atmospheric Condition: Clear, Temperature: 32 ℃, Humidity: 81%, Wind Speed (mph): 5.8NW). Ten nypa trees were randomly chosen on each date, resulting in a total of 30 sets of data in total (3 days x 10 trees), along with three control data sets (3 trees). The assembly drawing of the nypa sap collecting device is shown in Figure 3, and details of the components, materials and functions are summarised in Table 1.

Table 1. Components of nypa sap collecting device, materials and functions

No	Part	Material	Function
1	Netting-cap	PVC	• To prevent insects/rodents from entering the assembly • To equalize inside assembly temperature with ambient
2	Chamber	PET	• Main body: encloses the assembly to protect it from insects/pesticides. • Upper part; holds the net. • Hole; provides access for the gripper to the chamber. • End part; supports and secure casing position to the tapped stalk
3	Gripper	Food grade FDA Silicone	• To attach the assembly to the nypa stalk • To prevent insects/rodents from entering the assembly via the stalk • To accommodate various diameter sizes of nypa stalk • Has a remarkable degree of elasticity and stretch
4	Plastic Bag	HDPE Food grade	• To store the dropped sap
5	Clip	Stainless Steel 304	• To lock the position of the plastic bag (4) to the casing (6) • To hold the position of the casing (6) to the stalk
6	Casing	Bamboo	• To hold the plastic bag for nypa sap storage • To protect the plastic and nypa sap from pests' attack

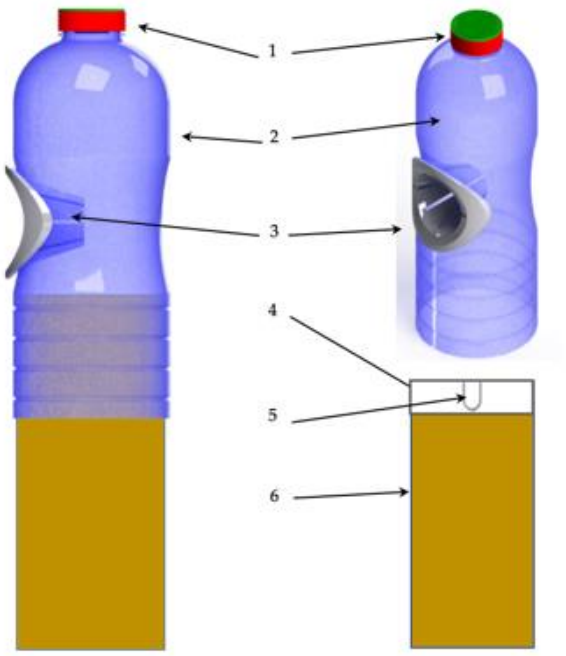

Figure 3. Assembly diagram of the nypa sap collecting device

Compounds such as polyethylene terephthalate (PET) have provided plastic bottles with several advantages such as toughness, energy savings and ease of production (Nistico, 2020). These advantages significantly contribute to the higher consumption of single-use plastic. Research by Ballerini *et al*., 2022 has found that single-use plastic bottles are the most abundant pollutant at riverbanks, posing harm to marine life, water quality, and indirectly affecting the livelihoods of fishermen (Saxena *et al*., 2022). Therefore, there is a need to educate and encourage the Apong community in Sarawak about the recycling and reuse of plastic bottles in Apong production. Furthermore, the reuse of the plastic bottle as a nypa sap collection vessel is convenient, easy to manufacture and cost-saving. Compared to glass, PET plastic bottles are lightweight (Benyathiar *et al*., 2022). Recycling plastic bottles provides significant environmental benefits, including the reduction of CO_2 emissions, mitigation of greenhouse effects, minimization of carbon footprints, and substantial savings in cost and pollution (Biron, 2017).

Time Study

A time study was conducted to determine the installation duration of the nypa sap collection device in a real-world environment. The identified traditional nypa sap tapper was provided with brief training prior to the experiment. The time study consisted of three primary processes, as summarised in Table 2, and the installation process and setup of the nypa sap collecting device are depicted in Figure 4.

Table 2. Installation process and description of the nypa sap collecting device

Process	Description
1.	Beat the inflorescence stalk.
2.	Scrape off the nypa stalk tip.
3.	Attach the gripper to the stalk (Item No. 3 in Table 1) follow by the chamber (Item No. 2 in Table 1).
4.	Place the plastic on the bamboo and secure the assembly with clips or string.
5.	Insert the bamboo from Step 4 into the chamber (Item No. 2 from Table 1).
6.	Sap collection (the following day): Remove the plastic from the bamboo (in Step 4) and tie it up.

Figure 4. Installation process and setup of nypa sap collecting device

A stopwatch was used to measure the time taken for each process, and the results were recorded. Steps 1 through 5 were executed consecutively, one after the other. Subsequently, the assembly was left overnight to allow for the accumulation of nypa sap droplets. Step 6 was

performed the following morning for sap collection. The time taken to remove and tie up the plastic from the assembly was also recorded, with all plastic samples appropriately labelled. Meanwhile, the installation of the traditional process (control) involved a similar procedure for nypa sap collection. Following a 16-hour period, the sap was harvested for analysis.

Collected Nypa Sap Profile and Physicochemical Properties

The collected sap from the time study was transported to the laboratory at Universiti Malaysia Sarawak, which is located approximately 30 minutes from Kampung Tambirat. The samples were stored in a cooler box filled with ice cubes to maintain a temperature of 20 °C and to slow down the fermentation process. Subsequently, all samples were subjected to a series of analyses to check for impurities, and to determine total soluble solids (TSS), pH, total dissolved solids (TDS), electrical conductivity (EC) and glucose content. The following procedures were followed for the analyses:

a) Impurities and colour observation

The sap samples were placed in glass bottles and labelled accordingly. The colour of the sap was observed and compared with each other using the naked eye. Drops of sap from each sample were examined under the LED Lab Trinocular Compound Microscope Model T120C to identify impurities. The microscope's magnification was set from 4X to 10X and 40X to obtain clear images. The images were saved and labelled according to the corresponding sap samples harvested from chosen nypa trees. Furthermore, the images were compared with existing literature to identify any foreign entities present in the samples.

b) Determination of TSS

The total soluble solids content of the sap was determined as °brix using a handheld refractometer. The refractometer measured the refractive index of the liquid (Sulaiman *et al*., 2020).A drop of the collected nypa sap was placed on the refractometer's sample zone, and the TSS reading in °brix was recorded. The brix scale, widely utilised in the food and beverage industries, represents the percentage of sucrose content in a solution (Toledo, 2014).The correlation between °brix and sucrose content is given as follows (Elewa *et al*., 2020):

1 °brix = 1 g of sucrose/ 100 g of solution (Eq. 1)

c) Determination of pH level, TDS, and EC

In this experiment, a Hanna HI98130 Combo pH, TDS and EC meter were utilised to determine the pH, TDS and EC value, respectively, of the nypa sap. EC and TDS are distinct parameters. Typically, TDS concentration is measured in ppm, while µs represents the EC (Rusydi, 2018). The correlation between TDS and EC is determined by the characteristics and nature of the dissolved cations and anions in the water. The relationship between TDS and EC of a solution can be described as follows (Thirumalini & Joseph, 2009):

$$TDS = A \times EC \quad \text{(Eq. 2)}$$

where A is a constant that typically ranges between 0.55 and 0.9 in conductivity measurements.

The meter was calibrated before use by dipping the probe into buffer solutions of pH 7.01 and 4.01 for pH calibration. For TDS/EC calibration, the probe was immersed in a calibration solution of 12.88 ms/cm. Next, a portion of the collected nypa sap was placed in a beaker, and the probe was immersed into the nypa sap sample. The pH, TDS and EC readings were recorded. After each measurement, the probe was removed and thoroughly rinsed with distilled water to prevent cross-contamination before the next use.

d) Glucose content

Traditional laboratory methods typically require specialised equipment and trained personnel. However, the use of a glucometer is relatively inexpensive, compact and easy to use in the field. According to a study by Fundador and Calumba (2020), the glucometer was able to accurately measure the sugar content in tested fruits, with an average error of only 3.8%. The ACCU-CHEK® Instant S blood glucometer was employed to determine the glucose content of the nypa sap. The two essential components of the glucometer are the sensor (test strips) and the detector (Tonyushkina & Nichols, 2009). A drop

of sap was placed on the strip dosing area inserted in the glucometer. A chemical reaction occurred when glucose was detected, producing a small electrical current proportionate to the amount of glucose content (Yanez, 2013). The value of the glucose content of the sample appeared on the LCD screen. The glucose concentration reading in mmol/L was recorded.

RESULTS AND DISCUSSION

The results of the stalk dimensions are summarised in Table 3. The results provide important input for defining the gripper size. The data were gathered from 33 trees representing a variety of stalk conditions from different locations. The minimum stalk diameter recorded was 21.38 mm, while the maximum stalk diameter was 55 mm. The variety of stalk sizes, as well as sap production, as also influenced by the age of the nypa tree, in line with Matsui *et al*. (2014).

Table 3. Maximum, minimum, average and range of nypa palm stalk diameter

Parameter	Measurement (mm)
Maximum diameter overall	55.00
Minimum diameter overall	21.38
Range (Maximum – minimum)	33.62
Average diameter overall	32.49

As depicted in Figure 5, the nypa stalk exhibits a smaller tip diameter that gradually increases towards the bottom. This information was taken into account during the gripper design process. Figure 6 illustrates the gripper design, featuring a narrow top radius tailored to fit the minimum stalk diameter and a wider bottom radius to accommodate the maximum stalk size. The gripper incorporates several slots connected by a thin layer of material, allowing for easy tearing to adapt to a wide range of stalk diameter differences, from the smallest to the largest ones.

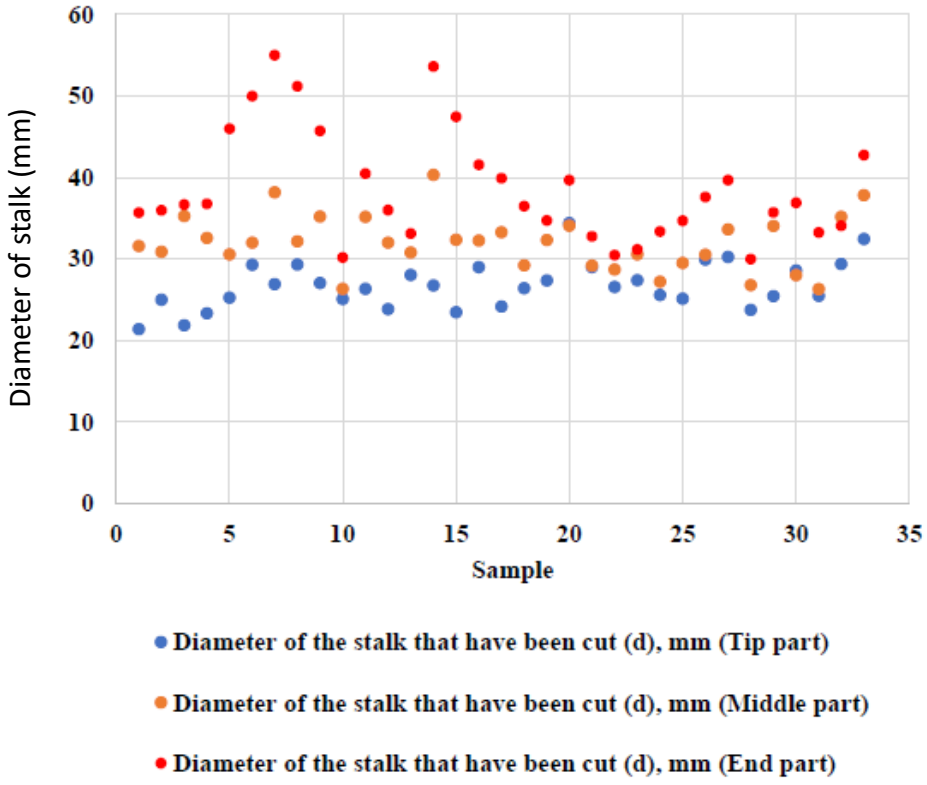

Figure 5. Tabulation of nypa palm stalk diameter at tip, middle, and end parts

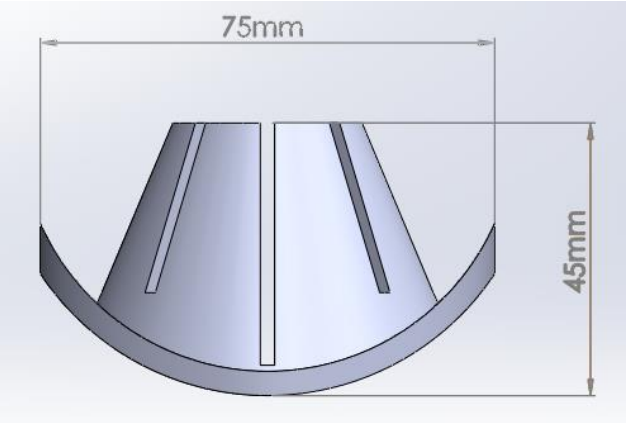

Figure 6. Gripper design of the nypa sap collecting device

As shown in Figure 5 and Table 3, the samples were randomly chosen to validate the versatility of the device, which can be adjusted to fit different stalk sizes and orientations.

Table 4 presents the volume of nypa sap collected for experiments conducted on 15th April, 18th May and 24th May 2022. Overall, the results indicate no significant difference in the techniques used to collect nypa sap (see Figure 7), except for Sample 10 from the experiment conducted on 15th April, which recorded no volume. This was due to an improperly installed collecting device that did not fit the stalk during assembly, resulting in sap dripping away from the designated storage area. Other factors that can affect nypa sap production include weather conditions, nypa tree age, stalk thickness and length, and frond diameter (Tonyushkina & Nichols, 2009; Madigal, 2020). Larger frond diameters are often associated with higher sap yields, and the best sap production is typically observed in middle-aged palms (Matsui *et al*., 2014; Nguyen *et al*., 2016).

Table 4. Volumes of collected nypa sap.

	15th April 2022	18th May 2022	24th May 2022
Sample	Volume (mL)	Volume (mL)	Volume (mL)
1	745	420	270
2	380	300	400
3	690	430	390
4	250	280	700
5	50	100	600
6	135	690	100
7	54	40	320
8	150	470	30
9	16	650	410
10	0	790	150
11	700	550	450

Time Study Results

The experiment aimed to assess the practicality of the developed device, which was measured by the time taken by the harvester to install the collecting device. Table 5 presents the average time taken to install the device by date. The total time represents the cumulative time taken for the entire process from Process 1 to Process 3. The results of the time study demonstrated a significant improvement after several repetitions. The total time taken on the third day was reduced by approximately 40% compared to the first day, resulting in a time of 49.66 seconds. This indicates that the developed device is user-friendly and practical, as the harvester becomes more accustomed to it over time.

Table 5. Time study for installation of nypa sap collecting device

Date	Process 1 (s)	Process 2 (s)	Process 3 (s)	Total time (s)
15/4/2022	23.78	36.64	21.02	80.44
18/5/2022	18.83	31.78	20.92	71.53
24/5/2022	10.74	22.12	16.8	49.66

Results of Collected Nypa Sap Profile and Physicochemical Properties

The condition of sap samples collected using the developed device (Samples 1 to 10) was compared and discussed with those collected using the traditional method using bamboo (Sample 11) to verify the performance of the developed device in comparison to the traditional method.

Impurities and Color Observation

The freshness of nypa sap is indicated by its colour, with milky-white denoting fermented sap and pale yellow indicating fresh sap (Madigal *et al*., 2020). All samples (1-11) underwent the same tapping process, lasting over 14 hours. Based on Figure 7, all samples were fermented. Upon observation, nypa sap from Samples 1-10, collected using the developed device, appeared milky-white and clean. In contrast, the sap from Sample 11, collected using bamboo, appeared yellowish-white. This is due to the bamboo used to store the sap, which has been repeatedly used, cleaned, and dried using smoke from firewood (Gunawan *et al*., 2020). Bamboo is a natural fibre material that reacts with the acidic properties of the sap, causing a yellowish colour. Moisture absorption is a natural phenomenon that occurs when using natural fibres due to their hydrophilic properties (Madigal *et al*., 2020). High-density polyethylene (HDPE) plastic, an organic material, is well-suited for nypa sap collection due to its high chemical resistance, including resistance to the acidic properties of the sap (Liu *et al*., 2018). Hence, HDPE is recommended for use in nypa sap collection.

Figure 7. Colour of nypa sap 14 hours after tapping process

Figure 8 shows images of impurities that exist in the collected sap. Samples 1 to 10 were collected using the developed device, while Sample 11 was collected using traditional bamboo (as a control). Only microbes were detected in Samples 1 to 10, with no other impurities found. However, debris or solid particles were found in Sample 11, likely due to the open-top bamboo being exposed to the environment. The sweet smell of the fresh sap attracts pests and rats, and without a cover, insects, rainwater and other solid particles (debris) can easily enter the bamboo.

The microbes observed under the microscope resemble yeast, which is consistent with previous studies. Yeast, such as *Saccharomyces cerevisiae*, is commonly found in nypa sap (Limtong *et al*., 2020). Yeast cells are oval-shaped, and their reproduction results in clusters of growing cells (Liu *et al*., 2018; Gunawan *et al*., 2020). Yeast reproduces through budding, an asexual reproduction method where a daughter cell is formed by pinching off a part of the parent cell (Monroy Salazar *et al*., 2016). These characteristics are evident in Samples 1 to 10. Nypa sap contains sugar and other compounds essential for microbial growth. Moreover, the high temperatures of the tropical climate in Sarawak, Malaysia, are conducive to microbial development (Chongkhong & Puangpee, 2018). As a result, yeast can grow rapidly, leading to the natural sugar fermentation of nypa sap.

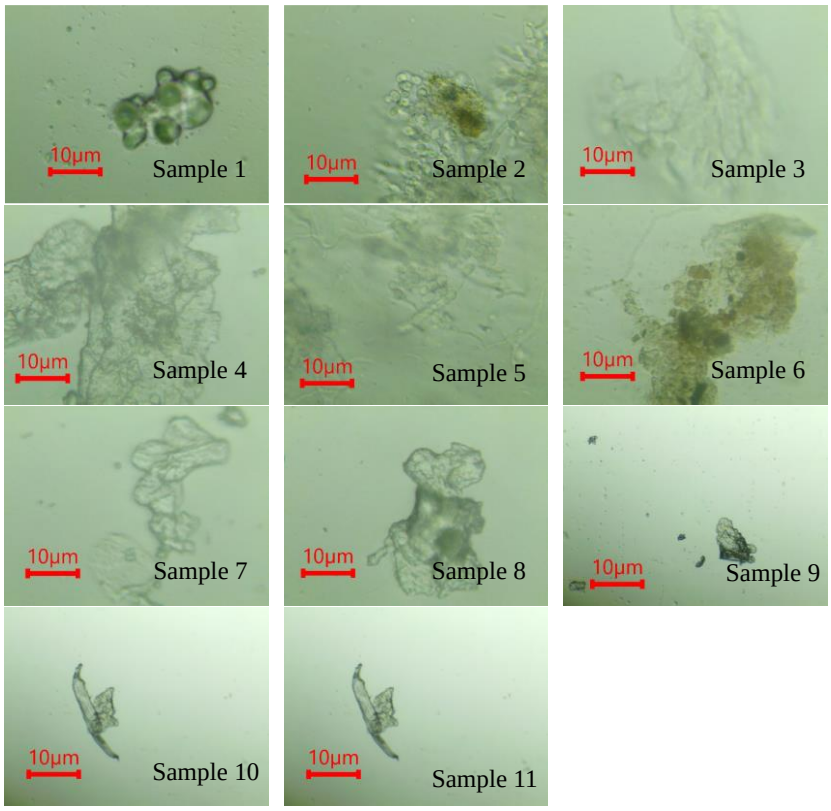

Figure 8. Microscopic observation of impurities in nypa sap samples (40× magnification)

The nypa sap collected using the developed device showed lower contamination compared to bamboo. Foreign particles, namely insects, maggots, and rat droppings, were evident in the sap collected using the traditional method, as shown in Figure 9(a). The wide open-top bamboo can be easily accessed by insects and rats. A sieve was used to filter the collected nypa sap. The accumulated foreign particles covered 1.6% of the total sieve area for the traditional method. Only a small spot (0.05%) was found on the sieve used to filter sap from the device, as shown in Figure 9(b). The tiny maggots found in the developed device were likely due to a small gap between the gripper and the nypa stalk. This occurred only in cases where the stalk had an uneven shape. Therefore, the developed device can effectively prevent insects and pests from contaminating the sap, with the exception of smaller insects measuring 2 mm and below.

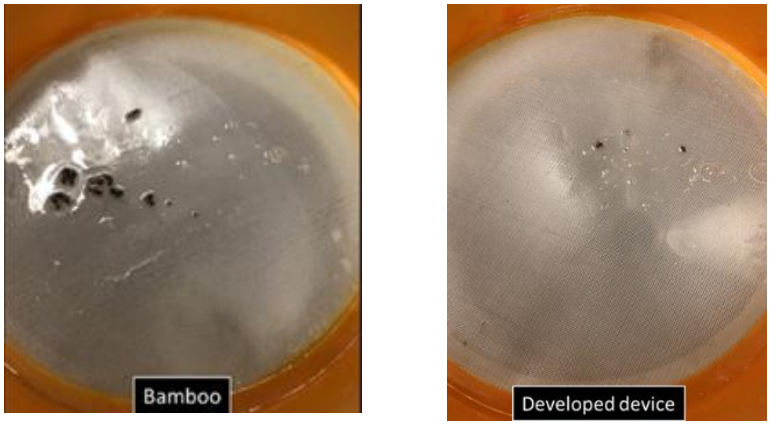

(a) (b)

Figure 9. Images of impurities collected from (a) the traditional method and (b) the developed device using a 0.08mm strainer.

Chemical Properties

Chemical properties are summarised in Table 6, 7 and 8 based on the experiment date, while comparisons between the experiments are shown in Table 9.

The TSS brix of nypa sap for Experiments 1, 2 and 3 are recorded in Tables 6 to 8, showing a range of 11–18%. Sample 11 served as a control, using bamboo for sap harvesting in Experiments 2 and 3. The TSS reading from Experiment 1 showed a lower average brix compared to Experiments 2 and 3. This is likely due to the rain that occurred on 5th April 2022, between 6 pm and 6 am in Kampung Tambirat, Sarawak, as recorded by the World Weather Online website. The sucrose content of the sap can be affected by weather conditions, with low TSS brix observed in sap collected after rainy days due to higher water content (Matsui *et al*., 2014). The results obtained in this research are mostly within the range reported in other studies from Indonesia, which ranged from 15-17 °brix, but lower than that of Thailand, which reported 22.9 °brix (Rachman & Sudarto, 1995; Phetrit *et al*., 2020). It is worth noting that Thai practitioners add kiam (*Cotylelobium lanceolatum Craib*) as a preservative in nypa sap to retard the fermentation process.

Tables 6 to 8 show the pH values for each sample collected throughout the experiments. There is no significant difference in pH between nypa sap collected using bamboo and the developed device. All samples were acidic, with pH values ranging between 3.35 and 4.34. These readings are within the range of 3.18 - 4.20 reported in another study (Semjonovs *et al*., 2014). The acidic pH indicates that the nypa sap has undergone fermentation. This is likely due to the long harvesting duration, which took overnight (about 17 to 18 hours) before undergoing the cooking process. Initially, the pH of fresh nypa sap is neutral, but gradually the acidity increases and the pH decreases as fermentation occurs (Tamunaidu & Saka, 2012).

Table 6. Chemical properties of nypa sap from Experiment 1 (15th April 2022).

Sample	brix (%)	pH	Glucose (mmol/L)	TDS (PPM)	EC (Us/cm)
1	12	3.44	21.60	2468	4936
2	12	3.44	28.60	2401	4802
3	13	3.89	27.20	2531	5062
4	12	3.44	29.70	2292	4584
5	11	3.35	26.90	2105	4210
6	16	4.34	32.60	2844	5688
7	16	4.07	31.40	2633	5266
8	12	3.44	27.10	2186	4372
9	13	3.80	28.40	2468	4936
10	12	3.44	27.10	2468	4936
11	13	3.70	28.00	2374	4748

Table 7. Chemical properties of nypa sap from Experiment 2 (18th May 2022).

Sample	brix (%)	pH	Glucose (mmol/L)	TDS (PPM)	EC (Us/cm)
1	13	3.53	31.10	2842	5684
2	15	3.71	H1	2330	4660
3	12	3.53	30.20	2478	4956
4	13	3.44	H1	2472	4944
5	16	3.89	H1	2872	5744
6	14	3.53	32.10	2419	4838
7	15	3.35	H1	2707	5414
8	16	3.71	32.90	2504	5008
9	13	3.44	H1	2201	4402
10	13	3.53	31.60	2671	5342
11	15	3.62	30.10	2726	5472

*H1 indicates that the value is greater than 33.30 mmol/L
(The instrument is unable to read values greater than 33.30 mmol/L)

Table 8. Chemical properties of nypa sap from Experiment 3 (24th May 2022).

Sample	brix (%)	pH	Glucose (mmol/L)	TDS (PPM)	EC (Us/cm)
1	16	3.89	H1	1943	3886
2	16	3.89	30.60	2511	5023
3	18	3.80	H1	2511	5023
4	14	3.71	H1	2282	4564
5	13	3.89	26.30	2282	4564
6	15	3.62	H1	2282	4564
7	15	3.98	H1	2651	5302
8	15	3.89	H1	2522	5044
9	13	3.71	H1	2225	4451
10	14	3.98	H1	2186	4372
11	14	3.97	25.9	2606	5213

*H1 indicates that the value is greater than 33.30 mmol/L
(The instrument is unable to read values greater than 33.30 mmol/L)

Table 9. Summary of chemical properties of nypa sap from all three experiments.

Experiment	Sample	brix (%)	pH	Glucose (mmol/L)	TDS (PPM)	EC (Us/cm)
1 (15th April 2022)	1-10	12	3.32	25.4	2193	4386
2 (18th May 2022)	1-10	14	3.57	32.4	2550	5099
	11 (control)	15	3.62	30.1	2726	5472
3 (24th May 2022)	1-10	15	3.84	32.3	2340	4679
	11 (control)	14	3.97	25.9	2606	5213

The acidity of sap is a result of microbial activities that convert sugars into ethanol (Tamunaidu & Saka, 2012; Yanez, 2013; Semjonovs *et al*., 2014).*Pichia* spp. and *Saccharomyces* spp. are among the main bacteria found in nypa sap responsible for fermentation (Yamagata *et al*., 1980). Additionally, other species of microbes such as *Hanseniaspora guilliermondii, Lachancea thermotolerans, Hanseniaspora vineae, Lachancea fermentati,* and *Torulaspora delbrueckii* have been identified in nypa sap (Limtong *et al*., 2020). The presence of these microbes may be due to the cleanliness of the harvester and the device used in the nypa sap harvesting process, as well as the long collecting time and open device that may be exposed to contaminants from the outside (Naknean *et al*., 2010). While the cleanliness of the device has been emphasised in this research, the personal cleanliness of the harvester may vary, which could explain the variability in pH readings observed in this research, even within the same experimental setting.

Fermentation of nypa sap typically begins a few hours after tapping and becomes more rapid over time. This justifies the acidic condition observed in the samples, as the local setting for sap collection in this research was set at 17 to 18 hours after tapping. A few samples collected using the developed device showed a higher pH value (pH = 4.34), indicating that proper cleanliness procedures are required to get a reliable quality of sap acidity. Furthermore, shortening the collecting period before temperatures get too hot (i.e., before sunrise) could be beneficial, as the ideal temperature for active yeast fermentation is reported to be 32 ˚C (Chongkhong & Puangpee, 2018).

The conductivity of a liquid is an indicator of the number of dissolved substances, chemicals, and minerals present in it. Higher amounts of these impurities will result in higher conductivity. During fermentation, the chemical compounds in nypa sap are broken down, leading to changes in electrical conductivity. Active fermentation activity can result in higher readings of TDS and EC at specific times. TDS and EC values are proportional, as described in Equation 2.

Low readings of TDS and EC were observed in the samples collected on rainy days. Regardless of weather conditions, on average, higher TDS and EC values were observed in samples collected using the traditional method compared to those collected using the collecting

device. The use of bamboo, which has been repeatedly smoked for sterilization, may contribute to impurities in the sap. The bamboo is exposed to smoke from the high-temperature burning of firewood, which can result in the formation of polycyclic aromatic hydrocarbons (PAHs). PAHs are a class of chemicals and carcinogens that naturally occur as a result of burning coal, oil, gas, wood, garbage and tobacco. PAHs are often found attached to stable particles in water, which can settle in sediment (Nwachukwu *et al*., 2019). In the case of nypa sap, the PAHs formed by the smoked bamboo may also be attracted to stable particles in the sap, which can settle in sediment. The deposited PAHs in the sediments can then remobilize into nypa sap, leading to an increase in conductivity and total dissolved solids. Therefore, a reduction of 7% to 11% in TDS and EC significantly improves sap purity.

Tables 6 to 8 present the glucose content of the collected nypa sap. Experiment 1 shows the lowest glucose content of the sap compared to Experiments 2 and 3. This is attributed to rain in Kampung Tambirat, Sarawak on 5th May 2022, between 6 p.m. and 6 a.m. (during Experiment 1) as recorded by the World Weather Online website. Plant photosynthesis rate is influenced by sunlight, and low sunlight intensity during rainy days can result in a decrease in photosynthesis rate (Lantemona *et al.,* 2013). This condition becomes a limiting factor for sugar production through metabolism. Additionally, the metabolic heat generated by microbial growth during fermentation is found to be proportional to oxygen consumption, with an average of 3.38 kcal per gram of O_2 (Minkevich & Eroshin, 1973). Since these mesophilic microbes grow best between 20 °C and 40 °C, proper sap storage requires ventilation space to disperse the heat produced by microbial respiration activities (Manpreet *et al*., 2005; Slaa & Gnode, 2009). This justifies why Experiment 1 and Sample 11 (control) from Experiments 2 and 3, which used traditional bamboo, showed lower glucose content compared to sap collected using the developed device. The traditional bamboo, which has an open top, provides good ventilation, thereby lowering the temperature inside the bamboo compared to the closed chamber of the device.

Furthermore, natural fermentation begins with an increase in lactic acid, followed by ethanol, and finally acetic acid (Somashekaraiah *et al*., 2019). *Saccharomyces* sp. is one of the bacteria found in nypa sap that is responsible for fermentation, as glucose is predominant in nypa sap, followed by fructose and sucrose (Phetrit *et al*., 2020). An increase in glucose content indicates an increase in fermentation rate. This is because, under aerobic conditions, the microbes ferment sucrose, with the yeast enzyme invertase breaking down the sugar into glucose and fructose as the first step (Marques *et al*., 2015). Fructose and glucose are then metabolised to carbon dioxide and several organic acids, with acetic and gluconic acids being formed through the conversion of glucose via gluconolactone (Lynch *et al*., 2019). The measurement principle of the glucometer is based on enzymatic reaction, which also measures the oxidation of glucose to gluconic acid. Therefore, an increase in glucometer reading also indicates the oxidation of glucose to gluconic acid or the conversion of sugar into acetic acid.

CONCLUSION

The chemical properties of nypa sap are measured by TSS and pH level. Initially, fresh sap has a neutral pH and high sucrose content. Gradually, it turns acidic due to the activities of microorganisms that convert sugars into ethanol (Nguyen *et al*., 2016). As sucrose is converted to simple sugars, such as glucose, the sucrose content of the sap decreases, which is indicated by a lower brix reading. However, the glucose content shows an adverse trend compared to the other two parameters. As time passes, the glucometer reading also increases, representing the oxidation of glucose into gluconic acid. The presence of gluconic acid imparts a sour taste to the nypa sap, indicating the level of fermentation. The freshness of the sap can be extended by controlling the fermentation process, such as by adding preservatives, which is a common practice in other countries like Thailand and Indonesia.

In conclusion, the physicochemical properties of the collected sap show no significant difference regardless of the collecting method used. However, the sap collected using the developed device improves the cleanliness condition of the sap compared to traditional bamboo. Physically, the new device has improved the cleanliness of the collected sap, with a reduction of about 97% in foreign

particles found in the sap compared to the traditional method. Furthermore, the chemical impurities of the sap are significantly improved as shown by the reduced TDS and EC readings. In terms of practicality, the device is easy to use, as indicated by a 40% reduction in the time taken to assemble the device compared to the first trial. The device is also versatile, as it can flexibly cope with various stalk conditions, such as vertical and curving orientations. Moreover, the performance of the developed device is expected to improve further by optimizing the standard operating procedures and incorporating preservatives in future experiments.

ACKNOWLEDGEMENT

The authors would like to express their gratitude for the funding support received from the Prime Minister Office, Malaysia through Dana Pembangunan Bumiputera (DPUB 2019) RG/A011/TERAJU-03/2019 and F02/SGS/1800 /2019. The authors also acknowledge the research facilities provided by Universiti Malaysia Sarawak and the Department of Agriculture, Sarawak, and cooperation from the local Sarawak Apong Community in Samarahan, Kampung Tambak, and Kampung Spaoh, Sarawak.

REFERENCES

Ballerini, T., Chaudon, N., Fournier, M., Coulomb, J.-P., Dumontet, B., Matuszak, E. & Poncet, J. (2022). Plastic pollution on Durance riverbank: First quantification and possible environmental measures to reduce it. *Frontiers in Sustainability*, 3:866982. DOI: 10.3389/frsus.2022.866982

Benyathiar, P., Kumar, P., Carpenter, G., Brace, J., & Mishra, D. K. (2022). Polyethylene terephthalate (PET) bottle-to-bottle recycling for the beverage industry: A review. *Polymers*, 14(12): 2366. DOI: 10.3390/polym14122366

Biron, M. (2017). Recycling: The first source of renewable plastics. In Biron, M. (ed.) *Industrial Applications of Renewable Plastics*, Oxford: William Andrew Publishing. pp. 67-114. DOI: 10.1016/B978-0-323-48065-9.00003-0

Chongkhong, S. & Puangpee, S. (2018). Alternative energy under the royal initiative of his majesty the king: ethanol from nipa sap using isolated yeast. *Songklanakarin Journal Science Technology,* 40(3): 648-658.

Elewa, M., El-Saady, G., Ibrahim, K., Tawfek, M. & Elhossieny, H. (2020). A novel method for brix measuring in raw sugar solution. *Egyptian Sugar Journal*, 15(0): 69-86. DOI: 10.21608/esugj.2020.209517

Fundador, E.O. & Calumba, K.F. (2020). Using a glucometer for home-based quantification of sugar in baked goods. *Philippine Journal of Science*, 149(4). DOI:10.56899/149.04.10

Gunawan, W., Maulani, R.R., Hati, E.P., Awaliyah, F., Afif, A.H. & Albab, R.G. (2020). Evaluation of palm sap (*Neera*) quality (*Arenga pinnata Merr*) in processing of house hold palm sugar (case study on Aren farmers in Gunung Halu Village, Gunung Halu district, West Bandung regency). *IOP Conference Series: Earth and Environmental Science*, 466. DOI: 10.1088/1755-1315/466/1/012001

Lantemona, H., Abadi, A.L., Rachmansyah, A. & Pontoh, J. (2013). Impact of altitude and seasons to volume, brix content, and chemical composition of aren sap in north sulawesi. *IOSR Journal of Environmental Science, Toxicology and Food Technology*, 4(2): 42-48. DOI: 10.9790/2402-0424248

Limtong, S., Am-In, S., Kaewwichian, R., Kaewkrajay, C. & Jindamorakot, S. (2020). Exploration of yeast communities in fresh coconut, palmyra, and nipa palm saps and ethanol-fermenting ability of isolated yeasts. *Antonie Van Leeuwenhoek*, 113(12): 2077-2095. DOI: 10.1007/s10482-020-01479-2

Liu, T., Huang, A., Geng, L.H., Lian, X.H., Chen, B.Y., Hsiao, B.S., Kuang, T.R. & Peng, X.F. (2018). Ultra-strong, tough and high wear resistance high-density polyethylene for structural engineering application: a facile strategy towards using the combination of extensional dynamic oscillatory shear flow and ultra-high-molecular-weight polyethylene. *Composites Science and Technology*, 167: 301-312. DOI: 10.1016/j.compscitech.2018.08.004

Lynch, K.M., Zannini, E., Wilkinson, S., Daenen, L. & Arendt, E.K. (2019). Physiology of acetic acid bacteria and their role in vinegar and fermented beverages. *Comprehensive Reviews in Food Science and Food Safety*, 18(3): 587-625. DOI: 10.1111/1541-4337.12440

Madigal, J.P.T., Cariaga, J.F., Suarez, T.C.E. & Agrupis, S.C. (2020). Assessment of the physico-chemico and microbiological changes during nipa (*Nypa fruticans*) sap fermentation collected from different sites in cagayan province, Philippines. *Indian Journal of Science and Technology*, 13(32): 3230-3236. DOI: 10.17485/IJST/v1 3i32.1251

Madigal, J.P.T., Calixto, B.G.S.C.G.S., Duldulao, M., Ubiña, T. D. & Agrupis, S. C. (2020). Development of nipa (*Nypa fruticans*) sap closed collection vessel. *Agro Bali: Agricultural Journal*, 3(2): 108-117. DOI: 10.37637/ab.v3i2.611

Manpreet, S., Sawraj, S., Sachin, D., Pankaj, S. & Banerjee, U.C. (2005). Influence of process parameters on the production of metabolites in solid-state fermentation. *Malaysian Journal of Microbiology*, 1(2): 1-9. DOI: 10.21161/mjm.120501

Marques, W.L., Raghavendran, V., Stambuk, B.U. & Gombert, A.K. (2015). Sucrose and *Saccharomyces cerevisiae*: a relationship most sweet. *FEMS Yeast Research*, 16(1): 1-16. DOI: 10.1093/femsyr/fov107

Matsui, N., Okimori, Y., Takahashi, F., Matsumura, K. & Bamroongrugsa, N. (2014). Nipa (*Nypa fruticans Wurmb*) sap collection in Southern Thailand I. Sap production and farm management. *Environment and Natural Resources Research*, 4(4): 75-88. DOI: 10.5539/enrr.v4n4p75

Minkevich, I.G. & Eroshin, V.K. (1973). Productivity and heat generation of fermentation under oxygen limitation. *Folia Microbiologica*, 18(5): 376-385. DOI: 10.1007/BF02875932

Monroy Salazar, H., Salem, A.Z.M., Kholif, A., Monroy, H., Pérez, L.S., Zamora, J.L. & Gutiérez, A. (2016). Yeast: description and structure. In Salem, A.Z.M., Kholif, A.E. & Puniya, A.K. (eds.) *Yeast Additive and Animal Production*, Delhi: Research Publishing Services. pp. 4-13.

Naknean, P., Meenune, M. & Roudaut, G. (2010). Characterization of palm sap harvested in Songkhla province, Southern Thailand. *International Food Research Journal,* 17(14): 977-986.

Nguyen, D. Van, Sethapokin, P., Rabemanolontsoa, H., Minami, E., Kawamoto, H. & Saka, S. (2016). Efficient production of acetic acid from nipa (*Nypa fruticans*) sap by Moorella thermoacetica (*f. Clostridium thermoaceticum*). *International Journal of Green Technology*, 2: 1-12.

Nistico, R. (2020). Polyethylene terephthalate (PET) in the packaging industry. *Polymer Testing*, 90: 106707 DOI: 10.1016/j.polymertesting.2020.106707

Nwachukwu, C., Hieu, M.V., Chládková, H. & Fadeyi, O. (2019). Strategy implementation drivers in correlation with strategic performance. *Management and Marketing Journal,* 17(1): 19-38.

Phetrit, R., Chaijan, M., Sorapukdee, S. & Panpipat, W. (2020). Characterization of nipa palm's (*Nypa fruticans Wurmb*.) sap and syrup as functional food ingredients. *Sugar Tech*, 22(1): 191-201. DOI: 10.1007/s12355-019-00756-3

Rachman, A.K., & Sudarto, Y. (1995). Nipah sumber pemanis baru. Yogyakarta: Kanisius.

Radam, R.R., Noor, H., Sari, M. & Lusyani, H. (2014). Chemical compounds of granulated palm sugar made from sap of nipa palm (*Nypa fruticans Wurmb*) growing in three different places. *Wetlands Environmental Management*, 2(1): 108-115.

Reed, D.R., & McDaniel, A.H. (2006). The Human Sweet Tooth. *BMC Oral Health*, 6(1): 17. DOI: 10.1186/1472-6831-6-S1-S17

Rusydi, A.F. (2018). Correlation between conductivity and total dissolved solid in various type of water: A review. *IOP Conference Series: Earth and Environmental*

Science, 118. DOI: 10.1088/1755-1315/118/1/012019

Sainz-Polo, M.A., Ramírez-Escudero, M., Lafraya, A., González, B., Marín-Navarro, J., Polaina, J. & Sanz-Aparicio, J. (2013). Three-dimensional structure of *Saccharomyces invertase*: Role of a non-catalytic domain in oligomerization and substrate specificity. *Journal of Biological Chemistry*, 288(14): 9755-9766. DOI: 10.1074/jbc.M112.446435

Saxena, A., Agarwal, V., Yadav, P., Tripathi, S., Kasliwal, A. & Ansari, H.S. (2022). Impact of single-use plastic on local communities in India. *International Journal of Scientific Research in Science, Engineering and Technology*, 9(5): 168–177. DOI: 10.32628/IJSRSE T229534

Semjonovs, P., Denina, I., Fomina, A., Patetko, A., Auzina, L., Upite, D., Upitis, A. & Danilevics, A. (2014). Development of birch (*Betula pendula Roth*.) sap based probiotic fermented beverage. *International Food Research Journal*, 21: 1763–1767.

Slaa, J. & Gnode, M. (2009). Yeast and fermentation: the optimal temperature. *Journal of Organic Chemistry: Chem. Dut. Aspects*, 134(1): a-c.

Somashekaraiah, R., Shruthi, B., Deepthi, B.V. & Sreenivasa, M.Y. (2019). Probiotic properties of lactic acid bacteria isolated from neera: A naturally fermenting coconut palm nectar. *Frontiers in Microbiology*, 10: 1–11. DOI: 10.3389/fmicb.2019.01382

Somorin, Y.M., Odeyemi, O.A. & Ateba, C.N. (2021). Salmonella is the most common foodborne pathogen in African food exports to the European Union: analysis of the rapid alert system for food and feed (1999–2019). *Food Control*, 123: 107849. DOI: 10.1016/j.foodcont.2020.107849

Sulaiman, S., Jafarzadeh, S., & Fazilah, A. (2020). Characterization of physicochemical and antioxidant properties of oil palm trunk saps as affected by the storage time in comparison to nipa sap. *Journal of Oil Palm Research*, 32(1): 75-82. DOI: 10.21894/jopr.2020.0014

Tamunaidu, P. & Saka, S. (2012). On-site sugar analysis and pre-treatment of nipa saps. *Green Energy and Technology*, 108: 121-126. DOI: 10.1007/978-4-431-54067-0_12

Thirumalini, S. & Joseph, K. (2009). Correlation between electrical conductivity and total dissolved solids in natural waters. *Malaysian Journal of Science*, 28(1): 55–61. DOI: 10.22452/mjs.vol28no1.7

Toledo, M. (2014). Brix-Sugar determination by density and refractometry. *Mettler Toledo*, 1-8.

Tonyushkina, K. & Nichols, J.H. (2009). Glucose meters: a review of technical challenges to obtaining accurate results. *Journal of Diabetes Science and Technology*, 3(4): 971–980. DOI: 10.1177/19322 9680900300446

Yanez, M.G. (2013). Glucose meter fundamentals and design. *Freescale Semiconductor*, AN4364.

Yamagata, K., Fujita, T., Sanchez, P.C. & Takahashi, R. (1980). Yeasts flora of palm wine in the Philippines. *Research Bulletin,* 13: 56-55.

Borneo Journal of Resource Science and Technology (2024), 14(1): 69-79
DOI: https:doi.org/10.33736/bjrst.6163.2024

Simulation of Hybrid Microbial Fuel Cell-Adsorption System Performance: Effect of Anode Size on Bio-Energy Generation and COD Consumption Rate

NUR FARUNITA MOHAMAD[1], IVY AI WEI TAN[*1], MOHAMMAD OMAR ABDULLAH[1], NORAZIAH ABDUL WAHAB[1] & DEVAGI KANAKARAJU[2]

[1]Department of Chemical Engineering and Energy Sustainability, Faculty of Engineering, Universiti Malaysia Sarawak, 94300 Kota Samarahan, Sarawak, Malaysia; [2]Faculty of Resource Science and Technology, Universiti Malaysia Sarawak, 94300, Kota Samarahan, Sarawak, Malaysia
*Corresponding author: awitan@unimas.my
Received: 11 October 2023 Accepted: 23 March 2024 Published: 30 June 2024

ABSTRACT

Landfill leachate discharged into watercourse without proper treatment can pollute the water source due to its high chemical oxygen demand (COD). The high pollutant load in landfill leachate has become one of the potential substrates in bio-energy generation by using microbial fuel cell (MFC). MFC integrated with adsorption system has been introduced as an approach to overcome the limitation of stand-alone MFC, which is able to treat the landfill leachate more effectively while simultaneously generating bio-energy. Anode size has been reported to have a significant influence on the power generation of MFC via lab-scale experiments, however the simulation studies on MFC are still limited. This study aimed to develop a simulation model to predict the effect of graphite fiber brush anode size on the performance of a single chamber air-cathode hybrid MFC-Adsorption system, in terms of COD removal and bio-energy generation. The highest power density of 1.33 mW/m^2 was achieved with 20% anode brush removed. The highest current generation of 2.37 mA and voltage of 7.11 mV was obtained with the largest anode surface area of 0.1288 m^2 and resistance of 2.76 Ω. The highest COD consumption by electrogenic microorganisms was 4.96 x 10^{-9} Lmol/mg, and predicted to decrease with decreasing anode size. The efficiency of the simulation model could be further improved by incorporating parameters such as charge transfer kinetic at anode and cathode, adsorption effect by activated carbon as well as the substrate and microbial population behaviour. The simulation model developed was significant towards enhancing the bio-energy generation and reducing the cost of MFC for industrial application.

Keywords: Bio-energy; chemical oxygen demand; landfill leachate; microbial fuel cell; simulation model

INTRODUCTION

Landfill leachate consists of various components characterised as high chemical oxygen demand (COD), biochemical oxygen demand (BOD), BOD/COD ratio, suspended solids, pH, turbidity, ammonium-nitrogen (NH_3-N) and heavy metals. Energy production from landfill leachate has become a recent interest due to the potential of this highly polluting wastewater as the source of bio-electricity generation (Tan *et al*., 2023). MFC has demonstrated advantages as compared to other wastewater treatment processes as MFC can convert substrate energy to electricity directly, and operate at ambient or low temperatures, thus producing less amount of excessive sludge (Sorgato *et al*., 2023). The MFC design for practical application as it single chamber air-cathode is the most suitable produces higher power generation, low cost and simple design (Samudro *et al*., 2022; Li *et al*., 2023). In terms of voltage generation and treatment efficiency, hybrid system is generally more reliable and efficient than a stand-alone MFC (Tee *et al*., 2016). Yazdi *et al*. (2016) obtained a higher power density of 2400 mW/m^2 by using 2.5 cm^2 graphite fiber brush (GFB) as an anode electrode material. However, the optimization of bio-energy through the MFC design still needs to be further researched for industrial application. Numerical studies on MFC can be extensively used to offer deeper insights into MFC performance (Gadkari *et al*., 2019a).

The performance of MFC depends on the improvement through modifying system architecture, materials and better understanding of the solution chemistry (Liang *et al*., 2022). The metabolic pathway of the microorganism and the potential of anode are the key parameters for cell potential determination. The anode used in MFC should be able to reduce the internal resistance and increase power density when placed together with the cathode. According to Sakai *et al.* (2018), the surface area of anode has an important role in energy production. Rossi *et al*. (2019) reported an 18% reduction in the power density with a larger anode due to increasing in the internal resistance. A shorter anode-brush diameter was found to maintain a closer spacing of electrodes which reduced the internal resistance and improved MFC performance (Lanas *et al*., 2014). In a single chamber MFC, a carbon brush with 27 cm^2 produced 48 mW/m^3 whereas an anode with 9 cm^2 produced 41 mW/m^3 (Houghton *et al*., 2016). As the number of experimental studies on MFC has been increasing, it is not the same for mathematical modelling and simulation studies. Mathematical models are able to help in understanding the influence of different operational, design and biological parameters affecting the MFC performance, and to optimize the new reactor configurations as well as aiding in up-scaling the technology (Ortiz-Martínez *et al*., 2015). Improvement in simulation design is crucial as the innovation of MFC for industrial application is restricted by the electrode material cost, requirement of precious metal, low power density and low performance of the system. These issues can be overcome at the lab scale, however the vital part is the performance on a large scale particularly when managing wastewater that does not have steady conditions with time (Logan, 2010). A few mathematical models have been developed to study the influence of anode on MFC performance, such as the model on bioanode (Gadkari *et al*., 2019b) and two-dimensional model of air-cathode MFC with GFB as anode (Gadkari *et al*., 2019a). Gadkari *et al*. (2019a) used Nelder-Mead Simplex algorithm for prediction of power generation to estimate the parameters in the model, which reported little change in power density around 15% to 60% of brush removed in which the power density was reduced by 21%.

Table 1 shows the development of MFC numerical studies. Limited numerical studies have focused on air-cathode MFC. Additionally, optimisation using simulation on hybrid MFC-Adsorption system has not been reported up to date, and the study on the effect of anode size in hybrid MFC-Adsorption system has not been found. Simulation study is significant towards the development of MFC for industrial application as the system is currently in its infancy stage due to the challenges on reducing the high cost and improving the power generation. Anode generally should have the characteristics of larger surface area, best chemical and microbial stability, high electrical conductivity, biocompatibility and inexpensive in cost (Liang *et al*., 2022). The power output of the system is determined by the wellness of biofilm attached to the anodic surface area. Thus, the best method to enhance the performance of the MFC is by increasing the affinity of the biofilm through anode modification (Banerjee *et al*., 2022). Therefore, the main focus of the present study was to develop a simulation model using Microsoft Excel 365 Proplus by correlating the anode size of a single chamber hybrid MFC-Adsorption system with the bio-energy generation of the system and COD consumption rate, by using landfill leachate as the MFC substrate. In addition, the current and voltage generated in the hybrid MFC-Adsorption system with different anode size were predicted through simulation of the maximum power densities.

MATERIALS AND METHODS

Simulation Design

The simulation used in this work was adopted from Gadkari *et al*. (2019a) which was the two-dimensional simulation focusing on single chamber air-cathode MFC. Microsoft Excel 365 Professional Plus was used to develop the simulation in predicting the bio-energy generation and COD consumption rate. GFB anode was represented in the simulation and was connected using twisted titanium wire and placed at the central of the closely packed-bed of granular activated carbon (GAC). The air-cathode existed as activated carbon fiber felt (ACFF) and was connected to the circuit by a copper rod. The electrode was exposed to air on its outer surface while being in contact with the earthen pot and hydrogel was applied evenly between them, following the configuration of the hybrid MFC-Adsorption system of Tee *et al*.

Table 1. Development of MFC numerical studies

Mathematical and simulation study on MFC	Description	Range of study	Reference
1-Dimensional mathematical model	Developed model coupling biological, heat and mass transfer processes occurring in MFC. Numerical tools: Microsoft Excel and MATLAB.	1. Effect on cathode and anode overpotential as a function of current density. 2. Effect of substrate concentration on biofilm thickness. 3. Effect of temperature on MFC performance. 4. Effect on biomass and acetate concentration as a function of current density.	Oliveira *et al*. (2013)
Modelling based on Freter equations	Developed model simulation towards electrochemical performance in batch and continuous mode of MFC operation. Numerical tools: MATLAB.	Batch mode: 1. Effect of initial substrate on external voltage. 2. Effect of external resistor on overall energy efficiency. Continuous mode: 1. Effect on power generation as a function of influent substrate concentration and dilution rate. 2. External resistor effect on the overall energy efficiency.	Lin *et al*. (2018)
Dynamic model based on bioanode kinetic	Developed model based on batch operated single chamber MFC with biotic anode and an air-cathode.	1. Effect of initial substrate concentration on maximum voltage, CE and COD removal rate. 2. Effect of external resistance on MFC performance.	Gadkari *et al*. (2019a)
2-Dimensional model	Developed model with charge transfer kinetic coupled to the mass balance for both anode and cathode electrode.	1. Effect of anode size on power densities. 2. Effect of anode distance from cathode on power densities. 3. Effect of initial substrate concentration on power densities, CE and COD removal rate.	Gadkari *et al*. (2019b)

(2016). The reactor was assumed to be operating in fed-batch mode. Anode GFB is known with high porosity characteristics. Gadkari *et al*. (2019a) successfully simulated the anode GFB by using a mathematical model to optimize the GFB anode-based air-cathode MFC in a directed way, which helped in optimizing the performance relationship across the scale. Therefore, a simulation on GFB anode size of hybrid MFC-Adsorption system was performed in this study to evaluate its effect on bio-energy generation.

The simulation incorporated a few assumptions for the development and simplicity. The parameters such as pH and temperature were neglected, carbon dioxide (CO_2) released during substrate oxidation in the anode stayed dissolved in the bulk solution, leachate and CO_2 remained in the anode chamber and did not diffuse to cathode assembly, similar with the oxygen from air-cathode which did not diffuse in the anode chamber. The substrate used was landfill leachate which functioned as the only electron donor in the anolyte. The effective porosity of the brush anode was remained when the concentration of bacteria/substrate changed. The last assumption was the reverse reaction of substrate oxidation at anode and oxygen reduction at cathode were negligible. The parameters of landfill leachate were obtained from Shanmugham (2019) while power generation values were obtained from Tee *et al*. (2016). The MFC working volume was 5.65 L whereas the GFB anode was designed as 100 mm in diameter and 360 mm long. The anode was maintained at 4 cm from the cathode. Other parameters were estimated by using the best fit correlation equation obtained using the Microsoft Excel 365 Professional Plus.

Calculation of Anode Surface Area

The area of GFB anode was calculated using Equation 1 [Eq. (1)] to estimate the power generation. The anode size was reduced by removing the sections of the brush incrementally from the side farthest from the cathode (Gadkari *et al*., 2019a). The same was used in this simulation study by maintaining the distance between the anode and cathode at 4 cm. The area of anode after the removal was calculated using Equation 2 [Eq. (2)]

$$A = 2\pi rh + 2\pi r^2 \qquad \text{Eq.(1)}$$

$$A_i = A_0 + A_0(i\%) \qquad \text{Eq.(2)}$$

where A (m^2) indicated surface area while h (m) was length of brush and r (m) was radius of brush. A_i (m^2) was area of anode after removal, A_0 (m^2) was initial area of brush, i indicated percent of removal.

Simulation Study of Hybrid MFC-Adsorption System

The first simulation was performed by comparing the trend with Gadkari *et al*. (2019a). The power density was predicted against the brush removal by using the maximum power density from Tee *et al*. (2016) as the reference. The power was calculated using Equation 3 (Eq.(3)) whereas the current generated for each anode size was calculated using Equation 4 (Eq.(4)). The voltage generated was calculated using Equation 5 (Eq.(5)). The second simulation was performed on the current generation against time by referring to the data of Penteado *et al*. (2018) where the maximum current value was calculated from the first correlation developed on power density. This study focused on the ratio of anode surface area to the volume of anode compartment (ESAVR) towards the performance of current generated (Penteado *et al*., 2018). The predicted values were used to calculate the voltage generated against time by using Equation 5.

$$P = P_d A \qquad \text{Eq.(3)}$$

$$I = \sqrt{\left(\frac{P}{R}\right)} \qquad \text{Eq.(4)}$$

$$V = IR \qquad \text{Eq.(5)}$$

where P (W) was power, P_d (W/m^2) was power density, A (m^2) was area of anode and I (A) was current. For voltage (V) calculation, the constant resistance, R of 30 Ω was multiplied with the current.

Prediction of COD Consumption Rate

The COD consumed in relation to the anode size was predicted by referring to Penteado *et al*. (2018). The COD consumption rate was predicted to decrease by 1000 mg/Lday with decreasing anode size. With the prediction of COD consumed in the hybrid MFC-Adsorption system, the fraction of COD or COD consumption by electrogenic microorganism (Lmol/mg) was then calculated using Equation 6 (Eq. (6)) (Penteado *et al*., 2018). For the largest anode surface area, the COD of landfill leachate was 729 mg/L (Shanmugham, 2019) and the consumption rate was 6.12 L/h (Tee *et al*., 2016), thus the COD consumption rate was 107,075.52 mg/Lday.

$$ratioelectrogenic = \frac{\frac{jA}{4F}}{rCOD} \qquad \text{Eq.(6)}$$

where $rCOD$ (mg/Lday) indicated the rate of COD consumed in the anode chamber, F (96,485 As/mol) was Faraday's constant, j (A/m^2) was current density and A (m^2) was anode surface area.

Parameters of Simulation Study

The parameters shown in Table 2 were used to simulate the effect of anode size on the bio-energy generation and COD consumption rate of the hybrid MFC-Adsorption system.

Table 2. Parameters of simulation studies

Parameter	Value	Unit	Reference
GFB initial diameter	100	mm	Tee *et al.* (2016)
GFB initial length	360	mm	Tee *et al.* (2016)
Maximum power density	1.21	mW/m^2	Tee *et al.* (2016)
Maximum current	2.37	mA	Tee *et al.* (2016)
Maximum voltage	0.66	mV	Estimated
Resistance	30	Ω	Estimated
COD	729	mg/L	Shanmugham (2019)
Volume of anode compartment	5.65	L	Tee *et al.* (2016)

RESULTS AND DISCUSSION

Effect of Anode Size on Bio-Energy Generation

In the first simulation, the bio-energy generation in terms of power, voltage and current in relation to the change of anode size was studied. The maximum power density (Figure 1(a)) showed insignificant change of about 1±0.3% to 40% of brush removed and predicted to show a greater decrease of 2% when compared to the results of Gadkari *et al*. (2019a) as shown in Figure 2. This was possibly due to the same type of anode used that had been heat-treated. The power density was the highest with 20% brush removed as the over-potential in the brush increased (Gadkari *et al*., 2019a). Additionally, the local current density and reaction rate was higher as the distance of brush end from cathode decreased. It could be observed in Figure 2 that the local current density and reaction rate in the brush anode decreased with decreasing anode size. The increase in 20% to 40% reduction of anode size indicated that the average local current density and reaction rate had reached its maximum capacity. The maximum average local current density and reaction rate showed a major drop in the case of 60% of brush removed, hence this caused the reduction in power density after a nearly constant power density was achieved between 20% to 40% of brush removed. Higher power density could be achieved by using a more conductive electrolyte as power density could be affected by the substrate concentration (Logan *et al*., 2015) which influenced the speed of bacteria in removing the oxygen and reducing oxygen mass transfer into the anode (Hays *et al*., 2011). Di Lorenzo *et al*. (2010) also suggested to include the mass transfer effect of a substrate in anode electrode for a better understanding of MFC behaviour.

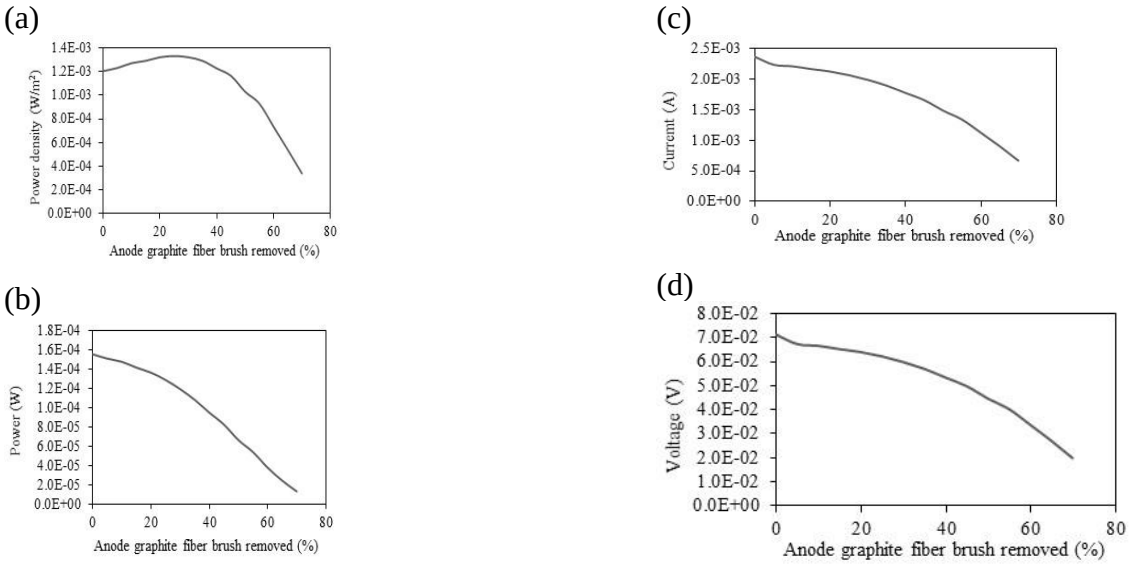

Figure 1. Simulation of (a) power density, (b) power, (c) current and (d) voltage generation in hybrid microbial fuel cell-Adsorption system against percentage of anode graphite fiber brush removed

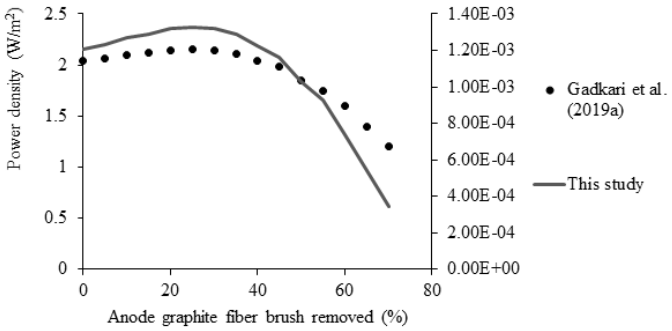

Figure 2. Predicted value of power density obtained from correlation to the corresponding value adopted from Gadkari *et al*. (2019a)

Power Generation in Hybrid MFC-Adsorption System

The power generated was found to decrease with decreasing anode size (Figure 1(b)). By comparing the gradient of the graph, an assumption could be drawn where huge changes in power generation occurred with 20% and 60% of brush removed. According to Rossi *et al*. (2019), lower power output was obtained with smaller anode primarily due to the decrease in cathode potential. The cathode performance could decrease because of cathode fouling (Yang *et al*., 2017). This was supported by Houghton *et al*. (2016) where increasing anode area did not improve the system performance since cathode had been the limiting factor for the power production. Houghton *et al*. (2016) also reported that anode electrode contributed to lower ohmic losses as compared to cathode electrode.

Current Generation in Hybrid MFC-Adsorption System

Figure 1(c) shows that the current generation decreased with the decreasing anode size with a fluctuation between no brush removal and 5% of brush removed. This simulation used 30 Ω resistance, which was different from the resistance value (27.6 Ω) used by Tee *et al*. (2016), which affected the current generation. Gadkari *et al*. (2019b) proved that the increase in the applied external resistance caused a decrease in the current density, coulombic efficiency and COD removal rate of the MFC. Kumar *et al*. (2018) explained that sufficient electrode spacing and surface of anode were obligated for bacterial growth as well as for electron transformation from anode to cathode. Lower current and power density were obtained with higher total internal impedance where diffusion resistance had been the contributor (Lanas *et al*., 2014). Wider spacing between the cathode and edge of anode brush also caused an increase in the total internal impedance (Cheng *et al*., 2006). In this simulation study, the electrode spacing could be reduced to less than 4 cm to generate a higher current. Close electrode spacing in the hybrid MFC-Adsorption system was significant due to the lower conductivity of substrate which resulted in higher ohmic losses. The anode acts as a surface for bacteria to associate to generate electron and proton during respiration (Kumar *et al*., 2018). Additionally, the current generation was highly dependent on the concentration of bacteria attached onto the surface of anode. This suggested that lower surface area for bacterial attachment would reduce the anoxic condition for the exoelectrogenic activity (Penteado *et al*., 2018). Less bacteria attached would reduce the electron transfer to the anode surface. The reduction of anode size caused a reduction of the surface area of brush anode from 0.1288 cm^2 to 0.1224 cm^2, thus resulted in the descending current generated. Generally, specific current generation also depended on current density that was dependent on the over-potential which was a function of electrode potential, electrolyte potential and equilibrium potential of the charge transfer reaction at the particular electrode (Gadkari *et al*., 2019a).

Voltage Generation in Hybrid MFC-Adsorption System

Figure 1(d) shows that the voltage generation demonstrated similar trend as the current generation, which decreased with the decreasing anode size. The simulation results showed that the highest anode area of 0.1288 m^2 produced the highest voltage of 0.71 mV. Wang *et al*. (2013) reported 97.9 mV was generated with higher anode graphite plate size of 81.1 cm^2 while smaller anode with 74.5 cm^2 surface area generated 71.5 mV. The higher voltage also indicated the higher amount of the attached biomass (Lin *et al*., 2018). The low voltage generation could be mainly due to the mediator-less MFC system which had caused most microorganism species to be inactive in transferring electron to the anode (Tee *et al*., 2016). The ease of electron transfer process in the bio-electrochemical system enhanced the voltage production. Mediator would act as the electron shuttler which enhanced the electron efficiency. However, a few studies have reported the unnecessary use of mediator which made the mediator-less MFC to be more commercially feasible since the electron generated was transferred to the anode surface by a few mechanisms such as through conductive appendages, direct contact, provided chemical mediators or self-produce mediators (Das & Mangwani, 2010; Kumar *et al*., 2016). Modification of anode was found to be able to increase the biofilm attached on its surface area to produce higher power output (Santoro *et al*., 2013). The comparison of the performance of the hybrid MFC-Adsorption system developed in this study with other MFC systems are summarized in Table 3. The power density

obtained was lower than previous studies due to smaller size of anode was used. Higher power density of hybrid MFC-Adsorption system with anode area of 0.1030 m^2 could be achieved by using a more conductive electrolyte as the substrate considering the low microbial kinetic of the landfill leachate.

Table 3. Comparison of performance of various microbial fuel cell (MFC) systems

Type of MFC	Anode type	Anode size	Findings		Reference
			Current	Power density	
Dual chamber	Graphite plate	74.5 cm^2 81.1 cm^2	186.2 µA 271.3 µA	NA	Wang *et al*. (2013)
Single chamber	Graphite pellets	12.5 cm^2 90 cm^2 499 cm^2 1247 cm^2	0.03 mA 0.067 mA 0.0171 mA 0.47 mA	0.01 W/m^3 0.043 W/m^3 0.247 W/m^3 8.1 W/m^3	Di Lorenzo *et al.* (2010)
Single chamber	Carbon brush	9 cm^2 18 cm^2 27 cm^2	NA	48 ± 1.3 W/m^3 44.5 ± 0.88 W/m^3 48 ± 1.3 W/m^3	Houghton *et al.* (2016)
Single chamber air-cathode	Carbon fiber brush	2.5 cm in diameter 1.2 cm in diameter 0.8 cm in diameter	0.32 mA/cm^2 0.29 mA/cm^2 0.23 mA/cm^2	1270 mW/m^2 910 mW/m^2 600 mW/m^2	Lanas *et al.* (2014)
Single chamber air-cathode	GFB	0.1288 m^2 0.1030 m^2 0.0772 m^2 0.0515 m^2	2.37 mA 2.13 mA 1.78 mA 1.12 mA	1.2 mW/m^2 1.32 mW/m^2 1.23 mW/m^2 0.736 mW/m^2	This study

*NA-not applicable

Optimisation of Bio-Energy Generation

The optimised current generation took shorter time to increase and achieved a stable state with higher ESAVR (Figure 3). The rapid increasing state indicated the start-up with prediction of a day extended to the function of decreasing ESAVR. The largest anode size was estimated to have ten days of start-up. The study simulated in terms of best fit graph on the first current generation against time which was for the largest surface area of anode by referring to Tee *et al.* (2016). The next current generation was estimated by taking the difference of the maximum current generation between the anode size. This resulted in the continuous plot of current generation against time. The low initial concentration of bacteria attached on the anode surface justified that more time was needed for the system to generate electricity (Wang *et al*., 2015). According to Angelaalincy *et al.* (2018), large surface area and robust structure played an important role for supporting the biofilm in MFC. Moreover, the presence of active electron transferring live organism at the outer layer of the biofilm caused high current generation (Sun *et al*., 2016). It was speculated that bacteria existed under more anoxic conditions with larger anode brush size. Therefore, more exoelectrogenic consortia developed on the anode brush in order to generate current. As the mass of biofilm increased over time, more brush could achieve sufficient anoxic condition and improved the current generation. Start-up for the removed brush was delayed until sufficient biofilm could consume oxygen in order for exoelectrogenic to grow (Penteado *et al*., 2018). However, high diffusion resistance was found in the electrochemical system as time elapsed due to the dead cell accumulated in the inner layer of the biofilm. This explained the lower current generation at lower surface area of anode. The presence of activated carbon in the anode compartment helped to shorten the start-up time due to the rough surface which offered high surface area for bacteria to grow and form a mature bio-membrane (Tee *et al*., 2016). Tee *et al*. (2016) took 10 days for start-up with 5.65 L working volume. Another study on hybrid MFC-Adsorption system by Selvanathan (2018) used palm oil mill effluent as the substrate reported three days for start-up with 655 mL of working volume and 300 µM methylene blue as the mediator. The start-up time was shorter due to

the mediated transfer of electrons from microorganism to anode. Penteado *et al*. (2018) explained that lower volume of anode chamber promoted the competition of microorganism towards substrate. The shorter time obtained in this simulation study was due to a more stable power over time could be achieved using GFB as the anode (Ahn & Logan, 2013).

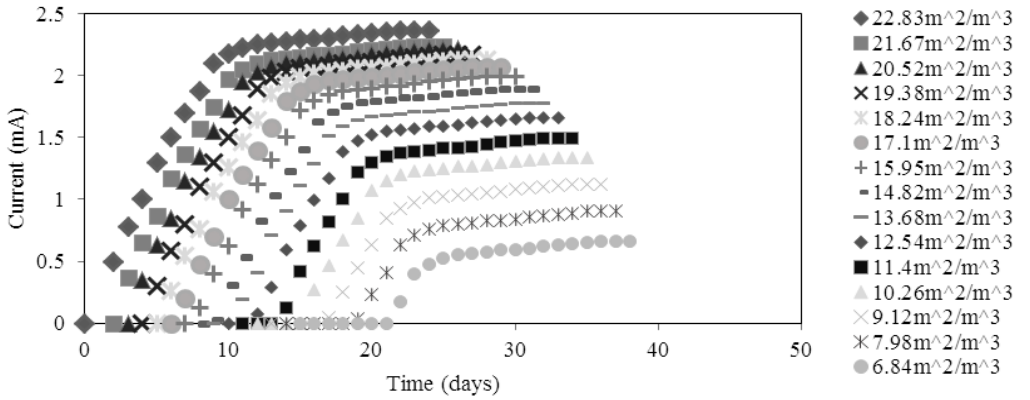

Figure 3. Optimized current generation of hybrid microbial fuel cell (MFC)-Adsorption system against time

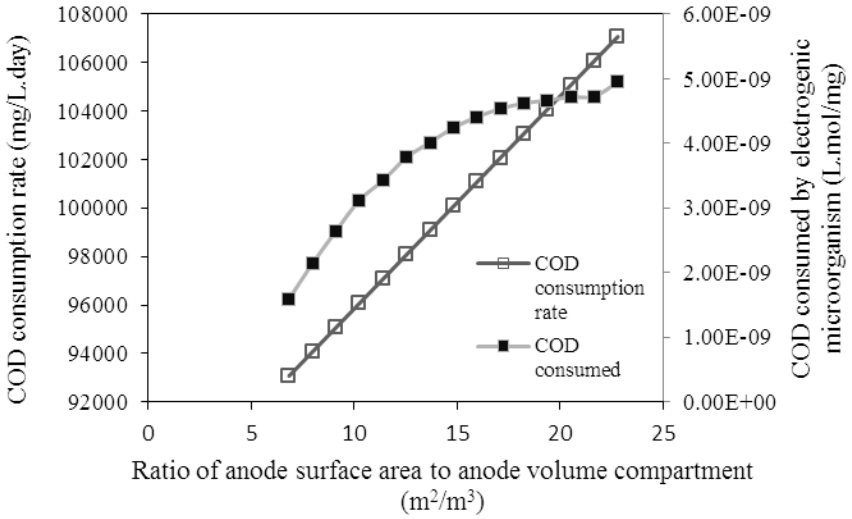

Figure 4. Chemical oxygen demand (COD) consumption rate and Chemical oxygen demand COD consumed by electrogenic microorganism in hybrid microbial fuel cell (MFC)-Adsorption system against ESAVR

Effect of Anode Size on COD Consumption Rate

The COD consumption rate was simulated by referring to Penteado *et al*. (2018) which focused on the effect of ESAVR. However, this study used different conditions by varying the anode surface area and assuming a constant anode volume whereas Penteado *et al*. (2018) varied the anode volume and assumed a constant anode electrode. The simulated COD consumption rate (Figure 4) showed a similar trend with Penteado *et al*. (2018). Fluctuation might occur depending on the load of a substrate which corresponds to the bacteria present in the load (Selvanathan, 2018). The COD consumption rate was also affected by the ESAVR where a higher ESAVR would increase the COD consumption rate. Several studies reported that higher COD removal was obtained when higher anode size was used. Wang *et al*. (2013) showed 14.86% and 6.87% of COD removal using 81.1 cm^2 and 74.5 cm^2 of anode graphite plate, respectively. Di Lorenzo *et al*. (2010) showed 70% of COD removal using 1247 cm^2 of graphite pellets as compared to the smaller anode size. The treatment efficiency depended on the total population of microorganism (Wang *et al*., 2015). Higher anode surface area led to higher nutrient consumption which indicated a positive effect on the degradation of the waste and promotion in the biomass formation. The COD

consumption rate also depended on the anode volume where a lower anode compartment resulted in a higher COD consumption rate due to more competition among microorganisms for food (Penteado *et al*., 2018). Larger anode surface area enhanced the power generation of the hybrid MFC-Adsorption system which suggested that the role of microorganism was fixed in anodic biofilm. Penteado *et al*. (2018) stated the significance of fraction of COD consumption by electrogenic microorganism which was related to the MFC performance. In this study, the highest COD consumed by electrogenic microorganism was 4.96 x 10^{-9} Lmol/mg, which was obtained with the largest anode surface area of 0.1288 m^2. The COD consumed by electrogenic microorganism decreased with decreasing ESAVR. This could be explained in terms of higher ohmic losses due to the microbial community selection in lower shear force which was affected by a smaller anode size (Penteado *et al*., 2018).

CONCLUSION

The performance of a hybrid MFC-Adsorption system in terms of bio-energy generation and COD consumption rate has been simulated using different GFB anode size. The highest power density of 1.33 mW/m^2 was obtained with 20% of anode brush removed. The power density obtained was lower than previous studies due to the smaller size of anode used. Higher power density with an anode area of 0.1030 m^2 could be achieved by using a more conductive electrolyte as the substrate considering the low microbial kinetic of the landfill leachate. The current and voltage generation demonstrated a decreasing trend with the reduction in anode size. Besides, the start-up time was shorter when a larger anode surface area was applied. The COD consumption rate and COD consumed by electrogenic microorganisms decreased with increasing ESAVR. The simulation model developed in this study could be further improved for better performance of the hybrid MFC-Adsorption system by considering other parameters such as the reaction rate in anode brush, charge transfer kinetics, substrate and microbial population behaviour as well as the mass transfer of air diffused in both anode and cathode electrodes. A more precise simulation and numerical study on the hybrid MFC-Adsorption system would offer deeper insights into the mechanism of the system operation and potentially help in optimising the system performance. Overall, the simulation model developed was significant towards enhancing the bio-energy generation and reducing the cost of MFC for industrial application.

ACKNOWLEDGEMENTS

The authors acknowledge Universiti Malaysia Sarawak (UNIMAS) for providing the research grant: Cross Disciplinary Research Grant F02/CDRG/1830/2019.

REFERENCES

Ahn, Y. & Logan, B.E. (2013). Domestic wastewater treatment using multi-electrode continuous flow MFCs with a separator electrode assembly design. *Applied Microbiology and Biotechnology*, 97: 409-416.

Angelaalincy, M.J., Krishnaraj, R.N., Shakambari, G., Ashokkumar, B., Kathiresan, S. & Varalakshmi, P. (2018). Biofilm engineering approaches for improving the performance of microbial fuel cells and bioelectrochemical systems. *Frontiers in Energy Research*, 6: 63.

Banerjee, A., Calay, R.K. & Mustafa, M. (2022). Review on material and design of anode for microbial fuel cell. *Energies*, 15: 2283.

Cheng, S., Liu, H. & Logan, B.E. (2006). Increased power generation in a continuous flow MFC with advective flow through the porous anode and reduced electrode spacing. *Environmental Science & Technology*, 40: 2426-2432.

Das, S. & Mangwani, N. (2010). Recent developments in microbial fuel cell: A review. *Journal of Scientific & Industrial Research*, 69: 727-731.

Di Lorenzo, M., Scott, K., Curtis, T.P. & Head, I.M. (2010). Effect of increasing anode surface area on the performance of a single chamber microbial fuel cell. *Chemical Engineering Journal*, 156: 40-48.

Gadkari, S., Gu, S. & Sadhukhan, J. (2019a). Two-dimensional mathematical model of an air cathode microbial fuel cell with graphite

fiber brush anode. *Journal of Power Sources*, 441: 227145.

Gadkari, S., Shemfe, M. & Sadhukhan, J. (2019b). Microbial fuel cells: A fast converging dynamic model for assessing system performance based on bioanode kinetics. *International Journal of Hydrogen Energy*, 44: 15377-15386.

Hays, S., Zhang, F. & Logan, B.E. (2011). Performance of two different types of anodes in membrane electrode assembly microbial fuel cell for power generation from domestic wastewater. *Journal of Power Sources*, 196: 8293-8300.

Houghton, J., Santoro, C., Soavi, F., Serov, A., Ieropoulos, I., Arbizzani, C. & Atanassov, P. (2016). Supercapacitive microbial fuel cell: Characterization and analysis for improved charge storage/delivery performance. *Bioresource Technology*, 218: 552-560.

Kumar, R., Singh, L. & Zularisam, A.W. (2016). Exoelectrogens: Recent advances in molecular drivers involved in extracellular electron transfer and strategies used to improve it for microbial fuel cell applications. *Renewable and Sustainable Energy Reviews*, 56: 1322-1336.

Kumar, R., Singh, L., Zularisam, A.W. & Hai, F.I. (2018). Microbial fuel cell is emerging as a versatile technology: A review on its possible applications, challenges and strategies to improve the performances. *International Journal of Energy Research*, 42: 369-394.

Lanas, V., Ahn, Y. & Logan, B.E. (2014). Effects of carbon brush anode size and loading on microbial fuel cell performance in batch and continuous mode. *Journal of Power Sources*, 247: 228-234.

Li, J., Lin, S., Zhang, Y., Wang, T., Luo, H. & Liu, G. (2023). Nitrogen removal with the physiological stratification of cathodic biofilm in air-cathode single-chamber microbial fuel cell under different external resistances. *Chemical Engineering Science*, 275: 118746.

Liang, H., Han, J., Yang, X., Qiao, Z. & Yin, T. (2022). Performance improvement of microbial fuel cells through assembling anodes modified with nanoscale materials. *Nanomaterials and Nanotechnology*, 12: 1-14.

Lin, H., Wu, S. & Zhu, J. (2018). Modeling power generation and energy efficiencies in air-cathode microbial fuel cells based on Freter equations. *Applied Science*, 8: 1983.

Logan, B.E. (2010). Scaling up microbial fuel cells and other bio-electrochemical systems. *Applied Microbiology and Biotechnology*, 85: 1665-1671.

Logan, B.E., Wallack, M.J., Kim, K.Y., He, W., Feng, Y. & Saikaly, P.E. (2015). Assessment of microbial fuel cell configurations and power density. *Environmental Science & Technology Letters*, 2: 206-214.

Oliveira, V.B., Simões, M., Melo, L.F. & Pinto, A.M.F.R. (2013). A 1D mathematical model for a microbial fuel cell. *Energy*, 61: 463-471.

Ortiz-Martínez, V.M., Salar-García, M.J., de los Ríos, A.P., Hernández-Fernández, F.J., Egea, J.A. & Lozano, L.J. (2015). Developments in microbial fuel cell modeling. *Chemical Engineering Journal*, 271: 50-60.

Penteado, E.D., Fernandez-Marchante, C.M., Zaiat, M., Gonzalez, E.R. & Rodrigo, M.A. (2018). Optimization of the performance of a microbial fuel cell using the ratio electrode-surface area / anode-compartment volume. *Brazilian Journal of Chemical Engineering*, 35: 141-146.

Rossi, R., Evans, P.J. & Logan, B.E. (2019). Impact of flow recirculation and anode dimensions on performance of a large-scale microbial fuel cell. *Journal of Power Sources*, 412: 294-300.

Sakai, K., Iwamura, S., Sumida, R., Ogino, I. & Mukai, S.R. (2018). Carbon paper with a high surface area prepared from carbon nanofibers obtained through the liquid pulse injection technique. *ACS Omega*, 3: 691-697.

Samudro, G., Imai, T. & Reungsang, A. (2022). Determination of optimum retention time in an air-cathode single-chamber microbial fuel cell batch-mode reactor by comparing different substrate types and concentrations. *Process Safety and Environmental Protection*, 162: 694-705.

Santoro, C., Ieropoulos, I., Greenman, J., Cristiani, P., Vadas, T., Mackay, A. & Li, B. (2013). Power generation and contaminant removal in single chamber microbial fuel cells (SCMFCs) treating human urine. *International Journal of Hydrogen Energy*, 38: 11543-11551.

Selvanathan, J.R. (2018). *Palm oil mill effluent treatment and bioenergy generation using hybrid microbial fuel cell-adsorption system.* (Thesis), Universiti Malaysia Sarawak, Malaysia.

Shanmugham, B. (2019). *Hybrid microbial fuel cell adsorption system with mediator for landfill leachate treatment and bioenergy generation.* (Thesis), Universiti Malaysia Sarawak, Malaysia.

Sorgato, A.C., Jeremias, T.C., Lobo, F.L. & Lapolli, F.R. (2023). Microbial fuel cell: Interplay of energy production, wastewater treatment, toxicity assessment with hydraulic retention time. *Environmental Research*, 231: 116159.

Sun, D., Chen, J., Huang, H., Liu, W., Ye, Y. & Cheng, S. (2016). The effect of biofilm thickness on electrochemical activity of *Geobacter sulfurreducens*. *International Journal of Hydrogen Energy*, 41: 16253-16258.

Tan, W., Yang, Z., Feng, Q., Su, H., Xu, L. & Liu, C. (2023). Effect of $NiCo_2O_4$ and Ni-P modified anodes on the treatment of aging landfill leachate by microbial fuel cells. *Journal of Power Sources*, 577: 233233.

Tee, P.-F., Abdullah, M.O., Tan, I.A.W., Mohamed Amin, M.A., Nolasco-Hipolito, C. & Bujang, K. (2016). Performance evaluation of a hybrid system for efficient palm oil mill effluent treatment via an air-cathode, tubular upflow microbial fuel cell coupled with a granular activated carbon adsorption. *Bioresource Technology*, 216: 478-485.

Wang, J., Zheng, Y., Jia, H. & Zhang, H. (2013). In situ investigation of processing property in combination with integration of microbial fuel cell and tubular membrane bioreactor. *Bioresource Technology*, 149: 163-168.

Wang, Y.L., Deen, M.J., Marsal, L.F., Hoff, A., Aguilar, Z.P. & Lin, Z.H. (2015). Solid-state electronics and photonics in biology and medicine 2. *ECS Transaction*, 69: 51-55.

Yang, W., Rossi, R., Tian, Y., Kim, K.-Y. & Logan, B.E. (2017). Mitigating external and internal cathode fouling using polymer bonded separator in microbial fuel cell. *Bioresource Technology*, 249: 1080-1084.

Yazdi, A.A., D'Angelo, L., Omer, N., Windiasti, G., Lu, X. & Xu, J. (2016). Carbon nanotube modification of microbial fuel cell electrodes. *Biosensors and Bioelectronic*, 85: 536-552.

Borneo Journal of Resource Science and Technology (2024), 14(1): 80-87
DOI: https:doi.org/10.33736/bjrst.5672.2024

Phytochemical Profiling of *Garcinia rostrata*, *Garcinia dryobalanosides* and *Garcinia cuneifolia* and Their Antibacterial Activity

NOR HISAM ZAMAKSHSHARI[1*], NUR FAZLIN ZAFIRAH ZAINE[1], DAYANG NURUL ANISA ABANG HEILMAN[1], AINAA NADIAH ABD HALIM[1], SURISA PHORNVILLAY[1], YEO KAI WEI[1], VIVIAN JONG YI[2] & FASIHUDDIN BADRUDDIN AHMAD[1]

[1] Faculty of Resource Science and Technology, Universiti Malaysia Sarawak, 94300 Kota Samarahan, Sarawak, Malaysia; [2] Fakulti Sains Gunaan, Universiti Technology Mara Sarawak, Kampus Samarahan 2, 94300 Kota Samarahan, Sarawak
*Corresponding authors: znhisam@unimas.my
Received: 9 May 2023 Accepted: 4 April 2024 Published: 30 June 2024

ABSTRACT

Garcinia spp. have been used in traditional medicine to treat various ailments, and recent studies have confirmed their pharmacological activities. In this context, the present study focused on three *Garcinia* spp., namely *Garcinia rostrata*, *Garcinia dryobalanoides* and *Garcinia cuneifolia*, which gain less attention in terms of their phytoconstituent and biological activity data. Methodologically, in this study, the phytochemical constituents of the three *Garcinia* sp. was determined through gas chromatography mass spectrometry (GC-MS) whereby the antimicrobial activity was evaluated using the Disc diffusion and Dilution method. The results showed that the extract from *Garcinia dryobalanoides* exhibited the most potent antibacterial activity against *Bacillus amyloliquefaciens* compared to the other species. The phytochemical analysis found that *Garcinia dryobalanoides* extract contained significant amounts of (Z)-18-Octadec-9-enolide and *n*-hexadecanoic acid, which are known to possess antibacterial properties. These major constituents were found to interact synergistically to produce the observed antibacterial activity. The findings suggested that *Garcinia dryobalanoides* could be a promising source for developing new antibiotics to combat bacterial infections. Overall, this study highlights the potential of *Garcinia* spp. for discovering new bioactivities, particularly their antibacterial properties. Further research is needed to explore the full range of phytochemical constituents and biological activities of these plants, which could lead to the development of new drugs to combat antibiotic resistance.

Keywords: Antimicrobial activity, *Garcinia*, GCMS, phytochemical analysis

INTRODUCTION

Plants have been used in medicine for a long time as natural remedies to cure diseases. Certain plant species have shown remarkable efficacy in combating microbial threats, implying a wealth of potential in the natural world (Parekh & Chanda, 2007). These properties were associated with the abundance of secondary metabolites such as phenolic compounds, terpenoids, flavonoids, and alkaloids (Othman *et al*., 2019; Kianfe *et al*., 2020). These compounds have an outstanding ability to prevent the growth of viruses, bacteria, and fungi.

Garcinia is the largest and taxonomically significant genus within the family Clusiaceae. It comprises nearly 250 species worldwide (Garden *et al*., 2020). The genus *Garcinia* is found abundantly in Malaysia (Khapare *et al*., 2020; Dominic *et al*., 2015), a tropical rainforest country that is rich with flora and fauna (Surbramaniam, 2013). The morphology of *Garcinia* varies depending on the species. Generally, *Garcinia* plants are evergreen trees or shrubs that can grow up to 20-25 m tall, although some species may be smaller (Wu *et al*., 2022). The leaves of *Garcinia* spp. are usually glossy and dark green, and they are arranged in pairs or whorls. The leaves can be simple or compound, and they range in size from 15 to 20 cm in length (Guedje *et al*., 2007). Meanwhile, its barks are usually brown or grey and are rough to the touch (Bora *et al*., 2017). *Garcinia* spp. is known for having good biological activities to combat many diseases owing to the existence of compounds that have significant therapeutic properties (Nguyen *et al*., 2017) such as oxygenated and prenylated xanthones. These compounds have excellent biological activity as

an anti-fungal (Adekunle *et al*., 2020), anti-inflammatory (Feng *et al*., 2021), anti-tumour (Jin *et al*., 2019), anti-oxidant (De Melo *et al.*, 2021), human immunodeficiency virus (HIV)-inhibitory (Corona *et al*., 2021) and antilipidemic properties (John *et al*., 2019).

To date, antibiotic resistance has been a major threat to global health, food security, and development. This escalating public health crisis crosses geographical and demographic boundaries, jeopardising the effective treatment of a wide range of infectious diseases in people of all ages and from all countries. In fact, infections such as pneumonia, tuberculosis, gonorrhoea, and salmonellosis are becoming more difficult to treat as antibiotics used to treat these diseases become less effective (WHO, 2020). This situation leads to an increased mortality rate hence, there is a need to search for a novel antibiotic to combat antibiotic resistance (Varela *et al*., 2021). Currently, there are 30,0000 antibiotic compounds that have been successfully identified from natural products (Thirumurugan *et al*., 2018). *Garcinia* is known for its anti-microbial activity in fighting various bacteria strains (Lin *et al*., 2021). For instance, *Garcinia gummi-gutta* essential oil contains high chemical constituents of (E)-β-farnesene and β-caryophyllene, which inhibits methicillin-resistant *Staphylococcus aureus* (MRSA) (Tan *et al*., 2020). Other than that, Garcigerin A and a-mangostin (xanthone) isolated from *Garcinia dulcis* show remarkable inhibition towards two pathogens, *S. aureus* and MRSA (Tamhid *et al*., 2019). Besides xanthone, bioflavonoids isolated from *Garcinia livingstonei* show excellent bacteria inhibition activity toward some nosocomial bacteria (Kaikabo and Eloff, 2011). Triterpene, namely Friedline isolated from *Garcinia latissima*, exhibits anti-bacterial activity against *Bacillus subtilis* (Ambarwati *et al*., 2019).

With this understanding, three Garcinia spp., namely *Garcinia dryobalanoides*, *Garcinia rostrata*, and *Garcinia cuneifolia* were investigated for their qualitative phytochemical analysis and their antimicrobial activity.

MATERIALS AND METHODS

Plant Material

The stem bark of *Garcinia rostrata* (UITM3022) was collected from Aluvial Forest, Jalan Sungai Moyan, Sarawak. For *Garcinia dryobalanoides* (UITM3032) and *Garcinia cuneifolia* (UITM 3025), the stem barks were collected from Semanggoh, and Keranggas Forest, Jalan Sungai Cina Matang, Sarawak, respectively. All samples were identified by a botanist.

Chemical and Solvent

A chromatography or an analytical grade solvent were used throughout this study. All chemicals were purchased from Merck (Darmstadt, Germany) and Sigma-Aldrich (Chemie, Steinheim, Germany)

Preparation of Plant Extract

The collected plant samples were air-dried and ground into fine powder. The powdered stem bark of *Garcinia rostrata*, *Garcinia dryobalanoides*, and *Garcinia cuneifolia* underwent maceration three times with increasing polarity solvents (hexane, ethyl acetate, and methanol) for 72 h. The macerated plant sample was then filtered, and the filtrates were allowed to evaporate under reduced pressure to obtain dry plant extracts of hexane, ethyl acetate, and methanol (Zamakshshari *et al*., 2016).

Anti-bacterial Assay

All bacteria stock cultures were preserved in Muller-Hinton Broth and stored at 4 °C. The antimicrobial activities were tested against two bacteria: two gram-positive (*Bacillus amyloliquefaciensand* and *S. aureus*) and two gram-negative (*Pseudomonas aeruginosa* and *Escherichia coli*). All of the bacteria strains were obtained from the Microbiology Laboratory at Universiti Malaysia Sarawak's Faculty of Resources Science and Technology. The diffusion method was applied to identify the antibacterial activities (Zamakshshari *et al*., 2022) with 1 mg/mL of concentration for each extract. The antimicrobial activities were assessed by measuring the diameter of zone inhibition after incubating the plates for 24 h at 37 °C. Positive and negative controls that were used for the antibacterial assay were streptomycin sulphate (10 µg/mL) and dimethyl sulfoxide (DMSO), respectively. Broth microdilution assay, on the other hand, were implemented to determine the minimum inhibitory concentration (MIC) the plant extract.

Serial dilutions of the plant extracts (1.0 mg/mL – 1.95 ug/mL) were used for the assay. Each well containing the diluted extract was supplemented with 20 µL of a 5 mg/mL TTC solution and incubated at 37 °C for 1 hour. Reduction of TTC to a pink formazan by viable microbes was used as an indicator of growth. The MIC value was determined from the lowest concentration that remained colourless. Then, from each MIC broth tube without visible growth, 100 µL of broth was pipetted onto Muller-Hinton agar and spread across the entire surface of the plate to determine the minimum bactericidal concentration (MBC). The plate was incubated for 18 – 24 h at 35 °C prior to examination of the colony growth on each plate.

Gas Chromatography Mass Spectrometry (GC-MS)

GC-MS was carried out using a Shimadzu GCMS-QP2010 Plus spectrometer. The constant pressure was set at 100.0 kPa and helium was used as the carrier gas. An RTX-5MS fused silica capillary column (30 m × 0.25 mm) with a film thickness of 0.25 µm was used in the GC-MS. Injection was performed in splitless mode at 300 °C in the injector. The temperature of the oven was increased by 4 °C/min from 40 to 160 °C (5-minute hold) and by 5 °C/min from 160 to 280 °C (15-minute hold). Each sample analysis was completed within a total run time of approximately 74 minutes. The GC-MS interface temperature was maintained at 280 °C. MS mode was used for analytical scanning between 45 and 500 atomic mass units (amu). The ion source temperature was set to 280 °C. Peaks were identified using the National Institute of Standards and Technology Mass Spectral Library (NIST17).

RESULTS & DISCUSSION

Extraction

The extraction of bioactive compounds from plants is essential for the nutraceutical and pharmaceutical industries. This process is critical to preserving the active ingredients in herbal plants and preventing their loss or destruction during preparation. Extracts obtained from plants provide a vast array of valuable compounds that are useful for further analysis and research. Therefore, the extraction step is vital before analysing the herbal plants for their potential benefits (Yahya *et al*., 2018). In this study, three *Garcinia* spp.: *Garcinia dyrobalanoides*, *Garcinia rostrata* and *Garcinia cuneifolia*, were extracted using maceration method with three solvents with different polarities namely ethyl acetate, methanol and hexane. The purpose of using three different polar solvents in the extraction of plants is to obtain a broad spectrum of chemical constituents that may have varying polarities and solubilities (Aissou *et al*., 2017). The results showed that *Garcinia dyrobalanoides* and *Garcinia rostrata* had a high percentage yield for the ethyl acetate extract compared to their methanol and hexane extracts (Table 1). This indicates that these two plant species are rich in semipolar compounds, which are soluble in ethyl acetate. On the other hand, the results showed that *Garcinia cuneifolia* had a high percentage yield of methanol extract compared to other extracts. This result indicated that *Garcinia cuneifolia* contains high-polar compounds that are more soluble in methanol. In addition, the findings suggested that the solvent used for plant extraction can significantly impact the yield and composition of the extract obtained.

Table 1. Percentage yield of extract obtained from *Garcinia dryobalanoides*, *Garcinia cuneifolia* and *Garcinia rostrata*

Species	Extract	Weight of plant sample (kg)	Extract weight (g)	Percentage yield (wt/wt)
Garcinia dryobalanoides	Hexane	3.40	41.40	1.22
	Ethyl Acetate		161.05	4.73
	Methanol		69.87	2.05
Garcinia cuneifolia	Hexane	0.51	2.66	0.52
	Ethyl Acetate		11.04	2.16
	Methanol		29.85	5.85
Garcinia rostrata	Hexane	1.32	3.07	0.23
	Ethyl Acetate		172.09	13.01
	Methanol		84.58	6.39

Antimicrobial Assay

The well diffusion method was used to screen the antimicrobial activity of extracts obtained from *Garcinia dryobalanoides*, *Garcinia rostrata* and *Garcinia cuneifolia* against selected bacteria. The screening results are tabulated in Table 2. A concentration of one mg/mL of the extract was used, as per the guidelines set by Pretto *et al*. (2004), which considers a plant extract with more than 1000 µg/mL as weak antimicrobial activity. All extracts of *Garcinia dryobalanoides* and the ethyl acetate extract of *Garcinia cuneifolia* showed good antimicrobial activity against *B. amyloliquefaciens* compared to other extracts. The antimicrobial activity is due to the presence of major compounds such as (Z)-18-octadec-9-enolide, n-hexadecanoic acid, 2-Propenoic acid, Octabenzone and 1,6,10,14,18,22-Tetracosahexaen-3-ol.
Meanwhile, none of the extracts demonstrated an inhibition zone against *S. aureus*. For the gram-negative bacteria, only the methanol extract of *Garcinia dryobalanoides* and the ethyl acetate extract of *Garcinia cuneifolia* showed more than a 10 mm inhibition zone against *E. coli* and *P. aeruginosa*, respectively. The extracts that showed more than a 10 mm inhibition zone were further evaluated for their minimum inhibitory concentration (MIC) value. The results showed that both ethyl acetate and methanol extracts of *Garcinia dryobalanoides* had MIC values of 500 µg/mL against *E. coli*, which are considered to have moderate antimicrobial activity (Pretto *et al.*, 2004). Moderate activity was also seen in the inhibition against *B. amyloliquefaciens* by *Garcinia dryobalanoides* and *Garcinia cuneifolia* extract. Only the ethyl acetate extract of *Garcinia dryobalanoides* gave a 250 µg/mL MIC value against *B. amyloliquefaciens*. Meanwhile, other extracts, such as hexane and methanol extract of *Garcinia dryobalanoides* and ethyl acetate extract of *Garcinia cuneifolia*, gave 500 µg/mL MIC values against *B. amyloliquefaciens*. It can be concluded that the evaluated Garcinia spp. exhibited bacteriostatic characteristics by their ability in inhibiting bacteria growth.

Table 2. Inhibition diameter of crude extract on garcinia species and positive control against selected microbes.

Plant	Extract	Inhibition zone (mm)			
		Bacteria strain tested			
		Bacillus amyloliquefaciens	*Staphyloccus aureus*	*Escherichia coli*	*Pseudomonas aeruginosa*
Garcinia dryobalanoides	Hexane	13.33 ± 0.57	NA	9.00 ± 0.00	NA
	Ethyl Acetate	14.33 ± 0.57	NA	10.00 ± 1.00	NA
	Methanol	11.66 ± 1.52	NA	11.00 ± 1.71	9.67 ± 0.57
Garcinia cuneifolia	Hexane	NA	NA	8.00 ± 1.00	NA
	Ethyl Acetate	14.00 ± 1.00	NA	9.33 ± 1.73	11.33 ± 0.57
	Methanol	NA	NA	9.00 ± 1.00	9.67 ± 0.57
Garcinia rostrata	Hexane	NA	NA	7.00 ± 1.00	NA
	Ethyl Acetate	8.67 ± 0.57	NA	9.33 ± 1.15	NA
	Methanol	NA	NA	9.00 ± 1.00	7.67 ± 0.57
Streptomycin		23.67 ± 0.57	24.33 ± 0.58	28.67 ± 0.57	26.00 ± 1.73
DMSO		NA	NA	NA	NA

GC-MS Analysis

The investigation on phytochemical was to analyse the chemical constituents present in various extracts of garcinia using GC-MS. The GC-MS is a powerful analytical technique that separates and identifies complex mixtures of chemicals present in a sample. The researchers analysed the chemical constituents of each extract and compared them to identify the common compounds present in most of the extracts. The results were documented in Table 3. Compounds with a selective index (SI) greater than 80% were identified with a compound name, whereas those with a SI less than 80% remained unclassified when their mass spectrum was compared to the NIST database. A total of 147 different chemical constituents were detected in all the *Garcinia* extracts, including phenols, terpenoids, acyclic alkene, phenylpropanoids, acid and others. Interestingly, the profiling of all *Garcinia* extracts revealed that (Z)-18-Octadec-9-enolide was present in each extract. This compound is also found as a

major component in other plant species such as *Imperata cylindrica* and *Millettia zechiana* (Lalthanpuii *et al*., 2019; Chama *et al*., 2022). The presence of this compound in *Garcinia* extracts suggests its potential as a bioactive compound in *Garcinia*. Furthermore, the GCMS analysis found nine compounds belonging to the family of terpenoids in some of the extracts. In general, terpenoids are cyclic unsaturated hydrocarbons that are linked to the basic isoprene skeleton and have constituent groups that vary in oxygen content. Terpenoids are present in most fruits and plants (Caputi & Aprea 2011). Previous research suggests that terpenoids have potential as protective agents and treatments for chronic illnesses including cancer and heart disease (Wagner, & Elmadfa, 2003).

Table 3. Forty Common chemical composition founds in three *Garcinia* spp.

No.	Compounds	% compound in extract (10mg extract)								
		Garcinia dryobalanoides			*Garcinia cuneifolia*			*Garcinia rostrata*		
		HEX	EA	MeOH	HEX	EA	MeOH	HEX	EA	MeOH
1	3H-3a,7-Methanoazulene	0.67	N.D	N.D	1.26	N.D	N.D	0.54	N.D	N.D
2	2,5-di-tert-Butyl-1,4-benzoquinone	0.32	0.17	N.D	N.D	N.D	N.D	N.D	N.D	N.D
3	1-Nonadecene	2.68	3.60	0.85	N.D	N.D	N.D	1.51	0.44	3.82
4	7,9-Di-tert-butyl-1-oxaspiro(4,5)deca-6,9-diene-2,8-dione	0.93	1.59	N.D	0.96	N.D	N.D	0.33	N.D	N.D
5	Benzenepropanoic acid	0.44	N.D	0.45	N.D	N.D	N.D	N.D	N.D	N.D
6	Glutaric acid	0.10	0.14	N.D	N.D	N.D	N.D	N.D	N.D	N.D
7	*n*-Hexadecanoic acid	6.71	9.27	N.D	17.33	6.41	0.23	2.57	2.88	7.03
8	9-Octadecenoic acid	0.30	0.79	1.48	N.D	N.D	0.19	N.D	N.D	N.D
9	Methyl stearate	1.24	1.46	0.52	N.D	0.65	N.D	0.49	0.48	0.97
10	(Z)-18-Octadec-9-enolide	6.61	12.86	8.21	45.26	27.01	5.04	9.57	13.42	28.04
11	Octadecanoic acid	2.05	2.21	N.D	N.D	1.35	N.D	N.D	N.D	N.D
12	1-Hexacosanol	3.60	4.67	N.D	N.D	N.D	N.D	N.D	N.D	N.D
13	2-Propenoic acid	2.80	2.52	1.12	N.D	6.47	N.D	1.13	3.04	6.55
14	Bis(2-ethylhexyl) phthalate	0.63	N.D	N.D	N.D	0.42	N.D	N.D	N.D	N.D
15	Tetrapentacontane	0.19	0.21	N.D	N.D	N.D	N.D	N.D	N.D	N.D
16	Octabenzone	7.26	8.31	2.20	N.D	10.48	N.D	0.70	2.45	5.16
17	alpha.-Tocospiro B	1.15	0.61	N.D	N.D	N.D	N.D	N.D	N.D	N.D
18	2,6,10,14-Hexadecatetraen-1-ol	3.22	3.85	N.D	N.D	N.D	N.D	0.78	N.D	N.D
19	(R)-2,8-Dimethyl-2-((3E,7E)-4,8,12-trimethyltrideca-3,7,11-trien-1-yl)chroman-6-ol	3.74	0.56	0.95	N.D	N.D	N.D	N.D	N.D	N.D
20	beta.-Sitosterol acetate	0.88	N.D	1.09	N.D	1.97	N.D	0.76	2.41	4.64
21	1,6,10,14,18,22-Tetracosahexaen-3-ol	22.82	14.00	18.00	N.D	10.66	N.D	4.19	N.D	N.D
22	Stigmasterol	1.70	1.90	3.78	N.D	N.D	N.D	N.D	N.D	N.D
23	Cyclopentadecanone	N.D	0.99	N.D	5.38	N.D	0.29	0.24	N.D	N.D
24	alpha.-Amyrin	N.D	1.90	3.69	N.D	N.D	23.26	N.D	N.D	N.D
25	gamma.-Sitostenone	N.D	0.53	N.D	N.D	N.D	7.97	N.D	N.D	N.D
26	Friedelan-3-one	N.D	2.27	8.88	N.D	N.D	32.99	10.07	9.26	11.19
27	beta.-Amyrone	N.D	0.53	N.D	N.D	N.D	0.64	N.D	N.D	N.D
28	(E)-9-Octadecenoic acid ethyl ester	N.D	N.D	0.57	N.D	2.56	N.D	N.D	N.D	N.D
29	1-Heptacosanol	N.D	N.D	2.26	N.D	1.77	N.D	2.18	1.90	4.59
30	24-Norursa-3,12-diene	N.D	N.D	4.66	N.D	N.D	N.D	0.52	N.D	N.D
31	Linoleic acid	N.D	N.D	6.72	1.49	1.40	N.D	3.07	N.D	N.D
32	Thunbergol	N.D	N.D	0.67	N.D	N.D	N.D	0.54	N.D	N.D
33	Tricyclo[20.8.0.0(7,16)]triacontane	N.D	N.D	28.68	N.D	N.D	N.D	52.29	38.52	13.37
34	Copaene	N.D	N.D	N.D	1.02	N.D	N.D	0.22	N.D	N.D
35	Caryophyllene	N.D	N.D	N.D	0.68	N.D	N.D	0.79	N.D	N.D
36	Pentadecanoic acid	N.D	N.D	N.D	N.D	0.43	N.D	N.D	0.36	N.D
37	Heptadecanolide	N.D	N.D	N.D	N.D	1.07	N.D	N.D	0.27	N.D
38	11,14-Eicosadienoic acid	N.D	N.D	N.D	N.D	0.78	N.D	N.D	0.28	0.80
39	28-Norolean-17-en-3-one	N.D	N.D	N.D	N.D	1.72	N.D	N.D	3.07	6.74
40	Stigmasta-5,22-dien-3-ol	N.D	N.D	N.D	N.D	1.67	N.D	N.D	0.85	N.D

HEX = hexane extract, EA= ethyl acetate extract, MeOH = methanol extract and N.D = not detected.

Correlation of Anti-BacteriaL Activity with Chemical Constituents of the Extract

The chemical constituents present in an extract contribute to the anti-bacterial activity. The results showed that the presence of major constituents such as (Z)-18-octadec-9-enolide, *n*-hexadecanoic acid, 2-Propenoic acid, Octabenzone and 1,6,10,14,18,22-Tetracosahexaen-3-ol in all *Garcinia dryobalanoides* extracts and the ethyl acetate extract of *Garcinia cuneifolia* has led to inhibition of *B. amyloliquefaciens*. These major compounds are interacted synergistically among them and increase their anti-microbial activity. Previous research reported that the presence of

n-hexadecanoic acid can moderately antibacterial activities against several bacteria strains, such as *K. pneumoniae, E. coli, B. subtilis*, and *S. aureus* at low maximum concentrations (Ganesan *et al*., 2022). Besides that, the presence of more than 30% of (Z)-18-Octadec-9-enolide in the extract is reported to lead to good antimicrobial activity (El-Sayed *et al*., 2023). However, even though some extracts contain those compounds as major constituents, the weak anti-bacterial activity shown might be due to antagonistic interactions between major and minor compounds. The synergistic and antagonistic interactions of chemical constituents in a plant extract refer to the way these constituents can interact with each other to produce either a greater or a lesser effect than expected. Synergistic interactions occur when two or more constituents work together to produce a stronger effect than each constituent could produce on its own (Caeser & Cech., 2019). Meanwhile, antagonistic interactions occur when two or more constituents work against each other, resulting in a weaker effect than expected (Guo *et al*., 2019).

CONCLUSION

The qualitative phytochemical analysis and antibacterial activity of three Garcinia spp., namely *Garcinia dryobalanoides*, *Garcinia rostrata*, and *Garcinia cuneifolia* towards four bacteria strains were fully established. Among all, *Garcinia dryobalanoides* extract demonstrated good biological activities compared to others owing to the synergistic interactions of chemical constituents present in the extract. This study is crucial as the identification of extract activities and phytochemical analysis is vital for herbal product development and acts as a bioactive marker or fingerprint for herbal standardisation. Despite that, further study on the isolation and extraction of chemical constituents from Garcinia species, specifically *Garcinia dryobalanoides* is essential to determine their potential as drug candidates to combat the antibiotic resistance that has become one of the most serious threats to world health, food security and development.

ACKNOWLEDGEMENTS

The authors express our utmost gratitude to Universiti Malaysia Sarawak (UNIMAS) for providing financial funding under the PILOT research (UNI/F07/PILOT/85386/2022) grant as well as research facilities and technical support. The Sarawak Biodiversity Centre (SBC) is also acknowledged.

REFERENCES

Adekunle, F.F., Similoluwa, F.A. & Adewale, A. S. (2020). Investigation of the effectiveness of biosynthesised gold nanoparticle from *Garcinia kola* leaves against fungal infections. *International Journal of Nanoparticles*, 12(4): 316-326.

Ambarwati, N.S.S., Elya, B., Malik, A., Hanafi, M. & Omar, H. (2019). Isolation, characterization, and antibacterial assay of friedelin from *Garcinia latissima* Miq. leaves. *Journal of Physics: Conference Series*, 1402(5): 055078.

Aissou, M., Chemat-Djenni, Z., Yara-Varón, E., Fabiano-Tixier, A.S. & Chemat, F. (2017). Limonene as an agro-chemical building block for the synthesis and extraction of bioactive compounds. *Comptes Rendus Chimie*, 20(4): 346-358.

Bora, N.S., Kakoti, B.B., Yadav, P., Gogoi, B. & Borah, S. (2017). Phyto-physicochemical, acute and subacute toxicity studies of *Garcinia lanceifolia* Roxb. A rare ethnomedicinal plant of Assam, India. *Indian Journal of Natural Products and Resources*, 8(4): 360-369.

Chama, M.A., Egyir, B. & Owusu, K.B.A. (2022). Phytochemical Composition and In Vitro Antibacterial Activities of *Millettia Chrysophylla* and *Millettia Zechiana*. *Journal of Science and Technology* (Ghana), 40(1): 66-85.

Corona, A., Seibt, S., Schaller, D., Schobert, R., Volkamer, A., Biersack, B. & Tramontano, E. (2021). Garcinol from *Garcinia indica* inhibits HIV-1 reverse transcriptase-associated ribonuclease H. *Archiv de Pharmazie*, 354(9): 2100123.

Caputi, L. & Aprea, E. (2011). Use of terpenoids as natural flavouring compounds in food industry. *Recent patents on food, nutrition & agriculture*, 3(1): 9-16.

Caesar, L. K., & Cech, N. B. (2019). Synergy and antagonism in natural product extracts: when 1+ 1 does not equal 2. *Natural product reports*, 36(6): 869-888.

Dominic G., Idris S., Md S.M.S., Umar S., Pearlycia B., William W.W.W., Md Harun N. (2015). Traditional Knowledge and Practices Related to Genus Citrus, *Garcinia*, *Mangifera* and *Nephelium* in Malaysia. *Open Access Library Journal*, 2(4): 1-11

De Melo, A.M., Almeida, F.L.C., De Melo Cavalcante, A.M., Ikeda, M., Barbi, R.C. T., Costa, B.P. & Ribani, R.H. (2021). *Garcinia brasiliensis* fruits and its by-products: Antioxidant activity, health effects and future food industry trends-A bibliometric review. *Trends in Food Science & Technology*, 112: 325-335.

El-Sayed, H., Hamada, M.A., Elhenawy, A.A., Sonbol, H., & Abdelsalam, A. (2023). Acetylcholine Esterase Inhibitory Effect, Antimicrobial, Antioxidant, Metabolomic Profiling, and an In Silico Study of Non-Polar Extract of The Halotolerant Marine Fungus *Penicillium chrysogenum* MZ945518. *Microorganisms*, 11(3): 769.

Feng, Z., Chen, J., Feng, L., Chen, C., Ye, Y. & Lin, L. (2021). Polyisoprenylated benzophenone derivatives from *Garcinia cambogia* and their anti-inflammatory activities. *Food & Function*, 12(14): 6432-6441.

Guedje, N.M., Zuidema, P.A., During, H., Foahom, B. & Lejoly, J. (2007). Tree bark as a non-timber forest product: The effect of bark collection on population structure and dynamics of *Garcinia lucida* Vesque. *Forest ecology and management*, 240(1-3): 1-12.

Garden, R. B. & Howrah, K. (2020). On the Correct Identity and Distribution of *Garcinia talbotii* Raizada ex Santapau (Clusiaceae) in Western Ghats, India. *Indian Forester*, 146(3): 272-275.

Ganesan, T., Subban, M., Christopher Leslee, D. B., Kuppannan, S.B. & Seedevi, P. (2022). Structural characterization of *n*-hexadecanoic acid from the leaves of Ipomoea eriocarpa and its antioxidant and antibacterial activities. *Biomass Conversion and Biorefinery*, 1-12.

Guo, Y., Ghirardo, A., Weber, B., Schnitzler, J. P., Benz, J.P. & Rosenkranz, M. (2019). Trichoderma species differ in their volatile profiles and in antagonism toward ectomycorrhiza *Laccaria bicolor*. *Frontiers in microbiology*, 10: 891.

Jin, S., Shi, K., Liu, L., Chen, Y. & Yang, G. (2019). Xanthones from the bark of *Garcinia xanthochymus* and the mechanism of induced apoptosis in human hepatocellular carcinoma HepG2 cells via the mitochondrial pathway. *International Journal of Molecular Sciences*, 20(19): 4803.

John, O.D., Brown, L., & Panchal, S.K. (2019). *Garcinia* fruits: Their potential to combat metabolic syndrome. Nutraceuticals and Natural Product Derivatives: Disease Prevention & Drug Discovery; Ullah, M., Ahmad, A., Eds, 39-80.

Kianfe, B.Y., Kühlborn, J., Tchuenguem, R. T., Tchegnitegni, B.T., Ponou, B. K., Groß, J., Teponno, R.B., Dzoyem, J.P., Opatz, T. & Tapondjou, L. A. (2020). Antimicrobial secondary metabolites from the medicinal plant *Crinum glaucum* A. Chev. (Amaryllidaceae). *South African Journal of Botany*, 133: 161-166.

Khapare, L.S., Kadam, J.H., & Shirke, G.D. (2020). Garcinia a medicinally potential genus in Western Ghats. *Journal of Pharmacognosy and Phytochemistry*, 9(5): 2750-2752.

Kaikabo A.A. & Elof J. N. (2011). Anti-bacterial activity of two bioflavonoids from *Garcinia livingstonei* leaves against *Mycobactrerium smegmatis*. *Journal of Ethnopharmacology*, 138: 253-255.

Lin, F., Li, P., Yue, G.G.L., Bik-San Lau, C., Kennelly, E. & Long, C. L. (2021). *Garcinia* Plants. *Medicinal Plants and Mushrooms of Yunnan Province of China* (pp. 193-216). CRC Press.

Lalthanpuii, P.B. & Lalchhandama, K. (2019). Chemical profiling, antibacterial and antiparasitic studies of *Imperata cylindrica*.

Journal of Applied Pharmaceutical Science, 9(12): 117-121.

Nguyen, D.C., Timmer, T.K., Davison, B.C. & McGrane, I.R. (2017). Possible *garcinia cambogia*- induced mania with psychosis: A case report. *Journal of Pharmacy Practice*, 32: 99–102.

Othman, L., Sleiman, A. & Abdel-Massih, R.M. (2019). Antimicrobial activity of polyphenols and alkaloids in middle eastern plants. *Frontiers in microbiology*, 10: 911.

Parekh, J. & Chanda, S. (2007). Antibacterial and phytochemical studies on twelve species of Indian medicinal plants. *African Journal of Biomedical Research*, 10(2): 175-181.

Pretto, J.B., Cechinel-Filho, V., Noldin, V.F., Sartori, M.R.K., Isaias, D.E.B., & Cruz, A. B. (2004). Anti-microbial activity of fractions and compounds from *Calophyllum brasiliense* (Clusiaceae/Guttiferae). *Zeitschrift Fur Naturforschung C*, 59(9–10): 657–662. DOI: 10.1515/znc-2004-9-1009

Subramaniam, V. (2013). Malaysian herbal heritage. Journal of Tropical Forest Science, 25(4): 592.

Tan, W.N., Tong, W.Y., Leong, C.R., Nik Mohamed Kamal, N.N.S., Muhamad, M., Lim, J.W., Khairuddean, M. & Her Man, M. B. (2020). Chemical composition of essential oil of *Garcinia gummi-gutta* and its antimicrobial and cytotoxic activities. *Journal of Essential Oil Bearing Plants*, 23(4): 832-842.

Tamhid, H.A. (2019). Chemical compounds and antibacterial activity of *Garcinia dulcis* (Roxb) kurz. *Jurnal Kedokteran dan Kesehatan Indonesia*, 10(1): 71-85.

Thirumurugan, D., Cholarajan, A., Raja, S.S.S. & Vijayakumar, R. (2018). An Introductory Chapter: Secondary Metabolites. *Secondary metabolites-sources and applications*. 1:13. DOI: 10.5772/intechopen.79766

Varela, M.F., Stephen, J., Lekshmi, M., Ojha, M., Wenzel, N., Sanford, L.M., Hernandez, A.J., Parvathi, A. & Kumar, S.H., (2021). Bacterial Resistance to Anti-microbial Agents. *Antibiotic*, 10: 593.

Wagner, K.H. & Elmadfa, I. (2003). Biological relevance of terpenoids. *Annals of Nutrition and metabolism*, *47*(3-4): 95-106.

Wu, P.P., Wang, Z., Jia, N.X., Dong, S.Q., Qu, X.Y., Qiao, X.G., Liu, C.C. & Guo, K. (2022). Vegetation Classification and Distribution Patterns in the South Slope of Yarlung Zangbo Grand Canyon National Nature Reserve, Eastern Himalayas. *Plants*, 11(9): 1194.

World Health Organization. (2020). Antimicrobial resistance. Available online at: https://www.who.int/news-room/fact-sheets/detail/antibiotic-resistance, Assessed on 14 May 2022.

Yahya, N.A., Attan, N. & Wahab, R. A. (2018). An overview of cosmeceutically relevant plant extracts and strategies for extraction of plant-based bioactive compounds. *Food and Bioproducts Processing*, 112: 69-85.

Zamakshshari, N.H., Ahmed, I.A., Didik, N.A. M., Nasharuddin, M.N.A., Hashim, N.M., & Abdullah, R. (2022). Chemical profile and antimicrobial activity of essential oil and methanol extract from peels of four *Durio zibethinus* L. varieties. *Biomass Conversion and Biorefinery*, 1-9.

Zamakshshari, N.H., Ee, G.C.L., Teh, S.S., Daud, S., Karunakaran, T., & Safinar, I. (2016). Natural Product Compounds from *Calophyllum depressinervosum*. *Pertanika Journal of Tropical Agricultural Science*, 39(2).

Borneo Journal of Resource Science and Technology (2024), 14(1): 88-97
DOI: https:doi.org/10.33736/bjrst.5958.2024

Experimental Study on Phytoremediation of Heavy Metal from Mine Wastewater by *Rumex nepalensis* Spreng.

GERA TECHANE*[1, 4], GEREMEW SAHILU[2] & ELFU AMARE[3]

[1]Ethiopian Institute of Water Resources, Addis Ababa University, Addis Ababa, Ethiopia; [2]Addis Ababa Institute of Technology, Addis Ababa University, Addis Ababa, Ethiopia; [3]School of Mechanical and Industrial Engineering, Ethiopian Institute of Technology, Mekelle University, Mekelle, Ethiopia; [4]Ministry of Mines, Federal Democratic Republic of Ethiopia
*Corresponding author: geratechane@gmail.com
Received: 12 August 2023 Accepted: 15 January 2024 Published: 30 June 2024

ABSTRACT

Tailings pond is considered as the main source of heavy metal pollution in gold mining areas. These heavy metals are directly released into fresh water without proper treatment. Phytoremediation process with the selected terrestrial plants may be an alternative solution for the mine wastewater treatment. In the current study, an experimental investigation found that *Rumex nepalensis* Spreng. has found a good accumulator of multi-metals in 15 days of experimental period. The results revealed that the removal efficiencies for Zn, Cu, Ni and Pb were 100%, 92%, 87%, and 67%, respectively. These indicate the plant showed its maximum accumulation of multi-metals. However, Pb reached saturation at the end of the 10th day, which makes its removal efficiency only in the first 10 days of the experimental period. The experiment revealed Pb and Ni which were above WHO standard for drinking water in the mine wastewater were made to permissible limit for these metals after the treatment.

Keywords: Mine wastewater, phytoremediation, *Rumex nepalensis* Spreng., tailings pond

INTRODUCTION

Rapid urbanization and development have considerably increased the demand for water, as it is a basic necessity of all living organisms (Mustafa & Hayder, 2021). However, some industrial activities introduce toxic pollutants directly into fresh water without proper treatment (Gupta & Shukla, 2020). Industrial wastewater is a major problem due to high concentrations of toxic pollutants, particularly heavy metals (Razzak *et al*., 2022). Heavy metal pollution has become a major global concern due to its toxicity (Demková *et al*., 2017; Sey and Belford, 2019; Agarwal *et al*., 2022). The presence of heavy metals in wastewater poses a significant risk as it can contaminate surface water and soil, ultimately finding its way into the food chain (Ahmad *et al*., 2022; Tong *et al*., 2022).

Gold processing often leads to the production of substantial quantities of tailings and wastewater, both of which can be sources of heavy metal contaminants (Manyuchi *et al*., 2022). Mine tailings are a mixture of finely powdered rock and water residual after gold has been extracted from a mine (Chen *et al.*, 2018). Mine tailings are the main heavy metal pollution source in gold mining areas (Zhang *et al*., 2020). A previous study has shown that the mine wastewater of the study area contains several heavy metals. Moreover, the mine wastewater is discharged to the nearby water bodies without proper treatment of heavy metals (Getaneh & Alemayehu, 2006). The release of toxic heavy metals from mine tailings can contaminate surface water, groundwater and agricultural soils (Bempah & Ewusi, 2016). Heavy metal contaminants are bio-accumulative and non-biodegradable (Dayal *et al*., 2016; Bouzekri *et al*., 2020) and have a potential to pose health risks to humans and aquatic life in the vicinity of mining areas (Liang *et al*., 2017; Adewumi & Laniyan, 2020).

Various conventional physicochemical and green biological techniques are applied to remove heavy metals. Conventional treatment methods including adsorption, coagulation, flocculation, chemical precipitation, membrane separation, ion exchange, flotation, and electrochemical technologies produce swift results, although they generate contaminated

slurry and more costly compared to bioremediation of heavy metals from wastewater (Razzak *et al*., 2022). Phytoremediation technique is a branch of bioremediation that employs the application of plants for the remediation of wastewater (Mustafa & Hayder, 2021). It is a cost-effective and environmental friendly technology of wastewater treatment (Kumar *et al.*, 2017). Heavy metal pollution and its repercussion for human health have increased research in developing low cost and sustainable remediation technology (Razzak *et al*., 2022). Therefore, the use of plants to remediate water pollution is currently attracting scientific community, as it provides a sustainable, cost-effective, less harmful and eco-friendly process (Kumar & Chopra, 2018; Razzak *et al*., 2022).

Rumex nepalensis is an herbaceous plant belongs to Polygonaceae family which has been used as traditional herbal medicine (Yadav *et al*., 2011). The plant has the antibacterial property against some strains of bacteria (Pal & Saha, 2003). The leafy vegetable of the *R. nepalensis* has antioxidant potential (Anusuya *et al*., 2016; Kumar & Singh, 2020) and its consumption will prevent aging related diseases (Anusuya *et al*., 2016). In Ethiopia, the plant is traditionally used for the treatment of stomach ache, tonsillitis, ascariasis, and uterine bleeding (Dabe *et al*., 2020). Moreover, some studies have shown the plant's potential for phytoremediation (Ahmad *et al*., 2022; Aras, 2022). A study undertaken in Uranium Mine of Southwestern China revealed the highest accumulation of uranium metal by the plant (Li *et al*., 2019).

Currently, various research results have been achieved in the phytoremediation of heavy metals from wastewater by using aquatic plant (Chaudhary & Sharma, 2019; Abbas *et al*., 2021; Panneerselvam & Priya, 2021). Aquatic plants are plants that grow in or near water and are either emergent, submersed, or floating (Balamoorthy *et al*., 2022). Aquatic plants have potential to absorb pollutants such as heavy metals found in domestic, agricultural and industrial wastewaters (Mustafa & Hayder, 2021). However, limited research has been done on the treatment of wastewater using terrestrial plants. Terrestrial plants are those plants which are largely dominating land surfaces (Beraldi-campesi, 2013). *Rumex nepalensis* was selected among other terrestrial plants based on previous research by Mengistu *et al*. (2023). In this study, the translocation factor which is the plant's ability to transport Cu, Ni and Pb in the upper part of the plant were reported 2.84, 1.5, and 3.0 respectively. These values can be considered as indicators for the plant's potential for phytoextraction (Waris *et al.*, 2022; Mengistu *et al.*, 2023). Furthermore, there were few studies which used terrestrial plants to treat particularly using real wastewater. Among the few reported studies, most of them used synthetic wastewater prepared in laboratories. Therefore, this work is an experimental investigation of heavy metal removal efficiency of *R. nepalensis* from mine wastewater at laboratory scale.

MATERIALS AND METHODS

Sample Collection

Wastewater sample was collected from Legadembi Gold Mine which is located at about 500 km south of the Capital, Addis Ababa. The longitude and latitude of tailing pond is 38.899453° and 5.7208514°. The wastewater sample was taken using polyethylene bottles, previously rinsed with mine water from the sampling site and brought to the laboratory for experimental investigation.

The herbaceous plant species, *R. nepalensis*, which was abundantly grown around the tailing pond was uprooted and packed in polyethylene bags and then transported to laboratory for the purpose of mine wastewater treatment. The plant was selected among other terrestrial plants based on literature review, its production of densely branched roots and high above-ground biomass (Ali *et al.* 2013). Moreover, the plant was selected among other plants based on previous research by Mengistu *et al.* (2023). In their study, the plant has showed efficient translocation of heavy metals especially, Cu, Ni and Pb in the upper part of the plant.

Experimental Setup

The experiment was performed at laboratory scale with adequate amount of sunlight and air by using *R. nepalensis* in order to investigate the percentage removal of heavy metals from mine wastewater (Figure 1). The plants were first cleaned of dirt and then the acclimatisation was undertaken. Acclimatisation process was carried out for three days, which is a process of adapting the plants to the new planting medium, and the

surrounding conditions (Ratna & Slamet, 2020). Plants with equal height and weight were used for each treatment pots containing 1 L of the mine wastewater which was filled up to the mark. One fresh and healthy plant was kept in each of the treatment pots. The wastewater sample without the plant species was used as control. The experiment was carried out for 15 days. This time was selected based on the work of Kothari *et al*. (2022) and Singh *et al*. (2021). Duplicate treatments were designed for each of the three variations of time (5 days, 10 days, and 15 days). Plants were removed from two containers in each of the respective time duration, and then the water samples kept for laboratory analysis. Distilled water was added daily to each container to compensate for water loss through plants transpiration and evaporation (Abbas *et al*., 2021). Hoagland solution of 5 mL (Wu *et al*., 2022) was added to the treatment pots each day. The Hoagland nutrient was prepared based on (Buta *et al*., 2014).

Analysis

The wastewater was examined before and after phytoremediation experiments for the selected heavy metals. Water samples were collected from the treatment pots on days: 5, 10, and 15 for analysis. The wastewater was digested according to EPA method 3051A (EPA, 2007) with modification, in a High Performance Microwave Digestion System (ETHOS UP milestone). 50 mL of wastewater was digested with mixtures of concentrated solutions of 5 mL of HNO_3 and 1 mL of HCl. The chemical reagents used were analytical or guaranteed reagent grade. Finally, the solution was transferred into a 50 mL volumetric flask and diluted to 50 mL using distilled water. The solution was then ready for the quantitative analysis of the heavy metals. Hence, the dilution factor becomes 1. Metal concentrations in water sample were calculated as follows Eq. (1):

$$C = \frac{Cs.Vs}{V} \quad \textbf{Eq. (1)}$$

Where: C = Metal concentration (mg/L) in water sample

C_s = Concentration of metal in digested dilute sample (mg/L)

V_s = Final volume of the digested sample solution (mL)

V = Volume of digested sample (mL)

For quality control purpose the same samples were analysed in duplicates and after every five samples, a calibration standard was analyzed to verify the response and efficiency of the analytical instrument. The accuracy of the method was confirmed by using known standard and the recovery of the tested samples using the following Eq. (2). The percentage recovery varied between 83.3% and 116.7%. These values are acceptable recovery which lies within a range of 80% - 120% as shown in Table 1.

$$\%\ \text{Recovery} = \frac{[\text{Spiked sample}] - [\text{Unspiked sample}]}{[\text{Amount added}]} \times 100 \quad \textbf{Eq. (2)}$$

Where, [ ] = concentrations

Table 1. Results of the recovery analysis for the wastewater samples

Heavy metal	Concentration before spiking	Concentration after spiking	Amount added	% Recovery
Cu	0.085±0.005	3.62±0.021	4 mg/L	88.3%
Zn	0.12±0.007	4.13±0.015		100.25%
Pb	0.025±0.005	4.09±0.082		101.6%
Ni	0.05±0.014	4.72±0.250		116.7%
Cd	0.00±0.000	3.96±0.014		99.0%

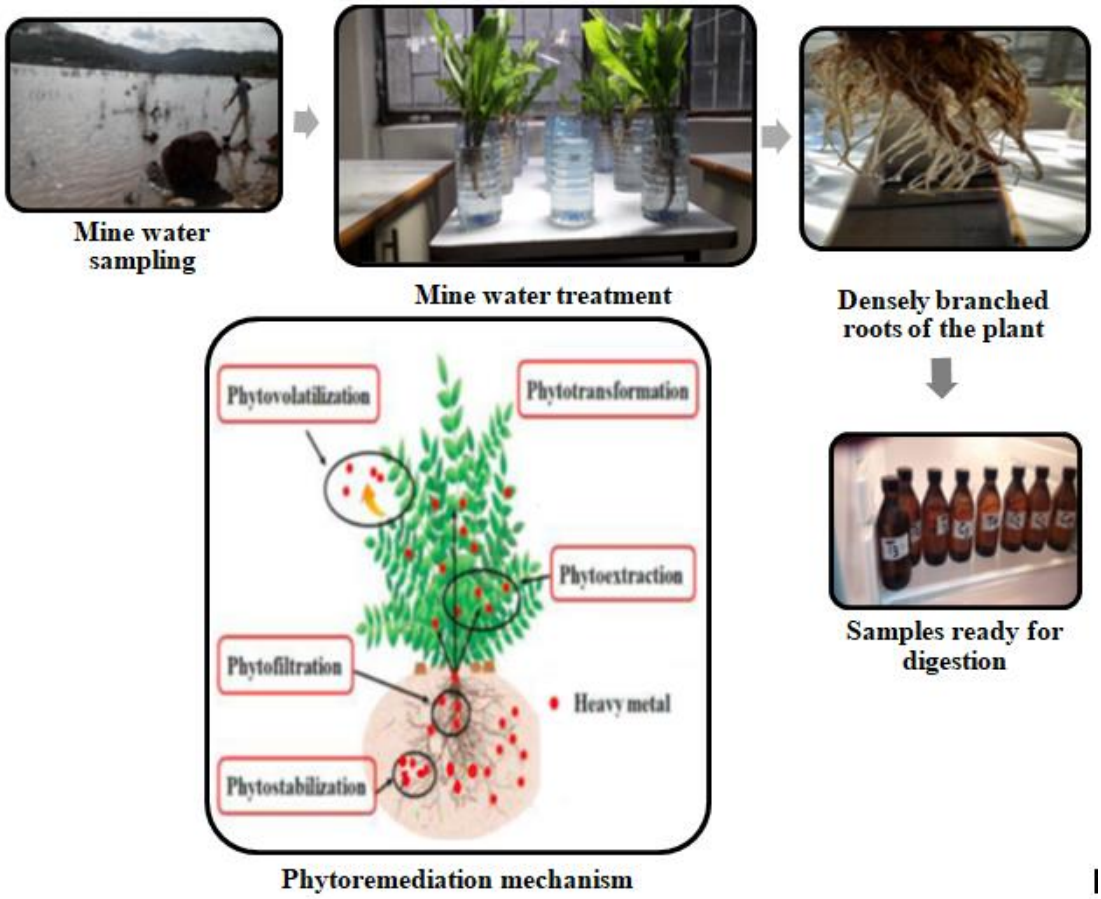

Figure 1. The experimental procedures and heavy metal removal mechanisms

In addition, Blank samples were digested following the same techniques employed for digesting the wastewater samples. Each blank were analysed for the metal contents (Cu, Cd, Zn, Pb and Ni) by MP-AES. The standard deviation (Std) of replicate blanks was calculated to determine method detection limit (MDL) using Eq. (3) (Butcher & Sneddon, 1998; Techane *et al.*, 2019).

MDL= blank mean + Std **Eq. (3)**

The method detection limits of the microwave assisted digestion for the wastewater samples in mg/L were 0.006, 0.010, 0.005, 0.001, and 0.020 for Cu, Cd, Zn, Pb and Ni metals, respectively.

The water samples were analysed for heavy metals Pb, Ni, Zn, Cu and Cd using Agilent Technologies 4200 Microwave Plasma Atomic Emission Spectrometer (MP-AES). Moreover, the pH of water samples was measured using sensION^{TM} + MM150, HACH. All statistical analyses were performed with Microsoft Excel and STATA 14.1. The removal efficiency of the heavy metals (Pb, Ni, Zn, Cu and Cd) was calculated using Eq. (4).

$$\text{Removal efficiency (\%)} = \frac{Ci - Cf}{Ci} \qquad \textbf{Eq. (4)}$$

Where, C_i= the initial concentrations of the heavy metals in the mine wastewater and C_f = the final concentrations of the heavy metals in the treated mine wastewater.

RESULTS AND DISCUSSION

The mechanism of removing heavy metals could be either by phytoextraction, phytostabilization, or phytovolatilization (Chen *et al*., 2023) as showed in Figure 1. Phytoextraction is the removal of heavy metals by aboveground tissues of the plant while phytostabilization is the plant's ability to resist high metal concentrations and halt them within their roots (Priya *et al.*, 2023). Metals are absorbed by the roots and enter the stem through xylem vessels, which are then passed to the stems and then to the leaves through photosynthetic mechanism (Ratna & Slamet, 2020). Real wastewater from tailings

pond of gold mining industry was used to test the phytoremediation potential of *R. nepalensis*. Time dependent removal efficiency of the plant is presented. Table 2 shows the results of the phytoremediation potential for 15 days in five days intervals. The mine waste water was analysed for Cd, Cu, Zn, Pb, and Ni before treatment, and also after five days, 10 days and 15 days of treatments with *R. nepalensis*. The analysis result of Cd was below detection limit both before and after treatments of the mine waste water. The contamination levels of the collected mine wastewater for Pb and Ni metals were beyond the safe limit of WHO for drinking water. The level of Pb and Ni in the tailings pond is about 1.5 and 3.4 times, respectively higher than the standard limit for drinking water (WHO, 2011). Moreover, the level of Ni in the initial mine wastewater is still slightly above the permissible limit set for wastewater discharge (WHO, 2006). Generally, the removal efficiencies exhibited an increasing trend as treatment days increases.

Table 2. The pH and heavy metal concentration (mg/L) before and after treatment

Parameters	Before phytoremediation	After phytoremediation			WHO limit drinking water* *	WHO limit wastewater*
	Co (Initial)	C1 (5^{th} day)	C2 (10^{th} day)	C3 (15^{th} day)		
pH	8.84	8.53	7.98	7.72	6.5-8.5	6.5-8.5
Cu	0.13	0.1	0.025	0.01	2	0.2
Zn	0.05	0.03	0.02	ND	3	2
Pb	0.015	0.01	0.005	0.005	0.01	0.5
Ni	0.24	0.17	0.05	0.08	0.07	0.2

(WHO, 2006*; WHO, 2011**)

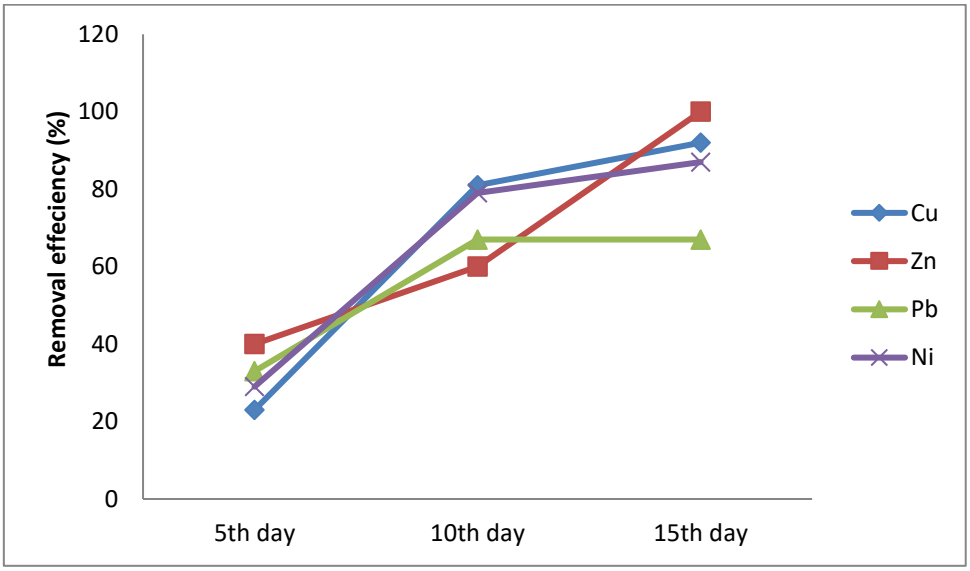

Figure 2. Removal efficiencies of varous metals at regular time interval

The pH values of the mine wastewater were decreased significantly during the phytoremediation using *R. nepalensis*. In this study, the pH in the three intervals of treatment: (5^{th}, 10^{th}, and 15^{th} day) was reduced by 3.51%, 9.73%, and 12.67% respectively. That means at the end of 15 days of treatment, the maximum pH reduction of 12.67% was recorded. In previous studies, (Singh *et al*., 2021) were reported the highest pH reduction of 10.75% in the treatment of paper mill effluent using *P. stratiotes* which was the decrease of pH values from 8.56 to 7.64. In addition, Azeez (2021) has also showed a maximum pH reduction of 7.6% from the sewage treatment unit using *Utricularia vulgaris* L. The variation of the pH might be due to the formation of transitional compounds during the microbial degradation of dissolved organic substances in the wastewater (Singh *et al*., 2021).

The initial concentration of Cu, Zn, Pb, and Ni in the untreated mine wastewater were 0.13

mg/L, 0.05 mg/L, 0.015 mg/L, and 0.24 mg/L, respectively. In other studies, Kothari *et al.* (2022) reported high concentrations of Cu (4.4 mg/L), Zn (7.0 mg/L), Pb (2.6 mg/L), and Ni (3.8 mg/L) in tannery effluents, which are all higher than the levels of the heavy metals in the untreated mine wastewater of this study. However, George *et al*. (2017) used initial concentrations of Cu (0.008 mg/L), Zn (0.05 mg/L), Pb (0 mg/L), and Ni (0.06 mg/L) in municipal wastewaters which are lower than the levels of heavy metals in this study. The concentration of heavy metals in our study decreased to 0.01 mg/L for Cu, 0.01 mg/L for Pb and 0.08 mg/L for Ni on the 15th day of the treatment, while Zn was below detection limit at this final treatment day. The maximum removal efficiencies for Zn, Cu, Ni, and Pb were 100%, 92%, 87%, and 67%, respectively, indicating the highest removal efficiency for Zn, followed by Cu, Ni, and finally Pb (**Error! Reference source not found.**). In other study Balamoorthy *et al*. (2022) has used the synthetic wastewater containing Cd, Pb, and Cu with initial concentrations of 0.25 mg/L, 0.5 mg/L, and 2 mg/L respectively, by introducing *Mimosa pudica* and treating them for 16 days. Their results showed that there was a reduction in Cd, Pb, and Cu to a concentration of 0.02 mg/L, 0.21 mg/L, and 0.4 mg/L level of heavy metals from the wastewater, respectively which showed the plant's ability to accumulate up to 92% of Cd, 58% of Pb, and 80% of Cu.

The concentration of Cu was 0.10 mg/L on the 5th day, 0.025 mg/L on the 10th day, and 0.01 mg/L at the end of the 15th day. The removal efficiency of *R. nepalensis* for Cu from the mine wastewater was enhanced from 23% on the 5th day to 81% on the 10th day and finally became 92% at the end of the treatment schedule. The rate of percentage removal of Cu metal increased as the uptake time increased (Abbas *et al*., 2021). The rate of absorption of Cu was 81% in the early days of treatment indicates at the first 10 days the accumulation process was achieved by the roots only and later the translocation of Cu was carried by the shoots of the plant (Balamoorthy *et al*., 2022). Abbas *et al*. (2021) has showed the highest percentage removal efficiency of Cu with 87.78% at 16 days experiment from industrial wastewater using *Typha latifolia.* Other study by Balamoorthy et al. (2022) which used a terrestrial plant, *Mimosa pudica,* also showed the improvement in the removal of Cu from wastewater from 40% on the 4th day to 80% at the end of the 16th day. Ahmad *et al*. (2022) have reported the potential of *R. nepalensis* which able to accumulate greater than 0.05 g/kg of Cu in its shoots. Furthermore, Aras (2022) has investigated the accumulation of 13.6 mg/L of Cu metal in *R. nepalensis* plant.

The concentration of Zn was recorded 0.03 mg/L on the 5th day, 0.02 mg/L on the 10th day and below detection limit at the end of the 15th day. The removal efficiency of *R. nepalensis* for Zn from the mine wastewater was enhanced from 40% on the 5th day to 60% on the 10th day and finally became 100% on the 15th day. Similar to Cu, the uptake of Zn by the plant has increased as time progressed. In other studies, Abbas *et al*. (2021) have showed the highest percentage removal efficiency of Zn with 75.81% at 16 days experiment from industrial wastewater using *T. latifolia.* Similarly, Azeez (2021) has reported the reduction of Zn in wastewater from 2.92 mg/L to 0.69 mg/L using *U. vulgaris* plant in 21 days of treatment, which is a percentage removal of about 76%. A laboratory-scale experimental investigation on phytoremediation of industrial effluent using *Nelumbo nucifera* Gaertn has also showed a reduction of Zn from 10.14 mg/L to 4.92 mg/L (Al-huqail *et al*., 2022). Moreover, in an investigation undertaken to determine the elemental content of heavy metals by Aras (2022) has reported a total of 45.5 mg/L of Zn in *R. nepalensis* plant.

Lead is among non-essential toxic metals. A continuous consumption of Pb polluted water leads to severe effects on human health such as brain diseases, cognitive and productivity problems, carcinogenic effects, kidney and bones diseases (Panneerselvam & Priya, 2021). The level of Pb in our study reduced to 0.01 mg/L on the 5th day, 0.005 mg/L on the 10th and 15th days. Unlike other heavy metals, the removal efficiency of *R. nepalensis* for Pb from the mine wastewater was recorded 33% on the 5th day to 67% on the 10th day and 15th day. This might be due to a low translocation of Pb to the shoot, which makes Pb immobile compared to the other heavy metals studied (Fritioff *et al*., 2010). From test results, it can be noticed that the root of *R. nepalensis* reached saturation at the end of the 10th day of treatment. This indicates the effective removal of Pb is on the 10th day. This finding is in agreement to a study undertaken by using a terrestrial plant known as

M. pudica which showed, the percentage of removal of Pb on the 16th day was found to be very less in amount compared to the percentage of removal of Cd and Cu (Balamoorthy *et al*., 2022). However, Ratna and Slamet (2020) have showed effective removal of Pb from industrial wastewater containing 0.42 mg/L using *Pistia stratiotes* in six days experiment. Similar to Zn and Cu of our study, the percentage removal of Ni has also enhanced as the treatment days increased.

CONCLUSION

Phytoremediation process with the terrestrial plant may be an alternative solution by putting the plants on a floating bed and keeping the roots in the wastewater. The study results evidenced that the removal efficiency of Zn, Cu, Ni, and Pb were 100%, 92%, 87%, and 67% respectively. The pH values of the wastewater were decreased significantly during the phytoremediation. The plant showed maximum accumulation of multi-metals. However, Pb reached saturation at the end of the 10th day, which makes its effective removal on the first 10 days of experimental period. From the present study, the mine wastewater should be treated by *R. nepalensis* for at least 10 days to reduce the toxic heavy metals especially Ni and Pb to their WHO standard limits. As this phytoremediation experiment has used a real type of wastewater with slightly lower concentrations of heavy metals, further studies are recommended with higher levels of heavy metals using synthetic wastewater or theoretical concentrations in laboratories.

AKNOWLEDGMENTS

The authors would like to acknowledge MIDROC Gold Mine PLC for allowing conducting the study within its license area. No specific grants from public, private, or nonprofit funding organizations were given for this research.

REFERENCE

Abbas, N., Butt, M.T., Ahmad, M.M. & Deeba, F. (2021). Phytoremediation potential of *Typha latifolia* and water hyacinth for removal of heavy metals from industrial wastewater. *Chemistry International*, *7*(2): 103-111.

Adewumi, A.J. & Laniyan, T.A. (2020). Total environment contamination, sources and risk assessments of metals in media from Anka artisanal gold mining area , Northwest Nigeria. *Science of the Total Environment*, *718*: 137235. DOI: 10.1016/j.scitotenv.2020.137235

Agarwal, A., Upadhyay, U., Sreedhar, I. & Anitha, K.L. (2022). Simulation studies of Cu (II) removal from aqueous solution using olive stone. *Cleaner Materials*, *5*(100128): 1-7. DOI: 10.1016/j.clema.2022.100128

Ahmad, I. Gul, S. Irum, M. &. Manzoor A.M. (2022). Accumulation of heavy metals in wild plants collected from the industrial sites - potential for phytoremediation. *International Journal of Environmental Science and Technology*. 20(5): 5441-5452.

Ahmad, S., Bashir, O., Anam, S., Haq, U., Amin, T., Rafiq, A., Ali, M., Heloisa, J. & Sher, F. (2022). Phytoremediation of heavy metals in soil and water : An eco-friendly , sustainable and multidisciplinary approachre. *Chemosphere*, 303: 1-10. DOI: 10.1016/j.chemosphere.2022.134788

Al-huqail, A.A., Kumar, P., Eid, E.M., Taher, M.A., Kumar, P., Adelodun, B., Andabaka, Ž., Mioˇ, B. & Kumar, V. (2022). Phytoremediation of Composite Industrial Effluent Using Sacred Lotus (*Nelumbo nucifera Gaertn*): A Lab-Scale Experimental Investigation. *Sustainability*, 14(15): 9500.

Ali, H., Khan, E. & Sajad, M. A. (2013). Phytoremediation of heavy metals-concepts and applications. Chemosphere, 91(7): 869-881.

Anusuya, N.R., Gomathi, S., Manian, V.S. & Menon, A. (2016). Evaluation of Basella rubra L ., *Rumex nepalensis Spreng* . and Commelina benghalensis L . for antioxidant activity. *International Journal of Pharmacy and Pharmaceutical Sciences*, 4(3): 714-720.

Aras, A. (2022). Determination of Trace Elements in *Rumex nepalensis* , *Inula discoidea* , *Tripleurospermum callosum* , and *Thymus migricus* Plants Using ICP-MS Application. *Journal of the Institute of Science and Technology*, 12(3): 1703-1710. DOI: 10.21597/jist.1103110

Azeez, N.M. (2021). Bioaccumulation and phytoremediation of some heavy metals (Mn , Cu , Zn and Pb) by bladderwort and duckweed. *Biodiversitas*, *22*(5): 2993-2998. DOI: 10.13057/biodiv/d220564

Balamoorthy, D., Velusamy, P., Rath, B. & Kabeto,

J. (2022). Removal of heavy metals from wastewater. *Journal of Civil Engineering, Science and Technology*, 13(1): 23-32. DOI: 10.33736/jcest.4473.2022

Bempah, C.K. & Ewusi, A. (2016). Heavy metals contamination and human health risk assessment around Obuasi gold mine in Ghana. *Environmental Monitoring and Assessment*, 188(5). DOI: 10.1007/s10661-016-5241-3

Beraldi-campesi, H. (2013). Early life on land and the first terrestrial ecosystems. *Beraldi-Campesi Ecological Processes*, 2(1): 1-17.

Bouzekri, S., El Hachimi, M.L., Kara, K., El Mahi, M. & Lotfi, E.M. (2020). Metal pollution assessment of surface water from the abandoned Pb mine Zaida, high Moulouya-Morocco. *Geosystem Engineering*, 23(4): 226-233. DOI: 10.1080/12269328.2020.1772125

Buta, E., Török, A., Csog, Á., Zongo, B., Cantor, M., Buta, M. & Majdik, C. (2014). Comparative Studies of the Phytoextraction Capacity of Five Aquatic Plants in Heavy Metal Contaminated Water. *Notulae Botanicae Horti Agrobotanici Cluj-Napoca*, 42(1): 173-179.

Butcher, D.J. and Sneddon, J.A. (1998) Practical Guide to Graphite Furnace Atomic Absorption Spectrometry. John Wiley and Sons, New York, pp. 34-149.

Chaudhary, E. & Sharma, P. (2019). Chromium and cadmium removal from wastewater using duckweed - *Lemna gibba L* . and ultrastructural deformation due to metal toxicity. *International Journal of Phytoremediation*, 21(3): 279-286. DOI: 10.1080/15226514.2018.1522614.

Chen, X., Feng, J., Mou, H., Liang, Z., Ding, T., Chen, S. & Li, F. (2023). Utilization of indole acetic acid with *Leucadendron rubrum* and *Rhododendron pulchrum* for the phytoremediation of heavy metals in the artificial soil made of municipal sewage sludge. *Toxics*, 11(1): 43.

Chen,Y., Jiang, X., Wang,Y. & Zhuang, D. (2018). Spatial characteristics of heavy metal pollution and the potential ecological risk of a typical mining area: A case study in China. *Process Safety and Environmental Protection* 113: 204-219.

Dabe, N.E., Kefale, A.T. & Dadi, T.L. (2020). Evaluation of Abortifacient Effect of *Rumex nepalensis Spreng* Among Pregnant Swiss Albino Rats : Laboratory-Based Study. *Journal of Experimental Pharmacology*. pp. 255-265

Dayal, S., Pratap, V., & Singh, M.K. (2020). Mathematical Approach to Describe Metal Concentration and Toxicity Growth by Laplace Transform. IOSR Journal of Mathematics, 12(3): 01–06. DOI: 10.9790/5728-1203060106.

Demková, L., Jezný, T. & Bobuľská, L. (2017). Assessment of soil heavy metal pollution in a former mining area–before and after the end of mining activities. *Soil and water Research*, 12(4): 229-236.

EPA. (2007). *Microwavemicrowave assisted acid digestion of sediments, sludges, soils, and oils:method 3051A*. pp. 1-30.

Fritioff, Å., Greger, M., Fritioff, A. & Greger, M. (2010). Aquatic and Terrestrial Plant Species with Potential to Remove Heavy Metals from Stormwater. *International Journal of Phytoremediation*, 5(3): 211-224. DOI: 10.1080/713779221

George, G.T., Gabriel, J.J., Nadu, T. & George, G.T. (2017). Phytoremediation of Heavy Metals from Municipal Waste Water by *Salvinia molesta Mitchell*. *Haya: The Saudi Journal of Life Sciences*, 2(3): 108-115. DOI:10.21276/haya

Getaneh, W. & Alemayehu, T. (2006). Metal contamination of the environment by placer and primary gold mining in the Adola region of southern Ethiopia. *Environmental Geology*, 50(3): 339-352. DOI: 10.1007/s00254-006-0213-5

Gupta, G. K. & Shukla, P. (2020). Insights into the resources generation from pulp and paper industry wastes: challenges, perspectives and innovations. *Bioresource Technology*, 297(9):122496

Kothari, R., Pandey, A., Ahmad, S., Mohan, H., Vinayak, S. & Tyagi, V.P. (2022). Utilization of *Chlorella pyrenoidosa* for Remediation of Common Effluent Treatment Plant Wastewater in Coupling with Co-relational Study : An Experimental Approach. *Bulletin of Environmental Contamination and Toxicology*, *108*(3): 507-517. DOI: 10.1007/s00128-021-03292-7

Kumar, V. & Chopra, A.K. (2018). Phytoremediation potential of water caltrop (*Trapa natans L.*) using municipal wastewater of the activated sludge process-based municipal wastewater treatment plant. *Environmental technology*, 39(1): 12-23.

Kumar, S. & Singh, P.K. (2020). Phytochemical investigation and antioxidant characterization of essential oil from roots of *Rumex nepalensis Spreng* high altitude of North India. *Materials Today: Proceedings*, 26: 3442-3448. DOI: 10.1016/j.matpr.2019.12.227

Li, R., Dong, F., Yang, G., Zhang, W., Zong, M., Nie, X., Zhou, L., Babar, A., Liu, J., Ram, B. K., Fan, C. & Zeng, Y. (2019). Characterization of Arsenic and Uranium Pollution Surrounding a Uranium Mine in Southwestern China and Phytoremediation Potential. *Polish Journal of Environmental Studies*, *28*(6): 173-185. DOI: 10.15244/pjoes/103446

Liang, Y., Yi, X., Dang, Z., Wang, Q., Luo, H. & Tang, J. (2017). Heavy metal contamination and health risk assessment in the vicinity of a tailing pond in Guangdong, China. *International Journal of Environmental Research and Public Health*, 14(12): 1557.

Manyuchi, M.M., Sukdeo, N. & Stinner, W. (2022). Potential to remove heavy metals and cyanide from gold mining wastewater using biochar. *Physics and Chemistry of the Earth*, 126:103110. DOI: 10.1016/j.pce.2022.103110

Mengistu, G. T., Sahilu, G., Mulat, W. & Amare, E. (2023). Assessment of native plants for their potential to remove trace metals around Legadembi tailings dam, Southern Ethiopia. *Environmental science and pollution research*, 30(19): 55615-55624.

Meyer, A., Grotefend, S., Gross, A., Wätzig, H. & Ott, I. (2012). Total reflection X-ray fluorescence spectrometry as a tool for the quantification of gold and platinum metallodrugs: determination of recovery rates and precision in the ppb concentration range. *Journal of pharmaceutical and biomedical analysis*, 70: 713-717.

Mustafa, H.M. & Hayder, G. (2021). Recent studies on applications of aquatic weed plants in phytoremediation of wastewater : A review article. *Ain Shams Engineering Journal*, 12(1): 355-365. DOI: 10.1016/j.asej.2020.05.009

Ratna, K.D.W & Slamet, I. (2020). The Effectiveness of Pistia stratiotes as Phytoremediation Agents in Reducing Lead (Pb) Levels in Batik Household Industrial Wastewater in Bakaran Village , Central Java-Indon. *Asian Journal of Biology*, 10(4): 68-73. DOI: 10.9734/ajob/2020/v10i430126

Pal, M. & Saha, B.P. (2003). Antibacterial Efficacy of *Rumex nepalensis Spreng* roots, *Phytotherapy research*, 17: 558-559. DOI: 10.1002/ptr.1162

Panneerselvam, B. & Priya, S. (2021). Phytoremediation potential of water hyacinth in heavy metal removal in chromium and lead contaminated water. *International Journal of Environmental Analytical Chemistry*, 1-16. DOI: 10.1080/03067319.2021.1901896

Priya, A. K., Muruganandam, M., Ali, S. S. & Kornaros, M. (2023). Clean-Up of Heavy Metals from Contaminated Soil by Phytoremediation: A Multidisciplinary and Eco-Friendly Approach. *Toxics*, 11(5): 422.

Razzak, S.A., Faruque, M.O., Alsheikh, Z., Alsheikhmohamad, L., Alkuroud, D., Alfayez, A., Hossain, S. M. Z. & Hossain, M. M. (2022). A comprehensive review on conventional and biological-driven heavy metals removal from industrial wastewater. *Environmental Advances*, 7:100168. DOI: 10.1016/j.envadv.2022.100168

Sey, E. & Belford, E.J. (2019). Levels of heavy metals and contamination status of a decommissioned tailings dam in Ghana. *EQA-International Journal of Environmental Quality*, 35: 33-50.

Singh, J., Kumar, V., Kumar, P., Kumar, P., Yadav, K.K., Cabral, M.S., Kamyab, H. & Chelliapan, S. (2021). An experimental investigation on phytoremediation performance of water lettuce (*Pistia stratiotes L.*) for pollutants removal from paper mill effluent. *Water Environment Research*, 1543-1553. DOI: 10.1002/wer.1536

Techane, G., Yadav, O. P. & Yadav, L. (2019). Atomic absorption spectroscopic determination of some heavy metal contents in tomato (Lycopersicon esculentum Mill) fruit and water used for irrigation. *Net Journal of Agricultural Science*, 7(1): 23-29.

Tong, L., Liang, T., Tian, Y., Zhang, Q. & Pan, Y. (2022). Research progress on treatment of mine wastewater by bentonite composite. *Arabian Journal of Geosciences*, 15:681. DOI: 10.1007/s12517-022-09981-9

Waris, M., Baig J.A., Talpur, F.N., Kazi, T.G. &. Afridi, H.I. (2022). An environmental field assessment of soil quality and phytoremediation of toxic metals from saline soil by selected halophytes. *Journal of Environmental Health Science & Engineering*, 20(1): 535-544.

WHO. (2006). *A compendium of standards for wastewater reuse in the Eastern*

Mediterranean Region (No. WHO-EM/CEH/142/E). pp. 1-19.

WHO. (2011). *Guideline for drinking water 4th Edition Geneva, Switzerland World Health Organization*. pp. 1-541.

Wu, A., Zhang, Y., Zhao, X., Li, J., Zhang, G., Shi, H. & Guo, L. (2022). Experimental Study on the Hydroponics of Wetland Plants for the Treatment of Acid Mine Drainage. *Sustainability*, 14, 2148: 1-13. DOI: 10.3390/su14042148

Yadav, S., Kumar, S., Jain, P., Pundir, R. K., Jadon, S. & Sharma, A. (2011). Antimicrobial activity of different extracts of roots of Rumex *nepalensis* Spreng . *Indian Journal of Natural Products and Resources*, 2(1): 65-69.

Zhang, W., Long, J., Zhang, X., Shen, W. & Wei, Z. (2020). Pollution and ecological risk evaluation of heavy metals in the soil and sediment around the HTM tailings pond, northeastern China. *International Journal of Environmental Research and Public Health*, 17(19): 1-10. DOI: 10.3390/ijerph17197072.

Borneo Journal of Resource Science and Technology (2024), 14(1): 98-111
DOI: https:doi.org/10.33736/bjrst.6010.2024

Inhibition of UVB-mediated Oxidative Stress in Immortalized HaCaT Keratinocytes by n-hexane Terpenoid Rich *Canarium odontophyllum* Extract (TRCO) as Evinced by Markers of Photodamage

AHMAD ROHI GHAZALI [1], YOGABAANU ULAGANATHAN[1], MUHAMMAD WAHIZUL HASWAN ABDUL AZIZ[1,2]* & DAYANG FREDALINA BASRI[3]

[1]Centre for Toxicology and Health Risk Studies (CORE), Faculty of Health Sciences, Universiti Kebangsaan Malaysia (UKM), Jalan Raja Muda Abdul Aziz, 50300 Kuala Lumpur, Federal Territory of Kuala Lumpur; [2]Department of Para-clinical Sciences, Faculty of Medicine and Health Sciences, Universiti Malaysia Sarawak (UNIMAS); [3]Centre for Diagnostic, Therapeutic & Investigative Studies (CODTIS), Faculty of Health Sciences, Universiti Kebangsaan Malaysia (UKM), Jalan Raja Muda Abdul Aziz, 50300 Kuala Lumpur, Federal Territory of Kuala Lumpur

*****Corresponding author: amwhaswan@unimas.my
Received: 24 August 2023 Accepted: 29 January 2024 Published: 30 June 2024

ABSTRACT

Acute exposure of eukaryotic cells to ultraviolet-B (UVB) radiation leads to a number of detrimental effects, one such prominent effect of UVB exposure is increased production of free radicals which can lead to oxidative damage. Although, the human skin is well equipped with endogenous antioxidant defence system, often increased levels of free radicals lead to oxidative damage in skin. Skin inflammation, accelerated skin aging, and formation of wrinkles are all consequences of UVB induced photodamage. Hence, it is posited that supplementation of an exogenous antioxidant derived from natural products could prevent and reduce oxidative damage in skin cells. This study set forth to investigate the antioxidative role of terpenoid rich *Canarium odontophyllum* Miq. (Dabai) extract on acute UVB-induced photodamage human keratinocyte cells (HaCaT). We first evaluated the antioxidative capacity of increasing concentrations of crude extracts of TRCO Dabai extracts (62.50 µg/mL, 125 µg/mL, 250 µg/mL, and 500 µg/mL) through FRAP assay. We found all the tested TRCO extract exhibited antioxidative capacity in dosage dependent manner. We further investigated the effects of pre-treatment 250 µg/mL and 500 µg/mL TRCO on UVB-induced photodamaged HaCaT cell by measuring oxidative stress markers of lipid peroxide (LPO content), protein carbonyl (PC) content, glutathione peroxidase (GSH-Px) and glutathione-S-transferase (GST) activities. Both 250 µg/mL and 500 µg/mL TRCO extract pre-treated UVB-induced HaCaT cell group exhibited significantly reduced lipid peroxides content and GST activity compared to the positive control ($p<0.05$). Pre-treatment of 250 µg/mL TRCO extract significant enhanced GSH-Px activity ($p<0.05$). However, no significant difference in protein carbonyl content could be established across all tested groups. Therefore, our results suggest that TRCO extract can offer protection against oxidative damages caused by UVB exposure, and said protective effects can be attributed by its antioxidant properties.

Keywords: *Canarium odontophyllum*, exogenous antioxidants, keratinocyte, oxidative photoaging, skin

INTRODUCTION

The epidermis layer of human skin forms the outermost protective barrier which defends against xenobiotic, environmental and pathogenic stressors (Grice & Segre, 2011). The epidermal layer provides physical separation between organisms and the external environment (Ghazali *et al*., 2020) which is important in negating effects of environmental stressors. However, the protective mechanism of skin is predominantly compromised by skin aging. Skin aging is influenced by both intrinsic and extrinsic factors which results in loss of cellular integrity thus resulting in altered functional roles (Landau, 2007). Intrinsic aging is a normal physiological occurrence that gradually leads loss of skin firmness, thickness as well as reduced capacity in skin repair mechanisms while extrinsic aging is caused due to environmental aspects like cosmetics, pollution, poor nutrition and UV irradiation, resulting in pre-mature skin aging, coarser skin, skin laxity and loss of cell elasticity (Zhang & Duan, 2018).UV irradiations are well-documented to be the primary external factor to accelerate

skin aging (Wang *et al*., 2019).

There are three types of UV radiations namely UVA (315- 400 nm), UVB (280 to 320 nm) and UVC (100 to 280 nm) except for UVC, two other ultraviolet radiations penetrate into skin in wavelength dependent manner. UVA radiation penetrates through epidermis and dermis layer while UVB radiation does not penetrate deeper than the epidermis layer (You *et al*., 2001). Although both UVA and UVB impose damaging effects to the skin, UVB radiation is considered more detrimental, as UVB radiations are shorter and can be directly absorbed by DNA causing mutations in pyrimidine bases of DNA leading to initiation of skin cancer (Mahendra *et al*., 2021). In particular, UVB ultraviolet irradiation accelerates the generation of free radicals (Wondrak *et al*., 2006).When the levels of free radicals exceed threshold levels, oxidative damage occurs, thus, leading to detrimental effects to cellular nucleic acids, cell membranes, cellular proteins and lipids (McDaniel *et al*., 2018).

Fortunately, skin cells are equipped with elaborate antioxidant defence system composing of enzymatic and non-enzymatic antioxidants which work in cohort to protect cells against oxidative damage. The roles of endogenous antioxidants against UV induced oxidative damage are classified into four major mechanisms; i) scavenging and quenching reactive species, ii) ending free radical chain reactions, iii) repairing molecular damages caused by radicals and iv) sequestration of transition metal ions (Aguilar *et al*., 2016). These functions are essential in inhibiting oxidant reactivity and in safe-guarding from cellular oxidative stress. However, the capacity of these endogenous antioxidants is not unlimited. Overexposure to UV can overwhelm the antioxidant defence system (Steenvoorden & Beijersbergen van Henegouwen, 1997). Therefore, additional photoprotection approaches are essential to maintain redox balance in cells thus avoiding further oxidative injury.

MATERIALS AND METHODS

Plant Material

Fresh leaves of *Canarium odontophyllum* Miq were collected in December 2019 from (1°26'03.2"N 110°25'52.1"E) Kuching, Sarawak. The specimen was brought in with export and research and development permits obtained from Sarawak Biodiversity Centre (Permit No: SBC-2020-EP-58-MWH & SBC-2019-RDP-20-MWH) by Dr. Muhammad Wahizul Haswan Aziz and Associate Prof Dr. Dayang Fredalina Basri, University Kebangsaan Malaysia (UKM). The specimen was deposited in UKM Herbarium with voucher number ID ID028/2020.

Preparation of leaf extract of *Canarium odontophyllum*

Solid-liquid solvent extraction method was employed to extract *Canarium odontophyllum* Miq. (Dabai) leaves extract. In the ratio of 1:10, 40g of *C. odontophyllum* air-dried and coarsely grounded leaves were soaked in 400 mL of n-hexane solvent for 48 hr at room temperature. After 48 hours, the mixture was filtered by using Whatman No.1 filter paper to collect the filtrate. The filtrate was then concentrated under reduced pressure using rotary evaporator until crude were formed. The obtained crude was allowed to air-dry under fume hood for 24 hr to remove remaining solvent. The resultant terpenoid rich crude was weighed. Terpenoid rich *C. odontophyllum* (TRCO) stock (1mg/mL) were prepared by diluting 1 mg of the crude in 1000mL of DMSO and kept at 4°C until further use. *C. odontophyllum* test concentration ranging from 62.50 µg/mL, 125 µg/mL, 250 µg/mL and 500 µg/mL were prepared by diluting the 1mg/mL of *C. odontophyllum* stock in distilled water and sterilised using 0.22 µm Millipore syringe filter.

Determination of *In Vitro* Antioxidant efficacy of *Canarium odontophyllum* Miq. Leaves Extract via Ferric Reducing Antioxidant Power (FRAP) Assay

The ferric reducing antioxidant power of TRCO were evaluated in accordance to (Benzie and Strain 1996). Essentially, in the presence of antioxidants, colorless ferric ion [Fe^{3+}-(2,4,6-Tris(2-pirydyl)-s-triazine)$_2$]$^{3+}$is reduced to insoluble Prussian blue ferrous ion-TPTZ complex [Fe^{2+}-(TPTZ)$_2$]$^{2+}$ in acidic medium. Firstly, FRAP working reagent were prepared in 10:1:1 ratio by mixing 30 mL of acetate buffer (30 mM, pH 3.6), 3 mL of $FeCl_3$ (20 mM) and 3 mL of TPTZ solution (10 mM). The FRAP

working reagent wrapped in aluminium foil and placed in 37°C water bath until use. A calibration curve using iron (II) sulphate $FeSO_4$ calibration is prepared with serially diluted concentrations that range from 100 to 1,000 µM. Ascorbic acid as positive control with concentrations ranging from 3.125 µg/mL to 50 µg/mL were also prepared. The *C. odontophyllum* Miq. test concentrations of 62.50 µg/mL, 125 µg/mL, 250 µg/mL and 500 µg/mL were also prepared. For the assay, 50 µL of $FeSO_4$, ascorbic acid solution and *C. odontophyllum* Miq. test extracts were added into respective wells in a 96-well plate in which each concentration consisted of quadruplicate (n=4). Then, 175 µL of pre-warmed FRAP reagent were added to the wells. Next, the plates were incubated at 37 ºC for 5 min. Finally, absorbance readings were taken at 595 nm using microplate reader. The FRAP values were expressed as ascorbic acid equivalent antioxidant capacity (AEAC) (Serbessa, 2019).

Cell culture

The immortalized human keratinocyte (HaCaT) cell lines were purchased from Elabscience USA, catalogue number EP-CL-0090). The cells were cultured in Dulbecco's Modified Eagle Medium (DMEM) containing glucose, L-glutamine and sodium pyruvate (HiMedia, India), 1% penicillin-streptomycin mixture (Nacalai Tesque, Japan) (Pen-Strep, 10 000 IU/mL) and supplemented with 15% foetal bovine serum (FBS) (Sigma-Aldrich®). The cells were maintained under standard cell culture conditions of 37°C,5% CO_2 and 95% humidity.

UVB Treatment of HaCaT Cells

HaCaT cells were seeded in 6 wells cell-culture plates at a density of 4 x 10^4 cell/mL. Cells were maintained in DMEM media supplemented with 1% pen-strep and 15 % FBS until 80% confluency were reached. The media was removed and cells were rinsed with sterile phosphate-buffered saline (PBS). Then, cells were divided into 250 µg/mL treatment group, 500 µg/mL treatment group, negative control, and positive control groups. The 250 µg/mL and 500 µg/mL treatment groups were pre-treated with 1 mL of 250 µg/mL and 500 µg/mL *C. odontophyllum* extract prepared in DMEM media. Whereas, both positive and negative control groups were added with 1 mL DMEM media only. Next, cells were incubated at 37 °C, 5% CO_2 and 95% humidity for 30 min. Upon incubation, 250 µg/mL, 500 µg/mL *C. odontophyllum* extracts treatment groups and positive control group were exposed to UVB radiation at 30 mJ/cm^2 without culture plate cover. Negative control group was not exposed UVB irradiation. Then, cells were washed twice with 1 mL ice-cold PBS for cell lysate preparation.

Cell lysates Preparation

Cell lysates were prepared by adding 400 µL of ice-cold RIPA lysis buffer to cells. Next, cells were incubated on ice for 5 min. Upon incubation, cells were gently scrapped and collected in micro-centrifuge tubes. The lysates were incubated in ice for 30 min on constant agitation. After incubation, cell lysates were centrifuged at 16128 RCF/g for 10 min at 4°C to remove cell debris. Supernatant of cell lysates were carefully collected and protein estimation was made based on BCA method.

Determination of Lipid Peroxides (LPO) Content, Protein Carbonyl (PC) Content, Glutathione Peroxidase (GPx) and Glutathione-S-Transferase (GST) Activity

The lipid peroxide (LPO) and protein carbonyl (PC) content as well as glutathione peroxidase (GPx) and glutathione-s-transferase (GST) activities of cell lysate samples were determined using relevant commercial kits from Elabscience® in accordance to manufacturer's instruction.

Statistical analysis

Data values are expressed in mean ± standard error of measurement (SEM) based on experiments performed in triplicates (n=3). One-way ANOVA test was carried out to compare means of various treatment groups. Significant level was set to 0.05 wherein results were considered statistically significant if $p<0.05$. IBM SPSS Statistics Version 23 and GraphPad Prism Version 9 were used for statistical analysis.

RESULTS

Antioxidant Capacity of n-hexane extract of *C. odontophyllum* Miq

The reducing capacity of TRCO were through FRAP Assay. The FRAP values were expressed as ascorbic acid equivalent antioxidant capacity (AAEAC) in the unit of µg AA (ascorbic acid)/g *C. odontophyllum* Miq leaves extract (Serbessa, 2019). TRCO extract with concentration of range of 62.50 µg/mL, 125 µg/mL, 250 µg/mL and 500 µg/mL were tested for its antioxidative capacity. Significant difference in FRAP values between all the tested extract concentrations were observed ($p< 0.05$). The highest FRAP value was exhibited by 500 µg/mL with 6.75±0.08 µgAA/g (Table 1), followed by 250 µg/mL expressing 4.27±0.06 µgAA/g, 125 µg/mL, with 1.66±0.03 µgAA/g while the lowest concentration of 62.50 µg/mL exhibited 1.11±0.07 µgAA/g (n=4) (Fig 1). All the FRAP values were statistically significant at $p<0.05$.

Table 1. Ascorbic Acid equivalent FRAP values of different concentrations of Terpenoid rich *Canarium odontophyllum* (TRCO) extracts

Concentration (µg/mL)	Ascorbic acid Equivalent FRAP values (µgAA/g)
62.5	1.11 ± 0.07
125	1.66 ± 0.03
250	4.27 ± 0.06
500	6.75 ± 0.08

Effects of TRCO Extract on Lipid Peroxides (LPO) Content on UVB-irradiated HaCaT Cells

In the present study, we assessed the effects of TRCO on lipid peroxides content in acute UVB exposed keratinocyte cells. We found that the highest concentration of lipid peroxides was exhibited in UVB only exposed HaCaT cells (Figure 2), whereas the control group (non-UVB exposed) exhibited lower lipid peroxide concentration. A statistically significant difference between UVB exposed and control group in lipid peroxide concentration was observed ($p<0.05$). Our result further demonstrated that pre-treatment with TRCO extracts prior to UVB exposure effectively reduces lipid peroxide content in HaCat cells (Figure 2). Notable lower lipid peroxide content was observed in both TRCO extracts pretreated UVB-exposed groups compared to UVB only exposed group. Both 250 µg/mL and 500 µg/mL TRCO treatment groups significantly reduced generation lipid peroxides in comparison to UVB only treated group ($p<0.05$). However, no significant difference in lipid peroxide content was observed between 250 µg/mL and 500 µg/mL TRCO. extracts pre-treated UVB exposed HaCat cells ($p<0.05$). Both 250 µg/mL and 500 µg/mL TRCO extracts pre-treated UVB exposed HaCat cells show no significant difference in LPO content compared to negative control group (non-UVB exposed group) ($p<0.05$).

Effects of TRCO Extract on Protein Carbonyl (PC) Content on UVB-irradiated HaCaT Cells

We assessed the effects of TRCO extracts in protein carbonyls formation in UVB exposed HaCaT cells. Highest protein carbonyl content was evident in UVB only exposed group (134.70 ± 15.21 nmol/mgprot) (Figure 3). However, when comparing protein carbonyl levels between UVB only exposed group to negative control group (108.20 ± 10.82 nmol/mgprot), no significant difference could not be established ($p<0.05$). We notice that the negative control group exhibited relatively high protein carbonyl content albeit the absence of UVB exposure. Pre-treatment of 250 µg/mL and 500 µg/mL TRCO extracts exhibited relatively lower protein carbonyl content compared to UVB exposed group. However, only 500 µg/mL TRCO extract pre-treatment group exhibited significant difference in PC content when compared to UVB only exposed group ($p<0.05$).

Effects of TRCO Extract on Glutathione Peroxidase (GPx) activity on UVB-irradiated HaCaT Cells

We investigated GPx activity in UVB irradiated HaCaT cells pre-treated with TRCO extracts. UVB exposed HaCaT cells exhibited significant depletion (Figure 4) in GPx activity (246.70 ± 21.45 U/mgprot) compared to control group (635.50 ± 10.38 U/mgprot) ($p<0.05$). The 250 µg/mL TRCO extract pre-treatment group

exhibited no loss of GPx activity, in fact it exhibited increased GPx activity than UVB only exposed group ($p<0.05$). GPx activity in 250 µg/mL TRCO extract pre-treated group were significantly higher than negative control group ($p<0.05$). However, we notice that 500 µg/mL TRCO extract pre-treated group exhibited significant depletion in GSH-Px activity compared to all other tested groups ($p<0.05$)

Effects of TRCO Extract on Glutathione-S-Transferase (GST) activity on UVB-irradiated HaCaT Cells

In our study GST activity in UVB only exposed HaCaT cells resulted in highest activity at 0.38 ± 0.29 U/mgprot (Figure 5). The negative control group revealed significantly lower GST enzyme activity 0.09 ± 0.10 U/mgprot) in comparison to UVB only exposed HaCaT cells ($p<0.05$). Both 250 µg/mL and 500 µg/mL TRCO extract pre-treatment groups expressed significantly reduced GST activity compared to UVB only exposed group ($p<0.05$).

DISCUSSION

UVB is one of the main causes of oxidative stress in skin. The duration and length of UVB exposure determines the severity of the effects. UVB radiation induces alterations in skin's biochemical compositions and mechanical functionality due to oxidative stress. Accelerated skin aging, formation of wrinkles and impoverished skin firmness are all signs of photodamage (Mishra *et al*., 2011). Although, the human skin is well equipped with endogenous antioxidant defence system comprising of a myriad of antioxidant molecules, often the increased levels of free radicals lead to depletion of said endogenous antioxidants (Babiarz *et al*., 2002). Therefore, application of exogenous antioxidants on skin may help negate ill effects caused by excessive free radicals during UVB exposure.

C. odontophyllum Miq (Dabai) is one such plant which is known for its nutritional and antioxidative values. *C.odontophyllum* Miq or colloquially known as "Dabai" is an indigenous plant to Borneo, Sarawak, Sabah, Brunei, Kalimantan, and Philippines. Many studies had been carried out on various parts of the Dabai plant to assess its nutritional and antioxidative values. *C. odontophyllum* plant extracts are recognized for its antioxidative activity against free radicals (Azlan *et al*., 2010),as well as for targeted cytotoxicity effects against many types solid cancers without harming normal cells (Latif *et al*., 2018). *C. odontophyllum* fruits are reported to exhibit high antioxidant capacity (Chew *et al*., 2011). The skin in particular is shown to contain polyphenols, phenolic and flavonoid compounds which is thought to be responsible for the antioxidative capacity (Chew *et al*., 2011). Various other studies have reported antioxidative activity in various parts of *C. odontophyllum* plants such as bark (Basri *et al*., 2016), pulp (Basri, 2014), peel (Yang *et al*., 2003; Chew *et al*., 2011) fruits and leaves (Basri, 2014; Basri, 2015).

To date, there are no published data available on the antioxidative capacity of n-hexane extracted *C. odontophyllum,* thereof, these results serve as the first reported data on antioxidative capacity of n-hexane extracts of *C. odontophyllum.*

The antioxidative properties in *C. odontophyllum* leaves extract is of particular interest because leaves are constantly exposed to UVB radiation stress and thereby, it is hypothesized to be equipped with photoprotective molecules composed of antioxidants in order to mitigate the formation of reactive oxygen species observed (Chu *et al*., 2008) . Protective antioxidants such as terpenes, flavonoids, tannins and polyphenols are well characterized in UVB induced leaves (Czegeny *et al*., 2016). *C. odontophyllum* leaves extracts were found to exhibit promising antioxidative values (Basri, 2014; Basri, 2015; Budin *et al*., 2018). These extracts were found to contain terpenoids, tannins and flavonoids. Previous gas chromatography (GC-MS) analysis on the n-hexane extracts of *C odontophyllum leaves* .wherein the major type of terpenoids were identified as spathulenol and phytol (Basri *et al*., 2022). The FRAP assay revealed antioxidative capacity in all the tested n-hexane *C. odontophyllum* leaves extracts. The antioxidative capacity in n-hexane *C. odontophyllum* leaves extracts could be contributed by the high presence of terpenoids. Studies on spathulenol and phytol terpenoids reveal antioxidative activities (do Nascimento *et al*., 2018, Islam; Ali *et al*., 2018)

Studies have confirmed that the presence of terpenoids exhibit high reducing activities and that, as the content of terpenoids increase the ferric reducing capacities also increases (Das *et al*., 2011, Greeshma & Murugan, 2018). Therefore, as previously mentioned by Abdul Aziz *et al*., (2022), terpenoid rich *C. odontophylum* (TRCO) leaf extract can offer antioxidative therapeutic effects.

In our study, n-hexane extracts of *C. odontophyllum* were found to exhibit protective effects when topically applied on human keratinocyte cells prior to acute UVB irradiation exposure. UVB is a potent generator of reactive oxygen species (ROS) in skin. Under normal circumstances, ROS are neutralized through the network of endogenous enzymatic and non-enzymatic antioxidants. However, when exposed to external stimuli such like UVB radiation, ROS levels are highly elevated, this occurrence results in overwhelmed endogenous antioxidant system which leads to oxidative stress. UVB irradiation is reported to not only elevate ROS levels but also most worryingly, it is responsible for the depletion of endogenous antioxidants such as glutathione peroxidase (GSH-Px) and Glutathione-S-Transferases (GST).

Glutathione peroxidase and glutathione-S-transferase are part of endogenous antioxidant defence system Jablonska *et al*., (2015) which help to preventing reactive oxygen species (ROS) induced oxidative stress in cells. Glutathione peroxidases are cytoprotective antioxidant selenoenzymes that plays two crucial roles; i) the primary function of GSH-Px is to catalyse the breakdown of hydrogen peroxides (H_2O_2), lipidic or non-lipidic peroxides to non-toxic products (e.g. water and oxygen) through oxidation of reduced glutathione (GSH), this activity of GSH-Px protects cells against lipid peroxidation and ii) to maintain redox balance between reduced glutathione (GSH) and oxidized glutathione (GSSG) in cells (Arthur, 2001; Xianyong *et al*., 2017)

Pre-treatment of n-hexane extract of *C. odontophyllum* at a low dose on acute UVB exposed human keratinocyte cells (HaCaT) resulted in high GSH-Px activity compared with untreated-UVB exposed groups. This could be due antioxidative activity of TRCO in maintaining redox balance by reducing formation free radicals upon UVB exposure. The increase in GSH-Px activity in exogenous antioxidant treated cells is similarly observed in many studies including (Arthur, 2001; Xu *et al*., 2018; Biernacki *et al*., 2021; Kunchana *et al*., 2021). The enhancement of GSH-Px activity also corroborates with the low levels of lipid peroxides observed. However, pre-treatment of a higher dose of n-hexane extract of *C. odontophyllum* revealed exhibited significant depletion in GSH-Px activity compared to all other tested groups ($p<0.05$). Instead of further enhancing or maintaining GSH-Px activity, 500 µg/mL TRCO dose depleted GSH-Px activity to even lower than UVB only exposed group. The reason for this contradictory behaviour of 500 µg/mL TRCO dose could indicate the depletion of reduced glutathione (GSH) in the UVB exposed cells. Xenobiotics are capable of inducing oxidative stress in cells which eventually leads to depletion of endogenous antioxidants in the process of maintaining cell redox homeostasis. Reduced glutathione (GSH) is part of endogenous antioxidant system which plays major role in the detoxification and neutralization of reactive oxygen species (ROS). GSH is also major substrate for the activity of GSH-Px (Eren & Selami, 2020). Therefore, depletion of GSH could lead to decreased GSH-Px activity. We presume that the depletion of GSH at 500 µg/mL TRCO extract is what affects the non-significant lipid peroxides and protein carbonyl content when compared with 250 µg/mL TRCO extract.

At higher concentration, it can be presumed that TRCO further aggravates the oxidative damage in cells which leads to severe depletion in GSH. This process eventually leads to the loss of activity in GSH-Px activity as observed in this study. Depletion of GSH can also mean the cells are activating cell death machinery which leads to apoptosis. Increased oxidative stress is linked to cellular damage and induction of cell death. Previous study by Abdul Aziz *et al*. (2022) on cell viability of HaCaT cells tested at 500 µg/mL TRCO provide evidences of decreased cell survivability with increment of TRCO concentration. Therefore, the severe depletion of GSH-Px activity may indicate cell death due to the increased oxidative damage. Studies have shown that the concentration of terpenoids determines the behaviour of terpenoids. At higher concentration, terpenoids act as pro-oxidants but at much lower concentrations it is

found to exert antioxidative effects (González & Gómez, 2012) Antioxidants such as ascorbate can function both as antioxidant and pro-oxidant on certain circumstances (Podmore *et al*., 1998). Beneficial antioxidants such as resveratrol, curcumin, coenzyme Q10, α-lipoic acid (He *et al*., 2017) is also known to act as pro-oxidants and produce overshooting of desired effects resulting fluctuations in redox balance.

GST are part of phase II detoxification enzymes (Townsend & Tew, 2003) which are largely responsible for detoxification of xenobiotics and electrophilic free radicals through conjugation with GSH. The mechanism of GST conjugation involves pairing xenobiotics with electrophilic centres to nucleophilic portions of GSH to detoxify and prevent toxic injuries to cells and tissues (Ishikawa, 1992).

TRCO extract pre-treated groups expressed significantly reduced GST activity compared to UVB only exposed group ($p<0.05$). This trend was similarly reported in (Monga *et al*., 2014). Reduced activity of GST in the TRCO pre-treated group compared to the untreated group could point out lower formation of free radicals and toxic products associated with UVB exposure. The reduced free radicals present can be attributed to antioxidative capacity of TRCO in scavenging free radicals thus leading overall reduction in GST activity. In the event of oxidative stress, antioxidative defence system are activated to reduce, eliminate, and detoxify free radicals to prevent oxidative damage to cells. In this case, treatment of exogenous antioxidant TRCO resulted in the overall reduction in free radicals and its associated oxidative stress products thus, not necessitating induction of high GST activity. Therefore, when there is a cellular redox balance, the need for elevated detoxification activity is lower (Benincasa *et al*., 2019). GSTs are not the only detoxification enzyme responsible for eliminating free radicals, but there are various other mechanisms involved in the elimination of free radicals as well which were not explored in this study. Many factors also affect the activity of GST enzyme for example the availability of GSH for the conjugation process which could be rate-limiting factor for GST activity. Therefore, further studies are needed to elucidate the involvement of major enzymatic and non-enzymatic antioxidants in the elimination of UVB induced free radicals in the presence of TRCO.

Lipid peroxidation on epidermal layers is a direct consequence of UVB irradiation exposure. Lipid peroxidation occurs due to the oxidative deterioration lipids by free radicals. It is initiated when ROS attacks and abstracts hydrogen from the methylene groups of lipids, resulting in lipid radicals. Elevated amount of ROS poses two consequences: i) impairing cell components and ii) activating specific signalling pathways (Finkel & Holbrook, 2000). The overwhelming amount of free radicals inflicts direct damage to lipids and leads to the production of lipid peroxidation products such as lipid peroxides, malondialdehyde (MDA), and 4-hydroxyalkenals (HAE/HNE). Most of these lipid peroxidation products are known to be highly toxic and mutagenic (Esterbauer *et al*., 1990) which causes injury in cells, tissues and organs (Ayala *et al*., 2014). Lipid peroxidation products are also strongly associated with photodamage and pre-mature skin aging (Alvarez & Stratton, 2008). Lipid peroxides are prominent indicators of lipid peroxidation which formed due to oxidative degradation of polyunsaturated fatty acids (PUFA) by free radicals.

In our study, we found that the highest concentration of lipid peroxides ($p<0.05$) was exhibited in UVB only exposed HaCaT cells, whereas the control group (untreated and non-UVB exposed) exhibited lower lipid peroxide concentration. The reason for the increased LPO formation upon UVB exposure can be majorly attributed to the lipid rich matrix of epidermal keratinocytes (Alvarez & Stratton, 2008). As we know, lipid peroxides are product of free radicals induced oxidation of polyunsaturated fatty acids. Skin epidermis is composed of polyunsaturated fatty acids such as linoleic acids which are found abundantly in ceramides, while arachidonic acid (AA) being the second most abundant (PUFA) (Knox & O'Boyle, 2021) and omega 3 fatty acids (Ziboh *et al*., 2000). These lipids could be primary targets of free radical species such as oxyl radicals, hydroxyl radicals and peroxyl radicals thus leading to increased formation of LPO. Our result is in accordance with Townsend and Tew (2003) that reported higher secretion of 8-isoprostane, an end product of lipid peroxidation in UVB- irradiated HaCaT cells compared control group and as well as

(Ishikawa, 1992) which reported similar inclination of increased lipid peroxidation product levels in UVB exposed group. Similar trend was also observed in few studies which evaluated effects of UVB radiation on lipid peroxidation products in keratinocyte cells (Chapkin *et al*., 1990; Afaq *et al*., 2007; Piao *et al*., 2013; Chen *et al*., 2015; Fehér *et al*., 2016; Fernando *et al*., 2016; Luangpraditkun *et al*., 2020; Lee *et al*., 2020).

We demonstrated that TRCO extracts of 250 µg/mL and 500 µg/mL were able significantly reduce the generation of lipid peroxidation products in HaCaT cells exposed to acute UVB exposure. The reduction in lipid peroxides formation is presumed to be due to terpenoid antioxidant content in TRCO extracts. Antioxidants are capable of scavenging free radicals which are formed due to acute and chronic UVB exposure. When HaCaT cells are pretreated with exogenous antioxidants such as TRCO extract, the generation of lipid peroxides are suppressed. Supplementation of exogenous antioxidant helps to scavenge excessive free radicals that are generated due to UVB exposure, thus, resulting in minimized lipid peroxide formation.

Similar to lipids and DNA, ROS induced oxidative stress also induces structural and functional modifications to cellular proteins due to protein oxidation. These structural modifications of protein molecules inevitably lead to loss of biological functions. Another prominent modification of proteins caused by ROS is the conversion of proteins to carbonyl derivatives (Sitte, 2003). Protein oxidation is a natural consequence of aerobic life, however environmental stimuli such as UV, chemotherapeutic drugs and hyperthermia can generate elevated amounts of ROS (Sitte, 2003). High amount of protein carbonyls were reported on keratinocytes cells that are exposed to UV radiation (Ogura *et al*., 2011). This is because UV-induced ROS reacts with amino acids of proteins in dermis and epidermis of skin to generate protein carbonyls (Yamawaki *et al*., 2019). Although the consequence of protein carbonyl accumulation in skin physiology remains unclear, studies have reported changes in skin colour (yellow-dark), alteration in collagen and extracellular matrix associated with photoaging (Uehleke, 2010), decreased moisture-holding capacity that leads to skin dryness and trans-epidermal water loss in stratum corneum as a result of elevated protein carbonyl levels (Baraibar, 2018; Yamawaki *et al*., 2019) and accelerated skin aging by amplifying decomposition of elastic fibres and collagens (Yamawaki *et al*., 2019). Even though, the body's innate antioxidant defence system is able to quench and eliminate ROS, excessive amount of ROS can lead to irreparable protein misfolding, to a large extend, which leads to selective proteolysis (Sitte, 2003). Therefore, strengthening the endogenous antioxidants with additional exogenous antioxidants in neutralizing the harmful effects of ROS could be a good strategy in reducing protein carbonyl induced skin damages.

This study assessed the effects of TRCO extracts in protein carbonyls formation in UVB exposed HaCaT cells. We found that pretreatment of 250 µg/mL and 500 µg/mL TRCO extracts exhibited relatively lower protein carbonyl content compared to UVB exposed group. However, when compared to UVB only exposed group, no significant difference in protein carbonyl content can be established ($p<0.05$). In fact, when comparing protein carbonyl levels between UVB only exposed group to control group, no statistical significance could not be established ($p<0.05$). We notice that the negative control group exhibited relatively high protein carbonyl content independent of any UVB exposure. This could be attributed to other oxidation processes including formation of carbonylated proteins through aldehyde and amino residues reaction due to lipid peroxidation (Chevion *et al*., 2000; Togni *et al*., 2019). The negligible induction of protein carbonyl content between the control group and UVB exposed group could be ascribable to few reasons; firstly, single exposure to UVB at low dose of 30 mJ/cm^2 may not be sufficient to induce notable increase in protein carbonyls. Study by Luangpraditkun *et al*. (2020) revealed enhanced protein carbonyl levels when HaCaT cells were exposed to single exposure of UVB at 60 mJ/cm^2. Secondly, possibly frequency of exposure to UVB may influence protein carbonyl content in keratinocytes. HaCaT cells which were exposed to repeated dose UVB irradiation were shown to express higher protein carbonyls content by Lee *et al*. (2020). Thirdly, a study by Ramachandran and Prasad (2008) provided that the extent of protein oxidation in living epidermal layer of skin is far less than

dermal layer due to high antioxidant capacity in the epidermis layer, thus, we presume that keratinocyte cells which is the major constituent of epidermal layer may also similar activities. Finally, the generation of protein carbonyls upon UVB exposure may require longer period of time to exhibit any substantial changes. Time-dependent fluctuations in reactive species upon UVB exposure is possible as different radical species act at different times (Sitte, 2003; Ogura *et al*., 2011). Study by Lee *et al*. (2013) reported higher protein carbonyl concentration when measured 2 hr after exposing HaCat cells to 30 mJ/cm^2, whereas in our study, cell lysates for protein carbonyl measurement were measured within 30 mins upon UVB exposure as we wanted to examine the immediate effects of UVB exposure on keratinocyte cells. Even though, 500 µg/mL TRCO extract significantly reduced protein carbonyl content in comparison to UVB only exposed HaCat group ($p<0.05$), the veritableness of this effect could not be established as both positive and negative controls indicate non-significant difference in protein carbonyl levels. Therefore, further studies are needed to establish the effects of TRCO in protein carbonyl content in UVB induced HaCat cell.

CONCLUSION

To summarise, UVB induced oxidative stress is a key factor in the onset and progression of photodamage and photoaging of the skin. Supplementation of exogenous antioxidants such as TRCO extracts as demonstrated in this study provide antioxidative and photoprotective effects against UVB. Specifically, TRCO gets involved in the prevention of UVB-mediated oxidative damage in HaCaT cells by lowering lipid peroxides levels, lowering glutathione-s-transferase activity (GST) and increasing glutathione peroxidase activity (GSH-Px). Taken together, TRCO appears to be a promising candidate as exogeneous antioxidant for protection against photoaging and photodamage.

ACKNOWLEDGEMENTS

This work was supported by the Government of Malaysia, Ministry of Science, Technology, and Innovation (Grant: Dana Impak Perdana DIP-2018-034)

Conflicts of Interest:

The authors declare no conflict of interest. The funders had no role in the design of the study; in the collection, analyses, or interpretation of data; in the writing of the manuscript; or in the decision to publish the results.

REFERENCES

Abdul Aziz, M.W.H., Basri, D.F., Masre, S.F. & Ghazali, R. (2022). Fatty acids and terpenoids from *Canarium odontophyllum* miq. leaf and their antioxidant and cytotoxic effects on uvb-induced immortalized human keratinocytes cells (HaCat). *Malaysian Applied Biology,* 51: 79-87. DOI: 10.55230/mabjournal.v51i3.2377

Afaq, F., Syed, D.N., Malik, A., Hadi, N., Sarfaraz, S., Kweon, M.H., Khan, N., Zaid, M.A. & Mukhtar, H. (2007). Delphinidin, an anthocyanidin in pigmented fruits and vegetables, protects human hacat keratinocytes and mouse skin against UVB-mediated oxidative stress and apoptosis. *Journal of Investigative Dermatology,* 127(1): 222-232. DOI: 10.1002/mc.20477

Aguilar, T., Navarro, B. & Mendoza Perez, J.A. (2016). Endogenous antioxidants: a review of their role in oxidative stress. *InTech*, DOI: 10.5772/65715

Alvarez, I. & Stratton, S. (2008). Effects of green tea polyphenols on UV-induced lipid peroxidation in skin cell models. *Cancer Research*, 68(9_Supplement): 3133.

Arthur, J.R. (2001). The glutathione peroxidases. *Cellular and Molecular Life Sciences,* 57(13-14): 1825-1835. DOI: 10.1007/pl00000664.

Ayala, A., Muñoz, M. & Argüelles, S. (2014). Lipid peroxidation: production, metabolism, and signaling mechanisms of malondialdehyde and 4-hydroxy-2-nonenal. *Oxidative Medicine and Cellular Longevity,* 2014: 360438. DOI: 10.1155/2014/360438

Azlan, A., Mohamad Nasir, N.N. & A, I. (2010). Antioxidant properties of methanolic extract of *Canarium odontophyllum* fruit.

International Food Research Journal, 17: 319-326.

Baraibar, M. (2018). Protein oxidation at the crossroad of skin & hair premature aging. DOI: 10.13140/RG.2.2.27864.44803

Basri, D. (2014). Preliminary screening for antimicrobial activity of the pulp of *Canarium odontophyllum* Miq. (dabai) fruit. *Global Journal of Pharmacology*, 8(2): 213-220. DOI: 10.5829/idosi.gjp.2014.8.2.82415

Basri, D. (2014). Screening of antioxidant phytoextracts of *Canarium odontophyllum* (Miq.) leaves in vitro. *IOSR Journal of Pharmacy*, 4: 1-6.

Basri, D. (2015). Leaves extract from *Canarium odontophyllum* Miq. (dabai) exhibits cytotoxic activity against human colorectal cancer cell HCT 116. *Natural Products Chemistry & Research*, 3: 1-4. DOI: 10.4172/2329-6836.1000166

Basri, D.F., Alamin, Z.A.Z. & Chan, K.M. (2016). Assessment of cytotoxicity and genotoxicity of stem bark extracts from *Canarium odontophyllum* Miq. (dabai) against HCT 116 human colorectal cancer cell line. *BMC Complementary and Alternative Medicine*, 16(1): 36. DOI: 10.1186/s12906-016-1015-2.

Benincasa, C., La Torre, C., Plastina, P., Fazio, A., Perri, E., Caroleo, M., Gallelli, L., Cannataro, R. & Cione, E. (2019). Hydroxytyrosyl oleate: improved extraction procedure from olive oil and by-products, and in vitro antioxidant and skin regenerative properties. *Antioxidants*, 8: 233. DOI: 10.3390/antiox8070233

Benzie, I.F.F. & Strain, J.J. (1996). The ferric reducing ability of plasma (FRAP) as a measure of "antioxidant power": the FRAP assay. *Analytical Biochemistry*, 239(1): 70-76.

Biernacki, M., Brzóska, M., Markowska, A., Gałażyn Sidorczuk, M., Cylwik, B., Gęgotek, A. & Skrzydlewska, E. (2021). Oxidative stress and its consequences in the blood of rats irradiated with UV: protective effect of cannabidiol. *Antioxidants*, 10: 821. DOI: 10.3390/antiox10060821

Budin, S.B., Kumar, S., Abd Warif, N.M., Mohd Saari, S. & Basri, D.F. (2018). Protective effect of aqueous extracts from *Canarium odontophyllum* Miq. leaf on liver in streptozotocin-induced diabetic rats. *Life Sciences, Medicine and Biomedicine*, 2(1). DOI:10.28916/lsmb.2.1.2018.5

Chapkin, R.S., Ziboh, V.A., Marcelo, C.L. & Voorhees, J.J. (1990). Metabolism of essential fatty acids by human epidermal enzyme preparations: evidence of chain elongation. *Journal of Lipid Research*, 27(9): 945-954. DOI:10.1016/S0022-2275(20)38771-X

Chen, A., Huang, X., Xue, Z., Cao, D., Huang, K., Chen, J., Pan, Y. & Gao, Y. (2015). The role of p21 in apoptosis, proliferation, cell cycle arrest, and antioxidant activity in UVB-irradiated human HaCaT keratinocytes. *Medical Science Monitor Basic Research*, 21: 86-95. DOI: 10.12659/MSMBR.893608

Chevion, M., Berenshtein, E. & Stadtman, E.R. (2000). Human studies related to protein oxidation: protein carbonyl content as a marker of damage. *Free Radical Research*, 33 Suppl: S99-108.

Chew, L.Y., Prasad, K.N., Amin, I., Azrina, A. & Lau C.Y. (2011). Nutritional composition and antioxidant properties of *Canarium odontophyllum* Miq. (dabai) fruits. *Journal of Food Composition and Analysis*, 24(4): 670-677. DOI:10.1016/j.jfca.2011.01.006

Czégény, G., Mátai, A. & Hideg, É. (2016). UV-B effects on leaves—oxidative stress and acclimation in controlled environments. *Plant Science*, 248: 57-63. DOI: 10.1016/j.plantsci.2016.04.013

Das, J., Mao, A.A. & Handique, P.J. (2011). Terpenoid compositions and antioxidant activities of two indian valerian oils from the Khasi Hills of north-east India. *Natural Products Communications*, 6(1). DOI: 10.1177/1934578X1100600131.

do Nascimento, K.F., Moreira, F.M.F., Alencar Santos, J., Kassuya, C.A.L., Croda, J.H.R.,

Cardoso, C.A.L., Vieira, M.d.C., Góis Ruiz, A.L.T., Ann Foglio, M., de Carvalho, J.E. & Formagio, A.S.N. (2018). Antioxidant, anti-inflammatory, antiproliferative and antimycobacterial activities of the essential oil of *Psidium guineense* Sw. and spathulenol. *Journal of Ethnopharmcolology,* 210: 351-358. DOI: 10.1016/j.jep.2017.08.030

Eren, S. & Selami, D. (2020). Glutathione peroxidase in health and diseases. *IntechOpen*. DOI: 10.5772/intechopen.91009

Esterbauer, H., Eckl, P. & Ortner, A. (1990). Possible mutagens derived from lipids and lipid precursors. *Mutation Research/Reviews in Genetic Toxicology,* 238(3): 223-233. DOI: 10.1016/0165-1110(90)90014-3

Fehér, P., Ujhelyi, Z., Varadi, J., Fenyvesi, F., Roka, E., Juhász, B., Varga, B., Bombicz, M., Priksz, D., Bácskay, I. & Vecsernyés, M. (2016). Efficacy of pre- and post-treatment by topical formulations containing dissolved and suspended *Silybum marianum* against UVB-induced oxidative stress in guinea pig and on HaCaT keratinocytes. *Molecules,* 21(10): 1269. DOI: 10.3390/molecules21101269

Fernando, M., Piao, M., Kang, K., Ryu, Y., Madduma Hewage, S., Chae, S. & Hyun, J. (2016). Rosmarinic acid attenuates cell damage against UVB radiation-induced oxidative stress via enhancing antioxidant effects in human HaCaT cells. *Biomolecules & Therapeutics*, 24: 75-84. DOI: 10.4062/biomolther.2015.069

Finkel, T. & Holbrook, N.J. (2000). Oxidants, oxidative stress and the biology of ageing. *Nature*, 408(6809): 239-247. DOI: 10.1038/35041687

Ghazali, R., Muralitharan, R., Soon, C., Salyam, T., Maulana, N., Thaha, U., Halim, R., Suhaifi, S., Khalid, M., Ahmad, A. & Kofli, N. (2020). Viability and antioxidant effects of traditional cooling rice powder (bedak sejuk) made from *Oryza sativa* ssp. Indica and *Oryza sativa* ssp. japonica on UVB-induced B164A5 melanoma cells. *Asian Pacific Journal of Cancer Prevention,* 21: 3381-3386. DOI: 10.31557/APJCP.2020.21.11.3381

González Burgos, E. & Gómez-Serranillos, M. (2012). Terpene compounds in nature: a review of their potential antioxidant activity. *Current Medicinal Chemistry,* 19. DOI:10.2174/092986712803833335

Greeshma Geetha, M. & Murugan, K. (2018). Antioxidant activities of terpenoids from *Thuidium tamariscellum* (c. muell.) bosch. and sande-lac. a moss. *Pharmacognosy Journal,* 10(4). DOI:10.5530/pj.2018.4.106

Grice, E.A. & Segre, J.A. (2011). The skin microbiome. *Nature Reviews Microbiology,* 9(4): 244-253. DOI:10.1038/nrmicro2537

Guo, C., Yang, J., Wei, J., Li, Y., Xu, J. & Jiang, Y. (2003). Antioxidant activities of peel, pulp and seed fractions of common fruits as determined by FRAP assay. *Nutrition Research,* 23(12): 1719-1726. DOI:10.1016/j.nutres.2003.08.005

He, L., He, T., Farrar, S., Ji, L., Liu T. & Ma, X. (2017). Antioxidants maintain cellular redox homeostasis by elimination of reactive oxygen species. *Cellular Physiology and Biochemistry,* 44(2): 532-553. DOI: 10.1159/000485089

Ishikawa, T. (1992). The ATP-dependent glutathione S-conjugate export pump. *Trends in Biochemical Sciences,* 17(11): 463-468. DOI: 10.1016/0968-0004(92)90489-v

Islam, M.T., Ali, E.S., Uddin, S.J., Shaw, S., Islam, M.A., Ahmed, M.I., Chandra Shill, M., Karmakar, U.K., Yarla, N.S., Khan, I.N., Billah, M.M., Pieczynska, M.D., Zengin, G., Malainer, C., Nicoletti, F., Gulei, D., Berindan-Neagoe, I., Apostolov, A., Banach, M., Yeung, A.W.K., El-Demerdash, A., Xiao, J., Dey, P., Yele, S., Jóźwik, A., Strzałkowska, N., Marchewka, J., Rengasamy, K.R.R., Horbańczuk, J., Kamal, M.A., Mubarak, M.S., Mishra, S.K., Shilpi, J.A. & Atanasov, A.G. (2018). Phytol: a review of biomedical activities. *Food and Chemical Toxicology*, 121: 82-94. DOI: 10.1016/j.fct.2018.08.032

Jablonska, E., Gromadzinska, J., Peplonska, B., Fendler, W., Reszka, E., Krol, M.B., Wieczorek, E., Bukowska, A., Gresner, P., Galicki, M., Zambrano Quispe, O., Morawiec, Z. & Wasowicz, W. (2015). Lipid peroxidation and glutathione peroxidase activity relationship in breast cancer depends on functional polymorphism of GPX1. *BMC Cancer*, 15(1): 657. DOI:10.1186/s12885-015-1680-4

Knox, S. & O'Boyle, N.M. (2021). Skin lipids in health and disease: a review. *Chemistry and Physics of Lipids*, 236: 105055. DOI: 10.1016/j.chemphyslip.2021.105055

Kunchana, K., Jarisarapurin, W., Chularojmontri, L. & Wattanapitayakul, S.K. (2021). Potential use of AmLa (*Phyllanthus emblica* L.) fruit extract to protect skin keratinocytes from inflammation and apoptosis after UVB irradiation. *Antioxidants*, 10(5): 703. DOI: 10.3390/antiox10050703

Landau, M. (2007). Exogenous factors in skin aging. environmental factors in skin diseases, E. Tur. *Current Problems in Dermatology*, 35: 1-13. DOI: 10.1159/000106405.

Latif, E., Basri, D., & Nagapan, T. (2018). Toxicological effect of *Canarium odontophyllum* extract against acute lymphoblastic leukemia CCL-119 cell line. *Journal of Environmental Science and Toxicology*, 3(1): 1-8. DOI:10.15226/2572-3162/3/1/00113

Lee, C., Park, G.H., Ahn, E.M., Kim, B.-A., Park, C.-I. & Jang, J.-H. (2013). Protective effect of *Codium fragile* against UVB-induced pro-inflammatory and oxidative damages in HaCaT cells and BALB/c mice. *Fitoterapia*, 86: 54-63. DOI: 10.1016/j.fitote.2013.01.020chu

Lin, C.B., Babiarz, L., Liebel, F., Kizoulis, M., Gendimenico, G.J., Seiberg, M., Roydon Price, E. & Fisher, D.E. (2002). Modulation of microphthalmia-associated transcription factor gene expression alters skin pigmentation. *Journal of Investigative Dermatology*, 119(6): 1330-1340. DOI: 10.1046/j.1523-1747.2002.19615.x

Luangpraditkun, K., Charoensit, P., Grandmottet, F., Viennet, C. & Viyoch, J. (2020). Photoprotective potential of the natural artocarpin against in vitro UVB-induced apoptosis. *Oxidative Medicine and Cellular Longevity*, 2020: 1042451. DOI:10.1155/2020/1042451

Mahendra, C., Zainal Abidin, S.A., Htar, T., Chuah, L., Khan, S., Ming, L.C., Ying, P.T., Counteracting the ramifications of UVB irradiation and photoaging with *Swietenia macrophylla* king seed. *Molecules*, 26: 2000. DOI: 10.3390/molecules26072000

McDaniel, D., Farris, P. & Valacchi, G. (2018). Atmospheric skin aging—contributors and inhibitors. *Journal of Cosmetic Dermatolology*, 17(2): 124-137. DOI: 10.1111/jocd.12518

Mishra, A., Mishra, A.K. & Chattopadhyay, P. (2011). Herbal cosmeceuticals for photoprotection from ultraviolet B radiation: a review. *Tropical Journal of Pharmaceutical Research*, 10. DOI:10.4314/TJPR.V10I3.7

Monga, J., Aggarwal, V., Suthar, S.K., Monika, Nongalleima, K. & Sharma, M. (2014). Topical (+)-catechin emulsified gel prevents DMBA/TPA-induced squamous cell carcinoma of the skin by modulating antioxidants and inflammatory biomarkers in BALB/c mice. *Food & Function*, 5(12): 3197-3207. DOI: 10.1039/c4fo00531g

Ogura, Y., Kuwahara, T., Akiyama, M., Tajima, S., Hattori, K., Okamoto, K., Okawa, S., Yamada, Y., Tagami, H., Takahashi, M. & Hirao, T. (2011). Dermal carbonyl modification is related to the yellowish color change of photo-aged Japanese facial skin. *Journal of Dermatolology Science*, 64(1): 45-52. DOI: 10.1016/j.jdermsci.2011.06.015

Oh, J.H., Lee, J.I., Karadeniz, F., Park, S.Y., Seo, Y. & Kong, C.-S. (2020). Antiphotoaging effects of 3,5-dicaffeoyl-epi-quinic acid via inhibition of matrix metalloproteinases in UVB-irradiated human keratinocytes. *Evidence-Based Complementary and Alternative Medicine*, 2020: 8949272. DOI: 10.1155/2020/8949272

Piao, M.J., Kang, K.A., Kim, K.C., Chae, S., Kim, G.O., Shin, T., Kim, H.S. & Hyun, J.W. (2013). Diphlorethohydroxycarmalol attenuated cell damage against UVB radiation via enhancing antioxidant effects and absorbing UVB ray in human HaCaT keratinocytes. *Environmental Toxicology and Pharmacology*, 36(2): 680-688. DOI: 10.1016/j.etap.2013.06.010

Podmore, I.D., Griffiths, H.R., Herbert, K.E., Mistry, N., Mistry, P. & Lunec, J. (1998). Vitamin C exhibits pro-oxidant properties. *Nature*, 392(6676): 559-559. DOI: 10.1038/33308

Prasad, K., Chew, L.Y., Khoo, H.E., Kong, K.W., Azlan, A. & A, I. (2010). Antioxidant capacities of peel, pulp, and seed fractions of *Canarium odontophyllum* Miq. fruit. *Journal of Biotechnology and Biomedicine*, 2010. DOI: 10.1155/2010/871379

Ramachandran, S. & Prasad, N.R. (2008). Effect of ursolic acid, a triterpenoid antioxidant, on ultraviolet-B radiation-induced cytotoxicity, lipid peroxidation and DNA damage in human lymphocytes. *Chemico-Biological Interactions*, 176(2): 99-107. DOI: 10.1016/j.cbi.2008.08.010

Serbessa, G.G. (2019). Antioxidant activities of avocado (*Persea americana* Mill.) and banana (*Musa paradisiac* L.) varieties. *Anatomy Physiology & Biochemistry International Journal*, 6(1): 9-14. DOI: 10.19080/APBIJ.2019.06.555678

Shao, H.-b., Chu, L.-y., Shao, M.-a., Jaleel, C.A. & Hong-mei, M. (2008). Higher plant antioxidants and redox signaling under environmental stresses. *Comptes Rendus Biologies*, 331(6): 433-441. DOI: 10.1016/j.crvi.2008.03.011

Sitte, N. (2003). Oxidative damage to proteins. Aging at the molecular level. T. von Zglinicki. Dordrecht, *Springer Netherlands*, 27-45. DOI: 10.1007/978-94-017-0667-4_3

Steenvoorden, D.P.T. & Beijersbergen van Henegouwen, G.M.J. (1997). The use of endogenous antioxidants to improve photoprotection. *Journal of Photochemistry and Photobiology B: Biology*, 41(1): 1-10. DOI: 10.1016/s1011-1344(97)00081-x

Togni, S., Maramaldi, G., Cavagnino, A., Corti, A. & Giacomelli, L. (2019). Vitachelox: protection of the skin against blue light-induced protein carbonylation. *Cosmetics*, 6(3): 49. DOI:10.3390/cosmetics6030049

Townsend, D.M. & Tew, K.D. (2003). The role of glutathione-S-transferase in anti-cancer drug resistance. *Oncogene*, 22(47): 7369-7375.DOI: 10.1038/sj.onc.1206940

Uehleke, H. (2010). Untersuchungen mit fluoreszenz-markierten Antikörpern: IV. Die Markierung von SPACEntikörpern mit Sulfochloriden fluoreszierender Farbstoffe. Schweizerische Zeitschrift für allgemeine Pathologie und Bakteriologie, 22(5): 724-729.

Wang, Y., Li, W., Xu, S., Hu, R., Zeng, Q., Liu, Q., Li, S., Lee, H., Chang, M. & Guan, L. (2019). Protective skin aging effects of cherry blossom extract (*Prunus yedoensis*) on oxidative stress and apoptosis in UVB-irradiated HaCaT cells. *Cytotechnology*, 71(2): 475-487. DOI: 10.1007/s10616-018-0215-7

Wondrak, G.T., Jacobson, M.K. & Jacobson, E.L. (2006). Endogenous UVA-photosensitizers: mediators of skin photodamage and novel targets for skin photoprotection. *Photochemical & Photobiological Sciences*, 5(2): 215-237. DOI: 10.1039/b504573h

Xianyong, M., Dun, D. & Weidong, C. (2017). Inhibitors and activators of SOD, GSH-Px, and CAT. *InTech*. DOI: 10.5772/65936

Xu, P., Zhang, M., Wang, X., Yan, Y., Chen, Y., Wu, W., Zhang, L. & Zhang, L. (2018) Antioxidative effect of quetiapine on acute ultraviolet-B-induced skin and HaCaT cell damage. *International Journal of Molecular Sciences*, 19. DOI: 10.3390/ijms19040953.

Yamawaki, Y., Mizutani, T., Okano, Y. & Masaki, H. (2019). The impact of carbonylated proteins on the skin and potential agents to block their effects.

Experimental Dermatology, 28(S1): 32-37. DOI: 10.1111/exd.13821

You, Y.-H., Lee, D.-H., Yoon, J.-H., Nakajima, S., Yasui, A. & Pfeifer, G.P. (2001). Cyclobutane pyrimidine dimers are responsible for the vast majority of mutations induced by UVB irradiation in mammalian cells*. *Journal of Biological Chemistry*, 276(48): 44688-44694. DOI: 10.1074/jbc.M107696200

Zhang, S. & Duan, E. (2018). Fighting against skin aging: the way from bench to bedside. *Cell Transplantation*, *27*(5): 729-738. DOI: 10.1177/0963689717725755

Ziboh, V., Miller, C. & Cho, Y.H. (2000). Metabolism of polyunsaturated fatty acids by skin epidermal enzymes: Generation of antiinflammatory and antiproliferative metabolites. *The American Journal of Clinical Nutrition*, 71: 361S-366S. DOI: 10.1093/ajcn/71.1.361s

Borneo Journal of Resource Science and Technology (2024), 14(1): 112-122
DOI: https:doi.org/10.33736/bjrst.6089.2024

Comparative Study of Drying Methods on Seaweeds (*Kappaphycus* sp. *and Padina* sp.) Based on Their Phytochemical and Polysaccharaide Content Located in Sabah

NAZIRAH MINGU[1], KHAIREE M. SAAD[2], HASMADI MAMAT[3], MD SHAFIQUZZAMAN SIDDIQUEE[4], MOHD HAFIZ ABD MAJID[1] & MOHD SANI SARJADI[1*]

[1]Faculty of Science and Natural Resources, Universiti Malaysia Sabah, Jalan UMS, 88400 Kota Kinabalu, Sabah, Malaysia; [2]SGS (M) Sdn. Bhd. Lot 146, Jalan Lama, Lok Kawi, 88200 Putatan, Sabah, Malaysia; [3]Faculty of Food Science and Nutrition, Universiti Malaysia Sabah, Jalan UMS, 88400 Kota Kinabalu, Sabah, Malaysia; [4]Biotechnology Research Institute, Universiti Malaysia Sabah, Jalan UMS, 88400 Kota Kinabalu, Sabah, Malaysia.
*Corresponding author: msani@ums.edu.my
Received: 18 September 2023 Accepted: 28 December 2023 Published: 30 June 2024

ABSTRACT

Seaweed, one of the marine resources is known for their precious active compound. The dehydration process is required before the ultilization of the seaweed. It helps to increase the shelf life and play a major role in the extraction of specific chemical components. This study was conducted to evaluate the effects of different drying treatments of two different seaweeds on its phytochemical contents and carrageenan properties. Seaweed used include edible seaweed which are *Kappaphycus* sp., and locally abundant seaweed *Padina* sp. Four (4) different drying methods used; namely sun-drying for five (5) days, air-drying for 14 days, freeze-drying for five (5) days, and oven drying with three different temperatures at 60 °C, 80 °C and 100 °C for six (6) h, respectively. The moisture content was measured, and air-dried seaweeds contain highest moisture content (19.32% - 16.21%). Methanol, MeOH was used as extraction solvent in the determination of phytochemicals content for total phenolic content (TPC) and total flavonoid content (TFC). Sodium hydroxide, was used to extract carrageenan from *Kappaphycus* sp., which was evaluated on their percentage yield. Oven dried at 100 °C extracts possessed lowest retention of phytochemicals content and carrageenan yield among all drying methods. This finding suggests that various drying methods applied significantly influenced the composition of seaweeds. Identifying the most effective post-harvest drying procedure for seaweed would be commercially advantageous.

Keywords: Carrageenan, drying, *Kappaphycus* sp., *Padina* sp., phytochemical.

INTRODUCTION

In Malaysia, Sabah is notable for being a fertile ground for the growth and consolidation of several types of seaweed. It is due to geographical factor of Sabah compared to peninsular Malaysia, Sabah is geographically located below the monsoon and typhoon belt (Fudholi *et al.*, 2010; Hussin and Khoso, 2017). Been introduced since 1978, cultivation of seaweed in Sabah continues widely developed for several industries and became a job opportunity to the people (Ahemad *et al.*, 2010). Seaweed is a species of marine plants and algae that grows in the ocean, rivers, mangroves, and lakes. Seaweed has been utilised since the old times as food, grain, compost and as a wellspring of restorative medications (Mishra *et al*., 1993). Seaweeds are categorised into three large groups which are red algae, green algae, and brown algae, according to the pigment present. There are more than 1500 species of seaweed in each of the groups (Morais *et al*., 2020). They also been studied for various applications, which can be incorporated into several value-added food products, animals feed, medicinal purpose, etc. as shown in Table 1.

Seaweed contains dietary fibres, vitamins, minerals, carotenoids and fatty acids. Other than that, high content of phenolics and flavonoids also reported in seaweed (Mei Ling *et al*., 2013). Phenolic compound is a diverse group of molecules covers a wide range of aromatic secondary metabolite families. These phenolic compounds in seaweed are able to combat oxidative stress (Mei Ling *et al*., 2013). Flavonoid is an essential antioxidant as it has

high redox potential. This content allowed seaweed to act as a great antioxidant. Several studies have conducted and reported the high antioxidant activities of various seaweed (Yap *et al*., 2019; Mei Ling *et al*., 2013; Belattmania *et al*., 2016).

Table 1. Applications of seaweed

Seaweed	Studies on Application	References
Saccharina japonica	Bio-oil production	Zeb *et al*. (2017)
Gelidium robustum	Biodegradable plastics	Freile-PelegrÍn *et al*. (2007)
Ascophyllum nodosum	Fertilizer	Abdel-Mawgoud *et al*. (2010)
Gracilaria cylindrica		Yadav *et al.* (2023)
Ulva rigida		Latique *et al.*, (2013)
Fucus spiralis		
	Dermatological	Freitas *et al*. (2020)
Kappaphycus alvarezii	Edible film	Watt *et al.* (2014)
Undaria pinnatifida	Skincare	Jesumani *et al*. (2019)
Fucus spiralis Linnaeus	Anti-Inflammatory	Lopes *et al*. (2014)
Mixture of brown and red seaweed	Biogas production	Nkemka & Murto (2012)
Gracilaria birdiae	Biofilter	Marinho-Soriano *et al*. (2009)
Hydrilla verticillata	Adsorbent	Baral *et al*. (2009)
Hypnea hippurodies L.	Formulated shampoo	Tha (2012)
Laminaria digitate	Biofuel production	Vanegas *et al.* (2014)

Carrageenan is a polysaccharide that commonly extracted from red seaweeds (Rodophyta). It usually used in food, cosmetic and pharmaceutical industries (Moey *et al.*, 2014; Tha, 2012; Lopes *et al*., 2014). According to Yong *et al.*, (2015), demand for carrageenan had increase. This has led to increase of cultivation of *Kappaphycus* sp. in Malaysia. Carrageenan is one of polysaccharides in seaweed other than agar and cellulose that contain galactose and glucose. Kappa-carrageenan (Figure 1) is used widely in food additives as it produces strong rigid gels (Ferdouse *et al.*, 2018). It is a colloid that used as stabilizer and thickening agent in food, cosmetic and pharmaceutical industries. Carrageenan is an alternating copolymer of α-(1–3)-D-galactose and ß-(1–4)-3,6-anhydro-D-galactose (Ili Balqis *et al.*, 2017). Two other classes of carrageenan are iota(ι)-carrageenan (Figure 2) and lambda(λ)-carrageenan (Figure 3). Iota-carrageenan comes mainly from *Eucheuma spinosum.* It gives a more elastic and soft structure while lambda-carrageenan is commonly from *Chondrus crispus* and it provides a creamy sensation in dairy products (Ferdouse *et al.*, 2018). The classification of carrageenan is according to the number of sulphate ester groups in each of them and the presence of 3,6-anhydro-D-galactose. Table 2 shows the difference of carrageenan.

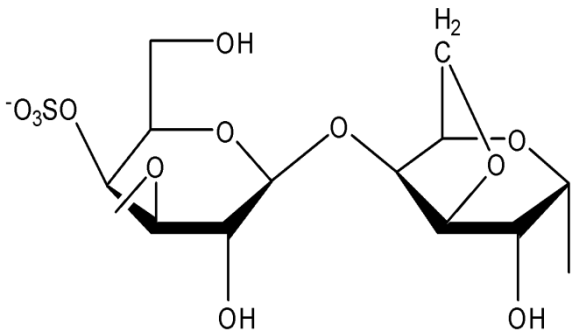

Figure 1. Kappa-carrageenan

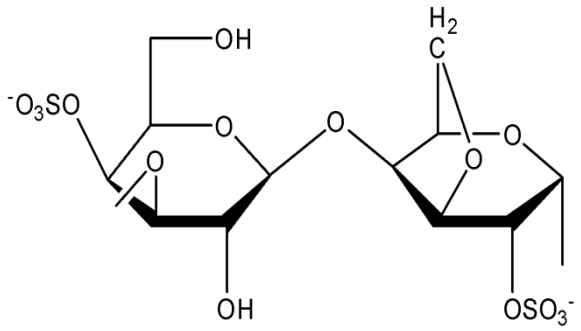

Figure 2. Iota-carrageenan

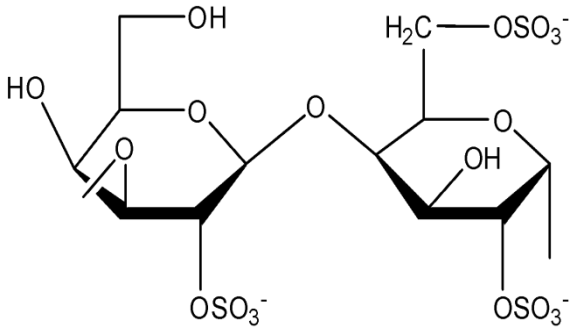

Figure 3. Lambda-carrageenan

Alginate is another type of polysaccharide extracted primarily from brown seaweeds (Phaeophyta). Commonly used in food, and actively studied on its pharmaceuticals, and biomedical applications for its gelling and binding properties (Salido *et al*., 2024). Figure 4 shows the chemical structures of sodium alginate that is known for its ability to form gels in the presence of divalent cations like calcium. In this study, alginate is extracted from brown seaweed, *Padina* sp.

In tropical countries like Malaysia, sun drying is a common method used to maintain the root products. Drying temperature affect bioactive compound and will degrade when dried at high temperature (Ismail *et al*., 2021). This study was conducted to investigate the impact of drying techniques on phytochemical content and polysaccharides extracted from *Kappaphycus* sp. and *Padina* sp. Methanol (80% v/v) was used for phytochemical content extraction and alkaline treatment for carrageenan extraction from *Kappaphycus* sp.

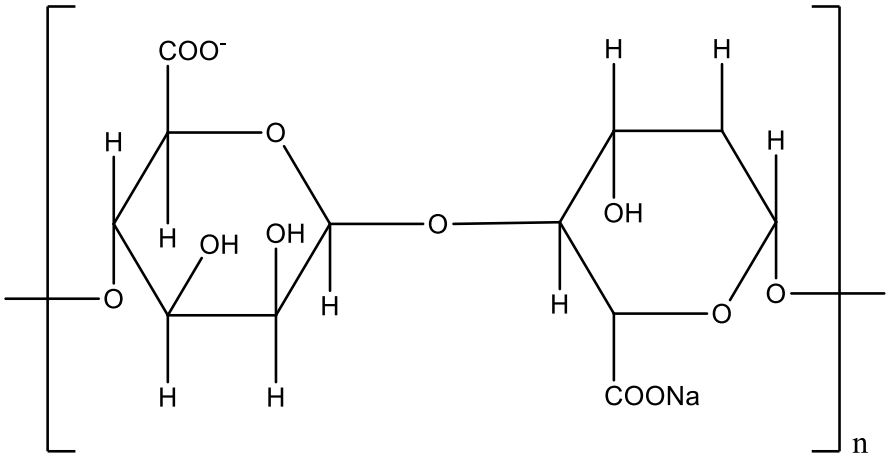

Figure 4. Sodium alginate structure

Table 2. Differences of carrageenan type (Shafie *et al*., 2022)

Name	Structure	Main sources	Usage
Kappa-carrageenan	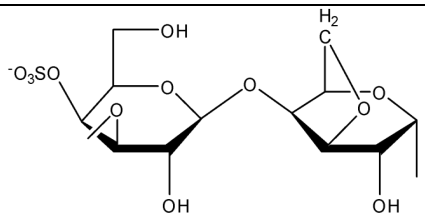	*Kappaphycus alvarezii*	• Thickening agent • Stabilising agent
Iota-carrageenan	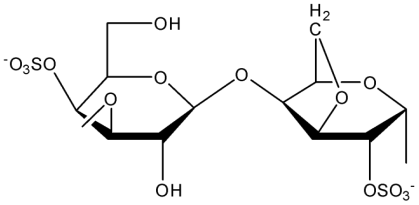	*Eucheuma spinosum*	• Elastic and soft structure
Lambda-carrageenan	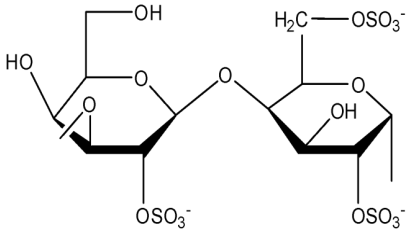	*Eucheuma gigartina*	• Thickening agent • Creamy product

MATERIALS & METHODS

Sample preparation

Both fresh *Kappaphycus* sp. and *Padina* sp. were collected from Semporna, Sabah. Seaweed was hand-picked from the cultivation locations. Harvests were occasionally cut by farmers using knives then followed by clean water wash and was sun-dried by laying on a horizontal platform before being delivered to Universiti Malaysia Sabah for experimental research purpose (Farhaduzzama *et al.*, 2023). *Kappaphycus* sp. labelled as (K) and *Padina* sp. labelled as (P). All seaweed was cleaned separately with tap water to remove epiphytes, salt and holdfast. Then, it was followed by washing with distilled water before continuing with drying process.

Drying process

Four different drying treatments were applied to both seaweeds under six different conditions. Washed seaweed was spread evenly in a single layer on trays except for freeze drying where the seaweeds were placed in a thermal container. Preliminary drying method was conducted to achieve constant weight of dried seaweed. Sun dry and freeze dry was held for 5 days, while air dry were held for 14 days. All oven dry samples were held for 6 hours. All dried samples applied were labelled as shown in Table 3. The moisture content of dried seaweed was taken and calculated using the following formula Eq.(1):

$$Moisture\ content\ (\%) = \frac{W1-W2}{W1} \times 100 \qquad \text{Eq.(1)}$$

Where,
W1: Weight (g) of sample before drying,
W2: Final weight (g) of sample after drying.

Extraction and determination of phytochemical content

Phytochemical content of dried seaweeds was extracted according to Neoh *et al.* (2021) with modification. Dried seaweed powders were extracted with 80% v/v of methanol with ratio sample: solvent of 1:20, w/v at room temperature. The mixture was sonicated for 30 minutes at 50 kHz in an Elmasonic S 180 H sonicator bath at 24°C, then shaken for 2 hours at room temperature in an incubator shaker. The

Table 3. Drying condition

Drying method	Condition for drying	Remark
Sun dry	5 days	SD
Freeze dry	-86 °C for 5 days	FD
Air dry	25 °C for 14 days	AD
Oven dry	100 °C for 6 hours	O1
Oven dry	80 °C for 6 hours	O2
Oven dry	60 °C for 6 hours	O3

extract was filtered through filter paper (Whatmann No. 1) before being stored at -20 °C for further analysis.

Total Phenolic Content (TPC)

Total phenolic content (TPC) from dried seaweed has been determined using Folin-Ciocalteu method by Ainsworth *et al.* (2007) with modification. About 100 µL of seaweed extract applied to 200 µL of Folin-Ciocalteu reagent. After five minutes, 800 µL of sodium carbonate applied to the mixture and allowed to stand in the dark room for 30 minutes. Gallic acid was used as standard. The results were expressed in the equivalent of 1 mg gallic acid equivalent per 1 g dried seaweed extract (mg GAE/g DS). A microplate spectrophotometer reader (Thermoscientific) against blank solution used to read absorbance at 765 nm. All measurements been performed in five replicates.

Total Flavonoid Content (TFC)

Total flavonoid content (TFC) been determined using the aluminium chloride calorimetric assay Neoh *et al.*, (2021) with modification. 120 µL of dried seaweed extract was used and added with 360 µL of methanol. After 5 minutes, 24 µL of aluminium chloride (10% w/v) was added to the mixture. 24 µL of potassium acetate was added to the mixture and the volume was made up to 1.2 mL with deionized water. The solution was well blended using vortex and sustained for 15 minutes in the dark room. Quercetin used as standard for standard calibration curve. Total flavonoid content was expressed as 1 mg quercetin equivalents in 1 g of dried seaweed (mg QUE/g DS). A microplate spectrophotometer reader against blank solution used to read absorbance at 510 nm. All measurements performed in five replicates.

Extraction and determination of carrageenan yield from *Kappaphycus* sp.

Carrageenan extraction for *Kappaphycus* sp. are according to Awalludin *et al.*, (2022) method with modification. five g of dried *Kappaphycus* sp. was heated in 200 mL of 1M NaOH and 200 mL of distilled water on a hot plate for 2 hours at 100°C. 100 mL of distilled water added, and the mixture then heated for another 2 hours. Yellowish-clear solution formed while heated. The mixture was filtered while hot and the solution was allowed to sustain in cold methanol overnight. The gel precipitate formed been centrifuge before filtered and oven dry at 60 °C for 6 hours. The yield of dried carrageenan was calculated using following formula; Eq. (2):

$$Carrageenan\ yield\ \% = \frac{Wc}{Wds} \times 100 \quad \text{Eq.(2)}$$

W_c: Weight (g) of dried carrageenan,
W_{ds}: Weight (g) of dried seaweed used.

Extraction and determination of alginate yield from *Padina* sp.

Sodium alginate extraction from *Padina* sp. was performed following method of Rashedy *et al.* (2021) with slight modifications. Approximately 0.5 g of dried samples was immersed in a 1% CaCl solution overnight. The solution was then separated, and the soaked seaweed was rinsed with deionized water two to three times. Subsequently, 5% HCl solution was added and maintained at room temperature overnight. The solution was then filtered, and the residue was washed again with deionized water three times. Alginate extraction was achieved by adding 3% of Na_2CO_3 and shake for an hour. The extract was filtered through a cheesecloth filter, and the filtrate was subjected to bleaching with a 2.5% (v:v) sodium hypochlorite solution. The extract sodium alginate was precipitated in ethanol and dried at 60 °C overnight. Alginate yield was determined using following formula; Eq.(3):

$$Polysaccharide\ yield\ \% = \frac{Weight\ (g)\ of\ dried\ alginate}{Weight\ (g)\ of\ dried\ seaweed} \times 100 \qquad \text{Eq.(3)}$$

RESULTS AND DISCUSSION

Moisture content

Table 4 shows the variation of moisture content for seaweeds at 6 drying methods ranged from 5.75% - 19.32% The orders of moisture content for *Kappaphycus* sp. among different drying methods in descending order are as follows: oven dry 100 °C (15.94%) > oven dry 80 °C (16.17%) > oven dry 100 °C (17.12%) > sun dry (18.29%) > air dry (19.32%). *Padina* sp. showed significantly lower moisture content than *Kappaphycus* sp., and this might be due to the difference in physical state of each selected seaweed. Physically, *Kappaphycus* sp. stored higher water content as it contained carrageenan, a hydrophilic compound (Farah Nurshahida *et al*., 2020). In addition, early research had shown that drying seaweed at temperatures above 50 °C caused its colour to darken due to degradation of chlorophyll within 2 hours, which led to a loss in phytochemical content (Uribe *et al*., 2018).

Table 4. Percentage yield of each seaweed

Seaweed	Drying techniques	Initial weight (g)	Final weight (g)	Yield (%)
Kappahycus sp.	SD	0.5030	0.4110	81.71
	AD	0.5113	0.4125	80.68
	FD	0.5001	0.4131	82.60
	O1	0.5140	0.4261	82.90
	O2	0.5073	0.4252	83.81
	O3	0.5021	0.4221	84.06
Padina sp.	SD	0.508	0.4562	89.82
	AD	0.5061	0.4243	83.83719
	FD	0.5013	0.448	89.36764
	O1	0.5011	0.465	92.79585
	O2	0.5021	0.472	94.00518
	O3	0.504	0.4753	94.30556

Phytochemical analysis

Total phenolic content (TPC) of *Kappaphycus* sp. ranged from 1.59 – 5.28 mg gallic acid equivalent (GAE) g^{-1} dried seaweed (DS) (Table 5). It can be observed that TPC varied with different drying methods. The order of TPC for *Kappaphycus* sp. across various drying methods in descending order are as follows: oven dry at 100 °C (1.45 ± 0.68 mg GAE/g DS) > sun dry (1.59 ± 0.9 mg GAE/g DS) > oven dry 80 °C (1.61 ± 0.28 mg GAE/g DS) > oven dry 60 °C (1.65 ± 0.78 mg GAE/g DS) > freeze dry (2.31 ± 0.24 mg GAE/g DS) > air dry (5.28 ± 0.29 mg GAE/g DS).

Table 5 also shows total flavonoid content (TFC) of *Kappaphycus* sp. ranged from 0.05 – 0.12 mg quercetin equivalent (QUE) g^{-1} dried seaweed (DS). The order of TFC for *Kappaphycus* sp. differ compared to its TPC. Order of extractability of flavonoids from *Kappaphycus* sp. in descending order are as follows: sun dry (0.12 ± 0.04 mg QUE/g DS) > oven dry 60 °C (0.07 ± 0.01 mg QUE/g DS) > freeze dry and oven dry 80 °C (0.06 ± 0.005 mg QUE/g DS) > air dry and oven dry 100 °C (0.05 ± 0.006 mg QUE/g DS).

Low TPC in *Padina* sp. extracted and different order compared to *Kappaphycus* sp. with ranged from 0.89 – 1.63 mg GAE g^{-1} dried seaweed (DS) as shown in Table 6. The order in descending order of TPC for *Padina* sp. are as follows: oven dry at 60 °C (0.89 ± 0.29 mg GAE/g DS) > freeze dry (0.97 ± 0.34 mg GAE/g DS) > oven dry 80 °C (1.25 ± 0.42 mg GAE/g DS) > oven dry 100 °C (1.34 ± 0.53 mg GAE/g DS) > air dry (1.58 ± 0.77 mg GAE/g DS) > sun dry (1.63 ± 0.31 mg GAE/g DS). Same table showed high TFC content in methanol extracts for *Padina* sp. It ranged from 0.31 – 0.95 mg quercetin equivalent (QUE) g^{-1} dried seaweed (DS). In this study, the order in descending order

for TFC in *Padina* sp. is same as its TPC content with sun dry (0.95 ± 0.05 mg QUE/g DS) contain the highest TFC and oven dry 60 °C (0.31 ± 0.005 mg QUE/g DS) contain the least TFC.

However, significant leaching of phenolic chemicals can be observed from sun drying and oven drying (100 °C) in *Kappaphycus* sp. This may be due to disability of the degrading enzyme polyphenol oxidase. In contrast, *Padina* sp. shows sun dried extract exhibit the highest phenolic content compared to other drying methods. Air drying still shows a higher TPC than other drying techniques. Oven dries of *Padina* sp. approved Gupta *et al.* (2011), where it stated that the percentage of total phenol and total flavonoid in dried seaweed will be reduced by 49-51% at temperatures below 40 °C and the reduction would be decreased as the drying temperature increased more than 41°C. Both phenolics and flavonoids content in Padina sp. increase in oven dries (60 °C > 80 °C > 100°C).

Table 5. Moisture content of *Kappaphycus* sp. and *Padina* sp. under different drying treatments.

Drying techniques	Moisture content (%)	
	Kappaphycus sp.	*Padina* sp.
SD	18.29	10.18
AD	19.32	16.21
FD	17.40	10.58
O1	17.12	7.19
O2	16.17	5.98
O3	15.94	5.75

Table 6. Phytochemical content of *Kappaphycus* sp.

Samples	Total Phenolics (mg GAE/g DS)[1]	Total Flavonoids (mg QUE/g DS)[2]
KSD	1.59 ± 0.9	0.12 ± 0.04
KAD	5.28 ± 0.29	0.05 ± 0.01
KFD	2.31 ± 0.24	0.06 ± 0.01
KO1	1.65 ± 0.78	0.07 ± 0.01
KO2	1.61 ± 0.28	0.06 ± 0.005
KO3	1.45 ± 0.68	0.05 ± 0.006

[1]Total phenolic content was expressed as mg gallic acid equivalents in 1g of dried seaweed (mg GAE/g DS)
[2]Total flavonoid content was expressed as mg quercetin equivalents in 1g of dried seaweed (mg QUE/g DS)

Carrageenan Yield

The drying process can alter both physical and chemical properties of the seaweed. The changes may impact the brittleness and texture which may influence the efficiency of subsequent carrageenan extraction processes. Figure 4 depicts the jelly-like carrageenan extracted from *Kappaphycus* sp. which is commonly utilised in food industries as thickening agent. Results show the percentage yield of carrageenan extracted from dried *Kappaphycus* sp. as shown in Figure 5. Carrageenan yield from *Kappaphycus* sp. varies depending on the drying techniques employed. These yields demonstrate variations attributed to the diverse drying methods applied to *Kappaphycus* sp. Carrageenan yield from *Kappaphycus* sp. treated with oven dry at 100 °C were significantly lower than other drying treatments. Meanwhile, oven dry at 80 °C yields higher carrageenan content than others, followed by air dry, oven dry at 60 °C, sun dry, freeze dry, and oven dry at 100 °C. High temperatures can cause rapid evaporation of moisture from seaweed. This may cause oven dry of *Kappaphycus* sp. at 100 °C yield low carrageenan as excessive moisture loss can hinder the extraction process and reduce carrageenan yield (de Faria *et al*., 2014).

Alginate Yield

Different drying techniques influence the alginate yield from *Padina* sp. as shown in Figure 6. Significant differences in alginate yield were observed by employing different drying methods on *Padina* sp. The result shows freeze – drying *Padina* sp. gives high yield of alginate compared to other drying techniques. Freeze – drying method involves freezing materials and removing moisture through sublimation, which help in reducing the potential for thermal

degradation. As the result, this method helps preserve the structure and functionality of carrageenan molecules, potentially leading to higher alginate yields. In contrast, oven dry at 80 °C gives low alginate yields as the heat applied on *Padina* sp. can alter the structural properties of alginate. The heat may denature the proteins in alginate that affecting its gelling and stabilising capabilities (Kelishomi *et al*., 2016).

CONCLUSION

In this study, different drying techniques on *Kappaphycus* sp. and *Padina* sp. were used to evaluate their phenolic and flavonoid content. The moisture content of seaweeds decreased along with the increase of temperature. Any type of processing and techniques applied such as high drying temperatures and extended drying may alter and lower certain phenol compounds in it (Li *et al*., 2006). Moreover, in the least presence of moisture, all plant cell components adhere to another and potentially make the extraction difficult, resulting in lower total phenolic content. The results from this study showed that different drying techniques affect TPC and TFC indicating that they differ depending on the drying conditions. The moderate temperature (60°C) and short drying period (6 hours) used in this process, shows the least affected total phenolic content. High temperature used to both seaweeds has led to a decrease of TPC. Sun-dried samples had the lowest levels of phenolic content. This is due to the longer drying duration (4 to 5 days in direct sunshine) and dehydration throughout the drying process, the phenolic content in the drying technique was impacted. This experimental data suggests the suitability of air drying as the best drying method for seaweed to preserve phenolic and flavonoid. Oven drying (80°C) is the best drying method applied on *Kappaphycus* sp. to conserve the carrageenan content. While for *Padina* sp., freeze drying is the beat drying method for high yield of alginate.

ACKNOWLEDGEMENTS

This study was supported by the Research Management Centre, Universiti Malaysia Sabah (UMS), Project code: DN20088.

REFERENCES

Abdel-Mawgoud, A.M.R., Tantaway, A.S., Hafez, M.M. & Habib, H.A. (2010). Seaweed extract improves growth, yield, and quality of different watermelon hybrids. *Research Journal of Agriculture and Biological Sciences*, 6(2): 161-168.

Ahemad Sade, I.A. & Ariff, M.R.M. (2010). The seaweed industry in Sabah, East Malaysia. *Journal of Southeast Asian Studies*, 11(1): 97-107.

Altemimi, A., Lakhssassi, N., Baharlouei, A., Watson, D.G. & Lightfoot, D.A. (2017). Phytochemicals: Extraction, isolation, and identification of bioactive compounds from plant extracts. *Plants*, 6(4): 42. DOI:10.3390/plants6040042

Awalludin, A., Mingu, N., Yaser, A.Z., Mamat, H., Kamaruzaman, K.A., Jamin, Z. & Sarjadi, M.S. (2021). Extraction and Physicochemical Properties of Refined Kappa-Carrageenan from Kappaphycus alvarezii Originated from Semporna, Sabah. Journal of Applied Science and Engineering, 25(3): 411-416. DOI:10.6180/jase.202206_25(3).0006

Baral, S.S., Das, N., Chaudhury, G.R. & Das, S.N. (2009). A preliminary study on the adsorptive removal of Cr (VI) using seaweed, *Hydrilla verticillata*. *Journal of Hazardous Materials*, 171(1-3): 358-369. DOI:10.1016/j.jhazmat.2009.06.011

Belattmania, Z., Engelen, A.H., Pereira, H., Serrão, E.A., Barakate, M., Elatouani, S. & Sabour, B. (2016). Potential uses of the brown seaweed *Cystoseira humilis* biomass: 2-Fatty acid composition, antioxidant and antibacterial activities. *Journal of Materials and Environmental Science*, 7(6): 2074-2081.

Boots, A.W., Haenen, G.R. & Bast, A. (2008). Health effects of quercetin: From antioxidant to nutraceutical. *European Journal of Pharmacology*. 58: 325-337. DOI:10.1016/j.ejphar.2008.03.008

Chellappan, D.K., Chellian, J., Leong, J.Q., Liaw, Y.Y., Gupta, G., Dua, K. & Palaniveloo, K. (2020). Biological and therapeutic potential of the edible brown marine seaweed *Padina australis* and their pharmacological mechanisms. *Journal of Tropical Biology & Conservation (JTBC)*, 17: 251-271. DOI:10.51200/jtbc.v17i.2667

de Faria, G.S.M., Hayashi, L. & Monteiro, A.R. (2014). Effect of drying temperature on carrageenan yield and quality of *Kappaphycus alvarezii* (*Rhodophyta, Solieriaceae*) cultivated in Brazil. *Journal of Applied Phycology*, 26: 917-922. DOI:10.1007/s10811-013-0172-7

Farah Nurshahida, M.S., Nazikussabah, Z., Subramaniam, S., Wan Faizal, W.I. & Nurul Aini, M.A. (2020). Physicochemical, Physical Characteristics and Antioxidant Activities of Three Edible Red Seaweeds (*Kappaphycus alvarezii, Eucheuma spinosum and Eucheuma striatum*) from Sabah, Malaysia, *IOP Conference Series: Materials Science and Engineering*, 991 (012048): 1-8. DOI:10.1088/1757-899X/991/1/012048

Farhaduzzaman, A.M., Khan, M.S., Hasan, M., Islam, R., Osman, M.H., Shovon, M.N.H., Haider, S.M.B., Kunda, M., Islam M.T. & Bhuyan, M.S. (2023). Seaweed Culture, Post-Harvest Processing, And Market Generation for Employment of Coastal Poor Communities in Cox's Bazar. *Journal of Applied Life Sciences and Environment*, 56(2): 231-244. DOI:10.46909/alse-562098

Ferdouse, F., Holdt, S.L., Smith, R., Murúa, P. & Yang, Z. (2018). The global status of seaweed production, trade and utilization. *Globefish Research Programme*, 124: 1-75.

Freitas, R.; Martins, A.; Silva, J.; Alves, C.; Pinteus, S.; Alves, J.; Teodoro, F.; Ribeiro, H.M.; Gonçalves, L.; Petrovski, Ž. Branco, L. & Pedrosa R. (2020). Highlighting the biological potential of the brown seaweed *Fucus spiralis* for skin applications. *Antioxidants*, 9(7)611: 1-21. DOI:10.3390/antiox90706112

Fudholi, A., Othman, M.Y., Ruslan, M.H., Yahya, M., Zaharim, A. & Sopian, K. (2011). The effects of drying air temperature and humidity on drying kinetics of seaweed. *Recent research in geography, geology, energy, environment and biomedicine*, 129-133. DOI:10.5555/2046174.2046196

Gupta, S., Cox, S. & Abu-Ghannam, N. (2011). Effect of different drying temperatures on the moisture and phytochemical constituents of edible Irish brown seaweed. *LWT-Food Science and Technology*, 44(5): 1266-1272. DOI:10.1016/j.lwt.2010.12.022

Hussin, H. & Khoso, A. (2017). Seaweed cultivation and coastal communities in Malaysia: An overview. *Asian Fisheries Science*, 30(2): 87-100. DOI:10.33997/j.afs.2017.30.2.003

Ili Balqis, A. M., Nor Khaizura, M.A.R., Russly, A.R. & Nur Hanani, Z.A. (2017). Effects of plasticizers on the physicochemical properties of kappa-carrageenan films extracted from Eucheuma cottonii, *International Journal of Biological Macromolecules*, 103: 721-732, DOI:10.1016/j.ijbiomac.2017.05.105.

Ilias, M.A., Ismail, A. & Othman, R. (2017). Analysis of carrageenan yield and gel strength of Kappaphycus species in Semporna Sabah. *Journal of Tropical Plant Physiology*, 9: 14-23.

Ismail, M.M., Komy, R.G.E. and Diab, M.H. (2021). Algal Bioactive Compounds and Their biological activities. *International Journal for Pharmaceutical Research Scholars*, 13(2):1440-1450. DOI:10.31838/ijpr/2021.13.02.198

Jesumani, V., Du, H., Aslam, M., Pei, P. & Huang, N. (2019). Potential use of seaweed bioactive compounds in skincare-A review. *Marine Drugs*, 17(12) 688: 1-19. DOI:10.3390/md17120688

Kelishomi, Z.H., Goliaei, B., Mahdavi, H., Nikoofar, A., Rahimi, M., Moosavi-Movahedi, A.A., Mamashli, F. & Bigdeli, B. (2016). Antioxidant activity of low molecular weight alginate produced by thermal treatment. *Food chemistry*, 196: 897-902. DOI:10.1016/j.foodchem.2015.09.091

Latique, S., Chernane, H., Mansori, M. & El Kaoua, M. (2013). Seaweed liquid fertilizer effect on physiological and biochemical parameters of bean plant (*Phaesolus vulgaris variety Paulista*) under hydroponic system. *European Scientific Journal*, 9(30): 174-191. DOI: 10.19044/ESJ.2013.V9N30P

Mei Ling, A.L., Yasir, S.M., Matanjun, P. & Abu Bakar, M.F (2013). Antioxidant activity, total phenolic and flavonoid contents of selected commercial seaweeds of Sabah, Malaysia. *International Journal of Pharmaceutical and Phytopharmacological Research (eIJPPR)*, *3*(3): 234-238.

Lopes, G., Daletos, G., Proksch, P., Andrade, P. B. & Valentão, P. (2014). Anti-inflammatory potential of monogalactosyl diacylglycerols and a monoacylglycerol from the edible brown seaweed *Fucus spiralis Linnaeus*. *Marine Drugs*, 12(3), 1406-1418. DOI:10.3390/md12031406

Marinho-Soriano, E., Nunes, S. O., Carneiro, M. A.A. & Pereira, D.C. (2009). Nutrients' removal from aquaculture wastewater using the macroalgae *Gracilaria birdiae*. *Biomass and Bioenergy*, 33(2), 327-331. DOI:10.1016/j.biombioe.2008.07.002

Mishra V.K.F, Temelli P.F., Shacklock O. & Craigie J.S. (1993) Lipids of the red alga *Palmaria palmata*. *Botanica Marina*. 36:169-174. DOI:10.1515/botm.1993.36.2.169

Moey, S.W., A. & Ahmad, I. (2014). Development, characterization and potential applications of edible film from seaweed (*Kappaphycus alvarezii*). *AIP Conference Proceedings.* 1614(1): 192-197. DOI:10.1063/1.4895194

Morais, T., Inácio, A., Coutinho, T., Ministro, M., Cotas, J., Pereira, L. & Bahcevandziev, K. (2020). Seaweed potential in the animal feed: A review. *Journal of Marine Science and Engineering*, 8(8)559: 1-24. DOI:10.3390/jmse8080559

Mujumdar, A. S. & Devahastin, S. (2000). Fundamental principles of drying. *Exergex*, Brossard, Canada, 1(1): 1-22.

Necas, J. & Bartosikova, L. (2013). Carrageenan: A Review. *Veterinarni Medicina*, 58(4): 187-205 DOI:10.17221/6758-VETMED

Neoh, Y.Y., Matanjun, P. & Lee, J.S. (2016). Comparative study of drying methods on chemical constituents of Malaysian red seaweed. *Drying Technology*, 34(14): 1745-1751. DOI:10.1080/07373937.2016.1212207

Neoh, Y.Y., Matanjun, P. & Lee, J.S. (2021). Effects of Various Drying Processes on Malaysian Brown Seaweed, *Sargassum polycystum* Pertaining to Antioxidants Content and Activity. *Transactions on Science and Technology*, 8(1): 25-37.

Nkemka, V.N. & Murto, M. (2012). Exploring strategies for seaweed hydrolysis: Effect on methane potential and heavy metal mobilisation. *Process Biochemistry*, 47(12): 2523-2526. DOI:10.1016/j.procbio.2012.06.022

Norra, I., Aminah, A., Suri, R. & Arif Zaidi, J. (2017). Effect of drying temperature on the content of fucoxanthin, phenolic and antioxidant activity of Malaysian brown seaweed, *Sargassum* sp. *Journal of tropical agriculture and food science*, 45(1), 2--36.

Nurshahida, M.F., Nazikussabah, Z., Subramaniam, S., Faizal, W.W. & Aini, M.N. (2020). Physicochemical, physical characteristics and antioxidant activities of three edible red seaweeds (*Kappaphycus alvarezii*, *Eucheuma spinosum* and *Eucheuma striatum*) from Sabah, Malaysia. *IOP Conference Series: Materials Science and Engineering*. 991(1)012001: 1-8. **DOI:**10.1088/1757-899X/991/1/012048

Ratti, C. (2001). Hot air and freeze-drying of high-value foods: A review. *Journal of Food Engineering*, 49(4): 311-319. DOI:10.1016/S0260-8774(00)00228-4

Salido, M., Soto, M. & Seoane, S. (2024). Seaweed: Nutritional and gastronomic perspective. A review, *Algal Research,*77 (103357):1-11. DOI:10.1016/j.algal.2023.103357.

Shafie, M.H., Kamal, M.L., Zulkiflee, F.F., Hasan, S., Uyup, N.H., Abdullah, S., Hussin, N.A.M., Tan, Y.C. & Zafarina, Z. (2022). Application of Carrageenan extract from red seaweed (Rhodophyta) in cosmetic products: A review. *Journal of the Indian Chemical Society*, 99(9) 100613: 1-7. DOI:10.1016/j.jics.2022.100613

Rashedy, S., Hafez, A.E.H., Mohamed S.M., Mahmoud, D. João, C., Leonel, P. & Anabela, R. (2021). Evaluation and Characterization of Alginate Extracted from Brown Seaweed Collected in the Red Sea, *Applied Sciences*, 11 (6290): 1-17. DOI:10.3390/app11146290

Uribe, E., Vega-Gálvez, A., Vargas, N., Pasten, A., Rodríguez, K. & Ah-Hen, K.S. (2018). Phytochemical components and amino acid profile of brown seaweed *Durvillaea antarctica* as affected by air drying temperature. *Journal of food science and technology*, 55(12): 4792-4801. DOI:10.1007/s13197-018-3412-7

Vanegas, C., Hernon, A. & Bartlett, J. (2014). Influence of Chemical, mechanical, and thermal pretreatment on the release of macromolecules from two irish seaweed species. *Separation Science and Technology*, 49(1): 30-38. DOI:10.1080/01496395.2013.830131

World Bank Group. (2016). Seaweed aquaculture for food security, income generation and environmental health in tropical developing countries. World Bank. DOI:10.1596/24919

Yadav, S.K., Yohannan, A.S.K. & Palanisamy, M. (2023). Seaweeds as Natural Resource for agar-agar Extraction in India- A Review, *Agro Economist - An International Journal*, 10(02): 201-208. DOI:10.30954/2394-8159.02.2023.13

Yap, W.F., Tay, V., Tan, S.H., Yow, Y.Y. & Chew, J. (2019). Decoding antioxidant and antibacterial potentials of Malaysian green seaweeds: *Caulerpa racemosa* and *Caulerpa lentillifera*. *Antibiotics*, 8(3)152: 1-18. DOI:10.3390/antibiotics8030152

Yong, Y.S., Yong, W.T.L., Ng, S.E., Anton, A. & Yassir, S. (2015). Chemical composition of farmed and micropropagated *Kappaphycus alvarezii (Rhodophyta, Gigartinales*), a commercially important seaweed in Malaysia. *Journal of Applied Phycology*, 27: 1271-1275. DOI:10.1007/s10811-014-0398-z

Zeb, H., Park, J., Riaz, A., Ryu, c. & Kim, J. (2017). High-yield bio-oil production from macroalgae (Saccharina japonica) in supercritical ethanol and its combustion behavior, *Chemical Engineering Journal*, 327: 79-90. DOI:10.1016/j.cej.2017.06.078.

Borneo Journal of Resource Science and Technology (2024), 14(1): 123-138
DOI: https:doi.org/10.33736/bjrst.5653.2024

Preliminary Characterisation of Lowland and Upland Rice from Sarawak, Malaysian Borneo

ZAZEVIA FRANK CLIFTON[1], FREDDY KUOK SAN YEO[1]*, RENEE PRISCILLA TRAWAS SYLVESTER EMBUAS[1], MEEKIONG KALU[1], ZINNIRAH SHABDIN[1] & LEE SAN LAI[2]

[1]Faculty of Resource Science and Technology, Universiti Malaysia Sarawak, Jalan Datuk Mohammad Musa, 94300, Kota Samarahan, Sarawak, Malaysia; [2]Agriculture Research Centre Semongok, KM20, Jalan Puncak Borneo, 93250, Kuching, Sarawak
*Corresponding author: yksfreddy@unimas.my
Received: 21 April 2023 Accepted: 08 May 2024 Published: 30 June 2024

ABSTRACT

Oryza sativa L. or commonly known as rice belongs to the family of Poaceae. In Malaysia, rice is normally cultivated either as lowland or upland rice. Sarawak is a state with diverse types of rice. All Sarawak rice are landraces. Despite the fact that Sarawak is rich in rice biodiversity, the assessment of the morphological traits which may provide basic information that is useful for the future breeding programs is still unavailable. The nomenclature of the landraces is based on the name given by the farmers. Problems arise when landraces having the same morphological characteristics were given different names and vice versa. In addition, the purity of seeds is unreliable. Common practices by the local farmers such as planting different rice landraces in the same field either in one plot or in different plots but very near to each other has contributed to the impurity of the seeds. The present study was undertaken with the objective to characterise the morphological traits of 22 lowland and 22 upland rice accessions from the North-Western region of Sarawak. The morphological traits observed on the 44 rice accessions *viz*., blade colour, ligule shape, ligule colour, auricle colour, heading days, flowering days, panicle type, culm length, panicle number, number of filled grain, seed length and grain colour exhibited variations. There are variations which may be considered in future Sarawak rice breeding programs.

Keywords: Lowland rice, *Oryza sativa*, rice breeding, Sarawak, upland rice

INTRODUCTION

Rice being the staple food of Malaysian is the country's most important crop. Food and Agriculture Organization reported that rice production in Malaysia for the year 2019 was 2.8 million tonnes, 3.6% more than the average rice production from the year 2014 to 2018 (Food and Agriculture Organization of the United Nations, 2019). Although the production shows an increasing trend, with the growing number of residents in Malaysia annually, the production of rice in the country is still considered insufficient to meet domestic demands. Malaysia still relies on the neighbouring countries such as Vietnam, Thailand, and Pakistan for importing rice (Khazanah Research Institute, 2019).

Sarawak is the country's fifth largest rice producing state, after Kedah, Perak, Kelantan and Perlis with 134, 260 ha of land planted with lowland and upland rice (Masni & Wasli, 2019). Rice is economically, socially and culturally important in Sarawak. There are two types of rice planted in Sarawak; lowland rice, which is grown in field that is either rain-fed or irrigated; and upland rice, which is grown in an area naturally well-drained without surface water accumulation (International Rice Research Institute [IRRI], n.d.). The state is very rich in the diversity of rice (Yeo *et al*., 2018). For example, Sarawak rice has different resistance towards *Pyricularia oryzae* (Lai *et al*., 2019; Yeo *et al*., 2024) and may have different defence mechanisms against *Scirpophaga incertulas* (Cheok *et al*., 2019;

Hamsein *et al*., 2020; Ling *et al*., 2020), and different toxicity response to antifungal nanoparticles (Tang *et al*., 2023), which are potential genetic resources for rice breeding.

Department of Agriculture, Sarawak has declared a total of 2011 rice accessions are currently deposited in the gene bank of Agriculture Research Centre (including imported accessions) (Department of Agriculture Sarawak, 2020). Sarawak rice accessions should be considered as landraces. The nomenclature of the landraces is based on the name given by the farmers. There is problem with identification when landraces having the same morphological characteristics were given different names or vice versa. The purity of farmer's seed is also unreliable because of the common practice of planting different rice landraces in the same field either in one plot or in different plots but very near to each other (Yeo *et al*., 2018).

Despite the fact that Sarawak is rich in rice biodiversity, the morphological characteristics of each Sarawak rice landrace are unclear. Thus far, no report is available describing the morphological characteristics of the Sarawak rice landraces. The information on morphological trait is useful for rice breeders in selecting parents of specific traits for breeding programs. Therefore, the objective of this study was to characterise the morphological traits of Sarawak rice landraces collected from the northwest region of Sarawak.

In order to allow unique individuals from each rice landrace collection (heterogenous population) to be assessed, Simple Sequence Repeats (SSR) marker was used in this study for genotyping and plant selection. SSR are commonly used for fingerprinting and effectively used for assessing the genetic diversity among closely related rice cultivar (Bhattarai *et al*., 2021) due to its ability to reveal polymorphism even in closely related varieties (Spada *et al*., 2004). Four SSR markers (RM1, RM279, RM489 and RM335) has been tested on 220 accessions. Out from 220 accessions, 44 accessions showed polymorphism.

MATERIALS AND METHODS

Collection and Pre-Selection of Rice Landrace

A total of 22 rice landraces (11 lowland and 11 upland landraces) were collected from different localities across different divisions in northwest region of Sarawak (Supplementary Table 1). A total of 10 seeds per landrace were germinated in different batches (Supplementary Table 2) in distilled water. Germinated seeds, were transplanted into trays containing planting medium of topsoil, compost and sand (3:2:1 ratio). Each seedling was considered as different accession (Total = 220 accessions). The seedlings were then genotyped using Simple Sequence Repeat (SSR) markers.

Young leaf samples, about 4-5 cm, were collected from the 220 accessions. Deoxyribonucleic acid (DNA) was extracted using Cetyltrimethylammonium Bromide protocol by Doyle and Doyle (1987). A total of 12 SSR markers were randomly chosen from RiceGenes database (www.gramene.org) representing the 12 chromosomes of rice. The 12 SSR markers were tested on two randomly selected accessions from different rice landrace. Four SSR markers (Supplementary Table 3) which showed polymorphisms were chosen for genotyping the 220 accessions. Polymerase Chain Reaction (PCR) amplification was performed by following Zhu *et al.* (2012). After electrophoresis, the agarose gel was stained with ethidium bromide and visualized.

From the 10 seedlings of each landrace, individuals with polymorphic genotype based on the four SSR markers were chosen for morphological characterisation without

replication. For a landrace, with ten seedlings having monomorphic genotype, one individual was selected randomly. In total, there were 44 accessions selected for morphological characterisation (22 accessions for lowland and upland rice, respectively).

The selected lowland rice accessions were transplanted into pots (13 inches, 5 gallons). Each pot was filled three-quarters full of soil mixture of topsoil, compost and sand (3:2:1 ratio). For pots used for planting lowland rice accessions, drainage holes were drilled on two sides of a pot, about 8 cm above the soil surface in the pot, to create a constant water level. Pots for upland rice accessions, had three drainage holes at the bottom to drain excess water. Watering was done once a day using tap water. The nitrogen, phosphorus and potassium (NPK) fertilizer (17.5:15.5:10) was used for fertilization. Ten grams of fertilizer was applied per pot per application. The first fertiliser application took place at roughly the same time with transplanting. The second application took place about 30-40 days after the first application. The third application took place during the flowering stage. The experiment was performed from October 2018 to June 2019, following the main rice planting season in Sarawak.

Morphological Characterisation

A total of 14 traits were selected from the International Rice Research Institute guidelines (International Board for Plant Genetic Resources & International Rice Research Institute Rice Advisory Committee, 1980) and 8 additional traits were added based on the observation of this study (Total = 22 morphological traits). Apart from observing morphological traits, developmental traits such as heading days (HD) and flowering days (FD) were studied throughout the experiment. All recorded characters, methods and criteria are shown in Supplementary Table 4. Thirteen quantitative morphological traits were compared between lowland and upland rice accessions. Student's t-test was used to analyse the data.

Cluster analysis was done based on nine qualitative traits. Data matrices were analysed using Paleontological Statistic (PAST) software version 4.03 to construct a dendrogram made up using Jaccard's coefficient, showing the relatedness between the 44 rice accessions.

RESULTS

Pre-Screening of Rice Accessions

A total of 44 accessions out of 220 accessions were selected based on their SSR marker genotype (Supplementary Table 5). From the 44 accessions, there were 22 accessions of lowland rice designated as UNIMAS-23 – UNIMAS-44 and 22 accessions of upland rice designated as UNIMAS-01 – UNIMAS-22.

Morphological Characterisation of Rice Accessions

A total of 22 traits were recorded for both lowland and upland accessions. There were nine qualitative and 13 quantitative traits along with two observed developmental traits (Supplementary Table 4).

Qualitative Traits.

Polymorphism was observed in seven of the nine qualitative traits in the present study (Table 1). The leaf blade colour (BC) showed polymorphisms among the 44 accessions. BC had three classes recorded *viz*. pale green, green and dark green in both types of rice accessions (Supplementary Figure 1). From the observed 22 lowland rice accessions, 12 accessions had pale green BC, eight recorded dark green and only two accessions (UNIMAS-32 and UNIMAS-41) recorded green BC. For upland rice accessions, four accessions were pale green,

12 accessions were green and the remaining accessions were dark green.

The ligule shape (LS) was polymorphic for lowland rice accessions but was monomorphic for upland rice accessions where all the accession had acute to acuminate LS. For lowland rice accessions, there were two groups of LS recorded: acute to acuminate and 2-cleft. Seventeen (78%) of lowland rice accessions were recorded as having acute to acuminate LS while five accessions had 2-cleft LS (Supplementary Figure 2).

The colour of ligule (LC) and auricles (AC) of lowland rice accessions were monomorphic. All of them had white coloured ligule and auricle. The LC and AC were polymorphic for upland rice accessions. All the upland rice accessions had white LC and AC, except for one accession (UNIMAS-07) having purple ligule and auricle (Supplementary Figure 2).

As for the panicle, the type of panicle (PT) separated the lowland and upland rice accessions into three different groups, *viz.*, compact, intermediate and open PT (Supplementary Figure 3). For lowland rice accessions, a total of 12 accessions had intermediate PT, three accessions (UNIMAS-31, UNIMAS-39 and UNIMAS-42) showed an open PT and two accessions (UNIMAS-37 and UNIMAS-38) with compact PT. Five other accessions did not produce any panicles during the period of observation. A majority, 14 out from 22 (64%) accessions were having intermediate PT and six accessions exhibited open PT. Only one accession (UNIMAS-15) was having compact PT. There was one upland accession (UNIMAS-22) that did not produce any panicles during the period of observation.

Secondary branches (SB) in a panicle were grouped into three types: absent, light and heavy (Supplementary Figure 4) in both lowland and upland accessions. Among the 17 lowland rice accessions that flowered, SB was absent in three accessions (UNIMAS-23, UNIMAS-24 and UNIMAS-28), 12 accessions recorded light SB and the remaining two accessions had heavy SB (UNIMAS-27 and UNIMAS-37) (Table 1). For the 21 upland rice accessions that flowered, SB was found absent in eight accessions. Another eight accessions were having light SB and the remaining five accessions (UNIMAS-07, UNIMAS-08, UNIMAS-15, UNIMAS-17, and UNIMAS-18) were having heavy SB (Table 1).

The seed shape (SS) varied, where three classes were recorded among the rice accessions that flowered: oblong, elliptic and linear (Supplementary Figure 5 & 6). Oblong and linear SS were recorded for the 17 flowered lowland rice accessions (Table 1), where 10 lowland rice accessions produced seeds with linear SS and the remaining seven lowland rice accessions had oblong SS. For the 21 flowered upland rice accessions, 20 had linear SS and one accession had elliptic SS (Table 1).

Variation was also observed among the flowered rice accessions in seed colour (SC). The lowland rice accessions were grouped into four categories of SC; (1) yellow, (2) pale yellow, (3) blackish yellow and (4) golden-brown husk colour (Supplementary Figure 5 & 6). Ten out of 17 flowered lowland rice accessions exhibited pale yellow SC; four accessions with yellow SC, two accessions had blackish yellow SC and one accession with golden brown SC (Table 1). On the other hand, the flowered upland rice accessions exhibited yellow, blackish yellow and golden-brown husk SC. A majority, 13 (62%) accessions were having yellow SC. Five other accessions (24%) were having blackish yellow SC and the remaining three accessions (UNIMAS-12, UNIMAS- 19 and UNIMAS-21) were having golden brown SC (14%) (Table 1).

Table 1. The characters of nine qualitative traits for the 44 rice accessions

Type	Accession	BC	LS	LC	AC	PT	SB	SS	SC	GC
LOWLAND	UNIMAS-23	1	1	1	1	2	0	2	4	1
	UNIMAS-24	3	1	1	1	2	0	2	2	4
	UNIMAS-25	1	1	1	1	2	1	2	2	3
	UNIMAS-26	1	1	1	1	2	1	2	2	4
	UNIMAS-27	1	1	1	1	2	2	2	3	1
	UNIMAS-28	1	1	1	1	2	0	4	2	3
	UNIMAS-29	3	2	1	1	2	1	2	3	4
	UNIMAS-30	1	2	1	1	2	1	4	1	1
	UNIMAS-31	1	1	1	1	3	1	4	2	2
	UNIMAS-32	2	2	1	1	2	1	4	1	2
	UNIMAS-33	1	2	1	1	N/A	N/A	N/A	N/A	N/A
	UNIMAS-34	1	1	1	1	N/A	N/A	N/A	N/A	N/A
	UNIMAS-35	3	1	1	1	2	1	4	2	2
	UNIMAS-36	3	1	1	1	2	1	4	2	2
	UNIMAS-37	3	1	1	1	1	2	2	2	2
	UNIMAS-38	3	1	1	1	1	1	4	2	6
	UNIMAS-39	3	1	1	1	3	1	4	2	2
	UNIMAS-40	3	1	1	1	N/A	N/A	N/A	N/A	N/A
	UNIMAS-41	2	1	1	1	N/A	N/A	N/A	N/A	N/A
	UNIMAS-42	1	1	1	1	3	1	4	1	1
	UNIMAS-43	1	2	1	1	2	1	4	1	1
	UNIMAS-44	1	1	1	1	N/A	N/A	N/A	N/A	N/A
UPLAND	UNIMAS-01	3	1	1	1	2	0	4	1	1
	UNIMAS-02	1	1	1	1	3	0	4	1	1
	UNIMAS-03	2	1	1	1	2	0	4	1	1
	UNIMAS-04	2	1	1	1	2	0	4	1	1
	UNIMAS-05	2	1	1	1	2	0	4	1	1
	UNIMAS-06	2	1	1	1	2	1	4	1	1
	UNIMAS-07	2	1	3	2	2	2	4	1	3
	UNIMAS-08	2	1	1	1	2	2	4	1	2
	UNIMAS-09	2	1	1	1	2	1	4	1	1
	UNIMAS-10	2	1	1	1	2	1	4	1	1
	UNIMAS-11	3	1	1	1	2	1	4	1	2
	UNIMAS-12	2	1	1	1	2	0	4	1	1
	UNIMAS-13	2	1	1	1	2	1	4	1	2
	UNIMAS-14	2	1	1	1	3	1	4	1	2
	UNIMAS-15	1	1	1	1	1	2	4	1	1
	UNIMAS-16	3	1	1	1	3	1	3	1	4
	UNIMAS-17	1	1	1	1	3	2	4	1	1
	UNIMAS-18	3	1	1	1	3	2	4	1	1
	UNIMAS-19	1	1	1	1	3	1	4	4	1
	UNIMAS-20	2	1	1	1	2	0	4	3	1
	UNIMAS-21	3	1	1	1	2	0	4	4	1
	UNIMAS-22	3	1	1	1	N/A	N/A	N/A	N/A	N/A

Note. N/A: Data Not Available. BC: Blade Colour (Scale: 1; Pale Green, 2; Green, 3; Dark Green, 4; Purple Tips, 5; Purple Margins, 6; Purple Blotch), LS: Ligule Shape (Scale: 1;Acute To Acuminate, 2; 2-Cleft, 3; Truncate), LC: Ligule Colour (Scale: 1; White, 2; Purple Lines, 3; Purple), AC: Auricle Colour (Scale:1; White, Or 2; Purple, 3; Pale Green), PT: Panicle Type (Scale: 1; Compact, 2; Intermediate, And 3; Open), SB: Secondary Branching (Scale: 0; Absent, 1; Light, 2; Heavy), SS: Seed Shape (Scale: 1; Round, 2; Oblong, 3; Elliptic, 4; Linear), SC: Seed Colour (Scale: 1; Yellow, 2; Pale Yellow, 3; Blackish Yellow, 4; Golden Brown), GC: Grain Colour (Scale: 1; Milky White, 2; Reddish Brown, 3; Dark Brown, 4; Black, 5; Greenish White, 6; Light Reddish Brown)

Grain colour (GC) also showed high polymorphism among the flowered rice accessions. The 17 flowered lowland rice accessions were grouped into five GC groups: milky white, light reddish-brown, reddish brown, dark brown, and black (Supplementary Figure 5). Meanwhile, the 21 flowered upland rice accessions were grouped into four different groups: milky white, reddish-brown, dark brown and black (Supplementary Figure 6).

Cluster analysis grouped the 44 rice accessions into two main clusters based on the similarity index (Figure 1). The first cluster consisted of 27 rice accessions and the second cluster consisted of 17 rice accessions (Table 2). Among the nine qualitative traits used for PAST analysis, SB seemed to be the main character which separated the 44 rice accessions into two clusters. The cluster with 27 accessions was

mainly consists of accessions with light (scale: 1) and heavy (scale: 2) SB. The other cluster consists of mostly accessions having absent (scale: 0) of SB.

Table 2. Clustering of 44 rice accessions based on nine qualitative traits using Jaccard's coefficient

Cluster	Number of Accessions	Accession
I	27	UNIMAS-42-SRI/L, UNIMAS-39-SAMA/L, UNIMAS-38-SAMA/L, UNIMAS-37-SAMA/L, UNIMAS-36-SAMA/L, UNIMAS-35-SAMA/L, UNIMAS-32-SAMA/L, UNIMAS-31-SAMA/L, UNIMAS-30-SAMA/L, UNIMAS-29-SRI/L, UNIMAS-19-SRI/U, UNIMAS-18-SRI/U, UNIMAS-17-SRI/U, UNIMAS-16-SRI/U, UNIMAS-15-SRI/U, UNIMAS-13-KCH/U, UNIMAS-06-KCH/U, UNIMAS-07-KCH/U, UNIMAS-08-KCH/U, UNIMAS-09-KCH/U, UNIMAS-10-KCH/U, UNIMAS-11-KCH/U, UNIMAS-14-KCH/U, UNIMAS-26-KCH/U, UNIMAS-42-SRI/L
II	17	UNIMAS-40-KCH/L, UNIMAS-21-SRI/U, UNIMAS-12-KCH/U, UNIMAS-05-KCH/U, UNIMAS-04-KCH/U, UNIMAS-03-SER/U, UNIMAS-02-SER/U, UNIMAS-01-SER/U, UNIMAS-20-SRI/U, UNIMAS-22-KCH/U, UNIMAS-08-KCH/U, UNIMAS-23-SER/L, UNIMAS-24-KCH/U , UNIMAS-28-SR1/L, UNIMAS-33-SR1/L, UNIMAS-34-SR1/L, UNIMAS-41-KCH/L, UNIMAS-44-SR1/L,

Note. The accession number followed by an abbreviation indicating the division where seeds were collected and either it is lowland or upland rice accession. SRI: Sri Aman, SAMA: Kota Samarahan, KCH: Kuching, SER: Serian, /L: lowland rice accession, /U: upland rice accession

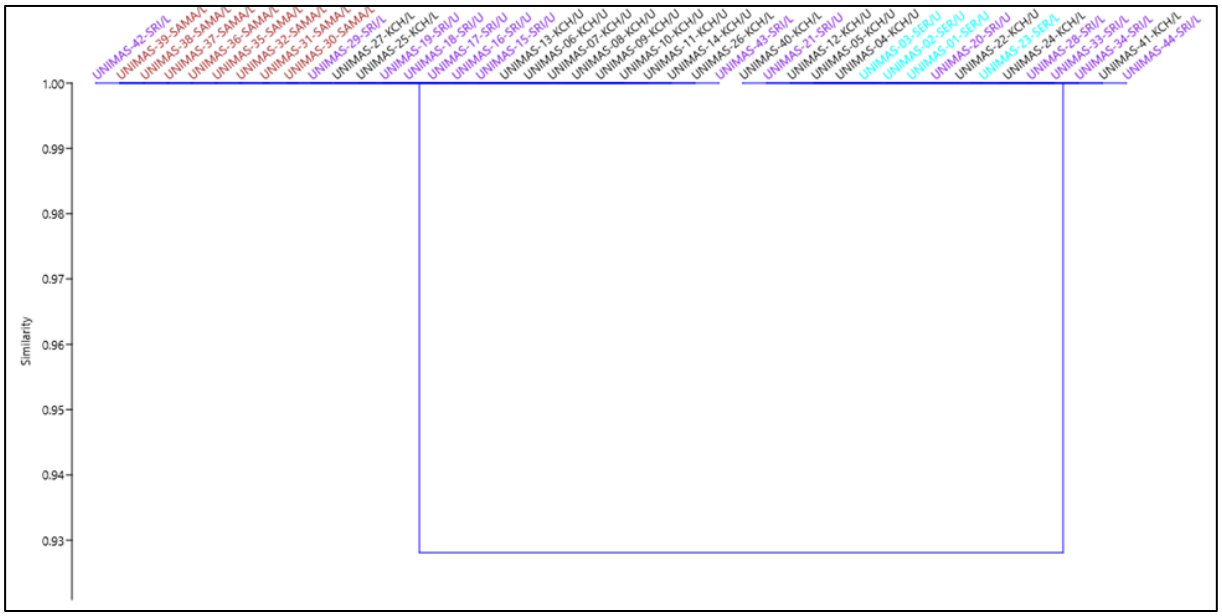

Figure 1. Dendrogram made up using Jaccard's coefficient of 44 rice accessions of lowland and upland rice from different divisions of the North-Western Region of Sarawak. *Note.* Purple: Sri Aman, Maroon: Kota Samarahan, Black: Kuching, Light Blue: Serian. Accession number followed by "/L" indicates lowland rice accession, "/U" indicates upland rice accession.

Quantitative Traits.

A total of 15 quantitative morphological traits of the 44 rice accessions are furnished in Table 3 and Table 4.

Plant height at five leaves stage or seedling height (SH) of lowland rice accessions (Table 3) ranged from 38.8 cm (UNIMAS-33) to 54.5 cm (UNIMAS-29). While among upland rice accessions, the SH ranged from 41.1 cm (UNIMAS-16) to 54.5 cm (UNIMAS-08) (Table 4). There was no significant difference in SH between lowland and upland rice accessions (Table 5).

At the mature stage, the plant height (PH) of lowland rice accessions (Table 3) ranged from 153.4 cm (UNIMAS-26) to 225.3 cm (UNIMAS-34). For upland rice accessions,

PH ranged from 90.9 cm (UNIMAS-09) to 201.2 cm (UNIMAS-07) (Table 4). In average, the lowland rice accessions were significantly taller than those upland rice accessions (Table 5).

Culm length (CL) for lowland rice accessions (Table 3) was ranging from 81.5 cm (UNIMAS-26) to 143.4 cm (UNIMAS-34). For upland rice accessions, the CL ranged from 40.7 cm (UNIMAS-02) to 115.7 cm (UNIMAS-22) (Table 4). The CL of lowland rice accessions was statistically longer than those of upland rice accessions (Table 5).

Culm diameter (CD) for lowland rice accessions (Table 3) ranged from 3.0 cm (UNIMAS-27, UNIMAS-37, UNIMAS-39, and UNIMAS-43) to 3.6 cm (UNIMAS-41). Among upland rice accessions, the mean of CD was 3.21 cm, ranging from 2.7 cm (UNIMAS-17) to 4.1 cm (UNIMAS-19) (Table 4). No significant difference was observed for CD between lowland and upland rice accessions (Table 5).

The leaf length (LL) observed among the lowland rice accessions ranged from 51.0 cm (UNIMAS-32) to 80.50 cm (UNIMAS-35) (Table 3), while 42.3 cm (UNIMAS-02) to 72.0 cm (UNIMAS-19) for upland rice accessions (Table 4). The LL was similar between the lowland and upland rice accessions (Table 5).

The leaf width (LW) for lowland rice accessions ranged from 1.1 cm (UNIMAS-25 and UNIMAS-44) to 2.2 cm (UNIMAS-31) (Table 3). With an average LW of 1.64 cm, lowland rice accessions had narrower LW as compared to those upland rice accessions (Table 5). The upland rice accessions had LW ranging from 1.4 cm (UNIMAS-04) to 2.1 cm (UNIMAS-03), with a mean of 1.79 cm (Table 4).

The number of panicles (NP) among the lowland rice accessions ranged from one (UNIMAS-25, UNIMAS-26, UNIMAS-28 and UNIMAS-41) to ten panicles per plant (Table 3), while NP among the upland accessions ranged from one (UNIMAS-20) to seven (UNIMAS-04 and UNIMAS-06) panicles per plant (Table 4). There was no significant difference in NP between the lowland and upland rice accessions (Table 5).

The mean length of panicle (LP) of lowland rice accessions (Table 3) was 29.23 cm, ranged from 24.5 cm (UNIMAS-25) to 35.6 cm (UNIMAS-23), similar to the LP of upland rice accessions averaged at 28.82 cm, ranging from 23.9 cm (UNIMAS-20) to 39.8 cm (UNIMAS-14) (Table 4 & 5).

The number of filled grains (NFG) per accession in lowland rice accessions, ranged from 84 grains (UNIMAS-42) to 1091 grains (UNIMAS-32) (Table 3). At an average of 443 grains per accession, the NFG of lowland rice accessions was similar to the NFG of upland rice accessions (Table 5), which ranged from 63 (UNIMAS-05) to 990 (UNIMAS-15) grains (Table 4).

The seed length (SL) ranged from 0.7 cm to 1.1 cm and 0.7 cm to 1.0 cm among lowland (Table 3) and upland rice accessions (Table 4 respectively. Seed width (SW) among the lowland rice accessions ranged from 0.2 cm to 0.4 cm (Table 3) and 0.2 cm to 0.3 cm for upland rice accessions (Table 4). The SL and SW did not show a significant difference between the lowland and upland rice accessions (Table 5).

The grain length (GL) among the lowland rice accessions had an average of 0.6 cm, ranging from 0.5 cm to 0.8 cm (Table 3). Among the upland rice accessions, the GL ranged from 0.6 cm to 0.9 cm (Table 4). For grain width (GW), the lowland rice accessions had an average of 0.19 cm, ranging from 0.2 cm to 0.3 cm (Table 3). The GW of upland rice accessions ranged from 0.15 cm to 0.2 cm (Table 4). The lowland rice accessions had shorter GL but wider GW than those of upland rice accessions (Table 5).

Table 3. The 13 quantitative traits and two development traits observed on 22 lowland rice accessions

Acc.	SH (cm)	PH (cm)	LL (cm)	LW (cm)	CL (cm)	CD (cm)	NP	LP (cm)	NFG	SL (cm)	SW (cm)	GL (cm)	GW (cm)	HD (days)	FD (days)
UNIMAS-23	51.4	168.2	53.2	1.5	113.5	3.5	3	35.6	320	1.0	0.3	0.5	0.2	125	154
UNIMAS-24	44.6	172.3	57.5	1.3	116.6	3.5	2	25.2	300	0.9	0.2	0.7	0.2	134	158
UNIMAS-25	40.3	172.6	62.8	1.1	108.3	3.2	1	24.5	250	0.7	0.3	0.6	0.2	134	158
UNIMAS-26	47.0	153.4	71.4	1.2	81.5	3.5	1	26.4	200	0.8	0.3	0.6	0.2	134	158
UNIMAS-27	46.8	174.0	70.9	1.6	101.5	3.0	2	30.1	159	0.8	0.3	0.5	0.2	119	145
UNIMAS-28	44.3	199.2	68.5	2.1	130.9	3.1	1	32.7	120	0.9	0.2	0.6	0.2	114	147
UNIMAS-29	54.5	187.5	74.8	1.9	114.6	3.4	6	28.3	660	1.0	0.4	0.6	0.2	130	159
UNIMAS-30	50.1	165.1	75.2	2.1	89.4	3.2	5	29.9	391	1.0	0.3	0.7	0.2	119	143
UNIMAS-31	48.9	173.6	54.1	2.2	121.6	3.4	8	24.6	690	1.1	0.2	0.7	0.2	112	140
UNIMAS-32	45.7	174.4	51.0	1.8	120.5	3.2	10	27.5	1091	1.0	0.2	0.7	0.2	113	138
UNIMAS-33	38.8	210.0	78.1	1.7	132.8	3.2	N/A	N/A	N/A	N/A	N/A	N/A	N/A	N/A	N/A
UNIMAS-34	42.4	225.3	80.3	1.6	143.4	3.3	N/A	N/A	N/A	N/A	N/A	N/A	N/A	N/A	N/A
UNIMAS-35	47.2	176.0	80.5	1.8	94.50	3.1	2	32.6	118	1.0	0.3	0.7	0.2	103	138
UNIMAS-36	40.8	189.4	71.4	1.7	118.0	3.2	2	34.5	274	1.0	0.3	0.8	0.2	89	117
UNIMAS-37	46.5	180.1	59.3	1.5	119.2	3.0	5	31.4	1055	0.8	0.3	0.6	0.3	86	115
UNIMAS-38	43.3	175.2	60.7	2.1	116.7	3.2	3	30.3	493	0.8	0.3	0.6	0.3	83	116
UNIMAS-39	39.5	170.8	65.8	1.9	103.2	3.0	2	28.2	696	0.9	0.3	0.6	0.2	89	118
UNIMAS-40	40.2	164.3	55.5	1.5	111.0	3.4	N/A	N/A	N/A	N/A	N/A	N/A	N/A	N/A	N/A
UNIMAS-41	43.4	159.5	57.0	1.7	105.2	3.6	N/A	N/A	N/A	N/A	N/A	N/A	N/A	N/A	N/A
UNIMAS-42	46.0	170.1	72.1	1.3	99.40	3.1	2	25.5	84	0.8	0.2	0.6	0.2	120	151
UNIMAS-43	48.2	173.0	70.7	1.3	106.1	3.0	7	29.6	630	0.9	0.2	0.6	0.2	111	138
UNIMAS-44	49.8	179.0	69.4	1.1	107.5	3.3	N/A	N/A	N/A	N/A	N/A	N/A	N/A	N/A	N/A

Note. Acc. indicates accession, N/A indicates data not available. SH: Seedling Height in centimetre, PH: Plant Height in centimetre, LL: Leaf Length in centimetre, LW: Leaf Width in centimetre, CL: Culm Length in centimetre, CD: Culm Diameter in centimetre, HD: Heading Days, FD: Flowering Days, NP: Number of Panicles, LP: Length of Panicle in Centimetre, NFG: Number of Filled Grains, SL: Seed Length, SW: Seed Width, GL: Grain Length, GW: Grain Width

Table 4. The 13 quantitative traits and two development traits observed on 22 upland rice accessions

Acc.	SH (cm)	PH (cm)	LL (cm)	LW (cm)	CL (cm)	CD (cm)	NP	LP (cm)	NFG	SL (cm)	SW (cm)	GL (cm)	GW (cm)	HD (days)	FD (days)
UNIMAS-01	46.3	127.3	54.1	1.8	65.7	3.2	5	33.5	276	1.0	0.2	0.7	0.2	124	151
UNIMAS-02	50.1	154.7	42.3	1.9	109.8	3.3	4	30.3	477	0.9	0.2	0.7	0.2	126	153
UNIMAS-03	47.1	139.4	67.8	2.1	88.9	3.1	5	24.5	407	0.8	0.2	0.6	0.2	112	140
UNIMAS-04	45.1	171.0	69.1	1.4	95.2	3.0	7	25.7	520	1.0	0.2	0.7	0.2	106	128
UNIMAS-05	44.9	172.1	70.1	1.8	90.1	2.9	3	26.7	63	1.0	0.2	0.7	0.2	103	132
UNIMAS-06	43.2	169.1	65.1	1.9	99.1	2.8	7	25.8	788	0.9	0.2	0.7	0.2	107	141

Continue ***Table 4:***

Acc.	SH (cm)	PH (cm)	LL (cm)	LW (cm)	CL (cm)	CD (cm)	NP	LP (cm)	NFG	SL (cm)	SW (cm)	GL (cm)	GW (cm)	HD (days)	FD (days)
UNIMAS-07	44.9	201.2	69.1	2.0	89.1	2.9	5	29.8	785	0.8	0.3	0.6	0.2	112	145
UNIMAS-08	54.5	185.6	58.2	1.8	100.7	3.3	6	27.9	627	0.9	0.2	0.8	0.2	112	142
UNIMAS-09	46.1	90.9	56.7	1.9	88.9	3.2	3	33.3	518	0.7	0.2	0.6	0.2	114	143
UNIMAS-10	49.1	149.9	57.4	1.7	85	3.4	4	32.1	413	0.9	0.2	0.8	0.2	102	127
UNIMAS-11	47.2	159.4	58.1	1.7	92.1	3.4	5	34.6	673	0.8	0.2	0.7	0.2	103	128
UNIMAS-12	48.1	159.9	58.7	1.5	87.1	3.1	2	24.7	158	0.8	0.2	0.6	0.2	126	146
UNIMAS-13	46.1	159.1	60.5	1.8	99.1	3.2	3	30.2	620	0.9	0.2	0.6	0.2	104	130
UNIMAS-14	49.1	163.5	63.4	1.8	102.1	3.3	3	39.8	710	0.8	0.2	0.6	0.2	99	129
UNIMAS-15	43.1	169.3	65.9	1.7	95.0	3.2	3	28.8	990	0.9	0.2	0.7	0.15	104	127
UNIMAS-16	41.1	167.3	70.0	1.9	80.8	2.9	3	26.3	687	0.9	0.2	0.7	0.2	101	131
UNIMAS-17	44.6	147.8	61.0	1.8	76.4	2.7	3	27.9	865	1.0	0.2	0.6	0.2	107	137
UNIMAS-18	46.1	139.9	70.2	1.9	40.7	3.1	5	25.4	723	0.9	0.2	0.9	0.2	94	128
UNIMAS-19	45.3	120.9	72.0	1.7	64.5	4.1	2	29.9	466	0.9	0.2	0.7	0.2	107	132
UNIMAS-20	45.7	196.7	65.3	1.7	91.0	2.9	1	23.9	120	0.9	0.3	0.7	0.2	103	140
UNIMAS-21	49.2	138.5	60.5	1.7	56.9	3.7	3	24.2	256	0.8	0.3	0.6	0.2	111	147
UNIMAS-22	49.4	175.2	64.0	1.8	115.7	3.8	N/A	N/A	N/A	N/A	N/A	N/A	N/A	N/A	N/A

Note. Acc. indicates accession, N/A indicates data not available. SH: Seedling Height in centimetre, PH: Plant Height in centimetre, LL: Leaf Length in centimetre, LW: Leaf Width in centimetre, CL: Culm Length in centimetre, CD: Culm Diameter in centimetre, HD: Heading Days, FD: Flowering Days, NP: Number of Panicles, LP: Length of Panicle in Centimetre, NFG: Number of Filled Grains, SL: Seed Length, SW: Seed Width, GL: Grain Length, GW: Grain Width

Table 5. Comparison of 13 quantitative morphological traits between lowland and upland rice accessions. The values indicate the mean ± standard error

Traits	Lowland	Upland
SH (cm)	45.44 ± 0.885	46.65 ± 0.614
*PH (cm)	177.86 ± 3.480	150.35 ± 6.160
LL (cm)	66.37 ± 1.950	65.61 ± 1.958
*LW (cm)	1.64 ± 0.071	1.79 ± 0.032
*CL (cm)	111.61 ± 3.046	87.00 ± 3.725
CD (cm)	3.25 ± 0.039	3.21 ± 0.072
NP	3.71 ±0.652	3.81± 0.321
LP (cm)	29.2294 ± 0.82657	28.8238 ± 0.89602
NFG	443.00 ±76.376	530.57 ±55.373
SL (cm)	0.90 ± 0.026	0.87 ± 0.017
SW (cm)	0.26 ± 0.010	0.21 ± 0.007
*GL (cm)	0.62 ± 0.019	0.72 ± 0.004
*GW (cm)	0.22 ± 0.005	0.19 ± 0.002

Note. Asterisk (*) indicates significant difference at $p<0.05$ (t-test). SH: Seedling Height, PH: Plant Height, LL: Leaf Length, LW: Leaf Width, CL: Culm Length, CD: Culm Diameter, NP: Number of Panicles, LP: Length of Panicles, NFG: Number of Filled Grains, SL: Seed Length, SW: Seed Width, GL: Grain Length, GW: Grain Width

For the developmental traits, the heading days (HD) of the lowland rice accessions ranged from 83 (UNIMAS-38) to 134 days (UNIMAS-24, UNIMAS-25 and UNIMAS-26) (Table 3), while the HD of upland rice accessions ranged from 94 days (UNIMAS-18) to 126 days (UNIMAS-02 and UNIMAS-12) (Table 4). The flowering days

(FD) of lowland rice accessions took around 115 days (UNIMAS-37) to 159 days (UNIMAS-29) (Table 3) and upland rice accessions recorded 127 days (UNIMAS-10 and UNIMAS-15) to 153 days (UNIMAS-02) of FD (Table 4).

DISCUSSION

Qualitative Traits as Morphological Marker

All qualitative traits observed in this study showed variations. Qualitative traits are considered morphological markers for the identification of rice landraces (Sinha & Mishra, 2013).

In the present study, it was observed that the leaf blade of lowland and upland rice accessions was grouped into three different classes of blade colour (BC) (Supplementary Figure 1). This trait is not reliable as a marker due to its dependence on environmental conditions. For example, the degree of the greenness observed on the leaf could be influenced by fertilizer applications, i.e. the nitrogen content of the leaf (Singh *et al*., 2002; Yang *et al*., 2015). Based on Leaf Colour Chart, pale green BC indicates nitrogen deficiency. Green BC indicates an elevated dose of nitrogenous fertilization. High nitrogenous content results in dark green BC (Bhupenchandra *et al*., 2021). The BC of this study may suggest there are variations in soil nitrogenous content even though same soil mixture was used and equal amount of fertilizers was applied. Another possibility to allow such colour variation would be genetic factor. According to Li *et al*. (2002), the colour of leaves is determined by the presence and concentration of pigments such as chlorophyll (green), carotenoids (yellow and orange), and anthocyanins (red and purple). The rice accessions of this study may have different concentrations of the different pigments, which results in colour variations.

Ligule is present in all the rice accessions in this study (Supplementary Figure 2). The morphology of ligule is important in the identification of grass species (de la Fuente & Ortunez, 2001; Rzanny *et al*., 2022). However, this trait may be insufficient for the identification of varieties of the same species. In this study, there were two ligule shapes (LS) observed for lowland rice accessions and only one for upland rice accessions. Based on the 44 rice accessions, LS may serve as one of the morphological markers to differentiate rice accessions, but not possible to differentiate between lowland and upland rice. The ligule colour may also serve as a morphological marker. There was one upland rice accession, UNIMAS-07 (Supplementary Figure 2), having purple ligule and auricle. The environmental dependency of this trait is unknown.

Seed shape (SS) is useful in identifying rice hybrids and is also valuable in the seed certification process to control seed standards (Kalaichelvan, 2009; Misra *et al*., 2023). Among the rice accessions in this study, they can be differentiated based on three SS: oblong, elliptic and linear (Supplementary Figure 5 & 6). Based on SS, this study speculates there is a presence of the sub-species tropical *japonica* (*javanica*) and *indica* among the 44 accessions. Rice accessions that have oblong or elliptic SS may be *javanica* rice. Those rice accessions with linear SS should be *indica* rice. This is based on the description available on the website of International Rice Research Institute (http://www.knowledgebank.irri.org/ericeproduction/0.5_Rice_races.htm).

Grain colour (GC) is a heritable character and has been used to categorise rice varieties (Maeda *et al*., 2014; Zhao *et al*., 2022). In the present study, the GC of the rice accessions were mostly milky white, followed by reddish-brown, black, dark brown and light brown. Pigmented rice may contain phenolic compounds and anthocyanin. It has been consumed as functional rice, as anthocyanin has been recognized as compound with health benefits due to its antioxidant activity,

anticancer, hypoglycemia and its anti-inflammatory effects (Maulani *et al*., 2018). GC is another morphological marker that is environmentally dependent. For example, grain discolouration due to disease may affect colour interpretation (Baite *et al*., 2020).

Cluster analysis based on nine qualitative traits has grouped the 44 rice accessions into two big clusters. Cluster I had a higher number of rice accessions compared to Cluster II. Cluster analysis revealed that there was no clustering according to seed origin (division), nor according to lowland or upland rice. The clustering was mainly based on secondary branching (SB) of the panicle. The rice accessions in Cluster I had light and heavy SB, which is of interest for yield breeding (refer to the discussion in the next section). The nine qualitative traits may not be sufficient to depict the rice accessions of one cluster are more genetically related nor genetically diverse from the accessions in the other clusters (Tejaswini *et al*., 2016).

According to Yeo *et al*. (2018), the registrations of a variety based on the name given by the farmers are unreliable. There is a possibility for a variety with a similar name, having different morphological characteristics. To support that, upland accessions UNIMAS-06 and UNIMAS-07 were clustered into a different group from UNIMAS-22 despite having the same name (Padi Merjat). Cultural practice by the local farmers where the rice seeds were inherited, transferred or exchanged between farmers might attribute to the diversity.

Direct and Indirect Yield Traits

According to IRRI (2002), plant height (PH) is divided into short (< 110 cm), medium (110 cm-130 cm) and tall (> 130 cm). Most of the rice accessions (41 accessions) in this study are considered tall. Only upland rice accession UNIMAS-09 is short (91 cm). Another two upland rice accessions, namely UNIMAS-01 (127.3 cm) and UNIMAS-19 (120.9 cm), are medium in height. In average, the lowland rice accessions of this study were taller than upland rice accessions (Table 5). Based on the plant height dynamic model of Wu *et al*. (2022), the lowland rice accessions in this study may have a higher risk of lodging compared to upland rice accession. Moreover, the culm lengths of lowland accessions were statistically longer than upland accessions in the present study. Lodging will reduce yield (Sunian *et al*., 2017).

The leaf length (LL) is known to vary between rice genotypes (Mehla & Kumar, 2008). All rice accessions in this study have long leaves based on IRRI (2002) except for upland rice accession UNIMAS-02, which has medium LL. Long leaves may not be preferable as compared to short leaves which will be more erect. Short leaves are uniformly distributed throughout the canopy, therefore mutual shading is reduced, and light is used more efficiently, thus contributing to yield (Tillier *et al*., 2023). Based on leaf width (LW), the rice accessions in this study are considered as having medium LW, except UNIMAS-28, UNIMAS-30, UNIMAS-31, UNIMAS-38 and UNIMAS-03 which have broad LW. Broad LW may not be preferable. A previous study suggested that narrower leaves are more beneficial under hot, dry and high-light habitats due to the ability to increase leaf heat exchange, avoid leaf damage and maintain leaf water content (Kang *et al*., 2021).

The rice accessions in this study had flowering time ranging from 115 to 159 days. According to the agronomy guide of IRRI (2015), the rice accessions in this study are most likely to have long crop duration, where from planting to harvest can take up to 160 days or longer. For lowland rice which has a long crop duration, it is recommended to be planted in irrigated or flood-prone fields (IRRI, 2015). The lowland rice accessions of this study were collected from farmers planting in rain-fed

field. Their production may be improved if planted in irrigated or flood-prone field.

There are five lowland rice accessions and one upland rice accession of this study that did not flower during the observation period. Many factors affect the flowering phase of rice. One of it is being photoperiod. Some Sarawak rice landraces, such as Biris and Bali are known to be photoperiod sensitive (Teo n.d; Saidon *et al*., 2017). This may be true for these six rice accessions in this study. These six rice accessions were germinated on the 30 November 2018. Seven other lowland rice accessions and two upland rice accessions which were germinated on the same date, however, manage to produce inflorescences. In future characterisation, all accessions should be germinated and transplanted at the same time.

The number of panicles (NP) observed in this study, at most, was up to 10 panicles per plant. The NP with filled grain is a key indicator of rice yield (Efisue *et al*., 2014). To support this, UNIMAS-32 and UNIMAS-06 of lowland and upland accessions, respectively, had higher NP, produced higher number of filled grains (NFG) (observation without statistical evidence). These results suggest that UNIMAS-32 and UNIMAS-06 can be considered for Sarawak rice breeding program to increase rice production.

Beside NP, panicle type (PT) and secondary branching (SB) were also observed (Supplementary Figure 3 & 4). PT of rice is referring to the mode of branching, the angle of the primary branches and the spikelet density (IRRI, 2002). Among the rice accessions in this study, three PT were observed, i.e. compact panicles, intermediate-type of panicles and open panicles (Supplementary Figure 3). Only three rice accessions had compact PT. Breeders usually selectively breed for compact PT to increase yield (Kalaichelvan, 2009). For SB, it is mainly regulated by the number of primary and secondary branches, which directly influences the total grain number (Agata *et al*., 2020). The stronger the branching pattern, the higher the yield. In this study, it is observed that the NFG was lower for those rice accessions, which have light SB or absent (observation without statistical evidence).

Among the rice accessions in this study, only lowland rice accession UNIMAS-37 and upland rice accession UNIMAS-15 were observed to have compact PT with heavy secondary branching. Unfortunately, these two accessions have low NP. They also have higher lodging risk (Wu *et al*., 2022) as their height can reach up to 180 cm and 169 cm, respectively. Lowland rice accession UNIMAS-32 and upland rice accession UNIMAS-06 have high NP but have intermediate PT and light SB. Using these accessions for breeding may require multi-parent crossing to stack the desired NP, PT and SB characters.

Grain size and shape are among the quality criteria being considered in developing rice varieties for commercial production (Custodio *et al*., 2019). Statistically, lowland rice accessions had shorter grain length and wider grain width compared to upland rice accessions (Table 5). However, according to the classification of ChePa *et al*. (2016) on Malaysian rice, all the observed accessions were having long to extra-long grains, ranging from 0.6-0.9 cm, except UNIMAS-23 (0.5 cm). Grains width (GW) observed in this study showed a range of 0.15 cm to 0.3 cm.

Based on grain size and seed shape as pointed out above, this study suggests that the rice accessions of this study may consists of *indica* and *javanica* rice. The grain length-width ratio for *indica* rice is usually above 2.2. For *japonica* rice, it falls below 2.01 (Rahman *et al*., 2020). Most rice accessions in this student have length-width ratio of *indica* rice. There are two accessions, UNIMAS-37 and UNIMAS-38,

which has a length-width ratio of *japonica* rice (approximately 2.0), further supporting the speculation based on seed shape.

There were variations in terms of grain shape recorded in this study. The Malaysian consumers mostly preferred rice having long shape (Ahmad Hanis *et al*., 2012). The rice accessions in this study, which has long shape characteristics, can be considered for Sarawak rice breeding program to achieve rice grain quality that meets customer preferences. Breeding programs need to engage with farmers through participatory approaches to better understand their preferences. Collaborative efforts between farmers, researchers, extension services, and consumers, help to ensure that newly developed rice varieties are aligned with the local needs and preferences.

CONCLUSION

In conclusion, a good variety of rice should be a well-balanced combination of high yield, quality and adaptability to different or targeted environments. The development and adoption of such varieties contribute to food security, economic viability for farmers, and the overall sustainability of rice production systems. Continuous collaboration between researchers, farmers, and other stakeholders is crucial for the successful development and dissemination of improved rice varieties.

The 44 rice accessions of lowland and upland rice collected from the North-Western region of Sarawak were successfully characterised based on their morphological traits. The morphological traits showed variations which may be useful for future rice breeding programs. Morphological markers are very important and all breeders are continuously looking for these markers that will enable them to characterise the plant materials for diversity study and to perform marker assisted selection. The current rice accessions showed a wide range of variability for the characters evaluated, which may be attributed to the diverse genetic background of the rice accessions. These variations could be the genetic resources for future breeding programs.

ACKNOWLEDGEMENTS

This study was funded by Ministry of Higher Education, Malaysia under Fundamental Research Grant Scheme (FRGS/1/2017/STG03/UNIMAS/03/2). The authors would like to acknowledge Universiti Malaysia Sarawak, for the facilities provided.

REFERENCES

Agata, A., Ando, K., Ota, S., Kojima, M., Takebayashi, Y., Takehara, S., Doi, K., Ueguchi-Tanaka, M., Suzuki, T., Sakakibara, H., Matsuoka, M., Ashikari, M., Inukai, Y., Kitano, H. & Hobo, T. (2020). Diverse panicle architecture results from various combinations of Prl5/GA20ox4 and Pbl6/APO1 alleles. Communications Biology, 3(1): 302. DOI:10.1038/s42003-020-1036-8

Ahmad Hanis, I.A.H., Jinap, S., Mad Nasir, S., Alias, R. & Muhammad Shahrim, A.K. (2012). Consumers' demand and willingness to pay for rice attributes in Malaysia. *International Food Research Journal*, 19(1): 363-369.

Baite, M.S., Raghu, S., Prabhukarthikeyan, S.R., Keerthana, U., Jambhulkar, N.N. & Rath, P.C. (2020). Disease incidence and yield loss in rice due to grain discolouration. Journal of Plant Diseases and Protection, 127(1): 9-13. DOI: 10.1007/s41348-019-00268-y

Bhattarai, G., Shi, A., Kandel, D.R., Solis-Gracia, N., da Silva, J.A. & Avila, C.A. (2021). Genome-wide simple sequence repeats (SSR) markers discovered from whole-genome sequence comparisons of multiple spinach accessions. *Scientific Report*, 11(1): 1-16.

Bhupenchandra, I., Athokpam, H.S., Singh, N.B., Soibam, H., Chongtham, S.K., Singh, L.K., Sinyorita, S., Devi, E.L., Bhagowati, S., Bora, S. S., Kumar, A., Devi, C.H.P. & Olivia, L.C. (2021). Leaf Color Chart (LCC): An instant tool for assessing nitrogen content in plant: A review. *The Pharma Innovation Journal*, 10(4): 1100-110.

Cheok, Y.H., Yeo, F.K.S. & Chong, Y.L. (2019). Oviposition behavior of *Scirpophaga incertulas*, the yellow stemborer (Lepidoptera: Crambidae) in a non-choice study. *Pertanika Journal of Tropical Agricultural Science*, 42(3): 1167-1172.

ChePa, N., Yusoff, N. & Ahmad, N. (2016). Determinants for grading Malaysian rice. American Institute of Physics Conference Proceedings, 1761(1): 020035. DOI: 10.1063/1.4960875

Custodio, M.C., Cuevas, R.P., Ynion, J., Laborte, A. G., Velasco, M.L. & Demont, M. (2019). Rice quality: How is it defined by consumers, industry, food scientists, and geneticists?. Trends in Food Science & Technology, 92: 122-137. DOI: 10.1016/j.tifs.2019.07.039

de la Fuente, V. & Ortunez, E. (2001). Festuca Sect. Eskia (Poaceae) in the Iberian Peninsula. Folia Geobotanica, 36(4): 385-421. DOI: 10.1007/BF02899988

Department of Agriculture Sarawak. (2020). *Agriculture Research Centre: Programmes*. Retrieved November 20, 2021, from https://doa.sarawak.gov.my/page-0-0-415-AGRICULTURE-RESEARCH-CENTRE-PROGRAMMES.html

Doyle, J.J. & Doyle, D.J.L. (1987). A rapid DNA isolation procedure for small quantities of fresh leaf tissue. *Phytochemistry*, 19: 1115.

Efisue, A.A., Bianca, C.U. & Orluchukwu, J.A. (2014). Effects of yield components on yield potential of some lowland rice (*Oryza sativa* L.) in coastal region of Southern Nigeria. Journal of Plant Breeding and Crop Science, 6(9): 119-127. DOI: 10.5897/JPBCS2014.0449

Food and Agriculture Organization of the United Nations. (2019). *GIEWS - Global information and early warning system.* Retrieved October 11, 2021, from https://www.fao.org/giewscountrybrief/country.jsp?code=MYS

Hamsein, N.N., Yeo, F.K.S., Sallehuddin, R., Mohamad, N.K., Kueh, F.T.F., Hussin, N.A. & Wan Ismail, W.N. (2020). Oviposition behaviour of *Scirpophaga incertulas* (Walker) (Lepidoptera: Pyralidae) on Sarawak rice landraces. Taiwania, 65(1): 95-99. DOI: 10.6165/tai.2020.65.95

International Board for Plant Genetic Resources & International Rice Research Institute Rice Advisory Committee. (1980). *Descriptors for rice, Oryza sativa L*. International Rice Research Institute.

International Rice Research Institute. (2002). *Standard evaluation system for rice (SES)*. Retrieved July 23, 2022, from http://www.knowledgebank.irri.org/images/docs/rice-standard-evaluation-system.pdf

International Rice Research Institute. (2015). *Steps to successful rice production*. Retrieved July 29, 2022, from http://knowledgebank. irri.org/images/docs/12-Steps-Required-for-Successful-Rice-Production.pdf

International Rice Research Institute (n.d.). *What is the difference between aerobic rice and upland rice?* Retrieved December 10, 2022, from http://www.knowledgebank.irri.org/step-by-step-production/growth/water-management/faqs-about-water-management/item/what-is-the-difference-between-aerobic-rice-and-upland-rice

Kalaichelvan, C. (2009). *Studies on identification of rice (Oryza sativa L.) cultivars using morphological and molecular markers* (Master thesis), Acarya Nayukulu Gogineni Ranga Agricultural University.

Kang, X., Li, Y., Zhou, J., Zhang, S., Li., C., Wang, J., Liu, W. & Qi, W. (2021). Response of leaf traits of eastern Qinghai-Tibetan broad-leaved woody plants to climatic factors. Frontiers in Plant Science, 12: 679726. DOI: 10.3389/fpls.2021.679726

Khazanah Research Institute. (2019). *The status of the paddy and rice industry in Malaysia*. Kuala Lumpur, Khazanah Research Rice Institute.

Lai, K.Y., Hussin, N.A., Mohammad, N.K., Hui, Y.T., Lai, L.S. & Yeo, F.K.S. (2019). Qualitative resistance of Sarawak rice landraces against *Pyricularia oryzae*. Borneo Journal of Resource Science and Technology, 9(2): 115-118. DOI: 10.33736/bjrst.1721.2019

Li, W., Zhang, Y., Mazumder, M.A.R., Pan, R. & Akhter, D. (2022). Research progresses on leaf color mutants. *Crop Design*, 1: 100015.

Ling, A.X.R., Yeo, F.K.S., Hamsein, N.N., Ting, H.M., Sidi, M., Wan Ismail, W.N., Taji, A.S. & Cheok, Y.H. (2020). Screening for Sarawak paddy landraces with resistance to yellow rice stem borer, *Scripophaga incertulas* (Walker) (Lepidoptera: Crambidae). Pertanika Journal of Tropical Agricultural Science, 43(4): 491-501. DOI: 10.47836/pjtas.43.4.06

Maeda, H., Yamaguchi, T., Omoteno, M., Takarada, T., Fujita, K., Murata, K., Iyama, Y., Kojima, Y., Morikawa, M., Ozaki, H., Mukaino, N., Kidani,

Y. & Ebitani, T. (2014). Genetic dissection of black grain rice by the development of a near isogenic line. Breeding Science, 64(2): 134-141. DOI: 10.1270/jsbbs.64.134

Masni, Z. & Wasli, M.E. (2019). Yield performance and nutrient uptake of red rice variety (MRM 16) at different NPK fertilizer rates. International Journal of Agronomy, 2: 1-6. DOI: 10.1155/2019/5134358

Maulani, R.R., Sumardi, D. & Adi, P. (2018). Total flavonoids and anthocyanins content of pigmented rice. *Drug Invention Today*, 12(2): 369-373.

Mehla, B.S. & Kumar, S. (2008). Use of morphological traits as descriptors for identification of rice genotypes. *Agricultural Science Digest*, 28(2): 101-104.

Misra, M.K., Harries, A. & Dadlani, M. (2023). Role of seed certification in quality assurance. Seed Science and Technology, 1: 172-199. DOI: 10.1007/978-981-19-5888-5_12

Rahman, M., Castillo, C.C. & Murphy, C. (2020). Agricultural systems in Bangladesh: The first archaeobotanical results from early historic Wari-Bateshwar and early Medieval Vikrampura. Archaeological and Anthropological Sciences, 12(1): 37-54. DOI: 10.1007/s12520-019-00991-5

Rzanny, M., Wittich, H.C., Mäder, P., Deggelmann, A., Boho, D. & Wäldchen, J. (2022). Image-based automated recognition of 31 *Poaceae* species: The most relevant perspectives. Frontiers in Plant Science, 12: 804140. DOI: 10.3389/fpls.2021.804140

Saidon, S.A., Hussain, Z.P.M.D., Ramli, A., Omar, O., Man, A., Ahmad, R. & Yusob, S.M. (2017). *Preliminary evaluation: New rice lines through improvement of selected Sarawak's traditional rice variety* [Poster Presentation]. Mardi Science Technology Exhibition.DOI: 10.13140/RG.2.2.15795.53281

Singh, B., Singh, Y., Ladha, J.K., Bronson, K.F., Balasubramanian, V., Singh, J. & Khind, C.S. (2002). Chlorophyll meter–and leaf color chart–based nitrogen management for rice and wheat in Northwestern India. Agronomy Journal, 94(4): 821-829. DOI: 10.2134/agronj2002.8210

Sinha, A.K. & Mishra, P.K. (2013). Agro-morphological characterization and morphology based genetic diversity analysis of landraces of rice variety (*Oryza sativa* L.) of Bankura district of West Bengal. *International Journal of Current Research*, 5(10): 2764-2769.

Spada, A., Mantegazza, R., Biloni, M., Capoali, E. & Sala, F. (2004). Italian rice varieties: historical data, molecular markers, and pedigrees to reveal their genetic relationships. *Plant Breed*, 123: 105-111.

Sunian, E., Ramli, A., Omar, O., Misman, S.N., Mohamad Saad, M., Jack, A. & Hashim, S. (2017). Evaluation on yield, yield component and physico-chemicals of advanced rice lines. *Journal of Tropical Agriculture and Food Science*, 45(2): 131-143.

Tang, A.S.O., Yeo, F.K.S., Chin, S.F., Wee, B.S. & Ngu-Schwemlein, M. (2023). Antifungal properties and phytotoxicity of ZnO nanoparticles - a genotypic dependent effect. Archives of Phytopathology and Plant Protection, 1(1): 1-20. DOI: 10.1080/03235408.2023.2251433

Tejaswini, K.L.Y., Manukonda, S., Rao, P.V.R., Kumar, B.N.V.S.R.R., Mohamad, L.A. & Raju, K. (2016). Cluster analysis studies in rice (*Oryza sativa* L.) using wards minimum variance method. *Journal of Agricultural and Crop Research*, 4(9): 129-139.

Teo, G. K. (n.d.). *Rice biodiversity*. Retrieved January 14, 2022, from https://doa.sarawak.gov.my/page-0-0-158-Rice-Bioderversity.html

Tillier, L.C., Murchie, E.H. & Sparkes, D.L. (2023). Does canopy angle influence radiation use efficiency of sugar beet? Field Crops Research, 293: 108841. DOI: 10.1016/j.fcr.2023108841

Wu, D.H., Chen, C.T. & Yang, M.D. (2022). Controlling the lodging risk of rice based on a plant height dynamic model. Botanical Studies, 63(1): 25. DOI: https://doi.org/10.1186/s40529-022-00356-7

Yang, X., Li, G., Luo, W. & Chen, L. (2015). Quantifying the relationship between leaf nitrogen content and growth dynamics and yield of muskmelon grown in plastic greenhouse. American Society for Horticultural Science, 50(11): 1677-1687. DOI: 10.21273/ HORTSCI.50.11.1677

Yeo, F.K.S., Meekiong, K., Shabdin, Z., Mohamad, N.K., Hussin, N.A. & Chung, H.H. (2018). Diversity of rice in Kampung Lebor, Serian - A first insight. In Yeo, F.K.S., Chong, Y.L. & Khan, F.A.A. (eds.). *Glimpses of Bornean Biodiversity*.

Kuching, Malaysia, Universiti Malaysia Sarawak Publisher. pp. 155-167.

Yeo, F.K.S., Rafael, E., Ewe, Z.H., Ang, P.S., Hussin, N., Vu Thanh, T.A., Chung, H.H., Lai, L.S., Ting, H. M. & Bao, Y. (2024). New variants of AvrPiz-t identified in *Pyricularia oryzae* from Malaysia. Plant Stress, 11(2024): 1-11. DOI: 10.1016/j.stress.2023.100322

Zhao, D., Zhang, C., Li, Q. & Liu, Q. (2022). Genetic control of grain appearance quality in rice. Biotechnology Advances, 60: 108014. DOI: 10.1016/j.biotechadv.2022.108014

Zhu, Y.F., Qin, G.C., Yang, W., Wang, J.C. & Zhu, S.J. (2012). Fingerprinting and variety identification of rice (*Oryza sativa* L.) based on simple sequence repeat markers. *Plant Omics Journal*, 5(4): 421-426.

Borneo Journal of Resource Science and Technology (2024), 14(1): 139-148
DOI: https:doi.org/10.33736/bjrst.5701.2024

Effects of Extraction Method on Yield, Phenolic and Flavonoid Content of Leaf, Stem and Root of *Cassia alata* Linn.

SCHLASTICA RAMIH ANAK BUNYA* & SAMUEL LIHAN

Institute of Biodiversity and Environmental Conservation, Universiti Malaysia Sarawak, 94300 Kota Samarahan, Sarawak, Malaysia
*Corresponding author: scholastica.rb@gmail.com
Received: 18 May 2023 Accepted: 8 May 2024 Published: 30 June 2024

ABSTRACT

The study of medicinal plants has gained significant interest among researchers because of their potential for therapeutic purposes and the production of natural drugs. In Sarawak, *Cassia alata* is one of the native plants used for medicinal purposes, such as treatment for constipation, ringworm, and other skin diseases. This study determined the yield of extraction, total phenolic content (TPC), and total flavonoid content (TFC) of the leaf, stem, and root of *C. alata* using various extraction methods and solvent extractions. The extractions were performed using soxhlet extraction (SE) and ultrasonic-assisted extraction (UAE) with ethanol and chloroform. Among all, the extract obtained from SE with ethanol solvent (SE-EtOH) showed the highest yield in all plant parts (leaf: 28.62 %, stem: 10.06 %, and root: 9.79 %). Meanwhile, the TPC and TFC estimated using the Folin-Ciocalteu phenol reagent and aluminium chloride colorimetric assay methods showed that the highest TPC and TFC were from the leaf extract obtained using UAE and chloroform (UAE-Chlo-L) with a TPC value of 117.436 mg GAE/g DW and a TFC value of 568.778 mg QE/g DW, respectively. Overall, the findings demonstrated that chloroform was an effective solvent system for all plant parts on the TPC and TFC, with the leaf part containing the greatest value, and that ultrasonic-assisted extraction was the best approach. This exploration is beneficial for the determination of methods that produce optimum yield, phenolic, and flavonoid content in *C. alata*'s species.

Keywords: *Cassia alata*, TPC, TFC, solvent system, soxhlet extraction, ultrasonic assisted extraction

INTRODUCTION

Plants possess a wide range of organic substances that are classified as primary and secondary metabolites. Primary metabolites such as phytosterols, acyl lipids, nucleotides, amino acids, and organic acids are fundamental for photosynthesis, reproduction, respiration, growth, and development (Wang *et al.*, 2022). Secondary metabolites are molecules that help plants interact with their surroundings (Adedeji & Babalola, 2020). Phenolics, flavonoids, alkaloids, terpenes, saponins, lipids and carbohydrates are the classes of secondary metabolites (Hussein & El-Anssary, 2019). The determination of secondary metabolites in plant extracts is important as it helps in supporting the development of modern medicines and supplements. According to Rahman *et al.*, (2022), the determination of total phenolic content (TPC) and total flavonoid content (TFC) are significant parameters to evaluate the potential health benefits of plant extracts such as antimicrobial, antioxidant and anti-inflammatory activity.

Phenolics are secondary plant metabolites with over 8000 structures, including lignans, tannins, phenolic acids, stilbenes, and flavonoids. They are commonly found in plant tissues such as in fruits, seeds, leaves, stems and roots. These phenolics are associated with various health benefits, such as anti-ageing (Dhalaria *et al*., 2020), anti-proliferative activities, anti-inflammatory and antioxidant properties (Cianciosi *et al*., 2018; Cardoso *et al*., 2020). The flavonoid, on the other hand, is a member of a group of polyphenolic-structured secondary plant metabolites. It has a wide range of biological effects, including hepatoprotective, anti-inflammatory (Jiang *et al*., 2019), antibacterial, antioxidant (Li *et al*., 2019), and anti-hyperlipidemic effects (Bencheikh *et al*., 2021).

Cassia alata, also called *Senna alata*, is one

of the native plants in the Leguminosae family with many medicinal uses. Its local name in Malaysia is "*pokok gelenggang*" (Mat Jusoh *et al*., 2023). In the Sarawak community, the leaves of *C. alata* have been used to treat constipation, ringworm, and other skin diseases by decoction and pounding (Bakar *et al*., 2023). Meanwhile, in Indonesia, the roots are used by the Dayak tribe to treat ringworm diseases (Az-Zahra *et al*., 2021). According to Fatmawati *et al.* (2020), *C. alata* has various pharmacological activities such as antibacterial, antidiabetic, anti-inflammatory, antifungal and antioxidant. For example, the ethanolic extracts from the leaves were suggested as potential active components for skin care products due to their antioxidant and anti-inflammatory properties (Saidin *et al.*, 2019). Besides, the bark and roots also showed antibacterial activity against *Salmonella enterica* serovar Typhimurium, *Staphylococcus aureus*, and *Escherichia coli* (Halim-Lim *et al.*, 2020). The various ethnomedicinal benefits of *C. alata* have prompted researchers to analyse plant sources for bioactive compounds. This approach is significant for developing new pharmaceutical and biological resources in healthcare systems (Vaou *et al*., 2021).

There is scant literature reported on the bioactive compounds of *C. alata* using different extraction methods and solvents (Oladeji *et al.*, 2020). Recently, researchers have gained interest in the application of soxhlet extraction (SE) and ultrasonic assisted extraction (UAE) using various solvents to extract secondary metabolites from plants (Ling *et al*., 2019). SE also known as "hot continuous extraction," is a traditional technique that is often used in small research settings. This process has significant exposure to dangerous and combustible organic solvents and uses a high amount of solvent, time, and energy (Thilakarathna *et al*., 2023). Meanwhile, the UAE uses the sonic cavitation effect of ultrasound to improve the surface contact between samples, solvents, and cell walls. Unlike SE, UAE is an advanced method that can reduce time and solvent consumption (Deng *et al*., 2022).

Therefore, the evaluation of different extraction methods and solvents is crucial in finding an optimum yield, phenolic and flavonoid content specifically in *C. alata*'s species. In this study, the yield, TPC and TFC of leaf, stem, and root extracts of *C. alata* were determined using soxhlet and ultrasonic assisted extraction. Subsequently, the extracts obtained from ethanol extraction were compared with those obtained from chloroform extraction. These results are significant for assessing the efficacy of the methods in determining the quantity of phenolic and flavonoid in *C. alata's* species.

MATERIALS AND METHODS

Materials

The chemicals used were ethanol (HmbG, Malaysia), chloroform (Merck, Germany), Folin-Ciocalteu reagent (Sigma Aldrich, USA), gallic acid solution (HiMedia, India), sodium carbonate (Na_2CO_3) solution (Merck, Germany), quercetin solution (Sigma Aldrich, USA), sodium nitrate ($NaNO_3$) solution (Merck, Germany), aluminium chloride ($AlCl_3$) solution (Merck, Germany), and sodium hydroxide (NaOH) solution (Merck, Germany).

Preparation of *C. alata* Samples

The *C. alata* plants were collected from the Kota Samarahan roadside (1˚27'40.968" N, 110˚24'50.5" E). The plants were identified by the flowers, which resemble a fluorescent yellow candle and grow in a vertical column from the plant (Oladeji *et al*., 2020). The collected plant samples were separated into leaf, stem, and root parts. They were properly cleaned before being chopped into small pieces, dried in an oven at 40 °C for 5 days to achieve constant weight and ground into a powder (Mugao *et al*., 2020).

Extraction of *C. alata* Samples

In SE, approximately 15 g of the samples were weighed and put in a thimble of a soxhlet apparatus containing 200 ml of extraction solvent and extracted for 6 hr (Mahyuddin *et al*., 2020). Meanwhile, in UAE, about 1 g of samples were put in a Schott bottle containing 40 ml of extraction solvent and extracted for 30 min using an ultrasonic water bath (Saifullah *et al*., 2020). The extraction solvents used were ethanol and chloroform.

Determination of Extraction Yield

After the extraction, the extracts were filtered through Whatman No. 1 filter paper, vacuum-

dried with a rotary evaporator and left to dry completely in the fume hood. The yield of extraction (%) was calculated as follows; Eq.(1):

Yield of extraction (%) = $W_0 / W_1 \times 100$ Eq.(1)

Where W_0 and W_1 are the weight of *C. alata* extracted from the sample (g) and the weight of the sample (g), respectively. To avoid any potential degradation, the resultant dried crude extracts were packed and kept at 4 ˚C.

Determination of Total Phenolic Content (TPC)

The TPC of *C. alata* extracts was determined using the Folin-Ciocalteu reagent and gallic acid as a standard solution (Ling *et al.*, 2019). Briefly, 0.125 ml of the extract was put into a test tube along with 0.5 ml of ultrapure water and 0.125 ml of Folin-Ciocalteu phenol reagent. After 3 min, 1.25 ml of 7% Na_2CO_3 was added, and then distilled water was added to top up the volume to 3 ml. The absorbance was measured at a wavelength of 760 nm using a Shimadzu UV-1900i spectrophotometer after 1 hr of incubation at room temperature and in a dark room. Figure 1 shows a calibration curve for gallic acid. The TPC of the extract was expressed as mg of gallic acid equivalent (GAE) per g of dry weight (mg GAE/ g DW) by comparing with the gallic acid calibration curve.

Determination of Total Flavonoid Content (TFC)

The TFC of *C. alata* extracts was determined using an aluminium chloride colourimetric assay and quercetin as the standard solution, according to Ling *et al.* (2019). About 4.8 ml of ultrapure water and 0.3 ml of a 5% $NaNO_3$ solution were added to a test tube after an aliquot of 0.2 ml of extract was added. After 5 min, 0.3 ml of 10% $AlCl_3$ was added, followed by 2 ml of 1M NaOH, and the remaining volume was brought to 10 ml with ultrapure water. The absorbance was determined at a wavelength of 414 nm. Figure 2 shows a quercetin calibration curve. The TFC of the extracts was expressed as mg quercetin equivalent per gram of dry weight (mg QE/ g DW) by comparing with the quercetin calibration curve.

Statistical Analysis

Results were expressed as mean ± standard deviation (n=3). Pearson correlation test was performed by using IBM SPSS Statistics 27 to determine the correlation between the TPC and TFC.

RESULTS AND DISCUSSION

Yield of Extraction

The extraction efficiency is significant as it can reduce the use of solvent volume, amount of dry sample, sampling time, energy costs, and extraction time per extraction (Zhang *et al.*, 2018). Table 1 shows the extraction yield of *C. alata.* The amount of extraction yield obtained increased from low polarity to high polarity of solvents as follows: chloroform > ethanol. The highest extraction yield was obtained by SE-EtOH, where the leaf at 28.62 ± 0.69% followed by the stem (10.06 ± 0.05%) and roots (9.79 ± 0.14%). In comparison, UAE-Chlo recorded a lower extraction yield for all parts of *C. alata*. Bui *et al.*, (2021) reported a similar trend in the extract yields of *Avicennia officinalis* leaf using ethanol (8.95 ± 0.69%) and chloroform (3.20 ± 0.57%).

Ethanol is a polar solvent which is particularly effective at extracting polar compounds, including a wide range of

Table 1. Extraction yield (%) of *C. alata* using SE and UAE

Extracts	Soxhlet extraction	Ultrasonic assisted extraction
EtOH-L	28.62 ± 0.69	11.80 ± 1.40
EtOH-S	10.06 ± 0.05	3.57 ± 0.59
EtOH-R	9.79 ± 0.14	2.00 ± 0.44
Chlo-L	8.50 ± 0.34	4.93 ± 0.42
Chlo-S	1.14 ± 0.34	0.83 ± 0.12
Chlo-R	1.30 ± 0.56	0.73 ± 0.12

phytochemicals such as flavonoids and alkaloids (Alara *et al.*, 2021). Meanwhile, chloroform, being a non-polar solvent is highly effective at extracting non-polar compounds such as lipids (Saini *et al.*, 2021). A greater yield in ethanol extracts showed that the presence of polar compounds was higher in *C. alata*. This is because polar compounds such as polar carbohydrates and glycosides are readily dissolved in polar solvents such as ethanol (Bitwell *et al.*, 2023). Similarly, Dirar *et al.*, (2019) reported that most of the components in *C. alata* are hydrophilic and water-soluble components. Therefore, ethanolic extracts showed a greater extraction yield of crude extracts than chloroform extracts.

As for plant parts, the leaf of *C. alata* showed a greater yield of crude extract than other plant parts. Similar to Halim-Lim *et al*. (2020), using 95% ethanol, the leaf extract (32.17%) of *C. alata* showed a higher yield than bark (30.53%) and root parts (30.05%). This is probably because leaves are rich in bioactive compounds responsible for protection against environmental stress factors such as UV radiation (Aguirre-Becerra *et al*., 2021). Meanwhile, for the extraction method, SE yielded higher yields compared to UAE, regardless of solvent extraction and plant part used. Similar to Das *et al.* (2019), the leaves of *Piper betle*'s extract yield resulted in 11.00 for SE, 10.33% for maceration, and 8.00 for UAE. According to Mahyuddin *et al*. (2020), the soxhlet apparatus cycles the same solvent through the samples completely, which ensures the fresh solvent is continually used to dissolve the targeted compounds. Over time, this can result in a more complete extraction of compounds with limited solubility. Therefore, the SE showed a greater yield of extraction than UAE and all plant parts.

Total Phenolic and Flavonoid Contents of *C. alata*

The total phenolic content (TPC) in *C. alata* was determined using Folic-Ciocalteu reagent. Meanwhile, an aluminium chloride colourimetric assay was used to determine the total flavonoid content TFC. As shown in Figure 1, the TPC was expressed in mg GAE/g DW and obtained from the calibration curve of gallic acid. For total flavonoid content of each extract was expressed in mg QE/g DW and obtained from the calibration curve of quercetin (Figure 2). The Pearson correlation coefficient was performed to show the strength and direction of the linear relationship of correlation. The Pearson correlation between TPC and TFC in this study was $r = 0.949$ (p-value < 0.01). This showed a positive correlation between TPC and TFC.

In this study, leaf extracts showed greater phenolic content, regardless of the extraction techniques and solvent used. The highest was obtained from the leaves part, extracted using UAE and chloroform (UAE-Chlo-L, 117.436 mg GAE/g DW) (Figure 3). Similar to TPC, the results presented in Figure 4 showed that the extracts from the leaves, extracted using UAE and chloroform had a significantly high flavonoid content (UAE-Chlo-L, 568.778 mg QE/g DW). The results showed that different parts of plants had different values of phenolic and flavonoid compounds.

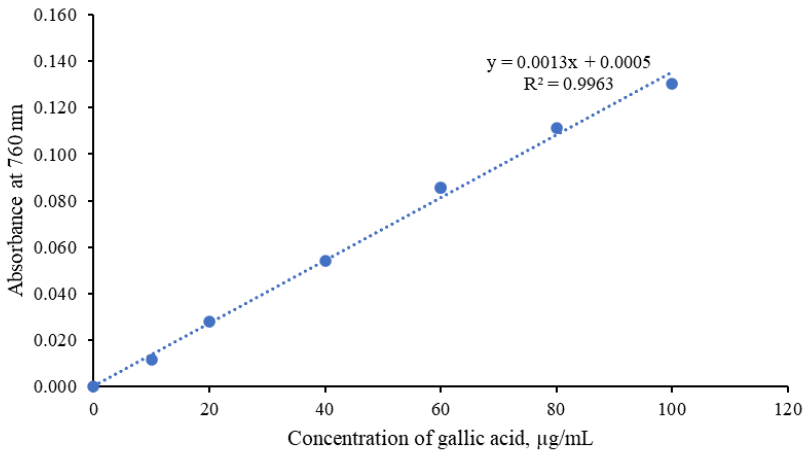

Figure 1. Gallic acid calibration curve

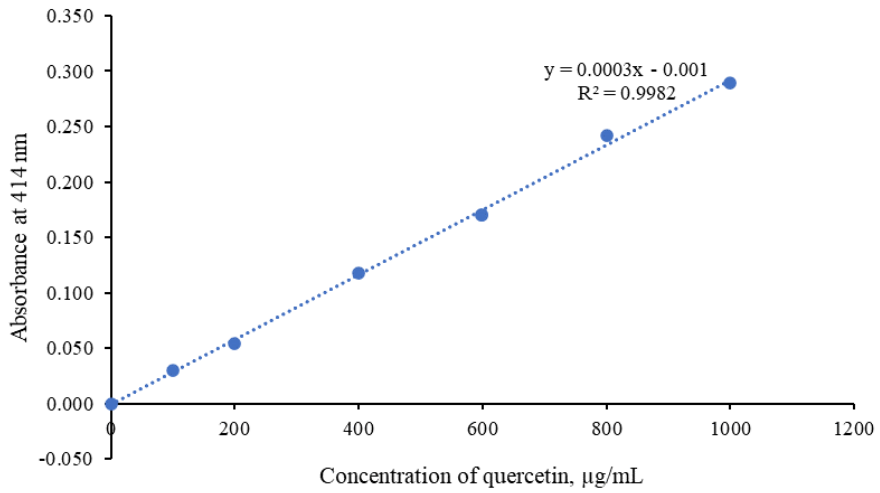

Figure 2. Quercetin calibration curve

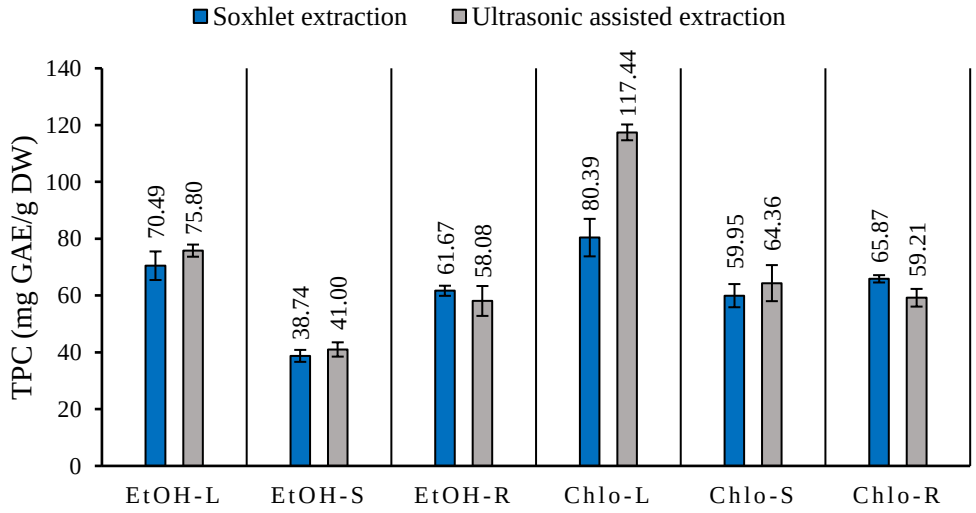

Figure 3. TPC of *C. alata* leaf, stem, and root using SE and UAE

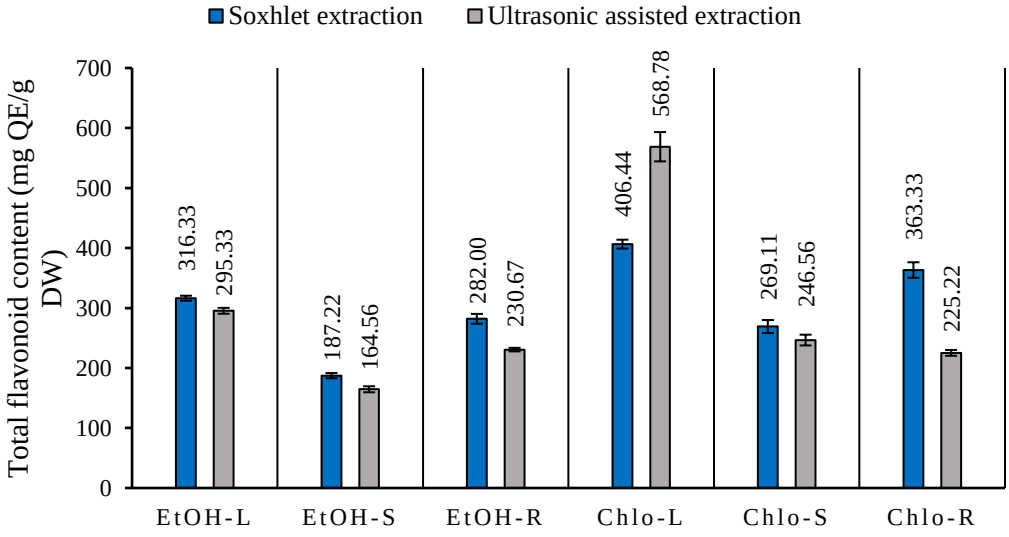

Figure 4. TFC of *C. alata* leaf, stem, and root using SE and UAE

Phytochemical compounds found in different plant parts may be responsible for the unique pharmacological effects in those parts (Sembiring *et al*., 2018). As a common plant response to these stresses, phenolic and flavonoid compounds are produced; these compounds have the ability to repair damaged tissues, absorb UV light, and repel parasites and pathogens (Clement *et al*., 2021). Less exposure is provided to the stems and roots to these factors. Therefore, evolutionary pressures on *C. alata* stems and roots to generate high concentrations of phenolic and flavonoid compounds are lower than on the leaves (Pachorkar & Patil, 2021). Additionally, environmental stressors such as UV radiation, pests, and pathogens affect the foliage more directly (Nantongo *et al*., 2018). As a result, phenolic and flavonoid compounds are more abundant in the leaves of *C. alata* than in its stems and roots. A study by Halim-Lim *et al.* (2020) also reported that the leaves of *C. alata* from water extract showed higher phenolic and flavonoid content than barks and roots.

As for the extraction techniques, UAE showed a better phenolic recovery in all extracts except for the roots extracted from both ethanol and chloroform (EtOH-R, Chlo-R). The ultrasound treatment successfully disrupted the cell wall of the plants, which also reduced particle size and enhanced solvent penetration into the plant matrix. This gave a higher surface of contact between trapped bioactive chemicals and the solvent, which improved the extraction efficiency (Das *et al.*, 2019). Romes *et al.* (2019) also reported the phenolic content of oil palm leaves from UAE was higher than SE and maceration extraction. Long exposure to high temperatures in SE could induce the degradation of bioactive compounds in the plants (Mohammadpour *et al.*, 2019). Therefore, UAE was effective for the recovery of the phenolic compound due to its short optimal extraction time and less quantity of solvents and samples used.

Meanwhile, for TFC, the results showed that SE provided a better recovery of flavonoid, except for the chloroform extract of leaves part (SE-Chlo-L, 406.444 mg QE/g DW) where the ultrasonic extract was higher (UAE-Chlo-L, 568.778 mg QE/g DW). However, the UAE is still competent because, even though the extraction used a small quantity of sample and solvent, it proved to be effective in extracting flavonoids. This agrees with Das *et al.* (2019), where a similar solid-to-solvent ratio was used for sonication, maceration, and soxhlet extraction, proving that sonication provides a better flavonoid recovery than other techniques. A higher solid-to-solvent ratio caused a higher concentration gradient, which raised the diffusion rate of the chemicals from the sample into the solvent (Elboughdiri, 2018: Jovanović *et al.*, 2021).

In this study, all the extracts obtained from chloroform showed a higher TPC compared to ethanol extracts. Similar results are obtained for TFC. A chloroform extract gives better TFC from all parts of *C. alata*, except for the ultrasonic extract of the roots (UAE-Chlo-R, 225.222 mg QE/g DW). The difference was slightly lower than the ultrasonic extract of roots by ethanol (UAE-EtOH-R, 230.667 mg QE/g DW) (Figure 4). These results are attributed to several factors such as the type of extraction solvent, its polarity index, and the solubility of the target compounds in chloroform as extraction solvent (Nguyen *et al.*, 2022).

According to Alara *et al.* (2021), chloroform might selectively extract certain phenolics that are less polar, which are not as effectively extracted by more polar solvents like ethanol or water. This selectivity of solvent extracts could result in a higher concentration of less polar phenolic compounds in chloroform extract. A study by Nguyen *et al.* (2022) also reported that ethyl acetate, acetone, and chloroform extracts of *Avicennia officinalis* L provided a higher TPC than ethanol, methanol, and dichloromethane extracts. Thus, chloroform in combination with UAE is a suitable method for the extraction of phenolic compounds. Meanwhile, SE is a suitable method for the extraction of flavonoids for all plant parts except for the Chlo-L. Based on the results, it is significant to choose the right solvent for phenolic and flavonoid extraction because the combination of extraction methods and solvent selection might provide a variety of outcomes.

CONCLUSION

Different extraction methods and solvent extracts generally affected the yield, phenolic and flavonoid content in *C. alata.* This study showed that extracts from the leaf of *C. alata*

performed better than the root and stem in terms of their extraction yield, TPC and TFC due to biological factors and environmental effects. With the exception of TFC in Chlo-R, the TPC and TFC in stem and root only show slight differences. Also, chloroform is a good choice of solvent for extracting phenolics and flavonoids due to the selectivity of less polar compounds in *C. alata.* For the extraction method, SE is better at extracting flavonoids except for the Chlo-L. Meanwhile, UAE is more efficient in extracting phenolic compounds except for the EtOH-R and Chlo-R. Thus, these findings provide data for selecting methods that produce optimal yield, phenolic and flavonoid contents in *C. alata*'s species.

ACKNOWLEDGEMENTS

This research study was funded by the UNI/I01/VC-HIRG/85485/P03-02/2022.

REFERENCES

Adedeji, A.A. & Babalola, O.O. (2020). Secondary metabolites as plant defensive strategy: A large role for small molecules in the near root region. *Planta*, 252(4): 61-73. DOI: 10.1007/s00425-020-03468-1

Aguirre-Becerra, H., Vazquez-Hernandez, M. C., Saenz de la O,D., Alvarado-Mariana, A., Guevara-Gonzalez, R.G., Garcia-Trejo, J.F. & Feregrino-Perez, A.A. (2021). Role of stress and defense in plant secondary metabolites production. *Bioactive Natural Products for Pharmaceutical Applications*, 140: 151-195. DOI: 10.1007/978-3-030-54027-2_5

Alara, O.R., Abdurahman, N.H. & Ukaegbu, C.I. (2021). Extraction of phenolic compounds: A review. *Current Research in Food Science*, 4: 200-214. DOI: 10.1016/j.crfs.2021.03.011

Az-Zahra, F.R., Sari, N.L.W., Saputry, R., Nugroho, G.D., Sunarto, Pribadi, T. & Setyawan, A.D. (2021). Traditional knowledge of the Dayak tribe (Borneo) in the use of medicinal plants. *Biodiversitas Journal of Biological Diversity*, 22(10): 4633-4647. DOI: 10.13057/biodiv/d221057

Bakar, F.A., Razzaq, K.W., Ahmad, K.I., Magiman, M.M., Rosli, Z., Seemab, A. & Faridah-Hanum, I. (2023). Diversity and utilization of ethnomedicinal plants in Sarawak, Borneo. *Malaysian Forester*, 86(1): 125-152.

Bencheikh, N., Bouhrim, M., Merrouni, I.A., Boutahiri, S., Kharchoufa, L., Addi, M., Tungmunnithum, D., Hano, C., Eto, B., Legssyer, A. & Elachouri, M. (2021). Antihyperlipidemic and antioxidant activities of flavonoid-rich extract of *Ziziphus lotus* (L.) Lam. fruits. *Applied Sciences*, 11(7788): 1-13. DOI: 10.3390/app11177788

Bitwell, C., Indra, S. Sen, Luke, C. & Kakoma, M.K. (2023). A review of modern and conventional extraction techniques and their applications for extracting phytochemicals from plants. *Scientific African*, 19: 1-19. DOI: 10.1016/j.sciaf.2023.e01585

Bui, N.T., Pham, T.L.T., Nguyen, K.T., Le, P.H. & Kim, K.H. (2021). Effect of extraction solvent on total phenol, flavonoid content, and antioxidant activity of *Avicennia officinalis*. *Biointerface Research in Applied Chemistry*, 12(2): 2678-2690. DOI: 10.33263/BRIAC122.26782690

Cardoso, R.R., Neto, R.O., dos Santos D'Almeida, C.T., do Nascimento, T.P., Pressete, CG., Azevedo, L., Martino, H.S.D., Cameron, L.C., Ferreira, M.S.L. & de Barros, F.A.R. (2020). Kombuchas from green and black teas have different phenolic profile, which impacts their antioxidant capacities, antibacterial and antiproliferative activities. *Food Research International*, 128: 1-10. DOI: 10.1016/j.foodres.2019.108782

Cianciosi, D., Forbes-Hernández, T.Y., Afrin, S., Gasparrini, M., Reboredo-Rodriguez, P., Manna, P.P., Zhang, J., Lamas, L.B., Flórez, S.M., Toyos, P.A., Quiles, J.L., Giampieri, F. & Battino, M. (2018). Phenolic compounds in honey and their associated health benefits: A review. *Molecules*, 23(9): 1-20. DOI: 10.3390/molecules23092322

Clement, O.U., Philomena, O.N., May, O.N., Onyinye, M.A. & Chisom, I.F. (2021). Phytochemical, proximate and mineral analysis of different parts of *Senna alata* Linn. *Research Journal of Biotechnology and Life Science,* 1(1): 18-15. DOI: 10.52589/RJBLSLLHPMRF6

Das, S., Ray, A., Nasim, N., Nayak, S. & Mohanty, S. (2019). Effect of different extraction techniques on total phenolic and flavonoid contents, and antioxidant activity of betelvine and quantification of its phenolic constituents by validated HPTLC method. *3 Biotech*, 9(1): 37-44. DOI: 10.1007/s13205-018-1565-8

Deng, Y., Wang, W., Zhao, S., Yang, X., Xu, W., Guo, M., Xu, E., Ding, T., Ye, X. & Liu, D. (2022). Ultrasound-assisted extraction of lipids as food components: Mechanism, solvent, feedstock, quality evaluation and coupled technologies-A review. *Trends in Food Science & Technology*, 122: 83-96. DOI: 10.1016/j.tifs.2022.01.034

Dhalaria, R., Verma, R., Kumar, D., Puri, S., Tapwal, A., Kumar, V., Nepovimova, E. & Kuca, K. (2020). Bioactive compounds of edible fruits with their anti-aging properties: A comprehensive review to prolong human life. *Antioxidants*, 9(11): 1-38. DOI: 10.3390/antiox9111123

Dirar, A.I., Alsaadi, D.H.M., Wada, M., Mohamed, M.A., Watanabe, T. & Devkota, H.P. (2019). Effects of extraction solvents on total phenolic and flavonoid contents and biological activities of extracts from Sudanese medicinal plants. *South African Journal of Botany*, 120: 261-267. DOI: 10.1016/j.sajb.2018.07.003

Elboughdiri, N. (2018). Effect of time, solvent-solid ratio, ethanol concentration and temperature on extraction yield of phenolic compounds from Olive leaves. *Engineering, Technology & Applied Science Research*, 8(2): 2805-2808. DOI: 10.48084/etasr.1983

Fatmawati, S., Yuliana, Purnomo, A.S. & Abu Bakar, M.F. (2020). Chemical constituents, usage and pharmacological activity of *Cassia alata*. *Heliyon*, 6(7): 1-11. DOI: 10.1016/j.heliyon.2020.e04396

Halim-Lim, S., Ramli, N.S., Fadzil, F.A. & Abd Rahim, M.H.A. (2020). The antimicrobial and antioxidant properties of *Cassia alata* extraction under different temperature profiles. *Food Research*, 1(5): 2166-2550.

Hussein, R.A. & El-Anssary, A.A. (2019). Plants secondary metabolites: The key drivers of the pharmacological actions of medicinal plants. *Herbal Medicine*, 1(3): 11-30.

Jiang, J., Yan, L., Shi, Z., Wang, L., Shan, L. & Efferth, T. (2019). Hepatoprotective and anti-inflammatory effects of total flavonoids of *Qu Zhi Ke* (peel of *Citrus changshan-huyou*) on non-alcoholic fatty liver disease in rats via modulation of NF-κB and MAPKs. *Phytomedicine*, 64: 153082-153091. DOI: 10.1016/j.phymed.2019.153082

Jovanović, A.A., Djordjević, V.B., Petrović, P.M., Pljevljakušić, D.S., Zdunić, G.M., Šavikin, K.P. & Bugarski, B.M. (2021). The influence of different extraction conditions on polyphenol content, antioxidant and antimicrobial activities of wild thyme. *Journal of Applied Research on Medicinal and Aromatic Plants*, 25: 100328-100335. DOI: 10.1016/j.jarmap.2021.100328

Li, Y.D., Guan, J.P., Tang, R.C. & Qiao, Y. F. (2019). Application of natural flavonoids to impart antioxidant and antibacterial activities to polyamide fiber for health care applications. *Antioxidants*, 8(8): 301-316. DOI: 10.3390/antiox8080301

Ling, Y.Y., Sook Fun, P., Yeop, A., Yusoff, M.M. & Gimbun, J. (2019). Assessment of maceration, ultrasonic and microwave assisted extraction for total phenolic content, total flavonoid content and kaempferol yield from *Cassia alata* via microstructures analysis. *Materials Today*, 19: 1273-1279. DOI: 10.1016/j.matpr.2019.11.133

Mahyuddin, H.S., Roshidi, M.A.H., Ferdosh, S. & Noh, A.L. (2020). Using soxhlet and supercritical fluid (SFE) methods. *Science*, 4(1): 9-12. DOI: 10.26480/gws.01.2020.09.12

Mat Jusoh, M.A.A., Aris, F., Mat Jalil, M.T., Ahmad Kamil, K. & Zakaria, N.A. (2023). A review of Malaysian medicinal plants with

potential anticancer activity. *Malaysian Applied Biology*, 52(1): 1-34. DOI: 10.55230/mabjournal.v52i1.2274

Mohammadpour, H., Sadrameli, S.M., Eslami, F. & Asoodeh, A. (2019). Optimization of ultrasound-assisted extraction of *Moringa peregrina* oil with response surface methodology and comparison with Soxhlet method. *Industrial Crops & Products*, 131: 106-116. DOI: 10.1016/j.indcrop.2019.01.030

Mugao, L.G., Muturi, P.W., Gichimu, B.M. & Njoroge, E.K. (2020). In vitro control of *Phytophthora infestans* and *Alternaria solani* using crude extracts and essential oils from selected plants. *International Journal of Agronomy*, 2020: 1-10. DOI: 10.1155/2020/8845692

Nantongo, J.S., Odoi, J.B., Abigaba, G. & Gwali, S. (2018). Variability of phenolic and alkaloid content in different plant parts of *Carissa edulis* Vahl and *Zanthoxylum chalybeum* Engl. *BMC Research Notes*, 11(125): 1-5. DOI: 10.1186/s13104-018-3238-4

Nguyen, N.V.T., Duong, N.T., Nguyen, K.N.H., Bui, N.T., Pham, T.L.T., Nguyen, K.T., Le, P.H. & Kim, K.H. (2022). Effect of extraction solvent on total phenol, flavonoid content, and antioxidant activity of *Avicennia officinalis*. *Biointerface Research in Applied Chemistry*, 12(2): 2678-2690. DOI: 10.33263/BRIAC122.26782690

Oladeji, O.S., Adelowo, F.E., Oluyori, A.P. & Bankole, D.T. (2020). Ethnobotanical description and biological activities of *Senna alata*. *Evidence-Based Complementary and Alternative Medicine*, 2020: 1-12. DOI: 10.1155/2020/2580259

Pachorkar, P.Y. & Patil, S.H. (2021). Therapeutic potential and characterization of *Senna alata*: An ethano-medicinal plant. *International Journal of Pharmaceutical Sciences and Research*, 12(9): 4985-4992. DOI: 10.13040/IJPSR.0975-8232.12(9).4985-92

Rahman, M.M., Rahaman, M.S., Islam, M.R., Rahman, F., Mithi, F.M., Alqahtani, T., Almikhlafi, M.A., Alghamdi, S.Q., Alruwaili, A.S., Hossain, S., Ahmed, M., Das, R., Emran, T. & Uddin, M.S. (2022). Role of phenolic compounds in human disease: Current knowledge and future prospects. *Molecules*, 27(233): 1-36. DOI: 10.3390/molecules27010233

Romes, N.B., Hamid, M.A., Hashim, S.E. & Wahab, R.A. (2019). Statistical modelling of ultrasonic-aided extraction of *Elaeis guineensis* leaves for better-quality yield and total phenolic content. *Indonesian Journal of Chemistry*, 19(3): 811-826. DOI: 10.22146/ijc.41603

Saini, R.K., Prasad, P., Shang, X. & Keum, Y.S. (2021). Advances in lipid extraction methods-A review. *International Journal of Molecular Sciences*, 22(24): 13643-13662. DOI: 10.3390/ijms222413643

Saidin, S.H., Azah, N., Ali, M., Hirmizi, N.M., Yusoff, N., Abdullah, Z., Markandan, S., Khoo, M., Pisar, M., Jamil, M., Lee, T.A., Hashim, N., Mohamed, S. & Caadir, S. (2019). Skin care active ingredients from *Senna alata* (L.) Roxb extracts. *Asian Journal of Pharmacognosy*, 3(1): 23-31.

Saifullah, M., McCullum, R., McCluskey, A. & Vuong, Q. (2020). Comparison of conventional extraction technique with ultrasound assisted extraction on recovery of phenolic compounds from lemon scented tea tree (*Leptospermum petersonii*) leaves. *Heliyon*, 6(4): 1-12. DOI: 10.1016/j.heliyon.2020.e03666

Sembiring, E.N., Elya, B. & Sauriasari, R. (2018). Phytochemical screening, total flavonoid and total phenolic content and antioxidant activity of different parts of *Caesalpinia bonduc* (L.) Roxb. *Pharmacognosy Journal*, 10(1): 123-127. DOI: 10.5530/pj.2018.1.22

Thilakarathna, R.C.N., Siow, L.F., Tang, T.K., Chan, E.S. & Lee, Y.Y. (2023). Physicochemical and antioxidative properties of ultrasound-assisted extraction of mahua (*Madhuca longifolia*) seed oil in comparison with conventional Soxhlet and mechanical extractions. *Ultrasonics Sonochemistry*, 92: 106280-106290. DOI: 10.1016/j.ultsonch.2022.106280

Vaou, N., Stavropoulou, E., Voidarou, C., Tsigalou, C. & Bezirtzoglou, E. (2021). Towards advances in medicinal plant antimicrobial activity: A review study on challenges and future perspectives. *Microorganisms*, 9(10): 1-28. DOI: 10.3390/microorganisms9102041

Wang, S., Li, Y., He, L., Yang, J., Fernie, A.R. & Luo, J. (2022). Natural variance at the interface of plant primary and specialized metabolism. *Current Opinion in Plant Biology*, 67: 102201-102221. DOI: 10.1016/j.pbi.2022.102201

Zhang, Q.W., Lin, L.G. & Ye, W.C. (2018). Techniques for extraction and isolation of natural products: A comprehensive review. *Chinese Medicine*, 13(20): 1-26. DOI: 10.1186/s13020-018-0177-x

Borneo Journal of Resource Science and Technology (2024), 14(1): 149-160
DOI: https:doi.org/10.33736/bjrst.5844.2024

Early Assessment of Forest Growth in a Logged over Coastal Lowland Mixed Dipterocarp Forest in Bintulu, Sarawak, Malaysia

KIAN HUAT ONG*, PEI LI YONG & ROLAND JUI HENG KUEH

Faculty of Agricultural and Forestry Sciences, Universiti Putra Malaysia Kampus Bintulu Sarawak, P. O. Box 396, 97008 Bintulu, Sarawak, Malaysia
*Corresponding author: okhuat@upm.edu.my
Received: 10 July 2023 Accepted: 19 January 2024 Published: 30 June 2024

ABSTRACT

Managing regrowth forests sustainably is a necessary tactic to address climate change as these forests' ability to capture and sequester carbon is much higher due to their potential high growth rate. These forests also retained high tree diversity if subjected to selective logging previously. The objectives of this study were to investigate growth rate of tree species in a logged over coastal lowland mixed dipterocarp forest. This study was carried out in 10 established plots (50 m × 20 m) at a logged-over forest in Universiti Putra Malaysia Bintulu Sarawak Campus, Sarawak, Malaysia and trees with 10 cm diameter breast height (dbh) and above were measured. There were 611 individual trees of 159 species and 43 families were found in a one-hectare. The majority of trees (86%) were found in smaller diameter classes (<30 cm) with only 2% in diameter classes of more than 50 cm. The study area still retains a mixed dipterocarp forest feature. The stand has a good growth rate. Overall *dbh* increment was 0.34 cm yr^{-1} with dipterocarps documented 0.39 cm yr^{-1}. A reverse growth dominance was observed in this study where smaller trees recorded higher growth. Thus contributing up to 72% of carbon sequestrated by this group of trees.

Keywords: Carbon sequestration, floristic composition, growth dominance, growth rate, logged-over lowland dipterocarp forest

INTRODUCTION

In 2020, about 31.1% of the earth's land surface is covered by forests with 45% found in the tropical region (FAO, 2020). Forest trees capture CO_2 from the air (one of the main greenhouse gases that causes climate change) and store carbon in biomass, forest litter and soil as they grow. Over a period of 19 years (2001 – 2019), annually it is estimated that global forests are able to remove 15.49 ± 19 Gt CO_2e. Tropical regions contributed 45.1% or 6.99 Gt CO_2e of this removal (Harris *et al*., 2021). The highest ability of tropical forests to capture and sequestration of carbon is due to the highest carbon density within this type of forests (FAO, 2020; Spawn, 2020). Thus managing forests sustainably including carbon capture is a crucial approach to help address climate change.

Changes in tree growth can have a significant impact, either shielding or impairing the increase in atmospheric CO_2. FAO (2020) estimated total carbon stock in forests at 662 Gt of which 45.2% in soil, 44.5% in living biomass, and 10.3% in dead wood and litter. South and Southeast Asia, Western and Central Africa, South America, Central America, and the Caribbean where most tropical forests can be found account for 53.7% of carbon found in living biomass (FAO, 2020). This indicates that tropical forests are a highly significant contributor to the global carbon budget. However, logged-over forests are now more widespread than unlogged forests in this region also. In the case of Borneo Island, Gaveau *et al*. (2014) estimated that by 2010 the total forested area only covers 52.8% of the island. Logged-over forests cover 46.2% of these persisted forests. They expected that about 42.0% or 88,150 km^2 of the remaining intact forests will be logged as they are categorized as production forest and only 32.2% of potential remain as intact forests in the coming decade. Although logged-over forests are more common, the understanding of carbon dynamics in response to timber harvesting in the tropics is limited. Following disturbance such as logging, forest regrowth is able to possibly provide a valuable carbon sink as forests regain their biomass during the succession process (Pugh *et*

al., 2019). Carbon sequestration potential due to biomass accumulation rate from natural forest regrowth is still sparse. Many countries are depending on default rates from the Intergovernmental Panel on Climate Change as they do not have nationally specific forest carbon accumulation rates (Lewis *et al.*, 2019). The available rates do not take into consideration variations in local land-use history and environmental conditions (Cook-Patton *et al*., 2020).

Production of timber in Malaysia is based on a selective management system with a periodic harvesting cycle of 25 – 30 years that was introduced in 1978 (Thang, 1987). A number of commercial trees above a certain diameter limit will be harvested. This management system is sustainable only if able to maintain timber production (potential harvestable trees recover in time) and continue to provide ecosystem services between cuts (Edwards *et al*., 2014). Therefore recovery of forest stock estimation becomes a critical component of sustainable forest management and is imposed by certification schemes (Nasi *et al*., 2012).

Forest certification, a market driven mechanism, gained traction after the United Nations Conference on Environment and Development, Earth Summit at Rio de Janeiro in 1992. The certification scheme aims to identify forest areas that are managed sustainably in terms of economic, social and environmental. An approach that allows timber harvesting to continue while at the same time ensuring forests are managed responsibly. In 1998 Malaysia Timber Certification Council was established and three years later, they launched their first certification scheme with the aim to encourage the implementation of sustainable forest management in Malaysia. This scheme was the first tropical forest scheme in the Asia Pacific region that gained endorsement by The Programme for the Endorsement of Forest Certification in May 2009.

The establishment of permanent sample plots is a crucial approach spelled out in the certification scheme documents in order to monitor and assess the health and vitality of the forests and the sustainability of managed forests. The plots are able to provide among other tree growth rates, regeneration status, and conditions of the forests. This collected information will be able to assist forest managers in determining the next harvesting cycle more accurately for their forest area. Information on the growth rate of tropical tree species found in the natural forests is still sparse especially in the logged-over forests. This study was conducted in an attempt to provide information on floristic composition, diameter, biomass and carbon content increments, and assessed the relationship between tree size and tree growth rate in a coastal logged-over lowland mixed-dipterocarp forest.

MATERIALS AND METHODS

Site Description and Plot Establishment

The study plots were established at a logged-over forest within Universiti Putra Malaysia Bintulu Sarawak Campus, Sarawak, Malaysia (Figure 1). The record from the Forest Department Sarawak indicated that this forest was selectively logged in 1977. In 1994, illegal logging activity was detected in this area resulting in major destruction with most of the trees with a diameter of 40 cm being felled. This forest is currently used for teaching and research purposes for forestry students. The forest area is situated at 20 – 110 m above sea level with an average annual rainfall of 2,327 mm. The soil in the area is acidic and classified as an Isohyperthermic Typic Dystropept known as the Nyalau soil series (Peli *et al*., 1984). One-hectare permanent sample plot was first established in 2007 by combining 10 subplots of 50 m × 20 m (Figure 2).

Diameter Measurement

All trees with a diameter of 10 cm and above at breast height (*dbh* – 1.3 m above ground height) were measured, tagged, identified and marked with a red paint to indicate the point of measurement. Remeasurement of *dbh* was conducted the following year at the marked measurement point.

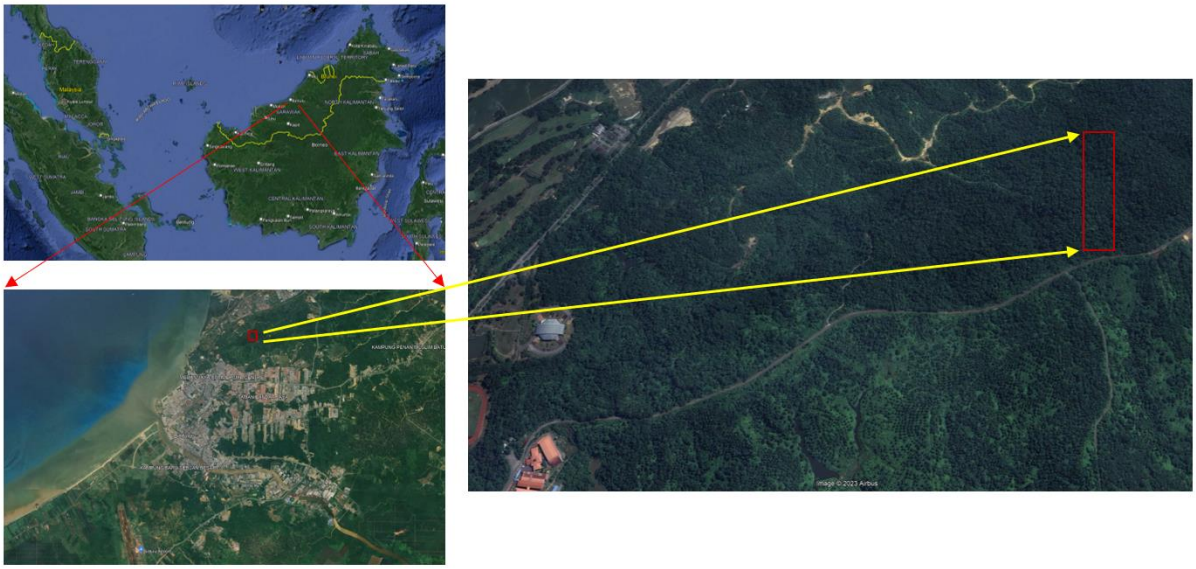

Figure 1. Study site location

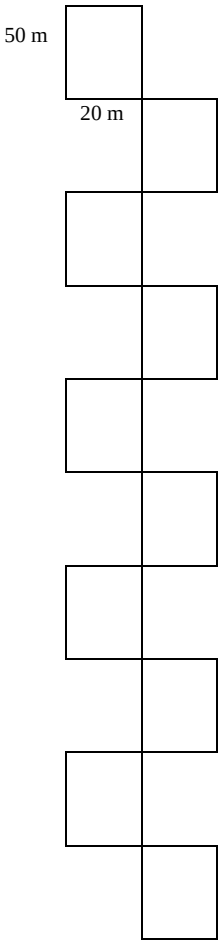

Figure 2. Plots layout

Data Analysis

Field data collected were quantitatively analyzed for growth dominance, biomass and carbon sequestration estimation, Important Value Index, species diversity and tree distribution within the study area. The methods are as follows:

Growth Dominance

The relationship between tree size and their

growth can be analyzed using growth dominance (GD) as proposed by Binkley (2004). This quantitative approach looks at how different tree sizes influence productivity (Soares *et al*., 2017). GD was calculated using the Eq. (1) proposed by West, (2014):

$$GD = 1 + \sum_{i=1}^{n}(x_i - x_{i-1})(y_i + y_{i-1}) \qquad \text{Eq. (1)}$$

where *n* is the number of trees found in the plot, *x* is the cumulative percentage in stem biomass, and *y* is the cumulative percentage increment in stem biomass.

Biomass and Carbon Sequestration Estimation

Manuri *et al*. (2016) allometric equation [Eq. (2)] for tropical dipterocarp forests was used to determine the aboveground biomass (AGB) of trees in the current study.

$$\text{AGB (kg)} = 0.215\ dbh^{2.533} \qquad \text{Eq. (2)}$$

The conversion factor of 0.471 was used to calculate carbon in AGB (Thomas & Martin, 2012). The ratio of 3.67 (weight of C in CO_2) was used to determine CO_2 captured by growing trees.

Importance Value Index

The importance value index (IVI) for tree species recorded in this study was calculated based formula Eq. (3), Eq. (4), Eq. (5) and Eq. (6) provided by Curtis and McIntosh (1951).

$$\text{Relative Density (RD)} = \frac{\text{density for a species}}{\text{total density for all species}} \times 100 \qquad \text{Eq. (3)}$$

$$\text{Relative Frequency (RF)} = \frac{\text{frequency value for a species}}{\text{total frequency for all species}} \times 100 \qquad \text{Eq. (4)}$$

$$\text{Relative Dominance (RDo)} = \frac{\text{dominance for a species}}{\text{total dominance for all species}} \times 100 \qquad \text{Eq. (5)}$$

$$\text{IVI} = \text{RD} + \text{RF} + \text{RD}_o \qquad \text{Eq. (6)}$$

Species Diversity and Tree Distribution

Shannon-Wiener index (Pielou, 1969) and Fisher's α index (Whittaker 1960) were two indices used in this study to determine the tree species diversity. Meanwhile Pielou's index (Pielou, 1969) and variance to mean ratio (Greig-Smith, 1983) were used to determine tree distribution and disperser within studied plots. The existence of Borneo endemic tree species and their conservation status was also determined. This is determined by referring to the Tree Flora of Sabah and Sarawak, the IUCN Red List, and the Red List of Bornean Endemic Dipterocarps (Bartholomew *et al*., 2021). Furthermore, a species-area curve was developed by plotting species number as a function of the sample plot size or area. This has been used in studies of community ecology which provides the fundamental component for conservation biology.

RESULTS AND DISCUSSION

Tree Diversity and Distribution, and Stand Floristic Composition

In an area of one hectare, a total of 45 families with 157 species were enumerated and 611 stems were recorded. Of these, 98 were identified at the species level and 59 were identified at the genus level. The number of tree species recorded in this logged-over forest was lower than the ranges reported in primary forests of Peninsular Malaysia and Borneo for elevation below 250 m (Proctor *et al*., 1983; Sukardjo *et al*., 1990; Manokaran & Swaine, 1994; Poulsen *et al*., 1996; Davies & Becker, 1996; Kartawinata *et al*., 2004; Small *et al*., 2004; Wilkie *et al*., 2004). Stand density in the current study was within the ranges reported by Proctor *et al*. (1983), Sukardio *et al*. (1990), Newbery *et al*. (1992), Manokaran and Swaine (1994), Poulsen *et al*. (1996), Davies and Becker (1996), Kartawinata *et al*. (2004), Small *et al*. (2004), and Wilkie *et al*. (2004) for primary forests of Peninsular Malaysia and Borneo (422–759 stems ha^{-1}). A total of 170 stems (or 27.8% of total stems) were from the Dipterocarpaceae family. A common feature in a mixed dipterocarp forest.

A species-area curve was developed to determine if the total number of species found in the current study signifies the total number of species in the whole studied area. A considerable number of species were steadily added as the number of subplots increased up to one hectare (Figure 3) which indicated that larger areas should be inventoried in order to get a better representative of tree species in this forest site. Similar results were reported by various authors who worked on tropical forests of Peninsular Malaysia, Borneo and Sumatra (Wyatt-Smith, 1966; Kartawinata *et al*., 1981;

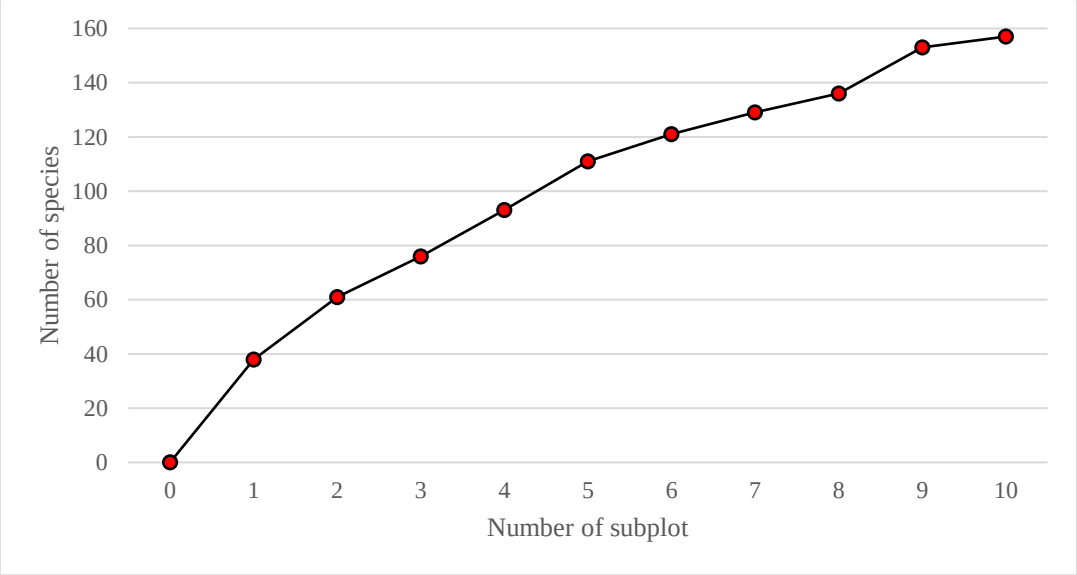

Figure 3. A species-area curve for this study

Riswan, 1982; Sist & Saridan, 1999; Kartawinata *et al*., 2004; Kueh *et al*., 2017).

In this study, a total of 45 tree families were recorded. Only a few tree families were speciose among the sites, with 34.5% represented by ten or more species. Dipterocarpaceae with 37 species (23.6% of total species recorded) and Euphorbiaceae with 15 species were the most speciose families in this study. These two families were commonly found in most of the lowland mixed dipterocarp forests around Borneo and Peninsular Malaysia. Meanwhile four (or 8.9%) families were represented by only a single species. This logged-over forest recorded a higher number of tree families than a few other primary forests in north Sumatra (Kartawinata *et al*., 2004) and Brunei on Borneo Island (Poulsen *et al*., 1996; Small *et al*., 2004).

The species diversity of this logged-over forest is categorised by a profusion of tree species with a low rate of occurrence resulting in high Shannon–Wiener and Fisher's α diversity indexes (4.52 and 67.66, respectively). About 42.7% (or 67 species) of tree species recorded were represented by a single individual. A higher number of single individuals representing a species is a common characteristic found in the lowland forest of Borneo (Poulsen *et al*., 1996; Small *et al*., 2004). Interestingly, tree species stems found within this logged-over forest were almost evenly distributed and dispersed (E = 0.90 and VMR = 0.99). This forest is dominated by a group of understorey species.

Xanthophyllum sp. (4.7%), *Rubroshorea macroptera* (4.6%) and *Litsea* sp. (3.4%) were the three dominant species found at this study site (Table S1). These three tree species also recorded the highest ecological weights among the species found with IVI values of more than 10 (Table S1). In this study, a total of 23 endemic species of Borneo were recorded (Table 1), with which 14 were from Dipterocarpaceae (37.8% of dipterocarps found in this site were endemic to Borneo). *Shorea praestans* is a critically endangered endemic species recorded in this logged-over forest based on the Red List of Bornean Endemic Dipterocarps (Bartholomew *et al*., 2021). Two endangered endemic species, *Hopea aequalis* and *Shorea domatiosa* (Bartholomew *et al*., 2021) also recorded on this site. Meanwhile, four

vulnerable endemic species, *Dipterocarpus stellatus*, *Neohopea isoptera*, *Rubroshorea quadrinervis*, and *Upuna borneensis* were recorded in this forest (Bartholomew *et al*., 2021).

Stand Diameter, Basal Area, Biomass, and Stand Growth

A total of 611 individuals with *dbh* ≥ 10 cm were recorded during this study. An inverted J-curve trend was observed in tree *dbh* classes in this forest, with the highest number of individuals having smaller tree *dbh* contributing to 63.0% (10–19.9 cm) of total stems recorded (Figure 4). The highest *dbh* was recorded for *Dryobalanops aromatica* at 83.0 cm. The average tree *dbh* was 20.3 cm with an annual rate of 0.34 cm yr^{-1}. The annual *dbh* growth for the dipterocarp was 0.39 cm yr^{-1}. Growth rates of *dbh* reduced as size increased (Figure 5), which resulted in small trees (*dbh* of 10.0 – 29.9 cm) contributing substantially more to AGB increment than large trees (Figure 6).

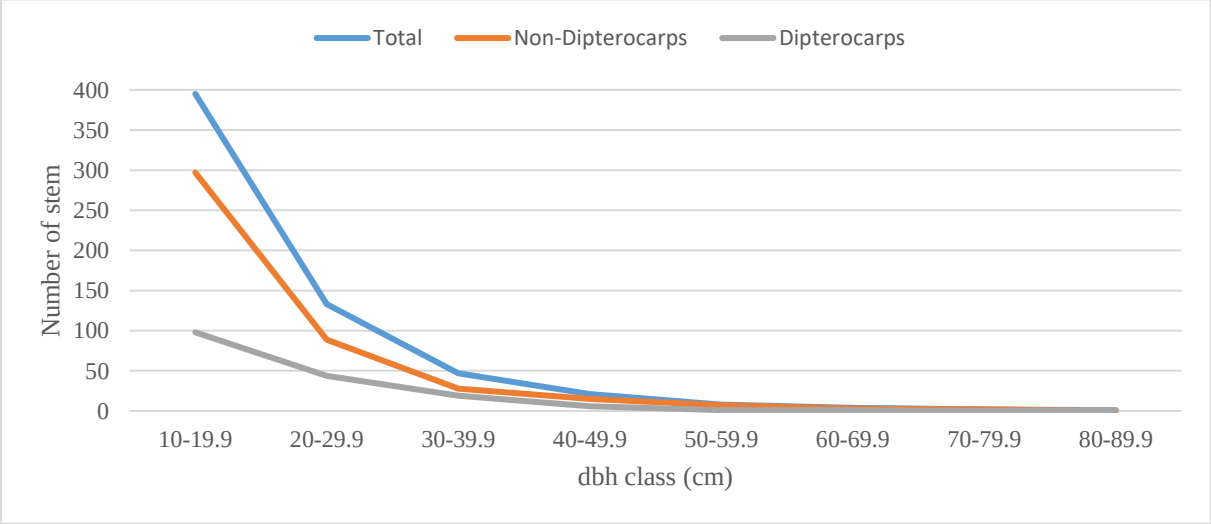

Figure 4. An inverted J-curve trend for tree diameter breast height classes in this study

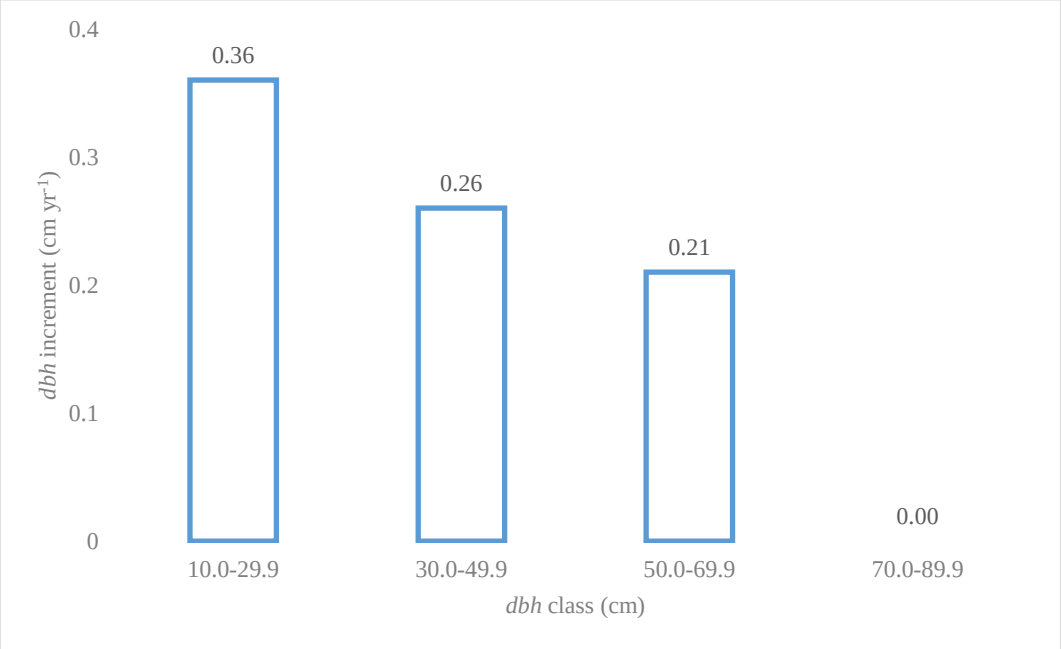

Figure 5. Annual diameter breast height growth rate according to diameter breast height classes

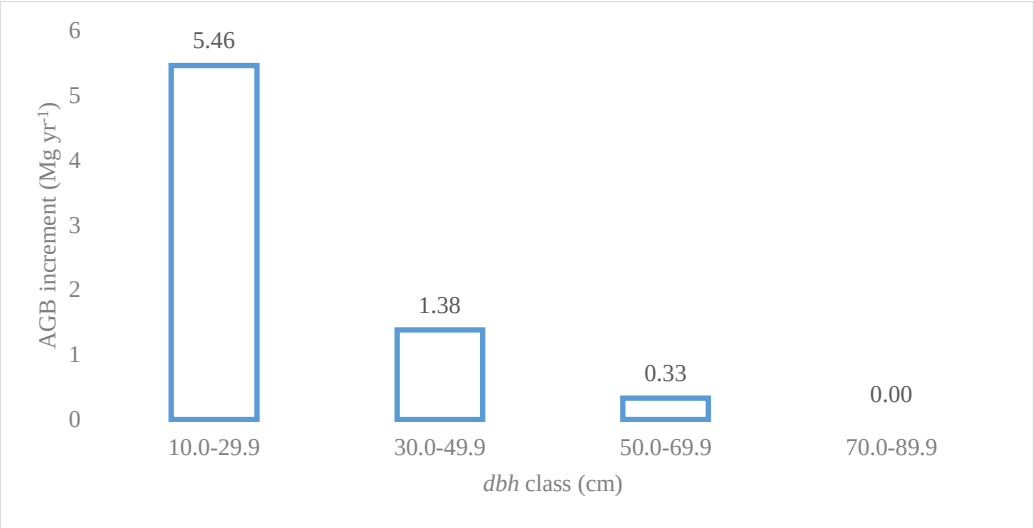

Figure 6. Above ground biomass increments according to diameter breast height classes

The total basal area in this forest was 25.16 m^2ha^{-1} (30.6% or 7.70 m^2 ha^{-1} contributed by dipterocarps) with annual growth of 0.64 m^2 ha^{-1} yr^{-1}. Meanwhile, total biomass was 435.03 t ha^{-1} (31.2% contributed by dipterocarps) with an annual of 11.51 t ha^{-1} yr^{-1}. In Sabah, Imai *et al*. (2012) found that dipterocarps contributed 43.4% of the total basal area when subjected to reduced-impact logging whilst the contribution of dipterocarps was lower (36.5%) in the area subjected to conventional logging.

In a dipterocarp forest of East Kalimantan, Sist and Nguyen-Thé (2002) reported a stand density of 530 stems ha^{-1} and a basal area of 35.1 m^2ha^{-1} before a logging operation. The number of stems was reduced to 402–498 stems ha^{-1} while the stands basal area was reduced to 18.7–28.7 m^2ha^{-1} four years after logging depending on logging intensities applied. In this study, our forest recorded higher stand density but similar stand basal area to that of East Kalimantan. Lower basal area per stem in the current study as compared to Sist and Nguyen-Thé (2002) report, might result in the indiscriminate felling of trees above 40 cm *dbh* during illegal logging operation years earlier in this forest.

Sist and Nguyen-Thé (2002) found that on average four years after logging, the overall *dbh* increment was 0.39 $cmyr^{-1}$ with dipterocarps recorded at 0.54 $cmyr^{-1}$. Meanwhile, the unlogged stand recorded *dbh* increment of 0.18–0.22 $cmyr^{-1}$ and a higher increment was recorded by dipterocarps (0.29–0.34 $cmyr^{-1}$). The current *dbh* increment was similar to the overall growth of logged-over stands in East Kalimantan. However, dipterocarp increment in this forest was considerably low when compared with the East Kalimantan site. The difference might be due to (i) recovery stages and (ii) a lesser number of larger *dbh* trees. It is well known that disturbed stands will experience a higher growth rate at the early stages of recovery (Chiew & Garcia, 1988; Thang & Yong, 1988; Sist & Nguyen-Thé, 2002: Bischoff *et al*., 2005). The forest in this study was subjected to logging more than 15 years ago while East Kalimantan stands only logged four years before. A higher number of large *dbh* (> 50 cm) was still available in East Kalimantan stands after logging while only 15 stems (2.5% of the total number of stems) larger than 50 cm were recorded on this site. Sist and Nguyen-Thé (2002) found that higher increment was recorded by trees with larger *dbh*. An opposite trend was observed in this forest, where smaller trees recorded a higher growth rate thus contributing more to AGB increments.

A reverse size-asymmetric of 0.42, where small trees contributed unduly more to stand increment than stand biomass, of GD was observed in this regrowth forest. Based on the conceptual model proposed by Binkley *et al*. (2006), the fourth phase of reverse GD could be observed in old growth forests. Higher growth of co-dominance and understorey trees and or reduction growth of dominant trees may result in reverse GD. A long-term observation would be required to assess the main factor contributing to reverse GD although decreasing growth of dominant trees is expected to be the main reason. A slower growth rate of large trees in forest

stands has been substantial research over the past few decades but the detailed mechanisms remain uncertain (Martinez-Vilalta *et al*., 2007; Hinckley *et al*., 2011). The current study only supports the general observation of the trend of diminished growth in larger trees, but is unable to give any insights into the mechanism involved.

Imai *et al*. (2014) conducted tree assessment in three different forest management units, i.e., Segaliud Lokan Forest Reserve in Sabah, Sapulut Forest Reserve in Sabah, and PT Ratah Timber in Kutai Barat, East Kalimantan. In the finding, they found that forest stands contained 345–670 stems ha^{-1} with 3.1–45.9 m^2ha^{-1} of basal area and 24–581 tha^{-1} of biomass in Segaliud Lokan Forest Reserve, 294–543 stems ha^{-1} with 3.6–51.4 m^2ha^{-1} of basal area and 25–653 tha^{-1} of biomass in Sapulut Forest Reserve, and 366–622 stems ha^{-1} with 4.7–66.2 m^2 ha^{-1} of basal area and 22– 969 t ha^{-1} of biomass in PT Ratah Timber. These variations of the tree density, volume and basal area per hectare depends on the degree of disturbances occurred in these areas. In an inventory work at Mulu National Park, Sarawak, Malaysia, Proctor *et al*. (1983) found that virgin dipterocarp forest contained 778 stems ha^{-1} with 57 m^2ha^{-1} of basal area and 650 tha^{-1} of biomass. They also recorded a stand density of 615–645 stems ha^{-1} with 28 m^2ha^{-1} of basal area and 210–250 tha^{-1} of biomass in poor alluvial forests. Meanwhile Kira (1978) estimated that undisturbed dipterocarp forest in Peninsular Malaysia contained 431 t ha^{-1} of biomass. The lower values of stand density, basal area and biomass in this study as compared with the Mulu forest (Proctor *et al*., 1983) as well as the Pasoh forest (Kira, 1978) indicated that this forest stand is still in a recovery stage and needs a longer time to reach climax stage. Stand and soil disturbance were still obvious after 15 years of recovery indicating that this stand was subjected to high logging intensity.

Carbon Sequestration

The smaller diameter size classes (10–29.9 cm) contributed 39.8% of the total AGB and carbon (Figure 7). About 86.4% of trees recorded in this study are found in these diameter size classes. Meanwhile trees more than 50 cm *dbh*, only added 26.3% to the total AGB and carbon although with simply 2.5% of total trees recorded. A total of 11.51 t $ha^{-1}yr^{-1}$ of AGB gained, 5.42 t C $ha^{-1}yr^{-1}$ was accumulated, and 19.87 t CO_2 $ha^{-1}yr^{-1}$ was sequestrated by trees in the current study with smaller diameter classes (10–29.9 cm) contributed 71.6%.

Based on 49 long-term forest monitoring plots across Borneo, Qie *et al*. (2017) estimated that AGB increment of intact forest interior plots (>100 m from the forest edge) at 0.91 t $ha^{-1}yr^{-1}$ while C gain is estimated at 0.43 t C $ha^{-1}yr^{-1}$ during 1958–2015.

Regrowth forests have a good possibility to capture carbon via tree growth as shown in this study reducing CO_2 emission. These forests are usually faster in gaining biomass than intact natural forests. These figures can serve as a baseline for understanding the contribution of regrowth forests in capturing and sequestering CO_2 from the atmosphere.

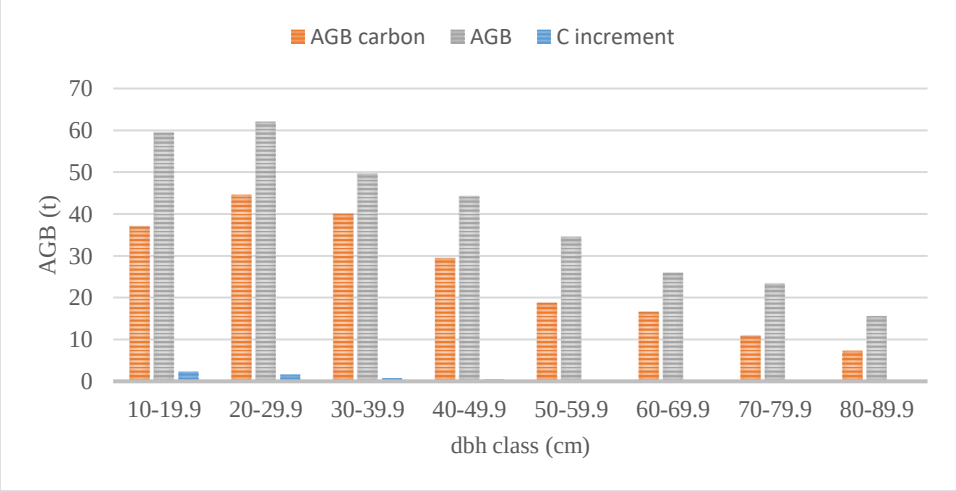

Figure 7. Aboveground biomass, and carbon content and increment according to diameter breast height classes

CONCLUSION

A total of 611 tree stems of 157 different species comprising 45 tree families were inventoried in a one-hectare area. Dipterocarpaceae and Euphorbiaceae dominated the area, a widespread characteristic of a mixed dipterocarp forest. The two most abundant species in this area were *Xanthophyllum* sp. and *R. macroptera*. A total of 23 Bornean endemic tree species were recorded with three species under the endangered species list (*R. praestans* – critically endangered; *H. aequalis* and *S. domatiosa* – endangered) indicating the area is high in conservation value.

In the current study, the *dbh* annual increment rate was 0.34 $cmyr^{-1}$ where smaller size trees recorded higher growth rates. Thus contributed markedly to AGB and carbon increment compared to larger trees. GD further confirmed that small trees contributed greatly to stand increment. From the early assessment of the growth data, it would suggest an indication of higher growth rate in regrowth forest in the current study which indicates high potential for carbon sequestration compared to intact forests. Long term monitoring of these data is still crucial to enhance our understanding of forest growth rates and the potential carbon sequestration of logged over forest

ACKNOWLEDGMENTS

We are thankful to George Bala Empin, Khairul Annuar Mohd. Suhailee, Muaish Sait, and the late Sylvester Sam for the field experiment.

REFERENCES

Bartholomew, D., Barstow, M., Randi, A., Cicuzza, D., Hoo, P.K., Juiling, S., Khoo, E., Kusumadewi, Y., Majapaum, R., Maryani, A.M., Maycock, C.R., Nilus, R., Pereira, J.T., Sang, J., Robiansyah, I., Sugau, J.B., Tanggaraju, S., Tsen, S. & Yiing, L.C. (2021). *The Red List of Bornean Endemic Dipterocarps*. Richmond, UK: Botanic Gardens Conservation International.

Binkley, D. (2004). A hypothesis about the interaction of tree dominance and stand production through stand development. *Forest Ecology and Management*, 190: 265-271. DOI: 10.1016/j.foreco.2003.10.018

Binkley, D., Kashian, D.M., Boyden, S., Kaye, M.W., Bradford, J.B., Arthur, M.A., Fornwalt, P.J. & Ryan, M.G. (2006). Pattern of growth dominance in forests of the Rocky Mountains, USA. *Forest Ecology and Management*, 236: 193-201. DOI: 10.1016/j.foreco.2006.09.001

Bischoff, W., Newbery, D.M., Lingenfelder, M., Schnaeckel, R., Petol, H., Madani, L. & Ridsdale, C.E. (2005). Secondary succession and dipterocarp recruitment in Bornean rain forest after logging. *Forest Ecology and Management*, 218: 174-192. DOI: 10.1016/j.foreco.2005.07.009

Chiew, K.Y. & Garcia, A. (1988). Growth and yield studies in the Yayasan Sabah Forest concession area. In Wan Razali, W.M., Chan, H.T. and Appanah, S. (eds.) *Proceedings of the Seminar on Growth and Yield in Tropical Mixed/Moist Forests*. Kuala Lumpur: Forest Research Institute Malaysia. pp. 192–204.

Cook-Patton, S.C., Leavitt, S.M., Gibbs, D., Harris, N.L., Lister, K., Anderson-Teixeita, K.J., Briggs, R.D., Chazdon, R.L., Crowther, T.W., Ellis, P.W., Griscom, H.P., Herrmann, V., Holl, K.D., Houghton, R.A., Larrosa, C., Lomax G., Lucas, R., Madsen, P., Malhi, Y., Paquette, A., Parker, J.D., Paul, K., Routh, D., Roxburgh, S., Saatchi, S.S., van den Hoogen, J., Walker, W.S., Wheeler C.E., Wood, S.A., Xu, L. & Griscom, B.W. (2020). Mapping potential carbon capture from global natural forest regrowth. *Nature*, 585: 545-550. DOI: 10.1038/s41586-020-2686-x

Curtis, J.T. & Mcintosh, R.P. (1951). An unpland forest continum in the prairie forest border region of Wisconsin. *Ecology*, 32: 476-496. DOI: 10.2307/1931725

Davies, S.J. & Becker, P. (1996). Floristic composition and stand structure of mixed dipterocarp forest and heath forests in Brunei Darussalam. *Journal of Tropical Forest Science*, 8: 542-569.

Edwards, D.P., Tobias, J.A., Sheil, D., Meijaard, E. & Laurance, W.F. (2014). Maintaining ecosystem function and services in logged tropical forests. *Trends in Ecology &*

Evolution, 29: 511-520. DOI: 10.1016/j.tree.2014.07.003

FAO. (2020). *Global Forest Resources Assessment 2020: Main report*. Rome: FAO. DOI: 10.4060/ca9825en

Gaveau, D.L.A., Sloan, S., Molidena, E., Yaen, H., Sheil, D., Abram, N.K., Ancrenaz, M., Nasi, R., Quinones, M., Wielaard, N. & Meijaard, E. (2014). Four decades of forest persistence, clearance and logging on Borneo. *PLoS ONE*, 9(7): e101654. DOI: 10.1371/journal.pone.0101654

Greig-Smith, P. (1983). *Quantitative plant ecology*. Oxford: Blackwell.

Harris, N.L., Gibbs, D.A., Baccini, A., Birdsey, R.A., de Bruin, S., Farina, M., Fatoyinbo, L., Hansen, M.C., Herold, M., Houghton, R.A., Potapov, P.V., Suarez, D.R., Roman-Cuesta, R.M., Saatchi, S.S., Slay, C.M., Turubanova, S.A. & Tyukavina, A. (2021). Global maps of twenty-first century forest carbon fluxes. *Nature Climate Change*, 11: 234-240. DOI: 10.1038/s41558-020-00976-6

Hinckley, T.M., Lachenbruch, B., Meinzer, F.C. & Dawson, T.E. (2011). A lifespan perspective on integrating structure and function in trees. In Meinzer, F., Lachenbruch, B. and Dawson, T. (eds.) *Size- and Age-Related Changes in Tree Structure and Function*. Tree Physiology, Volume 4. Dordrecht: Springer. pp. 3-30. DOI: 10.1007/978-94-007-1242-3_1

Imai, N., Seino, T., Aiba, S., Takyu, M., Titin, J. & Kitayama, K. (2012). Effects of selective logging on tree species diversity and composition of Bornean tropical rain forests at different spatial scales. *Plant Ecology*, 213: 1413-1424. DOI: 10.1007/s11258-012-0100-y.

Imai, N., Tanaka, A., Samejima, H., Sugau, J.B., Pereira, J.T., Titin, J., Kurniawan, Y. & Kitayama K. (2014). Tree community composition as an indicator in biodiversity monitoring of REDD+. *Forest Ecology and Management*, 313: 169-179. DOI: 10.1016/j.foreco.2013.10.041

Kartawinata, K., Rochadi, A. & Tukirin, P. (1981). Composition and structure of a lowland dipterocarp forest at Wanariset, East Kalimantan. *Malaysian Forester*, 44: 397-406.

Kartawinata, K., Samsoedin, I., Heriyanto, M. & Afriastini, J.J. (2004). A tree species inventory in a one-hectare plot at the Batang Gadis National Park, North Sumatra, Indonesia. *Reinwardtia*, 12: 145-157. DOI: 10.55981/reinwardtia.2004.60

Kira, T. (1978). Primary productivity of Pasoh Forest-a synthesis. *Malaysian Nature Journal*, 30: 291-297.

Kueh, R.J.H., Mang, N.G., Ong, K.H., Muaish, S., Sam, S., Empin, G.B., Rajanoran, T. & Sinus, C.R. (2017). Tree diversity at Payeh Maga montane forest, Sarawak, Borneo. *Journal of Tropical Biology and Conservation*, 14: 125-150.

Lewis, S.L., Wheeler, C.E., Mitchard, E.T.A. & Koch, A. (2019). Restoring natural forests is the best way to remove atmospheric carbon. *Nature*, 568(7750): 25-28. DOI: 10.1038/d41586-019-01026-8

Manokaran, N. & Swaine, M.D. (1994). *Population dynamics of trees in dipterocarp forests of Peninsular Malaysia.* Malaysian Forest Records No. 41. Kepong: Forest Research Institute Malaysia.

Manuri, S., Brack, C., Noor'an, F., Rusolono, T., Anggraini, S.M., Dotzauer, H. & Kumara, I. (2016). Improved allometric equations for tree aboveground biomass estimation in tropical dipterocarp forests of Kalimantan, Indonesia. *Forest Ecosystems*, 3: 28. DOI: 10.1186/s40663-016-0087-2

Martínez-Vilalta, J., Vanderklein, D. & Mencuccini, M. (2007). Tree height and age-related decline in growth in Scots pine (*Pinus sylvestris* L.). *Oecologia*, 150: 529-544. DOI: 10.1007/s00442-006-0552-7

Nasi, R., Billand, A. & Vanvliet, N. (2012). Managing for timber and biodiversity in the Amazon Basin. *Forest Ecology and Management*, 268: 103-111. DOI: 10.1016/j.foreco.2011.04.005

Newbery D.Mc.C., Campbell E.J.F., Lee Y.F., Ridsdale C.E. & Still M.J. (1992). Primary lowland dipterocarp forest at Danum Valley, Sabah Malaysia: structure, relative abundance and family composition. *Philosophical Transactions of the Royal Society London B*, 335: 341-356.

Peli, M., Ahmad Husni, M.H. & Ibrahim, M.Y. (1984). *Report and map of the detailed soil survey of UPM farm Bintulu Campus Sarawak*. Buletin Teknikal No. 1. Kuching: Universiti Pertanian Malaysia Cawangan Sarawak.

Pielou, E.C. (1969). *An introduction to mathematical ecology*. New York: Wiley.

Poulsen, A.D., Nielsen, I.C., Tan, S. & Balslev, H. (1996). A quantitative inventory of trees in one hectare of mixed dipterocarp forest in Temburong, Brunei Darussalam. In Edwards, D.S., Booth, W.E. and Choy, S.C. (eds.) *Tropical Rainforest Research — Current Issues*. Monographiae Biologicae, Volume 74. Dordrecht, Springer. pp. 139-150. DOI: 10.1007/978-94-009-1685-2_13

Proctor, J., Anderson, J.M., Chai, P. & Vallack H.W. (1983). Ecological studies in four contrasting lowland rain forests in Gunung Mulu National Park, Sarawak: I. Forest environment, structure and floristics. *Journal of Ecology*, 71: 237-260. DOI: 10.2307/2259975

Pugh, T.A.M., Lindeskog, M., Smith, B., Poulter, B., Arneth, A., Haverd, V. & Calle, L. (2019). Role of forest regrowth in global carbon sink dynamics. *Proceedings of the National Academy of Sciences*, 116: 4382-4387. DOI: 10.1073/pnas.1810512116

Qie, L., Lewis, S.L., Sullivan, M.J.P., Lopez-Gonzalez, G., Pickavance, G.C., Sunderland, T., Ashton, P., Hubau, W., Kamariah, A.S., Aiba, S.-I., Banin, L.F., Berry, N., Brearley, F.Q., Burslem, D.F.R.P., Dančák, M., Davies, S.J. Fredriksson, G., Hamer, K.C., Hédl, R., Lip, K.K., Kitayama, K., Krisnawati, H., Lhota, S., Malhi, Y., Maycock, C., Metali, F., Mirmanto, E., Nagy, L., Nilus, R., Ong, R., Pendry, C.A., Poulsen, A.D., Primack, R.B., Rutishauser, E., Samsoedin, I., Saragih, B., Sist, P., Slik, J.W.F., Sukri, R.S., Svátek, M., Tan, S., Tjoa, A., van Nieuwstadt, M., Vernimmen, R.R.E., Yassir, I., Kidd, P.S., Fitriadi, M., Nur Khalish, H.I., Rafizah, M.S., Layla Syaznie, A.L., Muhammad Shahruney, S. & Phillips, O.L. (2017). Long-term carbon sink in Borneo's forests halted by drought and vulnerable to edge effects. *Nature Communications*, 8: 1966. DOI: 10.1038/s41467-017-01997-0

Riswan, S. (1982). *Ecological studies on primary, secondary and experimentally cleared mixed dipterocarp forest and kerangas forest in East Kalimantan, Indonesia* (Ph.D. thesis), University of Aberdeen.

Sist, P. & Nguyen-The, N. (2002). Logging damage and the subsequent dynamics of a dipterocarp forest in East Kalimantan (1990–1996). *Forest Ecology and Management*, 165: 85-103. DOI: 10.1016/S0378-1127(01)00649-1

Sist, P. & Saridan, A. (1999). Stand structure and floristic composition of a primary lowland dipterocarp forest in East Kalimantan. *Journal of Tropical Forest Science*, 11: 704-722.

Small, A., Martin, T.G., Kitching, R.L. & Wong K.M. (2004). Contribution of tree species to the biodiversity of a 1ha Old World rainforest in Brunei, Borneo. *Biodiversity and Conservation*, 13: 2067-2088. DOI: 10.1023/B:BIOC.0000040001.72686.e8

Soares, A.A.V., Leite, H.G., Cruz, J.P. & Forrester, D.I. (2017). Development of stand structural heterogeneity and growth dominance in thinned *Eucalyptus* stands in Brazil. *Forest Ecology and Management*, 384: 339-346. DOI: 10.1016/j.foreco.2016.11.010

Spawn, S.A., Sullivan, C.C., Lark, T.J. & Gibbs, H.K. (2020). Harmonized global maps of above and belowground biomass carbon density in the year 2010. *Scientific Data*, 6,7(1): 112. DOI: 10.1038/s41597-020-0444-4

Sukardjo, S., Hagihara, A., Yamakura, T. & Ogawa, H. (1990). Floristic composition of a tropical rain forest in Indonesia Borneo.

Bulletin of the Nagoya University Forest, 10: 1-44.

Thang, H.C. & Yong, T.K. (1988). Status on growth and yield studies in Peninsular Malaysia. In Wan Razali, W.M., Chan, H.T. and Appanah, S. (eds.) *Proceedings of the Seminar on Growth and Yield in Tropical Mixed/Moist Forests*. Kuala Lumpur: Forest Research Institute Malaysia. pp. 137-148.

Thang, H.C. (1987). Forest management systems for tropical high forest, with special reference to Peninsular Malaysia. *Forest Ecology and Management*, 21: 3-20. DOI: 10.1016/0378-1127(87)90069-7

Thomas, S.C. & Martin, A.R. (2012). Carbon content of tree tissues: a synthesis. *Forests*, 3(2): 332-352. DOI: 10.3390/f3020332

West, P.W. (2014). Calculation of a growth dominance statistic for forest stands. *Forest Science*, 60: 1021-1023. DOI: 10.5849/forsci.13-186

Whittaker, R.H. (1960). Vegetation of the Siskiyou Mountains, Oregon and California. *Ecology Monographs*, 30: 279–338. DOI: 10.2307/1943563

Wilkie, P., Argent, G., Cambell, E. & Saridan, A. (2004). The diversity of 15 ha of lowland mixed dipterocarp forest, Central Kalimantan. *Biodiversity and Conservation*, 13: 695-708. DOI: 10.1023/B:BIOC.0000011721.04879.79

Wyatt-Smith, J. (1966). *Ecological studies on Malayan forests*. Malayan Forestry Department Research Pamphlet No. 52. Kuala Lumpur: Malayan Forestry Department.

Borneo Journal of Resource Science and Technology (2024), 14(1): 161-173
DOI: https:doi.org/10.33736/bjrst.6104.2024

Orchids of UNIMAS: Diversity in a Developed Campus Landscape

ALMUNAH ABD MUTALIB[1], AKMAL RAFFI[1*], MEEKIONG KALU[1] & FARAH ALIA NORDIN[2]

[1]Faculty of Resource Science and Technology, Universiti Malaysia Sarawak, 94300 Kota Samarahan, Sarawak, Malaysia; [2]School of Biological Sciences, Universiti Sains Malaysia, 11800, Gelugor, Pulau Pinang
*Corresponding author: mrmakmal@unimas.my
Received: 10 July 2023 Accepted: 4 April 2024 Published: 30 June 2024

ABSTRACT

For the past three decades, various biotic components in Universiti Malaysia Sarawak (UNIMAS) natural habitats have been studied but less attention given to the largest family of flowering plants, the Orchidaceae. A preliminary survey in the campus areas has resulted in the discovery of more than ten species of orchids. Therefore, in this study more field samplings were conducted throughout the UNIMAS campus focusing on the developed areas to unveil the potential of UNIMAS-developed areas as a growth ground for orchids. To date, 37 orchid species have been recorded from these areas; mainly found on the planted trees at the roadside and landscaped areas surrounding the academic buildings, while the terrestrial species were found to inhabit different types of disturbed habitat. Among them, *Dendrobium pensile* was identified as a new record to Sarawak while *Dendrobium pseudostriatellum* and *Pinalia biglandulosa* were endemic to Borneo. This study provides an insight into the orchid resiliency towards habitat alteration, landscape phorophytes species that can host orchids, and management of species in a developed landscape.

Keywords: Biodiversity, Borneo, orchids, phorophyte, university ecosystem.

INTRODUCTION

Universiti Malaysia Sarawak (UNIMAS) is a young university (established in 1993) and currently still undergoing some landscape changes for the development of many facilities such as the examination hall and hospital. The campus was initially developed in a lowland area with several natural habitats - which are represented by kerangas forest, mangrove area, peat swamp forest and secondary forest. These natural areas have caught the interest of many researchers to study their various biological components (UNIMAS Institutional Repository, 2022). However, for the past three decades less attention has been given to the largest family of flowering plants, the Orchidaceae. Recent botanical surveys on the campus areas extended from the parking lots of the Faculty of Resource Science and Technology to the forest fringes by the roadside have resulted in the discovery of more than ten species of orchid from different genera. The presence of the orchids outside of UNIMAS natural habitats indicates that its developed landscapes to some extend are suitable for the orchid's growth thus more species are anticipated to be enumerated (Wolken *et al.*, 2001; Stipkova & Kindlmann, 2021). The recorded epiphytic orchids were observed to benefit from the planted trees as hosts while the terrestrials were found to adapt to several types of environments – of which some were acknowledged to be uncommon for orchids (Beaman *et al.*, 2001; Wood, 2014). The capability of the developed landscapes for orchid growth was also evidenced by the high number of individuals among the sighted orchids (McCormick & Jacquemyn, 2013). This situation can infer the orchid's adaptation in disturbed and altered habitats to ensure their survivability. Thus, it is important to assess the species diversity to unveil the potential of UNIMAS-developed areas as a growth ground for orchids. This finding will add information on the orchid's resiliency in disturbed habitats and the planted landscape trees capability as orchid phorophytes in the developed landscapes.

MATERIALS & METHODS

Field Sampling and Samples Collection

This study was conducted at UNIMAS, Samarahan Campus (1° 28' N, 110° 25' E) from

February of 2021 to April of 2023. Convenience sampling (Speak *et al.*, 2018) was employed in a developed landscape of UNIMAS consisting of the areas surrounded by the building complexes and along the paved roads located in the main and east campus (Figure 1). The sighted orchids were photographed and their respective habitats and phorophytes (for epiphytic orchids) were documented accordingly. Samples were collected and kept as living specimens in the Orchidarium of UNIMAS.

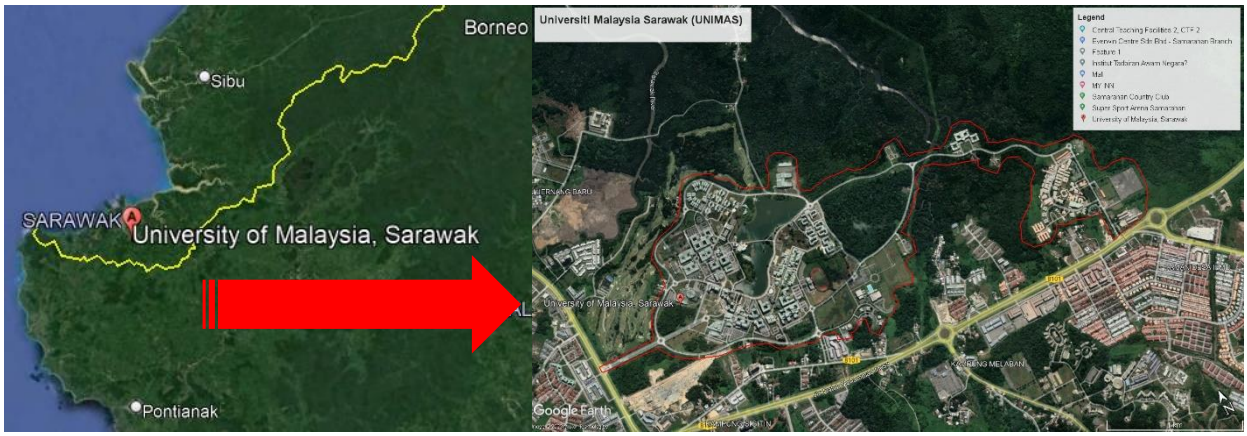

Figure 1. Location of Universiti Malaysia Sarawak (UNIMAS) indicating sampling sites (1° 27’ 34.79” N, 110° 26’ 23.39” E). Photo credit: Google Earth

Species Identification

The orchids’ taxonomic classification and distribution were determined using reliable sources such as Beaman *et al.* (2001), Wood (2014) and Plants of the World website: https://powo.science.kew.org/ (POWO, 2022). For the species that were not able to be identified up to species level (absence of flower), sp. will be denoted. Tree species that served as the phorophytes were identified based on the information provided by Boo *et al.*, (2006), Jabatan Landskap Negara (2008) and the National Parks of Singapore Flora & Fauna website : https://www.nparks.gov.sg/florafauna web/ (Nparks, 2022). The orchid's diversity was assessed *via* species richness where the number of the taxa in UNIMAS-developed campus landscapes was enumerated accordingly (Moore, 2013).

Orchids – Phorophyte Relationship

The analyses that were subjected to the individual counts were not included in this study due to the orchids' growing patterns that mostly documented growing in many clumps consisting of innumerable individuals with different growing phases and commonly found on the high point of host trees. Therefore, the relationships between epiphytic orchids and their phorophytes were analysed using the frequency of phorophytes (FP%) and orchids incidence (OI%). The analyses were adapted from Yulia and Budiharta (2011) with modifications as follows:

a. Frequency of phorophytes (FP%)

$$FP\% = \frac{\text{Number of phorophyte species (Np)}}{\text{Total number of phorophyte}} \times 100\% \quad \text{Eq.(1)}$$

b. Orchids incidences (OI%)

$$OI\% = \frac{\text{Number of incidences of epiphytic orchids (Ni)}}{\text{Total number of incidences}} \times 100\% \quad \text{Eq.(2)}$$

Subsequently, the zonation characteristics of the epiphytic orchids and the phorophyte were determined. For this investigation, a tree species with the highest incidences was chosen as the model phorophyte. The determination of the zonation of epiphytes on the host tree was adapted from Rasmussen and Rasmussen (2018) with a few modifications as follows: a) Zone I, the basal trunk (50 cm from ground), b) Zone II, the trunk (51 cm to primary branch), c) Zone III, basal part of the branch (primary branch to second branch), d) Zone IV, the middle part of the branch (second branch to third branch) and e) Zone V, the outer branch (third branch and its extension). While their respective numbers were enumerated based on the following categories: a) zero individuals b) small clump (1-10

individuals), c) medium clump (11-20 individuals) and robust clump (21 and more).

The bipartite network between phorophyte and epiphytic species was generated using RSoftware, Bipartite package (R Core Team, 2020) to create a graphical interaction between both variables (Morales-Linares *et al*., 2022). Data was tabulated in binary form according to the presence of epiphytic species on the phorophyte tree regardless of the number of orchid incidences.

RESULTS & DISCUSSION

Species Diversity in the Developed Area of UNIMAS Campus

In general, the distribution pattern of the orchids in the developed areas of UNIMAS was best described as constantly sparse and widespread in different environments. A total of 37 species from 19 genera were successfully recorded during the study (Table 1). All the genera belonged to the subfamily of Epidendroideae except *Zeuxine strateumatica* which was a member of Orchidoideae. Among the genera, *Dendrobium* displayed the highest number of species with 11 taxa followed by *Bulbophyllum* and then *Thrixspermum* while the remaining genera were represented by lesser species respectively. Although UNIMAS is a developed campus it had many to offer in terms of species diversity (Figure 2 & Figure 3) where we were able to document *Dendrobium pensile* (Figure 2e) which was later identified as a new record to Sarawak. The species diversity in the campus was also enriched by the documentation of two endemic taxa to Borneo *Dendorbium pseudostriatellum* (Figure 2f) and *Pinalia biglandulosa* (Figure 2h) that were previously localized in the peat swamp, hill forest and lower montane mossy forest habitats (Beaman *et al.*, 2001; Wood, 2014).

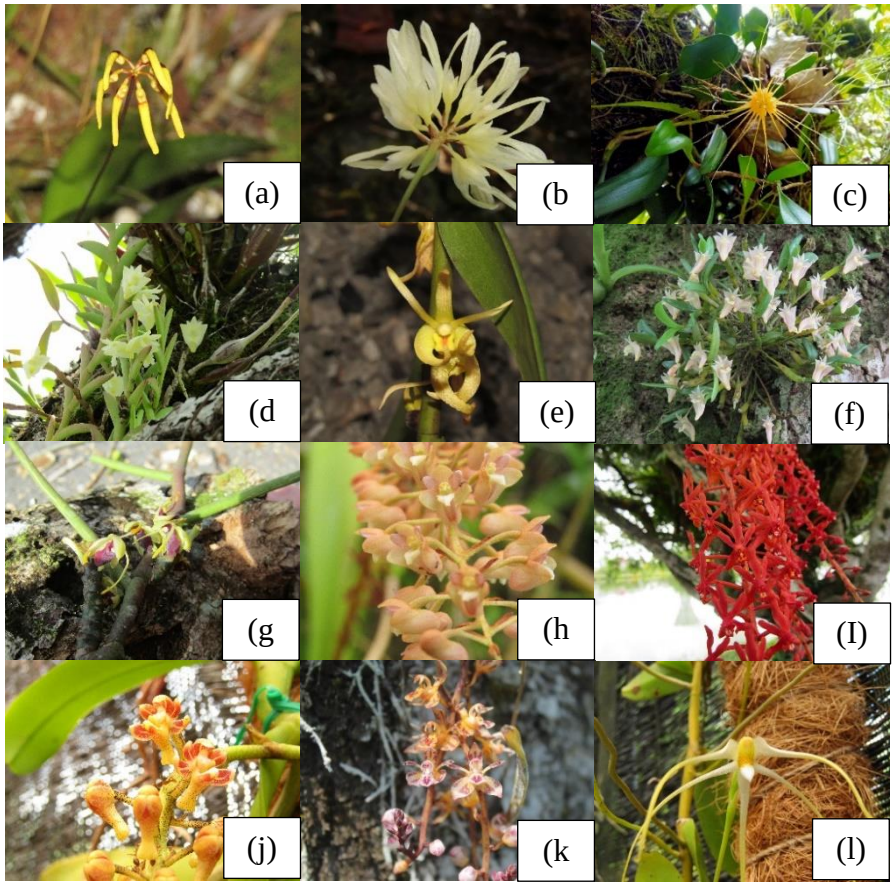

Figure 2. Selected epiphytic orchid species in UNIMAS developed campus landscape: (a) *Bulbophyllum brienianum*, (b) *Bulbophyllum purpurascens*, (c) *Bulbophyllum vaginatum*, (d) *Dendrobium kentrophyllum*, (e) *Dendrobium pensile**, (f) *Dendrobium pseudostriatellum***, (g) *Luisia antennifera*, (h) *Pinalia biglandulosa***, (i) *Renanthera elongata*, (j) *Robiquetia spathulata*, (k) *Thecostele alata* and (l) *Thrixspermum centipeda*. Photo credit: Akmal Raffi (c), Almunah A.M (a-b, d-j and l), & Haziah Musa (k)
*New record to Sarawak **Endemic to Borneo

Table 1. List of orchids species found in the developed urban landscape of UNIMAS. Note: Forest Fringes (FR), Planted Roadside Tree (PRT) and Planted Landscape Tree (PLT)

Subfamily	Genus	Species	Habitation in UNIMAS
Epidendroideae	*Acriopsis*	*Acriopsis liliifolia* (J.Koenig) Ormerod	Epiphytic on PRT & PLT
	Agrostophyllum	*Agrostophyllum* sp.	Epiphytic on PRT
	Arundina	*Arundina graminifolia* (D.Don) Hochr.	Terrestrial on FR
	Bromheadia	*Bromheadia finlaysoniana* (Lindl.) Miq.	Terrestrial on FR
	Bulbophyllum	*Bulbophyllum brienianum* (Rolfe) Merr.	Epiphytic on PLT & PRT
		Bulbophyllum cf. *grotianum*	Epiphytic on PRT
		B. medusae (Lindl.) Rchb.f.	Epiphytic on PRT
		B. purpurascens Teijsm. & Binn.	Epiphytic on PRT
		B. vaginatum (Lindl.) Rchb.f.	Epiphytic on PLT & PRT
	Cymbidium	*Cymbidium* sp.	Epiphyte on PLT & PRT
	Dendrobium	*Dendrobium convexum* Blume (Lindl.)	Epiphytic on PRT
		D. crumenatum Sw.	Epiphytic on PLT & PRT
		D. kentrophyllum Hook.f.	Epiphytic on PLT
		D. indivisum (Blume) Miq.	Epiphytic on PLT & PRT
		D. indragiriense Schltr.	Epiphytic on PLT & PRT
		D. pensile Ridl.	Epiphytic on PRT
		D. pseudostriatellum J.J.Wood & P.O'Byrne	Epiphytic on PLT & PRT
		D. rosellum Ridl.	Epiphytic on PRT
		D. secundum (Blume) Lindl. ex Wall.	Epiphytic on PRT
		D. setifolium Ridl.	Epiphytic on PLT & PRT
		Dendrobium sp. section Aporum.	Epiphytic on PRT
	Eulophia	*Eulophia graminea* Lindl.	Terrestrial on disturbed semi shaded area
	Luisia	*Luisia antennifera* Blume	Epiphytic on PRT
	Micropera	*Micropera callosa* (Blume) Garay	Epiphytic on PLT
	Oberonia	*Oberonia* sp.1	Epiphytic on PRT
		Oberonia sp.2	Epiphytic on PRT
	Oxystophyllum	*Oxystophyllum atrorubens* (Ridl.) M.A.Clem.	Epiphytic on PLT
	Pinalia	*Pinalia biglandulosa* (J.J.Sm.) Schuit., Y.P.Ng & H.A.Pedersen	Epiphytic on PLT & PRT
		P. cepifolia (Ridl.) J.J.Wood	Epiphytic on PLT & PRT
	Renanthera	*Renanthera elongata* (Blume) Lindl.	Epiphytic on PLT
	Robiquetia	*Robiquetia spathulata* (Blume) J.J.Sm.	Epiphytic on PLT & PRT
	Spathoglottis	*Spathoglottis plicata* Blume.	Terrestrial on grassy open area near drain
	Thecostele	*Thecostele alata* (Roxb.) C.S.P.Parish & Rchb.f.	Epiphytic on PRT
	Thrixspermum	*Thrixspermum amplexicaule* (Blume) Rchb.f.	Epiphytic on PLT & PRT
		T. centipeda Lour.	Epiphytic on PLT
		T. trichoglottis (Hook.f.) Kuntze	Epiphytic on PLT & PRT
Orchidoideae	*Zeuxine*	*Zeuxine strateumatica* (L.) Schltr.	Terrestrial on grassy open watery area

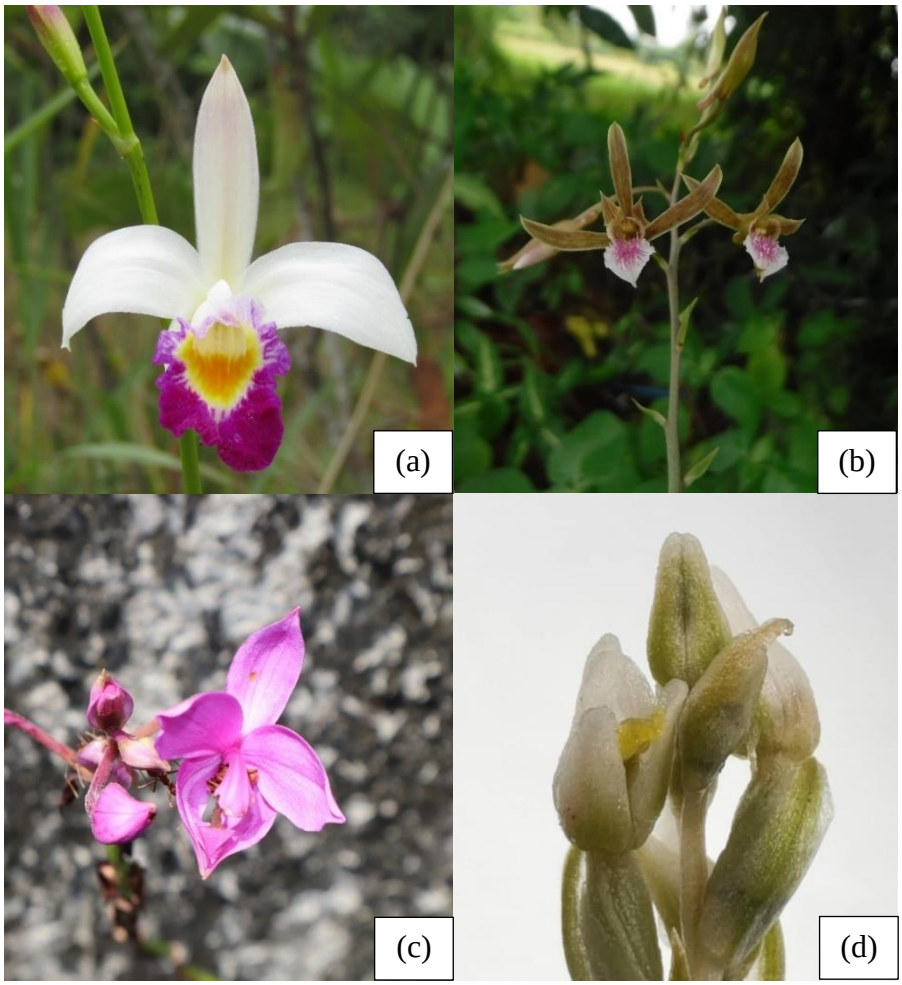

Figure 3. Selected terrestrial orchid species in UNIMAS developed campus landscape: (a) *Arundina graminifolia*, (b) *Eulophia graminea*, (c) *Spathoglottis plicata* and (d) *Zeuxine strateumatica*. Photo credit: Akmal Raffi (b & d), Almunah A.M (a) & Haziah Musa (c)

Uncharacterized Habitats for the Terrestrial Orchids in UNIMAS

Terrestrial orchids were observed to grow in the areas that were less visited by the campus community as they were not the main route for pedestrians to walk, open to semi-shaded areas, slightly wet to the water-logged ground and floored with grass. Among the terrestrial orchids, *Arundina graminifolia* and *Bromheadia finlaysoniana* were found near forest fringes, surrounded by tall grasses and layers of fern and for that, they were often to be mistakenly regarded as weeds. On the other hand, small-sized-orchid- *Zeuxine strateumatica* was found near the drain at the Faculty of Resource Science and Technology disguising itself among grasses. *Eulophia graminea* however was found in a disturbed area under a tree near the paved road meanwhile, *Spathoglottis plicata* was found in a drain with stagnant water along leaf litter and on an open area near the drain. All the terrestrial species were seen once or twice during the sampling period and could be categorized as small populations except for *Arundina gramnifolia* and *Bromheadia finlaysoniana* which could grow up to numerous individuals per population. However, maintenance activity done in the campus compound such as grass cutting and drain clearances posed a threat to these terrestrial orchids as workers were clueless about their existence and might destroy these orchids during their labour.

Epiphytic Orchids and the Phorophytic Ability of the Planted Landscape Trees in UNIMAS

The epiphytic orchids were represented by a total of 32 species and found on different planted landscape trees (Figure 4). The epiphytes displayed different propensities for host trees whereby some of them were restricted to only one phorophyte (with the lowest FP value of

0.74%) while others such as *Dendrobium crumenatum* (with the highest FP value of 31.15%) could grow up to 41 different host trees (Table 2). A higher value of FP indicated that the orchid species can be found on many different types of trees. On the other hand, the frequency for each epiphytic orchid can be depicted by the OI% where *D. crumenatum* resulted in 89.71% of incidences creating a large gap to the closest OI% of 2.73% displayed by *Pinalia biglandulosa* and the other species where the lowest percentage was 0.05%. Higher OI% indicated the species were commonly found compared to the other species with lower OI%.

In this study, more than 5000 individual trees have been observed in which they were classified to 54 tree species and about 1800 individual trees from 41 species were identified as phorophytes for orchids. Among them, *Andira inermis* (Figure 5a) which the phorophyte with the highest orchid incidences (17 orchids species) in which its zonation composition percentage was observed to be the highest in Zone IV followed by Zone III with 82.4% (14 species) and 70.6% (12 species) respectively (Figure 5b). All the orchid species were generally confined to the crown zones except four species- *Bulbophyllum medusae*, *D. crumenatum*, *D. secundum* and *P. biglandulosa* that were able to extend their occupancy to the trunk zones (Table 3). All of the epiphytic species attached to the phorophyte exist in a clump (Figure 5c) and will robustly occupied Zone III and Zone IV especially the *Bulbophyllum* group that can look like overgrown epiphytic plants and are often subjected to bark clearance by the maintenance activity by workers.

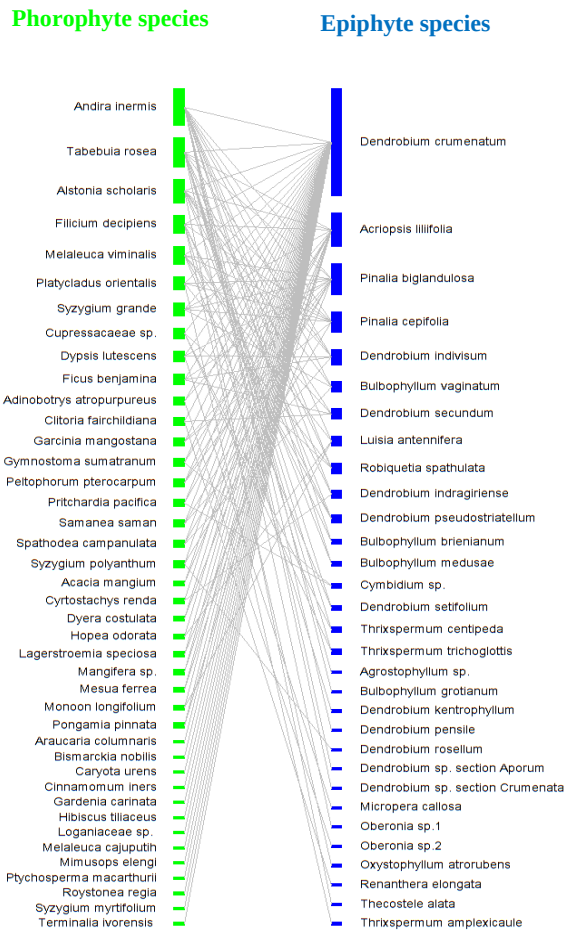

Figure 4. Bipartite Network of phorophyte and epiphytic orchid species of UNIMAS. Phorophyte species are connected by a line to their respective epiphytic orchid species that can host on the trees. The line indicates a two-way interaction between both variables with band height representing the number of connections made. Increased band height on phorophyte species means more species of orchids can be found on the tree and *vice versa*. Photo credit: RSoftware

Table 2. The epiphytic orchid species and the parametric value. Notes: Np = The number of phorophytes species of each epiphytic orchid, Ni = The number of incidences of each epiphytic orchid, FP% = The frequency percentage of phorophytes and OI% = The frequency percentage of orchid incidence.

Epiphytes in develop landscape of UNIMAS	Np	Ni	FP%	OI%
Dendrobium crumenatum Sw.	41	1840	30.15	89.71
Pinalia biglandulosa (J.J.Sm.) Schuit., Y.P.Ng & H.A.Pedersen	13	56	9.56	2.73
Acriopsis liliifolia (J.Koenig) Ormerod	13	33	9.56	1.61
Pinalia cepifolia (Ridl.) J.J.Wood	8	11	5.88	0.54
Dendrobium indivisum (Blume) Miq.	6	12	4.41	0.59
Dendrobium secundum (Blume) Lindl. ex Wall.	5	6	3.68	0.29
Robiquetia spathulata (Blume) J.J.Sm.	4	8	2.94	0.39
Luisia antennifera Blume	4	6	2.94	0.29
Bulbophyllum vaginatum (Lindl.) Rchb.f.	4	4	2.94	0.20
Dendrobium indragiriense Schltr.	3	13	2.21	0.63
Dendrobium setifolium Ridl.	3	9	2.21	0.44
Dendrobium convexum (Blume) Lindl.	3	4	2.21	0.20
Dendrobium pseudostriatellum J.J.Wood & P.O'Byrne	3	3	2.21	0.15
Thrixspermum trichoglottis (Hook.f.) Kuntze	2	10	1.47	0.49
Bulbophyllum medusae (Lindl.) Rchb.f.	2	6	1.47	0.29
Bulbophyllum brienianum (Rolfe) Merr.	2	5	1.47	0.24
Cymbidium sp.	2	4	1.47	0.20
Renanthera elongata (Blume) Lindl.	2	3	1.47	0.15
Dendrobium rosellum Ridl.	2	2	1.47	0.10
Thrixspermum amplexicaule (Blume) Rchb.f.	2	2	1.47	0.10
Bulbophyllum cf. *grotianum*	1	3	0.74	0.15
Agrostophyllum sp.	1	1	0.74	0.05
Bulbophyllum purpurascens Teijsm. & Binn.	1	1	0.74	0.05
Dendrobium kentrophyllum Hook.f.	1	1	0.74	0.05
Dendrobium pensile Ridl.	1	1	0.74	0.05
Dendrobium sp. section Aporum	1	1	0.74	0.05
Micropera callosa (Blume) Garay	1	1	0.74	0.05
Oberonia sp.1	1	1	0.74	0.05
Oberonia sp.2	1	1	0.74	0.05
Oxystophyllum atrorubens (Ridl.) M.A.Clem.	1	1	0.74	0.05
Thecostele alata (Roxb.) C.S.P.Parish & Rchb.f.	1	1	0.74	0.05
Thrixspermum centipeda Lour.	1	1	0.74	0.05

Table 3. List of orchid species on each zonation of *Andira inermis*.

Orchid species	Zone I	Zone II	Zone III	Zone IV	Zone V
Bulbophyllum brienianum (Rolfe) Merr.			+	+	
Bulbophyllum cf. *grotianum*			+	+	
Bulbophyllum medusae (Lindl.) Rchb.f.	+	+	+	+	
Bulbophyllum purpurascens Teijsm. & Binn.			+		
Bulbophyllum vaginatum (Lindl.) Rchb.f.			+	+	
Dendrobium convexum (Blume) Lindl.				+	
Dendrobium crumenatum Sw.	+	+	+	+	+
Dendrobium indivisum (Blume) Miq.				+	+
Dendrobium indragiriense Schltr.			+	+	+
Dendrobium pensile Ridl.			+		
Dendrobium rosellum Ridl.				+	+
Dendrobium secundum (Blume) Lindl. ex Wall.		+	+	+	
Dendrobium sp. section Aporum					+
Luisia antennifera Blume			+	+	
Pinalia biglandulosa (J.J.Sm.) Schuit., Y.P.Ng & H.A.Pedersen	+	+	+	+	+
Pinalia cepifolia (Ridl.) J.J.Wood			+	+	+
Robiquetia spathulata (Blume) J.J.Sm.				+	

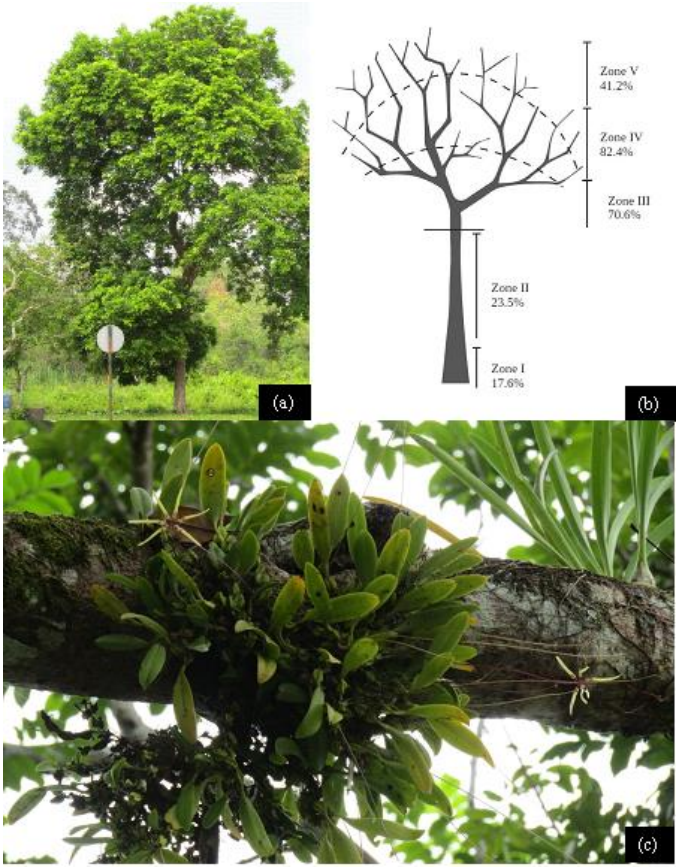

Figure 5. Selected phorophyte species for species diversity percentage per tree: (a) *Andira inermis* tree, (b) Different zonation for *Andira inermis* and the epiphytic orchid diversity percentage, (c) *Bulbophyllum brienianum* population on the branch of *Andira inermis* at zone III. Photo credit: Almunah A.M (a & c) & BioRender (b)

Orchids Diversity and the Survivability in the Built Environment of UNIMAS

The research on the diversity of orchid species among building complexes in tropical region were relatively new and limited study has been done on this topic but the attempts to introduce various species of orchids outside of their natural habitat for conservation have been a success (Izuddin *et al*., 2018, 2019a, 2019b). Figuratively, 37 species from this finding was relatively low compared with the number of orchid species in Sarawak's natural areas as such kerangas forest, limestone forest and mixed dipterocarp forest were all recorded more than 100 taxa however species in UNIMAS developed landscapes were closer to the number of orchid in peat swamp forest in Sarawak: 52 taxa but higher than mangrove forest species: less than 20 taxa (Beaman *et al*., 2001; Stephen *et al*., 2022). UNIMAS was built upon a natural lowland forest creating a unique mix of developed and natural areas where its developed areas were separated into the main campus and east campus by a natural forest in between that stretches for about a kilometre away from each area. The natural and developed areas on the campus were constantly altered such as land clearance for the development of new buildings and subjected to regular landscape maintenance, pruning, weeding and mowing. Additionally, UNIMAS in general experiences higher degree of temperature as a result of more buildings on the campus and lower rate of precipitation compared to natural tropical forests thus, all the orchid species found in this study can be categories as resilient types as they have been adapted to this environment. Their survivability can be inferred by the ecological attributes of the UNIMAS campus and the morphological characteristics of the orchids with their surroundings. Seeds from species such as *Dendrobium crumenatum, Spathoglottis plicata* and *Thrixspermum trichoglottis* were observed to be small, orchid seeds reportedly ranging from 0.1 to 6.0 mm and resulting them to be lightweight that can be produced massively inside the seed pod (Barthlott *et al*., 2014). Likewise, they would easily be dispersed by wind and can remain airborne longer and further away which could facilitate seed distribution in developed areas (Jersakova & Malinova, 2007). Where the fate of the dispersed seeds is highly dependent on the presence of needed factors for growth such as light, substrate moisture, mycorrhizal fungi, mineral nutrients and temperature on the medium they landed on (Rasmussen *et al*., 2015). The orchids on the campus most likely originated from the adjacent natural areas and the landscape transitions have allowed certain species to thrive in the altered environment. As such, all species were reported only inhabiting the natural forest of Sarawak where some of the areas were similar to that in UNIMAS except *Acriopsis liliifolia, Bromheadia finlaysoniana, Dendrobium crumenatum* and *Zeuxine strateumatica* that have been knowingly assimilating themselves in the open disturbed and developed ecosystem (Beaman *et al*., 2001; Rewicz *et al*., 2017). The occurrence of numeral orchid species in the UNIMAS campus landscape indicates that its land and planted trees were providing beneficial aid to accommodate their growth and survivability throughout the year. During the sampling period, the terrestrial species were mainly found in damp or watery and open spaces thus creating a better condition for juvenile orchids to grow. The water from the area would become a cellular source of electrons for photosynthesis to occur and the light from open space help them to boost their photosynthetic capacity especially by promoting their vegetative growth such as leaf expansion, stem extension and chloroplast development (Kami *et al.*, 2010; Bidlack & Jansky, 2017). Moreover, orchids have been reported to have lack of competitiveness and would thrive the best in area that has undergone land clearance in which there would be less struggle for orchids to uptake the nutrient that available in the area (Adamowski, 2006). Thus, reflecting the incidences of terrestrial orchids in this study that were mainly seen growing at forest fringes and roadside perimeters in which they were mainly covered with grasses or not more than three species of plants existing in the area. Apart from that, orchids are known to be associated with the presence of mycorrhizal fungi (McCormick & Jacquemyn, 2013). Therefore, the occurrence of terrestrial orchid species to some extent marked the existence of the mycorrhizae in the UNIMAS soil ecosystem. Mycorrhizal fungi were important towards orchid's seed germinations by providing exogenous 'endosperm' for nutrient supply to the seed growth until they reach photosynthetic phases (Arditti & Ghani, 2000; Jersakova & Milanova, 2007; Go & Raffi, 2017). Moreover, high number of epiphytic orchid species on the campus indicated the abundance

of mycorrhizal fungi inside the planted landscape trees of UNIMAS as trees in developed areas have been reported able to support the growth of orchid mycorrhizal fungi as well as orchids growth (Izuddin *et al*., 2018, 2019b). The seeds of epiphytic orchids would land on the tree barks of planted landscape trees of UNIMAS and get trapped within the bark crevices and can persist for years and remain viable even after experiencing different urban conditions (Izuddin *et al*., 2019b). Thus, the seed will germinate when their surrounding environments are suitable for their growth, in this case, the campus environment was proved to be favourable for the orchids to grow thus their significant incidences number throughout the campus developed landscape.

Three epiphytic species with higher FP% and OI% were observed to have larger pseudobulb namely *D. crumenatum*, *P. biglandulosa* and *A. liliifolia* in which the capability and efficiency of plants in storing water were reportedly increased with pseudobulb size (Li & Zhang, 2019) thus improving their survivability during dry season. Orchids species in the campus were likely exposed to harsher environment compared to forest as developed area were drier, hotter and windier (Chow *et al.,* 2019) therefore by having modification on their organ such as fleshy leaves, roots and stems especially in epiphytic species were helpful to accommodate their growth in the adverse climate. These modifications weren't only used to facilitate water uptake, but also nutrient absorption and storage as well as to reduce desiccation (De & Biswas, 2022). Orchids with high FP% were usually seen flowering and fruiting throughout the year and a similar phenomenon was reported in (Adamowski, 2006) where orchids in anthropogenic habitats were regularly and abundantly generating their reproductive structure. It has also been reported that a higher degree of urbanization initiates plants to advance their phenological phases such as leaf development, flowering and fruiting (Wohlfahrt *et al.,* 2019). Orchid's fertilization success in developed areas where its pollinator diversity was reduced (Wenzel *et al.,* 2019) was eased by having their pollen packed into pollinaria which helped to increase the efficacy of pollen transfer (Johnson *et al.,* 2005). This will allow orchids to produce numerous young recruits annually and able to increase their population size thus explaining why species with high FP% also have higher incidences (OI%). However, the population expansion of epiphytic species would rely more on the availability of phorophytes around the premises likewise, the campus offered more than 1800 individual trees that can support the existence of this epiphytic orchid. Among the 41 species of phorophyte that were able to host the epiphytic orchids four of them have been reported to be the phorophyte for orchids. The species were namely *Alstonia scholaris*¸ *Ficus benjamina*¸ *Tabebuia rosea* and *Samanea saman* as well as genera *Andira*, *Cinnamomum*, *Lagerstromia*, *Mangifera*, *Mesua* and *Syzygium* (Trapnell, 2006; Wood, 2014; Choden *et al.,* 2021; Rahayu & Yusri, 2022). This suggests the inclination of epiphytic orchids species in choosing certain phorophytes among other available tree species given they were occupying the same premises especially in a developed areas where the trees were planted prior and this preferable phorophyte species might have morphological characteristic such as bark rugosity, diameter, water holding and retention capacity and light penetration that can support the attachment and growth of orchids (Callaway *et al.,* 2002; Soetopo & Utami, 2020). It also opens the possibilities of planting known or suitable phorophyte will harbour more diverse epiphytic species including orchids (Sayago *et al.,* 2013). The result on species richness on phorophyte (*Andira inermis*) was profoundly on the crown strata of host tree which it was dense with the branches and twigs. This would provide an area for seed landing and population colonization as the angle between branches enables dust and leaf litter to accumulate and decompose thus supplying nutrients for the orchid to enhance their growth (Mojiol *et al.,* 2009; Izuddin *et al.,* 2018). Apart from that, the high distance of the crown from the ground would help the epiphytic orchid to reach for better light requirements as they were unable to extend their biomass to reach from the ground to the canopy (Spicer & Woods, 2022).

CONCLUSION

Overall, this study presented a total of 37 species of orchids has been found in UNIMAS and the phorophyte species for the epiphytic orchids were successfully identified. The general characteristics of the orchids to sustain their survivability in the campus area were discussed. The list of the orchid species provides an insight of the resiliency of certain species towards

habitat alteration and the epiphytic dependency on the phorophyte species to survive in campus area. Despite the rapid urbanization progress, we hope to raise awareness on orchids conservation and preservation program as it will help to curb the issues involving habitat destruction and illegal activities done towards the orchids. Furthermore, the study on urban orchids was still relatively low and more variables and parameters should be studied for orchids in their urban ecosystem to provide more information for further research.

ACKNOWLEDGEMENTS

This study was funded by the UNIMAS Small Scheme Grant (F07/SGS/2063/2021). Permission to conduct this study was granted by the Sarawak Forestry Corporation (Permit: SFC. 810-4/6/1-009 & Licence: No. 20230, No. 21652 & No. 21651). We are grateful to the following individuals: Sekudan Ak Tedong, Salim Arip, Saiffulrizan Sudirman, Nur Haziah Musa and Nur Khaleeda Ridzuan for their help during sampling period and Ivana Bilang for her help in facilitating data processing. The first author was supported by UNIMAS Zamalah Graduate Scholarship from 2023 – 2024.

REFERENCES

Adamowski, W. (2006). Expansion of native orchids in anthropogenous habitat. *Polish Botanical Studies*, 22, 35-44.

Arditti, J. & Ghani, A.K.B. (2000). Tansley Review No. 110.: Numerical and physical properties of orchid seeds and their biological implications. *New Phytologist*, 145: 367-421. DOI: 10.1046/j.1469-8137.2000.00587.x

Barthlott W., Große-Veldmann B. & Korotkova N. (2014). *Orchid seed diversity: A scanning electron microscopy survey*. Berlin: Botanic Garden and Botanical Museum Berlin-Dahlem.

Beaman, T.E., Wood, J.J., Beaman, R.S. & Beaman, J.H. (2001). *Orchids of Sarawak*. Kota Kinabalu, Malaysia: Natural History Publications (Borneo).

Bidlack, J.E. & Jansky, S.H. (2017). *Stern's introductory: Plant biology*. Fourteenth Edition. New York: McGraw-Hill. pp. 168.

Boo, C.M., Omar-Hor, H., Ou-Yang, K. & Ng, C.K. (2006). *1001 Garden Plants in Singapore.* Singapore: National Parks Board.

Callaway, R.M., Reinhart, K.O., Moore, G.W., Moore, D.J. & Pennings, S.C. (2002). Epiphyte host preferences and host traits: Mechanism for species-specific interactions. *Population Ecology*, 132: 221-230. DOI: 10.1007/s00442-002-0943-3

Choden, K., Jambay., Nepal, A., Choden & Suberi, B. (2021). Habitat ecology of epiphytic & terrestrial orchids in Langchenphu, Jomotsangkha Wildlife Sanctuary, Bhutan. *Indonesian Journal of Social and Environmental Issues*, 2(2): 143-154. DOI: 10.47540/ijsei.v2i2.256

Chow, W.T.L., Akbar, S.N.A.A, Heng, S.L. & Roth, M. (2016). Assessment of measured and perceived microclimates within a tropical urban forest. *Urban Forestry & Urban Greening*, 16: 62-75. DOI: 10.1016/j.ufug.2016.01.010

De, L.C. & Biswas, S.S. (2022). Adaptation mechanisms of epiphytic orchids: A review. *International Journal of Bio-resource and Stress Management*, 13(11): 1312-1322. DOI: 10.23910/1.2022.3115a

Go, R. & Raffi, A. (2017). *Discovering the wonders of Malaysian orchid: Unveiling Vanilla norashikiniana*. Selangor: Universiti Putra Malaysia Press.

Izuddin, M., Srivathsan, A., Lee, A.L., Yam, T.W. & Webb, E.L. (2019a). Availability of orchids mycorrhizal fungi on roadside trees in a tropical urban landscape. *Scientific Reports*, 9: 1-12. DOI: 10.1038/s41598-019-56049-y

Izuddin, M., Yam, T.W. & Webb, E.L. (2018). Specific niche requirements drive long-term survival and growth of translocated epiphytic orchids in an urbanised tropical landscape. *Urban Ecosystem*, 21: 531-540. DOI: 10.1007/s11252-018-0733-2

Izuddin, M., Yam, T.W. & Webb, E.L. (2019b). Germination niches and seed persistence of tropical epiphytic orchids in an urban

landscape. *Journal of Plant Research*, 132(3): 383-394. DOI: 10.1007/s10265-019-01110-0

Jabatan Landskap Negara (2008). *Pokok utama berbunga.* Kuala Lumpur, Malaysia: Jabatan Landskap Negara.

Jersakova, J. & Malinova, T. (2007). Spatial aspect of seed dispersal & seed recruitment in orchids. *New Phytologist*, 176: 237-241. DOI: 10.1111/j.1469-8137.2007.02223.x

Johnson, S.D., Neal, P.R. & Harder, L.D. (2005). Pollen fates and the limits on male reproductive success in an orchid population. *Biological Journal of the Linnean Society*, 86(2): 175-190. DOI: 10.1111/j.1095-8312.2005.00541.x

Kami, C., Lorrain, S., Hornitschek, P. & Frankhasuer, C. (2010). Light-regulated plant growth and development. *Current Topic in Developmental Biology*, 91: 29-66. DOI: 10.1016/S0070-2153(10)91002-8

Li, J.W. & Zhang, S.B. (2019). Physiological responses of orchid pseudobulbs to drought stress are related to their age and plant life form. *Plant Ecology*, 220: 83-96. DOI: 10.1007/s11258-018-00904-x

McCormick, M.K. & Jacquemyn, H. (2013). What constrains the distribution of orchid populations? *New Phytologist*, 202(2): 392-400. DOI: 10.1111/nph.12639

Mojiol, A.R., Jitinu, A.M.A., Adella, A., Ganang, G.M. & Nasly, N. (2009). Vascular epiphyte diversity at Pusat Sejadi, Kawang Forest Reserve, Sabah, Malaysia. *Journal of Sustainable Development*, 2(1): 121-127. DOI: 10.5539/jsd.v2n1p121

Morales-Linares, J., Carmona-Valdovinos, T.F. & Ortega-Ortiz, R.V. (2022). Habitat diversity promotes and structures orchid diversity and orchid-host tree interactions. *Flora*, 297: 1-8. DOI: 10.1016/j.flora.2022.152180

Moore, J.C. (2013). Diversity, taxonomy versus functional. In Levin, S.A. (ed.). *Encyclopedia of Biodiversity*. Second Edition. Amsterdam: Elsevier. pp. 648-656.

Nparks. (2022). *National Parks of Singapore: Flora & Fauna Web*. Retrieved August 10, 2022, from https://www.nparks.gov.sg/florafaunaweb/

POWO. (2022). *Plant of the World Online*. Retrieved May 15, 2022, from https://powo.science.kew.org/

R Core Team. (2020). *R: A Language and Environment for Statistical Computing*. R Foundation for Statistical Computing, Vienna, Austria. https://www.R-project.org/. Downloaded on 20 October 2022.

Rahayu, E.M.D. & Yusri, S. (2022). Habitat preferences of wild orchids in Bantimurung Bulusaurung National Park to model their suitable habitat in South Sulawesi. *Biodiversitas*, 23(1): 43-54. DOI: 10.13057/biodiv/d230106

Rasmussen, H.N., Dixon, K.W., Jersakova, J. & Tesitelova, T. (2015). Germination and seedling establishment in orchids: A complex of requirement. *Annals of Botany*, 116: 391-402. DOI: 10.1093/aob/mcv087

Rasmussen, H.N. & Rasmussen, F.N. (2018). The epiphytic habitat on a living host: Reflections on the orchid-tree relationship. *Botanical Journal of the Linnean Society*, 128: 456-472. DOI: 10.1093/botlinnean/box085

Rewicz, A., Bomanowska, A., Shevera, M.V., Kurowski, J.K., Krason, K. & Zielinska, K.M. (2017). Cities and disturbed areas as man-made shelters for orchid communities. *Notulae Botanicae Horti Agrobotanici Cluj-Napoca*, 45(1): 126-139. DOI: 10.15835/nbha45110519

Sayago, R., Lopezaraiza-Mikel, M., Quesada, M., Alvarez-Anorve, M.Y., Cascante-Marin, A. & Bastida, J.M. (2013). Evaluating factors that predict the structure commensalistic epiphyte-phorophyte network. *Proceeding of the Royal B Society*, 280(1756): 1-9. DOI: 10.1098/rspb.2012.2821

Soetopo, L. & Utami, A.P. (2020). Biodiversity exploration of host trees (phorophyte) of epiphyte orchids in the natural habitat. *IOP Conference Series: Earth and Environment*

Science, 449: 1-13. DOI: 10.1088/1755-1315/449/1/012029

Spicer, M.E & Woods, C.L. (2022). A case for studying biotic interaction in epiphyte ecology and evolution. *Perspective in Plant Ecology, Evolution and Systematics*, 54: 1-18. DOI: 10.1016/j.ppees.2021.125658

Speak, A., Escobedo, F.J., Russo, A. & Zerbe, S. (2018). Comparing convenience and probability sampling for urban ecology applications. *Journal of Applied Ecology*, 55(5): 2332-2342. DOI: 10.1111/1365-2664.13167

Stipkova, Z. & Kindlmann, P. (2021). Factors determining the distributions of orchids – A review with the examples from the Czech Republic. *European Journal of Environmental Sciences*, 11(1): 21-30. DOI: 10.14712/23361964.2021.3

Stephen, M., Almunah, A.M., Meekiong, K., Nordin, F.A., Razali, H., Haziah, M. & Raffi, A. (2022). Current state of knowledge on the orchids of Sarawak's peat swamps. *Sarawak Museum Journal*, LXXXV(106): 145-160. DOI: 10.61507/SMJ22-2022-9QRH-07

Trapnell, D.W. (2006). Variety of phorophytes species colonized by the neotropical epiphytes, *Laelia rubescens* (Orchidaceae). *Selbayana*, 27(1): 60-64. DOI: 10.2307/41760261

UNIMAS Institutional Repository. (2022). *Search results for orchid*. Retrieved June 20, 2022, from https://ir.unimas.my/.

Wenzel, A., Grass, I., Belavadi, V.V. & Tscharntke. T. (2019). How urbanization is driving pollinator diversity and pollination - A systematic review. *Biological Conservation*, 241: 1-15. DOI: 10.1016/j.biocon.2019.108321

Wohlfahrt, G., Tomelleri, E. & Hammerle, A. (2019). The urban imprint on plant phenology. *Nature Ecology & Evolution*, 3: 1668-1674. DOI: 10.1038/s41559-019-1017-9

Wolken, P.M., Sieg, C.H. & Williams, S.E. (2001). Quantifying suitable habitat of the threatened western prairie fringed orchid. *Journal of Range Management*, 54(5): 611-616. DOI: 10.2307/4003592

Wood, J.J. (2014). *Dendrobium of Borneo*. Kota Kinabalu, Malaysia: Natural History Publications (Borneo).

Yulia, N.D. & Budiharta, S. (2011). The diversity of epiphytic orchid and its host tree along Cemoro Sewu hiking pathway, Lawu Mountain, district of Magetan, East Java, Indonesia. *Journal of Nature Studies*, 10(2): 26-31.

Borneo Journal of Resource Science and Technology (2024), 14(1): 174-185
DOI: https:doi.org/10.33736/bjrst.5824.2024

REVIEW PAPER

Habitat Complexity Influencing Avian Community Structure, Conservation Management and its Implications in Malaysia

ABDUL MUHAIMIN BIN ABDUL HALIM[1] & NOR ATIQAH BINTI NORAZLIMI[1,2*]

[1]Department of Technology and Natural Resources, Faculty of Applied Sciences and Technology, Universiti Tun Hussein Onn Malaysia (Pagoh Campus), Pagoh Higher Education Hub, KM 1, Jalan Panchor, 84600 Muar, Johor, Malaysia; [2]Centre of Research for Sustainable Uses of Natural Resources, Universiti Tun Hussein Onn Malaysia, Johor, Malaysia
*Corresponding Author: atiqah@uthm.edu.my
Received: 5 July 2023 Accepted: 30 May 2024 Published: 30 June 2024

ABSTRACT

In this review, we explore the understanding of habitat complexity influencing the bird community with a special focus on Malaysia's recent case studies. Malaysia is one of the mega-diverse countries because it is gifted with the beauty of biodiversity. However, biodiversity resources are greatly affected by human activities such as mining operations, agricultural expansion, timber extraction, and hunting activity. In bird ecological research, habitat complexity is crucial because it affects biodiversity overall within species interactions and resource availability by evaluating environmental features including floristic composition and habitat heterogeneity. The positive relationship between habitat complexity and species diversity has been extensively documented. Complex habitats provide a variety of resources and niches, allowing different species to coexist. However, the advanced research methodologies, long-term monitoring, and a more nuanced understanding of the specific ecological processes influencing bird populations should be well emphasized. This review intends to fill in the gaps by critically analyzing potential conservation management strategies that might be adopted to increase habitat connectivity and minimize the negative effects of habitat loss on bird community structures in Malaysia.

Keywords: Bird diversity, conservation management, habitat complexity

INTRODUCTION

This paper review provided an overview of previous research on the definition of habitat complexity, the relationship between habitat complexity with species diversity and its effect on species diversity. This review next went over the analysis of 20 chosen papers from 2012 – 2022 about the habitat complexity of avian community structure in Malaysia. In addition, various topics have been covered in understanding habitat attributes used to measure habitat complexity and its impacts on bird diversity, the recent studies, gaps and future needs in the study of bird ecology as well as the potential conservation efforts and their implication to the conservation of bird populations in Malaysia.

For decades, researchers have been enthralled by various avian groups found in Malaysia, subsequently developing a profound understanding of the complex interactions between birds and their surroundings. Malaysia has the privilege to research the effect of habitat complexity in determining the distribution of bird communities as it is one of the mega-diversity countries in the world. Data from the Avibase (2022) database shows that Malaysia has 852 bird species belonging to 101 families, of which 18 are endemic species, 76 species are globally threatened and 17 are introduced species while Malaysia Nature Society (2022) issued the latest number with 814 bird species. Moreover, biodiversity resources are greatly affected by human activities such as mining operations, agricultural expansion, timber extraction, and the hunting of wild animals (Scanes, 2018, Atikah *et al.*, 2021). In Peninsular Malaysia, most pristine lowland dipterocarp forests have been exploited or harvested for timber business and development on commercial

crops and plantation areas (Atikah *et al.*, 2021). All these activities have surely reduced the diversity of the fauna to the extent that reflects the degree of habitat disturbance.

The spatiotemporal distribution of several important environmental resources influences the abundance of bird species. Moreover, the richness and diversity of bird species in terrestrial landscapes are directly correlated with habitat structure and floristic features; larger regions typically have a wider variety of habitats that different bird species can occupy (Mohd-Azlan *et al.*, 2015). Studies have demonstrated a connection between distinct bird species and various habitats. Birds are utilized as surrogates for determining the effects of habitat alteration because of their quick reaction to changing environments, which makes them ideal indicators of habitat quality, productivity, and stability (Vallecillo *et al.*, 2016). Hence, they are considered the most sensitive ecological indicators of the health of an ecosystem.

Understanding how various factors impact biodiversity is becoming more critical considering rapid ongoing global trends. It is essential to have a thorough knowledge of the relationships between habitat and fauna to manage the animal habitat, restore ecosystems, and support conservation practices (Morelli *et al*., 2013; Stirnemann *et al*., 2015). According to Stirnemann *et al.* (2015), most of the researches only focused on the correlations between the distribution and richness of species to the habitat offered by the physical structure of vegetation focusing on the quantity (e.g., cover area) rather than the complexity of habitat.

In conclusion, for successful conservation and management methods in Malaysia, it is critical to comprehend the impact of habitat complexity and variety on bird populations. Recent research has emphasized the significance of habitat variability in fostering robust bird groups and the beneficial association between habitat complexity and avian diversity (Stirnemann *et al.*, 2015). Malaysia may work to protect and restore various habitats by incorporating these findings into conservation planning, assuring the long-term survival of its outstanding bird species.

Definition of Habitat Complexity

In ecology, habitat complexity does not have a single definition of complexity - probably, there will never be one (Loke and Chisholm, 2022). Some researchers like Loke and Chisholm (2022), Carvalho and Barros (2017), Loke *et al.* (2015), Stein and Kreft (2015), Kovalenko *et al.* (2012) and Tokeshi and Arakaki (2012) have chosen their own preferred definition because of this ambiguity or have resorted to intuition. Furthermore, Kovalenko *et al*. (2012) stated that understanding how habitat complexity affects species distributions and trophic interactions is constrained by the ambiguity surrounding the terminologies used to define it, the metrics used to assess it, and the scales at which it is measured. The idea of habitat complexity indicates the coexistence of several "kinds" of elements that comprise a habitat – encompassing the presence of physical, structural and compositional features (Tokeshi and Arakaki, 2012; Loke *et al.*, 2015; Loke and Chisholm, 2022). Carvalho and Barros (2017) indicated "habitat complexity" as a measure of the absolute abundance of physical or structural components in a certain area – even in marine ecosystems. In addition, Carvalho and Barros (2017) conceptualized habitat complexity as a multidimensional measure that relates to a range of quantitative traits (such as the size, density and number of various structural elements) and qualitative traits (such as the composition or spatial arrangement of structural elements) of habitat attributes that may interact and have an impact on ecosystems at different levels. Moreover, Stein and Kreft (2015) proposed "habitat complexity" refers to vegetation including habitat structure and physical components – a multidimensional measure that incorporates a variety of factors such as landscape structure, spatial heterogeneity and resource distribution.

There are many approaches to measure or quantify the complexity of natural habitats so we can better understand how habitat complexity study was studied. Tokeshi and Araki (2012) emphasized that fractal geometry has been used to characterize habitat complexity by providing the hierarchical organization, spatial arrangement, and ecological processes occurring within the habitats. The multidimensional measure should be considered by including physical, chemical, and biological components while measuring the complexity of the habitat (Kovalenko *et al.*, 2012; Carvalho and Barros, 2017). Other than that, other methods mentioned

to quantify the habitat complexity – structural, functional, and landscape heterogeneity measurement (Stein and Kreft, 2015; Loke and Chisholm, 2022) while Loke *et al.* (2015) added feature artificial structure to enhance habitat complexity.

To conclude, habitat complexity can be defined as the existence of various components while considering the structural, physical and arrangement features (i.e., resources availability, soil type, vegetation, elevation, and climatic condition) within a habitat which can be influenced by fractal patterns to be quantified using several measures. Moreover, habitat complexity plays an important role in supporting biodiversity, the process of ecology, and conservation efforts because it can promote species richness and abundance as well as whole ecosystem health by providing more resources, niches, and microhabitats.

Relationship between Habitat Complexity and Species Diversity

The link between spatial environmental complexity and species diversity is a prominent topic in the field of ecology, evolution, and biogeography. Habitat complexity can arise from a variety of factors, such as structural heterogeneity, topographical variability, and the presence of biotic factors such as other species and their interactions. Since then, many studies have examined how environmental heterogeneity affects a wide range of taxonomic groups in many terrestrial and aquatic systems.

The habitat-heterogeneity theory, first put forth by MacArthur and MacArthur (1961), contends that a rise in the variety of habitats might result in a rise in species diversity. They explained when habitats are large enough to support various populations, then habitat variation may benefit diversity in some ways. The relationship between habitat complexity and species diversity has frequently been attributed to the surface area effect - ecosystems with greater levels of complexity typically create more favourable conditions for supporting higher species diversity (Kovalenko *et al*., 2012; St. Pierre and Kovalenko, 2014). Besides, Tokeshi & Arakaki (2012) added that a greater range of habitable area sizes might be available to species with a wider range of body sizes, hence promoting the richness of species, while Stein & Kreft (2015) suggested the idea that habitat complexity in abiotic or biotic environments expands the amount of available niche space, which permits more species to coexist. For example, greater vegetation density in a forest canopy can provide a range of microhabitats for insects, birds, and mammals, leading to greater species richness and diversity (Ghadiri *et al.*, 2012). Similarly, coral reefs with more complex structures, such as branching or tabular corals, tend to support higher biodiversity than simpler reef structures (Komyakova *et al.*, 2018).

Recent studies have also shown that habitat complexity can be influenced by the functional diversity of species in ecosystems. Functional diversity is the various ecological roles performed by different species including nutrient cycling, predation even pollination. Greater habitat complexity can enhance the diversity of functional traits in a community (Pease *et al.*, 2012; Schmera *et al.*, 2017), leading to greater functional redundancy and resilience in the face of disturbances such as climate change or habitat loss. For instance, a recent study by Coutinho *et al.* (2021) discovered that habitat complexity in the form of diverse microhabitats increased the functional diversity of bee colonies in agroecosystems. The study showed that bee species with different functional characteristics such as body size and foraging habits, were more likely to occur in agroecosystems with greater habitat complexity - which improved the functional diversity and stability of the bee community.

Even though there is a usually positive relationship between habitat complexity and species diversity, there are also some circumstances where increased complexity of habitat may not necessarily be advantageous to higher diversity. For example, in some cases as Fletcher *et al.* (2018) and Regolin *et al.* (2020), habitat fragmentation can increase the edge habitat and lead to higher habitat complexity, but this may not necessarily affect higher species diversity. Likewise, the effectiveness of habitat complexity in supporting diverse communities may be reduced by the presence of invasive species (Schirmel *et al.*, 2016) or other biotic stressors (Mayor-Pinto *et al.*, 2016; Michel *et al.*, 2016).

In conclusion, habitat complexity is

important in maintaining species diversity in ecosystems. Greater habitat complexity provides a wider range of resources and niches for organisms, which can increase species richness, functional diversity, and resilience to disturbances. Recent studies have shown that habitat complexity can also influence the functional diversity of communities (Pease *et al.*, 2012; Schmera *et al.*, 2017; Countiho *et al.*, 2021), highlighting the importance of preserving and restoring complex habitats to maintain biodiversity in the face of global environmental change.

Effect of Habitat Complexity on Species Diversity

A major factor in the loss of biodiversity worldwide is habitat destruction. Given the correlation between habitat complexity and biological richness, destruction involving structural simplification usually accounts for a significant portion of this loss. Numerous studies that evaluate the complexity of habitats only concentrate on the existence or absence of complex structures or a particular part of the complexity, most frequently the density of structural parts (St. Pierre & Kovalenko, 2014; Stirnemann *et al*., 2015). They added even though the mechanisms underlying this benefit are not fully understood, possible explanations include increased niches because of increased microhabitat availability, higher productivity, and a sampling effect linked to a larger surface area needs to be emphasized. Thus, Hanz *et al.* (2019) stated a study of the morphological diversity of species groups concluded that in more complex habitats, both group niche area and individual species niche constriction increase, which agrees with the bigger niche space hypothesis.

The environment contains a greater variety of habitats and microhabitats often lead to habitat complexity. Higher species diversity is the outcome of the variety of habitats because they produce niches and resources that may be used by various species for shelter, food resources or even nesting sites. For instance, the complexity of the habitat in a forest ecosystem can be reflected in the diversity of tree species, tree diameters, canopy cover, understory vegetation, fallen logs, and standing dead trees. Research by Regnery *et al.* (2013) focused on tree microhabitats in the forest and showed tree cavities and cracks on a tree can support important microhabitats for cavity-nesting bird and bat species. Paillet *et al.* (2018) commended that tree cavities found in forest can be important for cavity-nesting birds and bats while cracks and loose barks were particularly relevant for saproxylic beetles. This structural variety allows various species to fill distinct niches within the microhabitats in the forest, supporting a greater variety of species. Besides, abundant resources allow more species to live within the same macrohabitat. When the heterogeneity of habitat occurs, it can provide more different resources to occupy different species so it can reduce competition and promote species diversity too. For example, in a coral reef environment, different species of coral-associated fishes can be found inhabiting different coral species. Wehrberger and Herler (2014) concluded that corals reef can be settled with different types of coral species with a variety of structural complexity such as body size or crevices size that may be occupied by different species of fish based on their body sizes; compared to fish living in less complex reef corals, those linked with more complex microhabitats had distinct body morphologies of fishes.

However, it is believed that the presence of habitat complexity does not promise high species diversity in an area due to other environmental factors such as global warming and anthropogenic disturbance which causing habitat loss, especially the fragile microhabitats. Coral reefs are an example of a complex environment that may be extremely sensitive and fragile to many anthropogenic influences. For instance, coral bleaching episodes brought on by climate change may result in coral cover loss and a consequent drop in reef complexity (Graham, 2014; Pratchett *et al.*, 2018). Fish that depend on coral for refuge and feeding is frequently affected by coral bleaching due to the loss of structural complexity and habitat availability. Reduced fish numbers and variations in species richness can result from the loss of preferred habitats, with certain specialised fish species that depend on coral being particularly vulnerable (Graham, 2014; Pratchett *et al.*, 2018). While Novoa *et al.* (2021) stated structurally temperate forest habitat served partitioning niches to cater different types of birds with specific refuge, foraging and nesting needs can be destroyed by fire disturbance that naturally occurred by lightning and all the others were unintended

ignition by humans. They added after the fire episodes, the vegetation height and plant species abundance deteriorated respectively leading to a decline in overall bird diversity. Besides, environmental factors such as elevation cannot ensure the presence of habitat complexity supports high species diversity. As elevation increases, the habitat becomes less complex – foliage height and vegetation patches decreased can lead to the decline of bird diversity since fewer niches and food source availability as elevation is getting higher (Sam *et al.*, 2019).

MATERIALS AND METHODS

In this review article, the available literature by topic was searched using the Google Scholar databases from 2012 to 2022 and Preferred Reporting Items for Systematic Reviews (PRISMA) was performed to identify publications studying habitat complexity influencing bird community structure in Malaysia. We limited our search to peer-reviewed, articles in English, excluded reviews and grey literature (e.g., theses, technical reports, institutional dossiers) and used the combination of keywords to examine (i) correlations between habitat complexity, bird diversity and its conservation implications and (ii) habitat attributes used to measure habitat complexity that influencing bird community structure. The following keyword combinations were used for the search: "habitat complexity" AND "conservation" AND "bird diversity". An initial search resulted in 822 articles, which were limited to 20 articles after filtering with additional keywords such as “Malaysia” and “point counts”. Then the 20 chosen articles have been analyzed using Critical Thinking method to point out the main findings, sampling area, methods used, strengths and limitations of the studies into table (refer Supplementary Material: Table S1).

Habitat Complexity on Avian Community Structure in Malaysia

Measuring Habitat Complexity and its Impacts on Avian Community Structure

Successful conservation and management strategies depend on having a thorough understanding of the intricate interactions that exist between birds and their habitat. Because it affects the availability of resources, interactions between species, and biodiversity, habitat complexity is crucial in influencing the composition of bird groups. We shall examine the ideas of habitat complexity and its significance in studies of avian ecology. With the use of information collected from several studies carried out in Malaysia (refer to Supplementary Material, Table S1), different habitat characteristics are used to gauge habitat complexity. The subject matter will be supported by the cited publications, which offer insightful illustrations and proof.

Habitat attribute is defined as any living or non-living feature of the environment such as vegetation types, availability of food sources, temperature, moisture levels and shelter that provides resources necessary for a species in a particular habitat. Researchers have developed several variables to measure habitat complexity and evaluate its impacts on bird community structure. The floristic structure is one of the essential characteristics used to determine habitat complexity. In a selectively logged hill dipterocarp forest, Atikah *et al*. (2021) investigated the impact of vegetation structure on bird biodiversity. They found a significant correlation between bird species richness and abundance with habitat complexity, as measured by variables such as canopy cover, tree density, tree height and understory density. For instance, certain bird species may favour areas with dense undergrowth for nesting, while others may thrive in open canopy spaces for aerial foraging. In addition, microclimate factors are another characteristic to measure habitat complexity. For example, Rajpar and Zakaria (2015) delved into the relationship between bird populations and microclimate conditions such as temperature, humidity and wind patterns in shrub and open area in Selangor, Malaysia. Additionally, specific habitat variables, including the availability of perching sites, nesting materials, and foraging opportunities, play a pivotal role in shaping bird communities through their study. They suggested the diversity of birds can be positively impacted by adding bird-friendly elements to open spaces, such as creating artificial perching spots or keeping a range of plant species in shrub environments. Besides, Shafie *et al.* (2022) found different feeding guilds provide valuable insights into the trophic dynamics of the ecosystem, indicating the availability and diversity of food resources within the habitat. Differences in tree density,

canopy cover, understory vegetation, elevation gradients, the presence of microhabitats such as fallen logs, seasonal variability and biotic interactions could influence the diversity and abundance of bird species (Shafie *et al.*, 2022). Thus, a more complex habitat structure can provide a greater variety of niches, supporting a diverse community of birds with distinct habitat preferences.

Maintaining different bird populations and fostering environmental stability depends on habitat complexity. A habitat's inclusion of different structural components and vegetation offers birds a variety of resources, such as nesting spaces, feeding opportunities, and protection from predators. Atiqah *et al.* (2019) shed light on the intricate interplay between birds and tree species within oil palm agroforestry landscapes. They indicated the presence of different tree species provides a range of resources such as fruits, insects, and nesting sites, catering to the diverse dietary and nesting preferences of various bird species. Moreover, the vertical and horizontal heterogeneity in tree structures, including tall emergent trees, mid-story canopy layers, and a well-developed understory, offers birds a diverse array of perching, nesting, and foraging options (Atiqah *et al.*, 2019). Hence, conservation strategies that prioritize maintaining a rich diversity of tree species and structures within oil palm agroforestry landscapes can thus contribute significantly to bird conservation. As well, Razak *et al.* (2020) also showed that smallholdings with high oil palm productivity fostered significant avian species diversity and various feeding habits, demonstrating the beneficial association between habitat complexity and bird populations. High oil palm yield may indicate favourable conditions, such as adequate vegetation structure, sufficient food resources, and a relatively stable environment (Razak *et al.*, 2020). Next, Azhar *et al*. (2014) revealed that monoculture practices, characterized by the cultivation of a single crop of oil palm, can have distinct impacts on bird communities compared to polyculture practices involving the cultivation of multiple crops like bananas, coconuts, tapiocas, corns and sugar canes. Monoculture landscapes may limit the availability of diverse resources for birds, leading to a decrease in species richness. They added that polyculture practices, on the other hand, offer a more heterogeneous environment, providing a broader spectrum of resources crucial for supporting a diverse bird community. Integrating such findings into agricultural practices can help strike a balance between human needs and the preservation of avian biodiversity (Azhar *et al.*, 2014).

Numerous studies conducted in Malaysia have emphasised the beneficial effects of habitat complexity and variety on the composition of bird communities. Atikah *et al.* (2021) found that enhanced vegetation structure in hill dipterocarp forests with selective logging had a favourable impact on bird biodiversity. Furthermore, Shafie *et al.* (2022) noted that changes in habitat complexity in Terengganu's lowland dipterocarp woods resulted in variances in bird species distribution and abundance. Moreover, research has shown how critical habitat complexity is in supplying nutrients to bird populations. According to Razak *et al.* (2020), increased habitat diversity in agricultural settings can provide birds with better foraging possibilities by supporting a vast range of bird species and varied dietary guilds. Although there are typically favourable benefits of habitat complexity and variability in bird community composition in Malaysia, there are also adverse consequences related to ecosystem destruction and fragmentation. The destruction of habitat, which is a result of anthropogenic practices like deforestation and agricultural activities, is harmful to bird groups. Ismail *et al*. (2012) found less variety in the avifauna in the man-made Putrajaya wetlands, which are flanked by urban and farming areas. Similarly, Azman *et al.* (2019) showed that although supporting bird diversity, paddy fields in Peninsular Malaysia had fewer species than undisturbed native habitats. Birds' access to adequate nesting locations, food supplies, and secure shelter is limited by habitat degradation and dissipation which harms species diversity and population levels. Furthermore, modifications in the complexity of the ecosystem might affect bird populations by changing the microclimate. Rajpar and Zakaria (2015) showed that open-area and shrub areas exhibited distinctive microclimate features, affecting bird numbers and species diversity. Bird numbers, nesting success, and the capacity to locate food and shelter are all impacted by changes in daily temperature, humidity, and plant structure brought on by habitat changes. These results underline how crucial it is to preserve habitat complexity and reduce habitat

loss to guarantee the long-term survival of bird groups in Malaysia.

To sum up, habitat complexity demonstrated a vital role in shaping bird community structures. Various habitat attributes such as floristic structure, microclimate conditions, and specific habitat variables significantly influence bird species richness, abundance, and distribution since they can provide essential resources for nesting, feeding, and protection within the habitat. conservation initiatives should concentrate on protecting and rebuilding habitats with various structures and compositions to lessen the detrimental impacts of habitat loss and fragmentation on bird populations. To preserve robust and healthy bird populations in Malaysia, it is vital to promote habitat connectivity, safeguard crucial areas for avian biodiversity, and apply sustainable land utilization practices.

Recent Studies, Gaps, and needs on Avian Ecology in Malaysia

The bird population in Malaysia is remarkably diverse and is important to ecological research. The composition, number, and ecological roles of bird populations have been extensively studied in a variety of ecosystems in Malaysia. These findings highlight how crucial it is to preserve and comprehend bird groups to manage and conserve the environment. The selected 20 papers from 2012 to 2022 showed a variety of studies on bird ecology that focused on habitat complexity. Table S1 shows the ideas of critical thinking within the chosen papers.

It has been discovered that differences in vegetation systems have a major influence on the diversity and composition of bird communities (Amir *et al.*, 2015; Atikah *et al*., 2021). They highlighted the need for an understanding of avian responses to diverse environments considering not only land use but also specific structural elements within habitats. The link between bird richness and climatic attributes (temperature, humidity and wind patterns) and habitat factors (perching sites, nesting materials and foraging opportunities) has also been investigated, indicating the various impacts that various environments have on avian community structure (Rajpar & Zakaria, 2015).

But some research gaps must be studied. For instance, further research is needed to comprehend the impact of habitat complexity in altered landscapes like agricultural ecosystems (Kadir *et al.*, 2021; Atiqah *et al.*, 2019; Azhar *et al.*, 2024). Furthermore, little is known about how populations of nocturnal bird species react to habitat complexity (Yahya *et al.*, 2020). Further research is required to fully understand how habitat complexity affects bird populations specifically in fragile microhabitats like mangrove environments (Amir *et al*., 2015; Mohd-Azlan *et al.*, 2015).

Understanding the spatial dynamics of bird populations is crucial for effective habitat management and conservation, especially in landscapes undergoing rapid changes. Future studies could focus on incorporating more precise environmental variables, considering seasonal fluctuations and microclimatic conditions that may influence bird behaviour, breeding success and overall population dynamics by employing advanced modelling techniques and monitoring technologies to improve, predict and mitigate an effective conservation management strategy for bird populations (Rajpar and Zakaria, 2015; Martins *et al.*, 2021).

In summary, studies in the future should concentrate on longer observations to determine conservation measures and investigate spatio-temporal dynamics to narrow these gaps. The effect of habitat complexity on bird community structure across various habitats and land-use types must also be fully understood by requiring a multi-faceted approach, including advanced research methodologies, long-term monitoring, and a more nuanced understanding of the specific ecological processes influencing bird populations. Addressing these gaps will not only contribute to academic knowledge but will also enhance the effectiveness of conservation initiatives, ensuring the sustained health of avian communities in the face of environmental changes and anthropogenic pressures.

Prospective Conservation Management and its Conservation Implications

Future strategies that take habitat complexity and varieties into account are required for the conservation control of bird populations in Malaysia. By promoting a mix of local plant species, adopting varied crop structures and polyculture approaches to agricultural

landscapes can mimic natural habitats and then provide more suitable homes for avian species such as granivorous, fructivorous and insectivorous species (Azhar *et al.*, 2014; Atiqah *et al.*, 2019). Next, technology improvements provide conservationists with useful tools. Important information on habitat features, shifts in the landscape, and species dispersion may be obtained via remote sensing, GIS, and satellite imaging (Amir *et al.*, 2015; Atikah *et al.*, 2021; Martins *et al.*, 2021). Besides, Martins *et al.* (2021) and Azhar *et al.* (2014) added that sophisticated statistical techniques and occupancy modelling enhance and provide a robust framework for assessing habitat preferences, population trends, and the impact of environmental variables on bird species also aiding in evidence-based conservation decision-making. Moreover, conservation players or shareholders may acquire accurate knowledge of habitat complexity and prioritize conservation actions by fusing these technologies with field studies. Additionally, community involvement and citizen science programmes or online open crowd-source communities such as eBird, Inaturalist and BirdNet are essential for bird conservation (Puan *et al.*, 2019; Razak *et al.*, 2020). Other than that, the feeling of ownership and mutual accountability for habitat rehabilitation initiatives is fostered by engaging local people in bird population observation and monitoring as well as awareness-raising through educational programmes (Ismail *et al.*, 2012).

Marini *et al.* (2019) underlined the concept of species-habitat networks that emphasizes the interconnectedness of complexity of habitats with bird diversity and highlighted the need for a holistic approach to landscape management. They suggested establishing and preserving ecological corridors that link habitats that can facilitate the movement of bird species so it can enhance genetic diversity, reduces fragmentation, and provide birds with access to various resources throughout their life cycles. While Fraixedas *et al.* (2020) asked to strengthen a comprehensive bird monitoring program among scientists, conservationists, and citizen scientists to track bird populations, identify trends, and assess the impact of habitat management strategies because the continuous monitoring allows for adaptive conservation practices that respond to changing conditions and emerging threats.

In conclusion, ecological connection conservation, technology improvements, and local involvement are crucial for the management of bird conservation in Malaysia. Malaysia may increase habitat complexity and variability, eventually protecting its bird species, by embracing polyculture cropping, recovering ecological corridors, using technology for surveillance and empirical studies, and involving local people. By putting these strategies into practice, Malaysia may increase habitat variability and complexity, both of which have a favourable impact on the structure of bird communities and promote the long-term preservation of its avian biodiversity.

CONCLUSION

The complexity of the habitat is important in avian ecology study because it influences resource availability and interactions among species as well as biodiversity as a whole. By analyzing environmental characteristics like floristic composition and habitat heterogeneity, researchers may learn more about the interactions between birds and their surroundings. Future studies should focus on longer-term observations of the impact of habitat complexity on bird community structure across a range of habitats and land-use types to identify conservation priorities and fill in knowledge gaps. Moreover, a study into the functional relationships between bird species and their habitats, as well as the application of research findings in conservation contexts, will lead to an improvement in conservation and management techniques. Adopting sustainable land management practices, restoring ecological connectedness, utilizing technology improvements in monitoring and research, and encouraging citizen science and community involvement are potential strategies for managing bird conservation in Malaysia. Malaysia can work towards successful habitat management and the preservation of its abundant bird species by putting these future strategies into practice.

ACKNOWLEDGMENTS

This research was supported by Universiti Tun Hussein Onn Malaysia through Tier 1 Grant Research (Q509) and Postgraduates Research Grant (GPPS) (Vot Q237). Therefore, we would like to dedicate our gratitude to all parties

involved either directly or indirectly in making this paper a success.

REFERENCES

Amir, A., Hafidzi, M.N. & Ariffin, H.K. (2015). Diversity and density of birds at mangroves and oil palm plantations in two different regions in Selangor, Malaysia. *ARPN Journal of Agricultural and Biological Science*, *10*(11): 407-416.

Atikah, S.N., Yahya, M.S., Norhisham, A.R., Kamarudin, N., Sanusi, R. & Azhar, B. (2021). Effects of vegetation structure on avian biodiversity in a selectively logged hill dipterocarp forest. *Global Ecology and Conservation*, 28: e01660. DOI: 10.1016/j.gecco.2021.e01660.

Atiqah, N., Yahya, M.S., Aisyah, S., Ashton-Butt, A. & Azhar, B. (2019). Birds associated with different tree species and structures in oil palm agroforestry landscapes in Malaysia. *Emu-Austral Ornithology*, 119(4): 397-401. DOI: 10.1080/01584197.2019.1621680.

Avibase (2022). Checklist of birds of Malaysia. Bird Checklists of the World.Avibase. Available from https://avibase.bsc-eoc.org/checklist.jsp?region=MY

Azhar, B., Puan, C.L., Zakaria, M., Hassan, N. & Arif, M. (2014). Effects of monoculture and polyculture practices in oil palm smallholdings on tropical farmland birds. *Basic and Applied Ecology*, 15(4): 336-346. DOI: 10.1016/j.baae.2014.06.001.

Azman, N.M., Sah, S.A.M., Ahmad, A. & Rosely, N.F. (2019). Contribution of rice fields to bird diversity in Peninsular Malaysia. *Sains Malaysiana*, 48(9): 1811-1821. DOI: 10.17576/jsm-2019-4809-02.

Carvalho, L.R.S. & Barros, F. (2017). Physical habitat structure in marine ecosystems: the meaning of complexity and heterogeneity. *Hydrobiologia*, 797: 1-9. DOI: 10.1007/s10750-017-3160-0.

Coutinho, J.G., Hipólito, J., Santos, R.L., Moreira, E.F., Boscolo, D. & Viana, B.F. (2021). Landscape structure is a major driver of bee functional diversity in crops. *Frontiers in Ecology and Evolution*, 9: 624835. DOI: 10.3389/fevo.2021.624835.

Fletcher, R.J., Didham, R.K., Banks-Leite, C., Barlow, J., Ewers, R.M., Rosindell, J., Holt, R.D., Gonzalez, A., Pardini, R., Damschen, E. I., Melo, F.P.L., Ries, L., Prevedello, J.A., Tscharntke, T., Laurance, W. F., Lovejoy, T.E. & Haddad, N.M. (2018). Is habitat fragmentation good for biodiversity? *Biological Conservation*, 226: 9–15. DOI: 10.1016/j.biocon.2018.07.022.

Fraixedas, S., Lindén, A., Piha, M., Cabeza, M., Gregory, R. & Lehikoinen, A. (2020). A state-of-the-art review on birds as indicators of biodiversity: Advances, challenges, and future directions. *Ecological Indicators*, 118: 106728. DOI: 10.1016/j.ecolind.2020.106728.

Ghadiri Khanaposhtani, M., Kaboli, M., Karami, M. & Etemad, V. (2012). Effect of habitat complexity on richness, abundance and distributional pattern of forest birds. Environmental management, 50, 296-303. https://doi.org/10.1007/s00267-012-9877-7.

Graham, N.A. (2014). Habitat complexity: Coral structural loss leads to fisheries declines. *Current Biology*, 24(9): R359-R361. DOI: 10.1016/j.cub.2014.03.069.

Hanz, D.M., Böhning-Gaese, K., Ferger, S.W., Fritz, S.A., Neuschulz, E.L., Quitián, M., Santillán, V., Töpfer, T. & Schleuning, M. (2018). Functional and phylogenetic diversity of bird assemblages are filtered by different biotic factors on tropical mountains. *Journal of Biogeography*, 46(2): 291–303. DOI: 10.1111/jbi.13489.

Ismail, A., Rahman, F. & Zulkifli, S.Z. (2012). Status, composition, and diversity of avifauna in the artificial Putrajaya wetlands and comparison with its two neighboring habitats. *Tropical Natural History*, 12(2): 137-145.

Kadir, R.A., Mohammad, M.I. & Zulkifli, S.Z. (2021). Impact of Forest Fragment on Bird Community at the Bukit Kuantan Rubber Forest Plantation. *EDP Sciences*, 305: 05004. DOI: 10.1051/e3sconf/202130505004.

Komyakova, V., Jones, G.P. & Munday, P.L. (2018). Strong effects of coral species on the

diversity and structure of reef fish communities: A multi-scale analysis. *PloS one*, 13(8): e0202206. DOI: 10.1007/s10750-011-0974-z.

Kovalenko, K.E., Thomaz, S.M. & Warfe, D.M. (2012). Habitat complexity: approaches and future directions. *Hydrobiologia*, 685(1): 1-17. DOI: 10.1371/journal.pone.0202206.

Lee, W., Sompud, J., Pei, K.J., Sudin, M., Goh, C., Liau, P., Yahya, F. & Abdullah, A.J.S. (2018). Avifauna community in timber production area in Segaliud-Lokan Forest Reserve, Sabah. *Transactions on Science and Technology*, 5(2): 137–142

Loke, L.H. & Chisholm, R.A. (2022). Measuring habitat complexity and spatial heterogeneity in ecology. *Ecology Letters*, 25(10): 2269–2288. DOI: 10.1111/ele.14084.

Loke, L.H., Ladle, R.J., Bouma, T.J. & Todd, P.A. (2015). Creating complex habitats for restoration and reconciliation. *Ecological Engineering*, 77: 307-313. DOI: 10.1016/j.ecoleng.2015.01.037.

MacArthur, R.H., & MacArthur, J.W. (1961). On bird species diversity. *Ecology*, 42(3): 594-598. DOI: 10.2307/1932254

Marini, L., Bartomeus, I., Rader, R. & Lami, F. (2019). Species–habitat networks: A tool to improve landscape management for conservation. *Journal of Applied Ecology*, 56(4): 923-928. DOI: 10.1111/1365-2664.13337.

Martins, C.O., Olaniyi, O.E. & Zakaria, M. (2021). Ecological factors and spatial heterogeneity of Terrestrial Birds in Peninsular Malaysia. In *IOP Conference Series: Earth and Environmental Science*, 736(1): 012035. IOP Publishing. DOI: 10.1088/1755-1315/736/1/012035.

Martins, C.O., Olaniyi, O.E. & Zakaria, M. (2021). Environmental Factors and Spatial Heterogeneity Affect Occupancy Estimates of Waterbirds in Peninsular Malaysia. *Ornithological Science*, 20(1): 39-55. DOI: 10.2326/osj.20.39.

Mayer-Pinto, M., Matias, M. G. & Coleman, R. A. (2016). The interplay between habitat structure and chemical contaminants on biotic responses of benthic organisms. *PeerJ*, 4: e1985. DOI: 10.7287/PEERJ.PREPRINTS.1783.

Michel, V.T., Jiménez-Franco, M.V., Naef-Daenzer, B. & Grüebler, M.U. (2016). Intraguild predator drives forest edge avoidance of a mesopredator. *Ecosphere*, 7(3): e01229. DOI: 10.1002/ecs2.1229.

Mohd-Azlan, J., Noske, R.A. & Lawes, M.J. (2015). The role of habitat heterogeneity in structuring mangrove bird assemblages. *Diversity*, 7(2): 118-136. DOI: 10.3390/d7020118.

Morelli, F., Pruscini, F., Santolini, R., Perna, P., Benedetti, Y. & Sisti, D. (2013). Landscape heterogeneity metrics as indicators of bird diversity: determining the optimal spatial scales in different landscapes. *Ecological indicators*, 34: 372-379. DOI: 10.1016/j.ecolind.2018.03.011.

Novoa, F.J., Altamirano, T.A., Bonacic, C., Martin, K. & Ibarra, J.T. (2021). Fire regimes shape biodiversity: responses of avian guilds to burned forests in Andean temperate ecosystems of southern Chile. *Avian Conservation & Ecology*, 16(2): 22. DOI: 10.5751/ACE-01999-160222.

Paillet, Y., Archaux, F., Du Puy, S., Bouget, C., Boulanger, V., Debaive, N., ... & Guilbert, E. (2018). The indicator side of tree microhabitats: A multi-taxon approach based on bats, birds, and saproxylic beetles. *Journal of Applied Ecology*, 55(5): 2147-2159. DOI: 10.1111/1365-2664.13181.

Pease, A.A., González-Díaz, A.A., Rodiles-Hernández, R.O.C.I.O. & Winemiller, K.O. (2012). Functional diversity and trait–environment relationships of stream fish assemblages in a large tropical catchment. *Freshwater Biology*, 57(5): 1060-1075. DOI: 10.1111/j.1365-2427.2012.02768.x.

Pratchett, M.S., Thompson, C.A., Hoey, A.S., Cowman, P.F. & Wilson, S.K. (2018). Effects of coral bleaching and coral loss on the structure and function of reef fish assemblages. Coral bleaching: *Patterns, processes, causes and consequences*, 265-293. DOI: 10.1007/978-3-319-75393-5_11.

Puan, C.L., Yeong, K.L., Ong, K.W., Fauzi, M.I.A., Yahya, M.S. & Khoo, S.S. (2019). Influence of landscape matrix on urban bird abundance: evidence from Malaysian citizen science data. *Journal of Asia-Pacific Biodiversity*, 12(3): 369-375. DOI: 10.1016/j.japb.2019.03.008.

Rajpar, M.N. & Zakaria, M. (2014). Effects of habitat characteristics on waterbird distribution and richness in wetland ecosystem of Malaysia. *Journal of Wildlife and Parks*, 28: 105-120.

Rajpar, M.N. & Zakaria, M. (2015). Bird abundance and its relationship with microclimate and habitat variables in open-area and shrub habitats in Selangor, Peninsular Malaysia. JAPS: *Journal of Animal & Plant Sciences*, 25(1).

Razak, S.A., Saadun, N., Azhar, B. & Lindenmayer, D.B. (2020). Smallholdings with high oil palm yield also support high bird species richness and diverse feeding guilds. *Environmental Research Letters*, 15(9): 094031. DOI: 10.1088/1748-9326/aba2a5.

Regnery, B., Couvet, D., Kubarek, L., Julien, J.F. & Kerbiriou, C. (2013). Tree microhabitats as indicators of bird and bat communities in Mediterranean forests. *Ecological Indicators*, 34: 221-230. DOI: 10.1016/j.ecolind.2013.05.003.

Regolin, A.L., Muylaert, R.L., Crestani, A.C., Dáttilo, W. & Ribeiro, M.C. (2020). Seed dispersal by Neotropical bats in human-disturbed landscapes. *Wildlife Research*, 48(1): 1-6. DOI: 10.1071/WR19138.

Sam, K., Koane, B., Bardos, D.C., Jeppy, S. & Novotny, V. (2019). Species richness of birds along a complete rain forest elevational gradient in the tropics: Habitat complexity and food resources matter. *Journal of Biogeography*, 46(2): 279-290. DOI: 10.1111/jbi.13482.

Scanes, C.G. (2018). Human activity and habitat loss: destruction, fragmentation, and degradation. In *Animals and human society*, 451-482. Academic Press. DOI: 10.1016/B978-0-12-805247-1.00026-5.

Schirmel, J., Bundschuh, M., Entling, M.H., Kowarik, I. & Buchholz, S. (2016). Impacts of invasive plants on resident animals across ecosystems, taxa, and feeding types: a global assessment. *Global Change Biology*, 22(2): 594-603. DOI: 10.1111/gcb.13093.

Schmera, D., Heino, J., Podani, J., Erős, T. & Dolédec, S. (2017). Functional diversity: a review of methodology and current knowledge in freshwater macroinvertebrate research. *Hydrobiologia*, 787: 27-44. DOI: 10.1007/s10750-016-2974-5.

Shafie, N.J., Anuar, H., David, G., Ahmad, A. & Abdullah, M.T. (2022). Bird species composition, density, and feeding guilds in contrasting lowland dipterocarp forests of Terengganu, Peninsular Malaysia. *Tropical Ecology*, 1-11. DOI: 10.1007/s42965-022-00267-5.

Sompud, J., Kee, S.L., Sompud, C.B., Emily, A. G. & Igau, O.A. (2016). The correlations between bird relative abundance with the stem density in two years old *Acacia mangium* plantation at Sabah Forest Industries, Sipitang. *Transactions on Science and Technology*, 3(1-2): 136-142.

Stein, A. & Kreft, H. (2015). Terminology and quantification of environmental heterogeneity in species-richness research. *Biological Reviews*, 90(3): 815-836. DOI: 10.1111/brv.12135.

Stirnemann, I.A., Ikin, K., Gibbons, P., Blanchard, W. & Lindenmayer, D.B. (2015). Measuring habitat heterogeneity reveals new insights into bird community composition. *Oecologia*, 177(3): 733-746. DOI: 10.1007/s00442-014-3134-0.

St. Pierre, J.I., & Kovalenko, K.E. (2014). Effect of habitat complexity attributes on species richness. *Ecosphere*, 5(2): 1-10. DOI: 10.1890/ES13-00323.1

Styring, A.R., Ragai, R., Zakaria, M. & Sheldon, F.H. (2016). Foraging ecology and occurrence of 7 sympatric babbler species (Timaliidae) in the lowland rainforest of Borneo and peninsular Malaysia. *Current Zoology*, 62(4): 345-355. DOI: 10.1093/cz/zow022.

Tokeshi, M. & Arakaki, S. (2012). Habitat complexity in aquatic systems: fractals and

beyond. *Hydrobiologia*, 685(1): 27-47. DOI: 10.1007/s10750-011-0832-z.

Vallecillo, S., Maes, J., Polce, C. & Lavalle, C. (2016). A habitat quality indicator for common birds in Europe based on species distribution models. *Ecological Indicators*, 69: 488-499. DOI: 10.1016/j.ecolind.2016.05.008.

Varasteh Moradi, H., Zakaria, M. & K Robinson, S. (2014). Understorey bird responses to the edge-interior gradient in an isolated tropical rainforest of Malaysia. *Environmental Resources Research*, 1(2): 203-232. DOI: 10.22069/IJERR.2014.1695.

Wehrberger, F. & Herler, J. (2014). Microhabitat characteristics influence the shape and size of coral-associated fishes. *Marine Ecology Progress Series*, 500: 203-214. DOI: 10.3354/meps10689.

Whelan, C.J., Şekercioğlu, Ç.H. & Wenny, D.G. (2015). Why birds matter: from economic ornithology to ecosystem services. *Journal of Ornithology*, 156(1): 227-238. DOI: 10.1007/s10336-015-1229-y.

Yahya, M.S., Puan, C.L., Atikah, S.N. & Azhar, B. (2020). Density and diversity of nocturnal birds in oil palm smallholdings in Peninsular Malaysia. *J Oil Palm Res*, 32: 57-63. DOI: 10.21894/jopr.2020.0011.

Yahya, M.S., Puan, C.L., Azhar, B., Atikah, S.N. & Ghazali, A. (2016). Nocturnal bird composition in relation to habitat heterogeneity in small scale oil palm agriculture in Malaysia. *Agriculture, Ecosystems & Environment*, 233: 140-146. DOI: 10.1016/j.agee.2016.09.003.

Zakaria, M. & Rajpar, M.N. (2015). Assessing the fauna diversity of Marudu Bay mangrove forest, Sabah, Malaysia, for future conservation. *Diversity*, 7(2): 137-148. DOI: 10.3390/d7020137.

Borneo Journal of Resource Science and Technology (2024), 14(1): 186-200
DOI: https:doi.org/10.33736/bjrst.6246.2024

The Comparison of the Histological Skin Structures of Common Sunda Toad (*Duttaphrynus melanostictus*) and Grass Frog (*Fejervarya limnocharis*)

ZI QI LIM[1], AHMAD HATA RASIT*[2] & RAMLAH ZAINUDIN*[1]

[1]Faculty of Resource Science and Technology, Universiti Malaysia Sarawak, 94300 Kota Samarahan, Sarawak, Malaysia; [2]Faculty of Medicine and Health Sciences, Universiti Malaysia Sarawak, 94300 Kota Samarahan, Sarawak, Malaysia
*Corresponding authors: rahata@unimas.my; zramlah@unimas.my
Received: 2 November 2023 Accepted: 17 April 2024 Published: 30 June 2024

ABSTRACT

Anuran skin preserves all functional activities, especially for respiration and water regulation. *Duttaphrynus melanostictus* and *Fejervarya limnocharis* are the common species found in Borneo lowlands and are well-adapted to humans. Hence, they can reproduce quickly and rapidly in great numbers in the urban area. This study aims to select these urban-type anurans and describe the skin structure and glands. Four regions of skin samples were obtained, namely Dorsal Head (DH), Dorsal Centre (DC), Ventral Head (VH) and Ventral Centre (VC). The microscopic slides were prepared accordingly as in the histological techniques including skin grossing, fixing, processing, embedding, sectioning and were stained with Haematoxylin and Eosin staining. The seromucous glands are most prevalent in all four regions for both species. Parotoid glands are clearly visible in the skin structure of *D. melanostictus*, while there is a lack of parotoid glands in *F. limnocharis*. Nonetheless, *F. limnocharis* contains regular rows of glands, whereas the distribution of glands in *D. melanostictus* is scattered. In addition, *D. melanostictus* possess dermal bones, which are absent in *F. limnocharis*. Since anuran skin is a mucosal surface that in constant direct contact with the environment, their adaptations to harsh habitats should be reflected in the skin, particularly in the urban and invasive species in this study.

Keywords: *Duttaphrynus melanostictus*, *Fejervarya limnocharis*, glands, skin histology, urban-types anuran

INTRODUCTION

An anuran's skin consists of epidermis and dermis, which is the largest and heaviest single organ of the body. Their skin can be described as the mucosal surface which will be in constant and direct contact with the aquatic and terrestrial environments that are microbial diverse and laden (Varga *et al.*, 2019). Thus, they must be adapted to the demands of both habitats with their soft, moist integument. All the functional activities of the anuran skin are preserved by the skin of amphibian, which cooperates with the cardiac and respiratory systems (Zainudin *et al.*, 2018). Hence, for efficient cutaneous respiration and reduced evaporative water losses, their skin compensates for them by osmotic reabsorption when in contact with water. In addition, anuran skin is the essential innate organ of immunity, constituting a complex network of physical, chemical, immunological, and microbiological barriers, serving as the first line of deference against pathogens in the environment (Varga *et al.*, 2019). Their skin is composed of a lot of chemical compounds secreted from the glands that may play an important role as a defensive mechanism against potential predators and as a protection against ectoparasites (Moreno-Gómez *et al.*, 2014). Most of the anurans have mucous, granular, and seromucous glands, which granular glands are also called poison glands. In the dermal layer, all these glands play different functions and vary in size and surface area. Interestingly, toads have parotoid glands and warts on their skin. When toads are disturbed, they will secrete a milky and latex-like toxin that makes them smell nasty and harmful to predators (Inger *et al*., 2017). In the same way, toads also possess the granular gland that aids in protecting them from enemies and inflict insects that might harm them.

Duttaphrynus melanostictus, is a stocky and medium-sized to large true toad belongs to the family Bufonidae. The dark crests that border the eyelids and extend downwards on either side of the eye, as well as the round warts of various sizes on the back, make *D. melanostictus* easy to

be recognised (Inger *et al.*, 2017). The body of *D. melanostictus* has a variety of colour of greyish or reddish brown throughout the distribution range, without markings other than the dark edges of the warts (Inger *et al.*, 2017). *Duttaphrynus melanostictus* have black-tipped, hooked toes that lack adhesion pads and webbing on front toes, and only have extremely small webbing on hind toes. In addition, this species lacks the dorsolateral and supratympanic folds (Jaafar *et al.*, 2009).

Fejervarya limnocharis, is a small true frog in the family Dicroglossidae. Long, narrow head, a slender and oval body is the feature of this species. Based on Inger *et al.* (2017), the skin is finely pebbled, with a series of low and interrupted ridges on the back that form a line of bumps down the rump and sides. In addition, *F. limnocharis* lacks a loose skin fold on the outside of the fifth hind toes but does have a small metatarsal tubercle (Jaafar *et al.*, 2009). There are the distinctive brown and white streaks on its lips. According to Inger *et al.* (2017), *F. limnocharis* has darker blotches on its rusty brown to brownish grey in colour back, often with U- or W-shaped marking between the shoulders. Majority of them also have a light stripe down the middle of the back from the nose to the anus.

As anurans exhibit high levels of genetic structure, strong habitat association conferred by ecological and physiological constraints, with low dispersal ability, they can be described as excellent models for evolutionary studies (Avise, 2009). Their skin is sensitive to the climatic factors including temperature and precipitation, which helps in adapting to changes in the environment. However, most histological studies have focused on the family Ranidae, Megophryidae and Rhacophoridae, and there is a lack of histological study on the skin structure of the common Sunda Toad (*Duttaphrynus melanostictus*) and Grass Frog (*Fejervarya limnocharis*). As both *D. melanostictus* and *F. limnocharis* are urban anuran species and well-adapted to human activities and typically inhabit agricultural areas, drains, road verges, lawns, and football pitches, they can be easily found in the lowland of Borneo. This allows them to reproduce and live in large numbers in urban area. Usually, the differences between frog and toad are based on their skin structure. Thus, this study, these urban-type anurans taken from similar habitat and distribution were selected to compare their skin structures. The findings may aid in the understanding of the adaptation of these anuran species to urbanisation.

MATERIALS AND METHODS

Study Areas

A total of three study sites in Sarawak were chosen for sample collection. The study sites consisted of one protected area, Matang Wildlife Centre (1˚36.917’ N, 110˚10.470’ E), and two unprotected areas: UNIMAS (1˚28.013’ N, 110˚25.694’ E) and Mayor Song Swee Guan Park (1˚31.664’ N, 110˚22.409’ E).

Field Technique

The field surveys were carried out at night between 1830 to 2200 hours, during the period of the anurans are most active. Visual Encounter Survey (VES) and sound detection were used to systematically search for anurans. The shine of anurans’ eyes can be detected with the use of headlamps, and their calls can assist to locate them. Important details including the time and date of capture, microhabitat, and the distance from the nearest water source were labelled on the plastic. Besides that, the captured anurans were measured and identified. The body mass, snout-vent length (SVL) and tibia-fibula length (TFL) were taken and recorded (Table 1).

Table 1. Field data of samples analysed in this study for skin structures

No.	Field ID	Species	Date	Hour	Measurements			Age	Gender
					SVL (mm)	TFL (mm)	Weight (g)		
1	UW193	*Fejervarya limnocharis*	2/4/2023	2005	57	29	18	Adult	Female
2	MSSG01	*Duttaphrynus melanostictus*	7/4/2023	1936	70	29	40	Adult	Male
3	MSSG02	*Duttaphrynus melanostictus*	7/4/2023	1943	79	27	42	Adult	Female
4	MSSG04	*Fejervarya limnocharis*	10/4/2023	2025	52	27	12	Adult	Male

Histological Preparations

After completing all measurement and identification procedures, two individuals of *Duttaphrynus melanostictus* and two individuals of *Fejervarya limnocharis* anurans were euthanised with absolute ethanol. The tissues were then taken and preserved in absolute ethanol for the preservation of DNA tissue. The dorsal and ventral skin of the anurans were taken, mounted on filter paper, and fixed with 10% formalin. Six steps were conducted which include skin grossing, fixing, processing, embedding, sectioning, and staining.

The initial step in preparing the slide is skin grossing, in which the skin is cut out and placed in a casket. The essential step in skin grossing is fixation with 10% formalin for 24 hours. The skins were then placed into the processor machine following the standard protocol. During skin embedding, the samples were transferred to the Tissue Embedding Center 'Tissue-Tek˚TEC°' for skin block preparation. The tissues were embedded with paraffin for rigidity. The tissues were more resistant to sectioning because the paraffin penetrates all intercellular spaces and even into the cells (Junqueira & Carneiro, 2005). The block of tissues was trimmed and sectioned when it had been solidified and hardened. The thickness of the ribbons is 4.0 µm. The ribbon with the skin tissue was put in 50 ˚C hot water and mounted on labelled microscope slides.

As the majority of tissues are colourless, it will be challenging to observe the unstained tissues under a microscope (Junqueira & Carneiro, 2005). Thus, the modified Haematoxylin and Eosin (H & E) protocol was used (Sungif, 2017). The transparent appearance of the basic structure became pinkish-red with eosin staining, while haematoxylin stained the acidic structures purplish-blue. The tissue was then mounted using Distryene Plasticizer Xylene (DPX) and covered with a cover slip.

Skin Structure Analysis

All slides were visualised and examined using a Leica ICC50 HD microscope with 40x magnification and Leica LAZ EZ software. Four regions of the skin were analysed (Figure 1 & Figure 2), including the Dorsal Head (DH), Dorsal Centre (DC), Ventral Head (VH) and Ventral Centre (VC). Ten random skin slides in each of the four regions observed represent the dorsal and ventral parts of each skin area of frogs and toads. Thus, there were 40 skin slides (N) for each individual to be analysed, with 10 slides each for DH, DC, VH, and VC. Analysis and measurements were performed using ImageJ 1.15k software, with the glands numeration of 10 slides per region counted in units and the gland area measured in millimetres (mm). The Mann-Whitney Rank Sum Test was used to distinguish between *D. melanostictus* and *F. limnocharis* based on the number of glands present and the area of the glands. The data from the Mann-Whitney Rank Sum Test were analysed by using Statistical Package for the Social Science (SPSS) software.

Figure 1. Dorsal and ventral skin regions of *D. melanostictus* for histological study. The skin regions were denoted as: DH-dorsal head, DC-dorsal centre, VH-ventral head, and VC-ventral centre

Figure 2. Dorsal and ventral skin regions of *F. limnocharis* for histological study. The skin regions were denoted as: DH-dorsal head, DC-dorsal centre, VH-ventral head, and VC-ventral centre

RESULTS

Histology of Anuran Skin

Both *Duttaphrynus melanostictus* and *Fejervarya limnocharis* have two skin layers comprised of the epidermis and dermis (Figure 3). The epidermis layer of the skin in both species consists of stratum corneum, stratum spinosum and stratum germinativum, which serve to distinguish the internal cellular environment from the external physical environment. The stratum corneum is the outermost thin layer of the epidermis, while the innermost thick layer of the epidermis is called the stratum germinativum. In addition, the intermediate layer between the stratum corneum and the regenerative stratum germinativum layer is called the stratum spinosum (Varga *et al.*, 2019). The dermis layer which located below the epidermis layers, is composed of stratum spongiosum and stratum compactum. The stratum spongiosum is the outer layer of the dermis and is composed of loosely packed connective tissue. The loose connective tissue helps in maintaining the presence of glands including seromucous glands, mucous glands, and granular glands. The stratum spongiosum of *D. melanostictus* is thicker than *F. limnocharis*, as the size of glands in *D. melanostictus* is larger than in *F. limnocharis*. Furthermore, there is the presence of ground substance in both species, which is visible at the basal of the stratum spongiosum. Besides, the stratum compactum is made of dense organised connective tissue that is rich in collagen fibres and fibroblasts (Ponssa *et al.*, 2017). Stratum compactum also functions to separate between the skin layer and muscle layer.

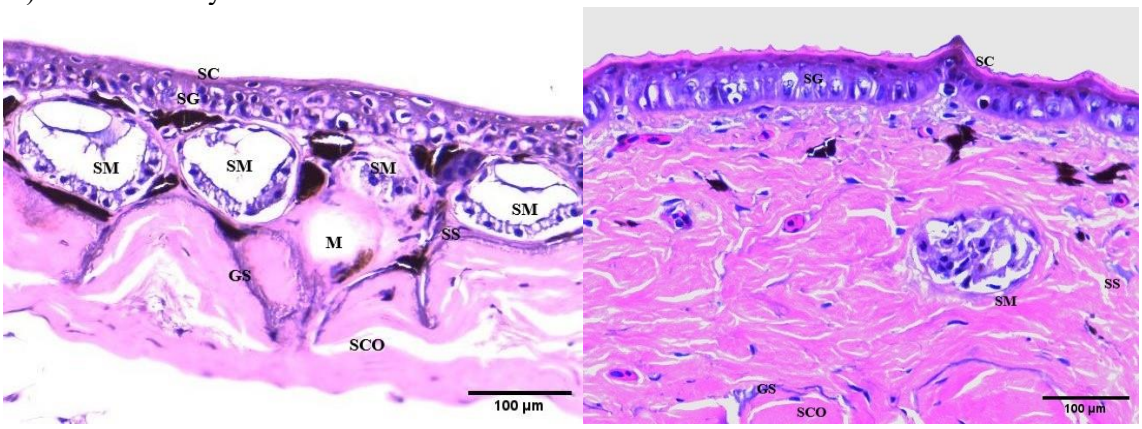

Figure 3. Histological section of the dorsal skin of *Fejervarya limnocharis* (left) and *Duttaphrynus melanostictus* (right), stained using H&E at 40x magnification. M, Mucous Glands; SM, Seromucous Glands; SC, Stratum corneum; SG, Stratum germinativum; SS, Stratum spongiosum; SCO, Stratum compactum; GS, Ground Substance

Histology of Anuran Glands

The anuran skin has several essential glands. In *D. melanostictus*, there are four types of glands present, which are mucous, seromucous, granular, and parotoid glands. *Fejervarya limnocharis*, in contrast, has only three types of glands: mucous, seromucous, and granular glands. The glands of *D. melanostictus* are found to be larger but fewer than the glands of *F. limnocharis*. In addition, the glands in *F. limnocharis* are arranged in orderly rows, while the glands arrangement of *D. melanostictus* is scattered. In contrast to the mucous and granular glands, the seromucous gland is the most prevalent in both species. Seromucous glands are mixed glands that consist of mucous and granular glands. They also include observable nuclei at the two layers of the cells. Seromucous glands also have the acinus that is bordered by simple and squamous-shaped cells, with abundant mitochondria. Besides that, mucous glands lack of cytoplasm in the acinus, giving the character an empty appearance. Despite having the same acinus lined by squamous-shaped cells similar to seromucous glands, this characteristic can distinguish mucous glands from seromucous glands. There is a low quantity of mucous glands found in *D. melanostictus* and *F. limnocharis*. Furthermore, granular glands, also known as poison glands, have a lumen filled with acinus that is made up of vacuolated, heterogeneous, and visible granular material and nuclei (Mills & Prum, 1984). In both species, the granular glands have a larger size than other glands (Figure 4).

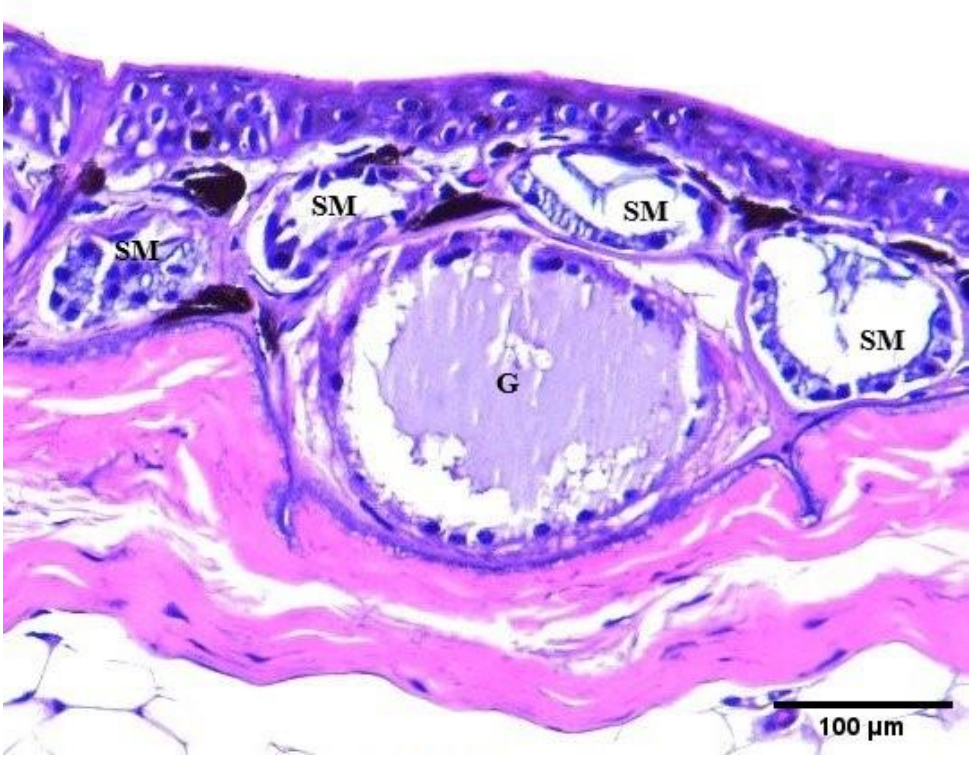

Figure 4. Glands present in the dorsal skin of *Fejervarya limnocharis*, stained using H&E at 40x magnification. SM, Seromucous Glands; G, Granular Gland

The existence of parotoid glands distinguishes the skin structures of *D. melanostictus* and *F. limnocharis*. This gland is found only in toad species, including *D. melanostictus*. Parotoid glands are made up of an accumulation of poison-producing granular alveoli. In this research, the dorsal head of *D. melanostictus* contains the structure of parotoid glands (Figure 5 & Figure 6). Compared to the granular glands in the other dorsal skin of *D. melanostictus*, the granular glands in parotoid glands (dorsal head) are particularly enormous. The dermal bones (Figure 7) found in *D. melanostictus* are also able to differentiate the skin structure between *D. melanostictus* and *F. limnocharis*. The dermal bones are clearly visible in almost all the observed slides of the dorsal parts (dorsal head and dorsal centre) of *D. melanostictus* skin.

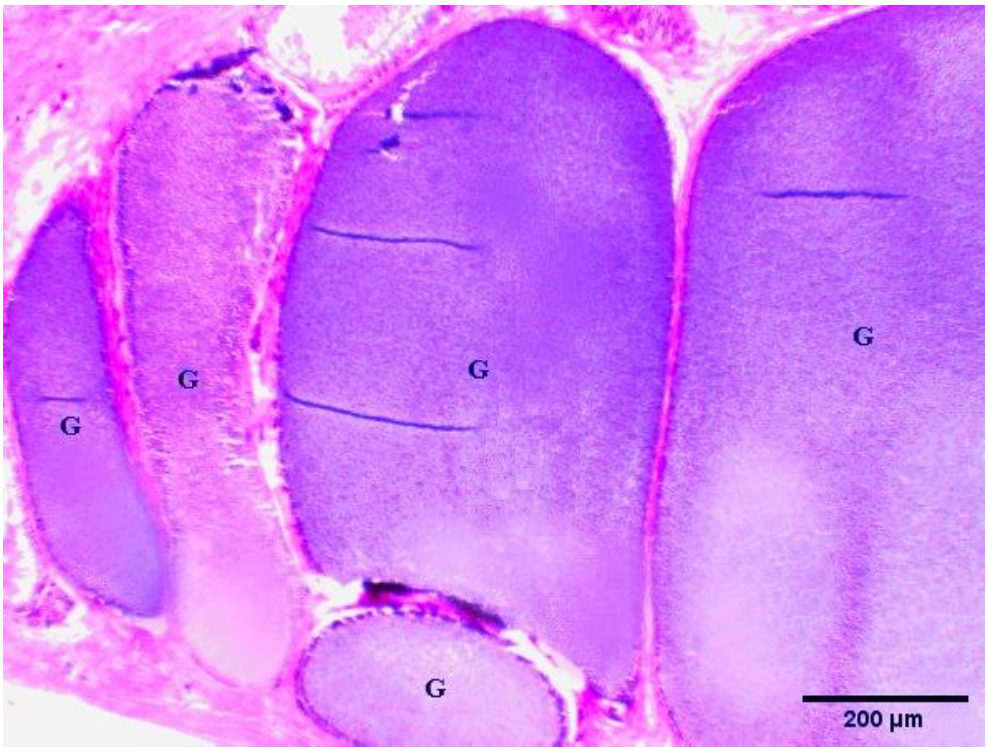

Figure 5. The parotoid gland (dorsal head) of *Duttaphrynus melanostictus* showing the distribution of granular glands, stained using H&E at 4x magnification. G, Granular Gland

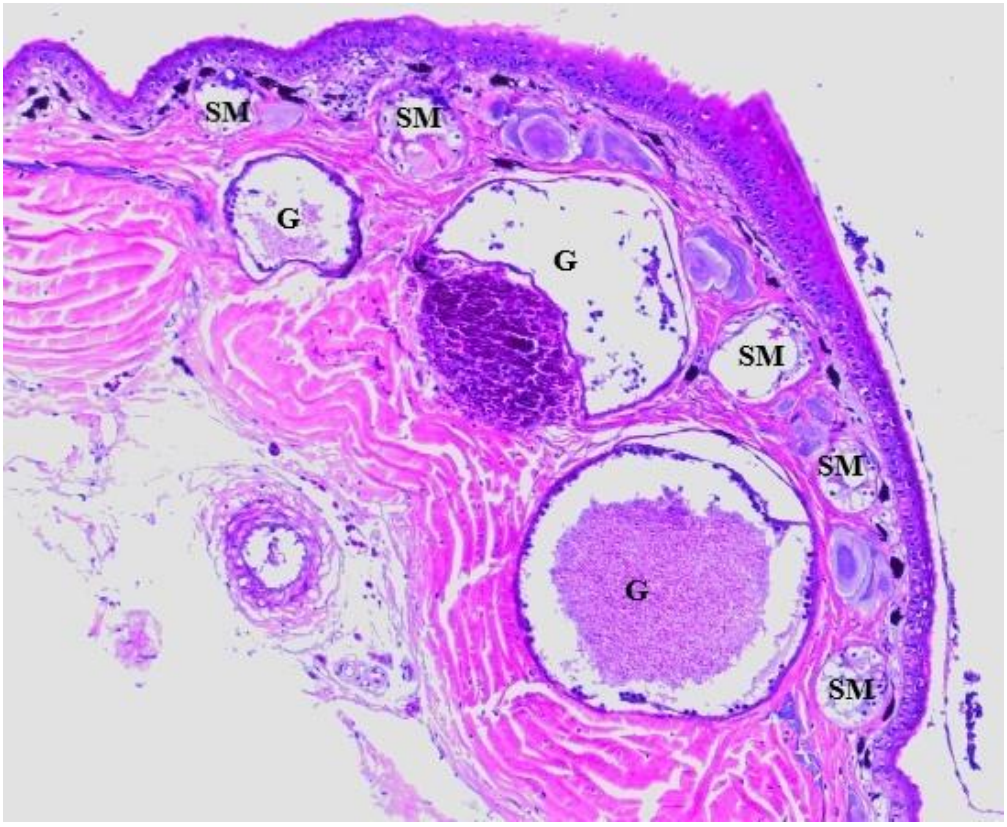

Figure 6. The parotoid gland (dorsal head) of *Duttaphrynus melanostictus* showing the distribution of seromucous and granular glands, stained using H&E at 10x magnification. SM, Seromucous Glands; G, Granular Gland

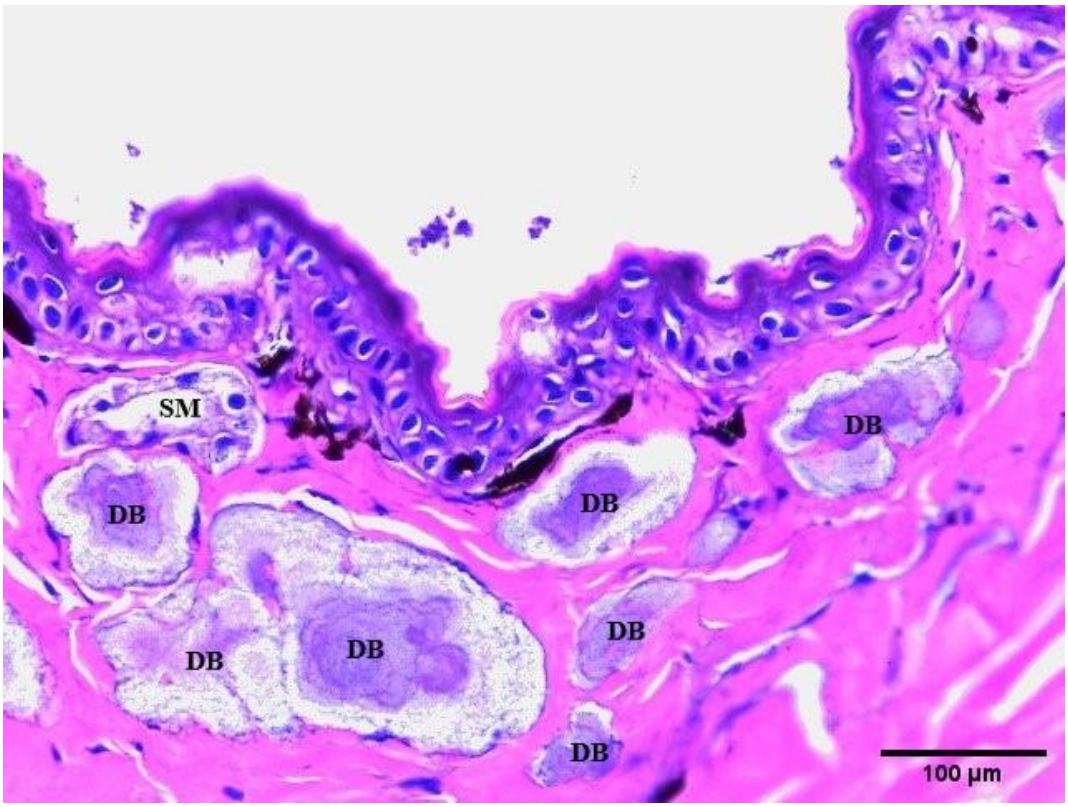

Figure 7. Dermal bone present in *Duttaphrynus melanostictus*, stained using H&E at 40x magnification. SM, Seromucous Glands; DB, Dermal Bone

Glands Numeration Between *Duttaphrynus melanostictus* and *Fejervarya limnocharis*

As the data in this research are not normally distributed and the sample sizes are small, the Mann-Whitney Rank Sum Test is an alternative to the t-test. The Mann-Whitney Rank Sum Test is a type of non-parametric test, in which the ranks of sample data from two independent populations are taken into account. In the dorsal head of *D. melanostictus* and *F. limnocharis* (Table 2 & Table 3), there is sufficient evidence to conclude that there is a significant difference in the seromucous glands present ($U = 8$, $n_1 = n_2 = 20$, $p=0.001< 0.05$ two-tailed) between the two species at 5% significance level. However, there are no statistically significant differences in the number of mucous glands ($U = 180$, $n_1 = n_2 = 20$, $p=0.298>0.05$ two-tailed) and granular glands ($U = 190$, $n_1 = n_2 = 20$, $p= 0.681 >0.05$ two-tailed) between the skin structures of *D. melanostictus* and *F. limnocharis*.

The analysis of gland numeration reveals no significant difference in the granular glands ($U = 191.5$, $n_1 = n_2 =20$, $p= 0.689 >0.05$ two-tailed) at the dorsal centre. Conversely, the significant differences in the mucous and seromucous glands present in the skin structure of *D. melanostictus* and *F. limnocharis* were observed, with values of $U = 160$, $n_1 = n_2 = 20$, $p = 0.037 < 0.05$ two-tailed and $U = 24$, $n_1 = n_2 = 20$, $p= 0.001 <0.05$ two-tailed, respectively. Additionally, it was discovered that the significant difference in the seromucous glands between these two species was found greater than the significant difference in the mucous glands between the skin structures of *D. melanostictus* and *F. limnocharis*.

In the ventral head, there is a significant difference only in the seromucous glands ($U = 15$, $n_1 = n_2 = 20$, $p= 0.001 < 0.05$ two-tailed) between the skin structures of *D. melanostictus* and *F. limnocharis* at 5% significance level. The mucous ($U = 180$, $n_1 = n_2 = 20$, $p=0.152 >0.05$ two-tailed) and granular glands ($U=190$, $n_1 = n_2 = 20$, $p=0.317 >0.05$ two-tailed) do not show statistically significant differences.

Table 2. Summarised data of numeration of glands on the dorsal head, dorsal centre, ventral head, and ventral centre between *Duttaphrynus melanostictus* and *Fejervarya limnocharis*

Skin Area	Types of Glands	Number of Glands		Mean	N	Standard Deviation	Median
		F. limnocharis	*D. melanostictus*				
Dorsal Head	Mucous	3	1	0.1	40	0.30382	0
	Seromucous	88	26	2.85	40	1.86121	2
	Granular	4	3	0.175	40	0.38481	0
Dorsal Centre	Mucous	4	0	0.1	40	0.30382	0
	Seromucous	77	31	2.7	40	1.57219	2
	Granular	3	3	0.15	40	0.42667	0
Ventral Head	Mucous	0	2	0.05	40	0.22072	0
	Seromucous	75	38	2.825	40	1.21713	3
	Granular	0	1	0.025	40	0.15811	0
Ventral Centre	Mucous	6	0	0.15	40	0.42667	0
	Seromucous	77	39	2.9	40	1.35495	3
	Granular	0	2	0.05	40	0.22072	0

Both mucous ($U = 150$, $n_1 = n_2 = 20$, $p= 0.018 < 0.05$ two-tailed) and seromucous glands ($U = 35$, $n_1 = n_2 = 20$, $p=0.001<0.05$ two-tailed) present in the ventral centre of *D. melanostictus* and *F. limnocharis* skin structure show a significant difference at 5% significance level. There is no significant difference in the number of granular glands present in the skin structure between *D. melanostictus* and *F. limnocharis* with the value of $U = 180$, $n_1 = n_2 = 20$, $p=0.152 > 0.05$ two-tailed.

It can be concluded that the number of seromucous glands in four regions (dorsal head, dorsal centre, ventral head, and ventral centre) of *D. melanostictus* and *F. limnocharis* skin structure showed a significant difference and able to distinguish between *D. melanostictus* and *F. limnocharis*.

Table 3. Summarised Mann-Whitney Rank Sum Test statistics of numeration of glands on the dorsal head, dorsal centre, ventral head, and ventral centre between *Duttaphrynus melanostictus* and *Fejervarya limnocharis*

Skin Area	Dorsal Head			Dorsal Centre			Ventral Head			Ventral Centre		
	M	SM	G	M	SM	G	M	SM	G	M	SM	G
Mann-Whitney U	180	8	190	160	24	191.5	180	15	190	150	35	180
Sig.	0.298	0.001	0.681	0.037	0.001	0.689	0.152	0.001	0.317	0.018	0.001	0.152

Notes: M= Mucous Glands, SM= Seromucous Glands, G= Granular Glands

Area of Glands Between *Duttaphrynus melanostictus* and *Fejervarya limnocharis*

The area of glands between *D. melanostictus* and *F. limnocharis* was tested by using the Mann-Whitney Rank Sum Test (Table 4 & Table 5). There is only a statistically significant difference can be observed in the dorsal head, which is the area of seromucous glands ($U = 51$, $n_1 = n_2 = 20$, $p=0.001<0.05$ two-tailed) between *D. melanostictus* and *F. limnocharis* skin structure at 5% significance level. However, the areas of mucous and granular glands showed no significant differences between these two

species, with the value of U = 180.5, $n_1 = n_2 = 20$, p=0.311>0.05 two-tailed and U = 194, $n_1 = n_2 = 20$, p=0.806>0.05 two-tailed, respectively.

In the dorsal centre, *D. melanostictus* and *F. limnocharis* have significant differences in the two types of area of glands, which are the area of mucous (U = 160, $n_1 = n_2 = 20$, p=0.038<0.05 two-tailed) and seromucous glands (U = 47, $n_1 = n_2 = 20$, p=0.001<0.05 two-tailed) at 5% significance level. However, the area of seromucous glands shows an extremely substantial difference between *D. melanostictus* and *F. limnocharis* skin structures compared to the area of mucous gland. Besides, there is also consists of the area of granular glands (U = 187, $n_1 = n_2 = 20$, p=0.541> 0.05 two-tailed), although it shows no significant difference between *D. melanostictus* and *F. limnocharis* skin structures.

Table 4. Summarised data of area of glands (mm^2) on the dorsal head, dorsal centre, ventral head and ventral centre between *Duttaphrynus melanostictus* and *Fejervarya limnocharis*

Skin Area	Types of Glands	Area of Glands (mm^2)		Mean	N	Standard Deviation	Median
		F. limnocharis	*D. melanostictus*				
Dorsal Head	Mucous	0.01128	0.00567	0.0004	40	0.00141	0
	Seromucous	0.15661	0.57413	0.0183	40	0.01717	0.009
	Granular	0.10668	0.27488	0.0095	40	0.02797	0
Dorsal Centre	Mucous	0.02618	0	0.0007	40	0.00222	0
	Seromucous	0.17372	0.5533	0.0182	40	0.01844	0.0119
	Granular	0.0189	0.19588	0.0054	40	0.01976	0
Ventral Head	Mucous	0	0.11316	0.0028	40	0.01479	0
	Seromucous	0.18575	0.78894	0.0244	40	0.03072	0.0126
	Granular	0	0.08813	0.0022	40	0.01393	0
Ventral Centre	Mucous	0.01701	0	0.0004	40	0.00122	0
	Seromucous	0.16496	0.57194	0.0184	40	0.01546	0.0132
	Granular	0	0.18539	0.0046	40	0.02323	0

In the ventral head, there is sufficient evidence to conclude that there is a significant difference between the areas of seromucous glands in *D. melanostictus* and *F. limnocharis* skin structures at 5% significance level. The null hypothesis is rejected as the area of seromucous glands (U = 9, $n_1 = n_2 = 20$, p=0.001<0.05 two-tailed) can prove the difference between these two species. In contrast, the analysis of the areas of mucous and granular glands shows values trending towards similarities between *D. melanostictus* and *F. limnocharis* skin structures, with U = 180, $n_1 = n_2 = 20$, p = 0.152>0.05 two-tailed and U = 190, $n_1 = n_2 = 20$, p=0.317>0.05 two-tailed, respectively.

The areas of mucous (U = 150, $n_1 = n_2 = 20$, p=0.019<0.05 two-tailed) and seromucous glands (U = 20, $n_1 = n_2 = 20$, p=0.001<0.05 two-tailed) in the ventral centre have an effect on the significant difference between *D. melanostictus* and *F. limnocharis* skin structures. There is no significant difference in the area of granular glands in the skin structures between *D. melanostictus* and *F. limnocharis* with the value of U = 180, $n_1 = n_2 = 20$, p=0.152>0.05 two-tailed.

The area of seromucous glands in the dorsal head, dorsal centre, ventral head, and ventral centre in *D. melanostictus* and *F. limnocharis* had been proved to have a highly significant difference in the area of glands present in *D. melanostictus* and *F. limnocharis* skin structure with a significant level of $\propto = 0.05$. It can be said that the area of seromucous glands in *D. melanostictus* has a large difference compared to the area of seromucous glands in *F. limnocharis* skin structure.

Table 5. Summarised Mann-Whitney Rank Sum Test Statistics of area of glands (mm^2) on the dorsal head, dorsal centre, ventral head and ventral centre between *Duttaphrynus melanostictus* and *Fejervarya limnocharis*

Skin Area	Dorsal Head			Dorsal Centre			Ventral Head			Ventral Centre		
	M	SM	G	M	SM	G	M	SM	G	M	SM	G
Mann-Whitney U	180.5	51	194	160	47	187	180	9	190	150	20	180
Sig.	0.311	0.001	0.806	0.038	0.001	0.541	0.152	0.001	0.317	0.019	0.001	0.152

Notes: M= Mucous Glands, SM= Seromucous Glands, G= Granular Glands

DISCUSSION

Urbanisation is accelerating worldwide, which means that the increasing population growth and the demand for basic life have resulted in the cities' inhabitation with the modification of landscapes dominated by architectural structural for human benefit. However, urbanisation has fundamentally altered the composition of wildlife communities, leading to biodiversity loss and the development of more species to urban areas (Bradley & Altizer, 2007). For instance, *Duttaphrynus melanostictus* and *Fejervarya limnocharis* are both urban anuran species, which can be well adapted to an environment disturbed by human activities. Fortunately, the existence of urban green lands aids some species in reducing habitat loss and preserving water runoff from impervious urban surfaces as well as serving as the breeding habitat for amphibians, particularly for anurans (Zhang *et al.*, 2015). As they adapt to urban environments, their skin structure must have some changes and becomes sensitive to the environment. This is due to the fact that the essential role of skin as the anuran's mechanical barrier, medium for ion transports and water regulation, sensor apparatus, part of chemical defence mechanism, respiratory organ, and sodium reservoir, that aid in anuran survival (Barlian *et al.*, 2011).

There are obvious distinguishes in skin morphology, with frogs having a thin layer of moist, soft textured skin and toads having a thick layer of dry, rough skin. Nevertheless, both possess epidermis and dermis layers. In the epidermis, the stratum corneum is formed of a thin layer of keratinized cells (Varga *et al.*, 2019), owing to the anuran skin usually "naked" with the absence of the covering with scales, feathers, or hair characters (Sungif, 2017). The keratinized cells that contain the substance alfakeratin are the alternative cells to assist prevent the loss of humidity and respond to environmental contamination (Barlian *et al.*, 2011). The thickness of the stratum corneum of *F. limnocharis*, nevertheless, is thinner than the stratum corneum of *D. melanostictus*. This is because the skin of *D. melanostictus* is water-tight and consists of warts, cones and spines, which induce the stratum corneum to thicken and become more densely packed with keratins (Elias & Shapiro, 1957). Thus, *F. limnocharis* is more susceptible to environmental contaminants and less tolerable to the resistance of water movement between internal and external environments (Campbell *et al.*, 2012), compared with *D. melanostictus*. *Fejervarya limnocharis* shows antibacterial activity against to environmental contaminants such as *Streptococcus pneumoniae* multidrug-resistant, in contrast to the forest frog, *Limnonectes macrodon* (Suhyana *et al.*, 2015). As a result, the stratum corneum of *F. limnocharis* still has the function of reducing water loss via evaporative dehydration and barrier to environmental contaminants without the existence of warts, cones, and spines in the skin. Hence, this becomes a proof that both *D. melanostictus* and *F. limnocharis* adapt to the urban areas, but *D. melanostictus* can be more tolerant to the warmer ambient temperature. In addition, stratum germinativum is also present as the innermost layer of the epidermis, which is the thick layer of the epidermis in *D. melanostictus* and *F. limnocharis* skin structure. This stratum provides strong adherence to the dermis underneath and conducts cell division (Maderson, 2010), which produces the outermost layer of the epidermis and develops into the uppermost layer of keratin (Sungif, 2017). Furthermore, the stratum spinosum, which serves as the intermediate layer between the stratum corneum and the stratum germinativum, is composed of oval to round terminally differentiating cells in the layer of the epidermis (Varga *et al.*, 2019). Different types of

cells such as epithelial cells, immune cells, as well as chromatophores which function as the producers of pigmentation patterns, are present in this layer (Cömden *et al.*, 2023).

There is also the observation of the dermis layer compasses of stratum spongiosum and stratum compactum. The outermost layer of the dermis, the stratum spongiosum, consists of loosely packed connective tissue. In both *D. melanostictus* and *F. limnocharis*, the loosely packed connected tissue helps to maintain the seromucous glands, mucous glands, and granular glands. Thus, the stratum spongiosum can be described as the gland's storage place. Despite this, the stratum spongiosum of *D. melanostictus* is thicker than *F. limnocharis*. This is due to the skin of *D. melanostictus* containing glands that are larger than those found in *F. limnocharis*, and the area-to-skin ratio of glands in *D. melanostictus* is higher than in the skin of *F. limnocharis*. Furthermore, the existence of stratum compactum in both species' skin structure aids in separating the skin layer and muscle layer. Therefore, it is composed of a substantial density of organized connective tissue that is abundant in collagen fibres and fibroblasts (Ponssa *et al.*, 2017). It can be inferred that the thickness of stratum spongiosum and stratum compactum in *D. melanostictus* is thicker than in *F. limnocharis*, as *D. melanostictus* has the enormous size of glands that require more physical support to maintain in the dermis of the skin.

According to Zainudin *et al.* (2018), the ground substance, which can be observed at the basal of the stratum spongiosum of both species, is a type of spongy moisture agent that serves to provide fluid to the interior of the stratum spongiosum. This is essential for urban-type anurans, as they are mostly in dry and terrestrial environments. This is because some urban-type anurans might not be able to alter their skin properties in response to changing environmental conditions, and the presence of ground substance can aid the skin in maintaining moisture (Zainudin *et al.*, 2018). In the comparison of *D. melanostictus* and *F. limnocharis* skin structure, *F. limnocharis* has a thicker ground substance than those in *D. melanostictus* skin structure. In addition, the less or lack of mucous glands in *D. melanostictus* skin structure can be described as the skin of *D. melanostictus* can gain moisture directly from the substrate (Zainudin *et al.*, 2018). This can be explained that *D. melanostictus* can be more adaptable and survive in terrestrial habitats, compared with *F. limnocharis*. It also can be concluded that *D. melanostictus* has the capacity to adjust and change its skin properties to fit the different types of environments.

The dermal bones were discovered on the dorsal parts of the skin of *D. melanostictus*, consistent with *Pelobatrachus nasutus* (Zainudin *et al.*, 2018), which is a condition corresponds to dermal ossifications. These dermal bones on the head and back of the pumpkin toadlets are visible through particularly thin skin due to fluorescence patterns (Goutte *et al.*, 2019), which may serve as intra-specific communication signals or as reinforcement for their aposematic colouration (Bowler, 2019). Such characteristics aid in alerting prospective predators to their toxicity. This suggests that the dermal bone of *D. melanostictus* may have the same function as the dermal bone in pumpkin toadlets.

All the exocrine glands appear in the stratum spongiosum, including mucous, seromucous, and granular glands, but only the toad species (*D. melanostictus* in this research) has the parotoid glands on the dorsal head skin section. Parotoid glands are the developed glandular accumulation in various body regions, and these glands are located in the dorsum of the head in *D. melanostictus* (Mariano *et al.*, 2019). and consists mainly of large alveoli with a milky secretion (Toledo *et al.,* 1992). Thus, this becomes a reason that the skin of *D. melanostictus* is thicker than *F. limnocharis*, as the parotoid glands near the eyes require physical support (Rais, 2012). The arrangement of alveoli in the parotoid glands of *D. melanostictus* shared a similar structure with *Phryoidis juxtaspera* in a honeycomb-like arrangement (Sungif, 2017). A large variety of alkaloids and steroids are present in the milky and latex-like toxins secreted by parotoid glands (Toledo *et al.,* 1992; Mariano *et al.*, 2019). This toxin acts as the chemical barrier against predators of microbial infection. Consequently, the toad venom produced by the dried toxin secretions of parotoid glands has high medicinal value to traditional Chinese medicine (Yang *et al.*, 2023). In addition, the granular glands in parotoid glands, on the dorsal head of *D. melanostictus* in this research, are enormous.

This explained the numeration of granular glands that had been measured in *D. melanostictus* lower than in *F. limnocharis*. It is because the measurements and calculations were taken when the magnification of the microscope was 40x, while the majority of the granular glands could only be observed in full detail in the microscope at a magnification of 4x or 10x. Apart from the parotoid glands, the granular glands in both species secrete the toxins containing peptides, amines and alkaloids that can protect them from microorganisms that exist on their skin surface and are fatal to prospective predators (Zainudin *et al.*, 2018). According to Rasit *et al.* (2018), this gland also has the potential for medical application, which produces secretion-containing peptides. Thus, the granular glands are most abundant at the dorsal part of the skin since these areas are typically exposed to the environment during both species are foraging, resting, or mating (Rasit *et al.*, 2018). Interestingly, the rate of epithelialisation of anuran skin wound is influenced by the concentration of granular glands (Rasit *et al.*, 2018; Rasit *et al.*, 2023).

In comparison to granular and mucous glands, the seromucous glands are significantly more prevalent in the dorsal and ventral parts of these two species. As seromucous glands are the mixed glands of mucous and granular, they also secrete toxins that serve the same functions as those secreted by the granular glands. Even though *D. melanostictus* has parotoid glands in the dorsal head of the body, the granular and seromucous glands also can aid in immunity to environmental variables. The granular and seromucous glands are the sole protective structures in the skin of *F. limnocharis* due to the absence of parotoid glands. Besides, the seromucous glands are exhibiting over the entire body in the skin structure of *D. melanostictus* and *F. limnocharis*. As the seromucous glands consist of mucous, they help preserve skin moisture and provide wet conditions for all regions of the body (Sungif, 2017). It can be assumed that the more seromucous glands emerge inside the skin of the anuran, the longer duration the anuran can stay and thrive in drier conditions. Additionally, it is possible to say that having seromucous glands is equivalent to compacting both types of glands in one way. This may be the strategy of *D. melanostictus* and *F. limnocharis* to be able to adapt, colonise and inhabit dry environments terrestrial that may lack of water sources or humidity (Razali, 2017).

The mucous glands, nonetheless, have a low quantity found in the skin structure *D. melanostictus* and *F. limnocharis*. The enumeration of mucous glands on the dorsal centre and ventral centre showed only significant differences between *D. melanostictus* and *F. limnocharis*. This is due to the dorsal centre and ventral centre of *D. melanostictus* lacking mucous glands. As the mucous glands are the ones that primarily focus on gas exchange and water balance (Mailho-Fontana *et al.*, 2017), the mucous glands produce a clear secretion that acts as the lubricant in water and is composed of glycoproteins such as mucin, mucinogen, sialic acid and carbohydrate residue including galactose and fructose (Garg *et al.*, 2008). The reason the skin of *F. limnocharis* contains a smaller number of mucous glands may be the adaptation to dry habitat, as their preference for hiding in the marshes or ponds to minimise water loss via evaporation and maintain a stable body temperature (Lillywhite & Licht, 1975). At the same time, it has been hypothesized that *D. melanostictus*, which has fewer or no mucous glands, may adapt to the drier environment by having a large size of the body since it has a greater volume to hold onto water and comparatively less surface area to lose it (Sungif, 2017). However, it also can be argued that the use of skin regions to identify glands may not be appropriate as the ventral head of these two species may not be in direct contact with the substrate.

The area of granular glands presents in *D. melanostictus* and *F. limnocharis* shows insufficient evidence to conclude that the significant differences between these two species on the dorsal head, dorsal centre, ventral head, and ventral centre. This is because of the large size of the majority of the granular glands in the skin structure of *D. melanostictus*, which necessitates the use of the microscope with 4x magnification to observe the whole of the glands. In addition, there is a lack of granular glands in the ventral regions of *F. limnocharis* skin structure. This is due to most granular glands are on the dorsal head, where they serve to protect *F. limnocharis* from potential predators and ectoparasites (Moreno-Gómez *et al.*, 2014). In contrast, there is a statistically significant difference in the area of seromucous glands present in both species' dorsal head, dorsal centre, ventral head, and ventral centre. As the

area of seromucous glands in *D. melanostictus* is about 3.5 times greater than those in *F. limnocharis* skin structure, the difference between these two species can be detected obviously. Compared to the seromucous glands in *F. limnocharis* skin structure, the seromucous glands in *D. melanostictus* revealed less in amount but a larger size. This results in the stratum spongiosum in *D. melanostictus* being thicker than in *F. limnocharis*. This may be due to the large total body size of *D. melanostictus*. Besides, the area of mucous glands on the dorsal centre, ventral head and ventral centre showed a significant difference between *D. melanostictus* and *F. limnocharis* skin structure. This is because the small number of mucous glands in the skin structure of *D.* melanostictus, as it may adapt to dry environments by its large body size.

The seromucous glands are most abundant in all parts of the skin areas (dorsal head, dorsal centre, ventral head, and ventral centre) with significant differences in the number of glands present and the area of the glands present in *D. melanostictus* and *F. limnocharis*. The seromucous glands are arguably the most essential glands required for both species. The seromucous and parotoid glands can demonstrate that the skin structure of *D. melanostictus* is different from *F. limnocharis* skin structure. As these anurans are urban species, the number and area of glands aid in determining their adaptation to the surrounding environments. Thus, this study supports the opinion that the distribution of mucous and seromucous glands in different skin regions can reflect the habits of *Pelobatrachus nasutus* in their natural habitat (Zainudin *et al.*, 2018). According to Rasit *et al.* (2023), the mucous glands are critical to represent the water quality of the habitats, as a low quantity of mucous glands in both species can prove that low water quality in urban areas. This also suggests that the large number of seromucous glands serves to defend against high levels of microbial activity in the water resources, facilitate the diffusion of oxygen through the skin (Rasit *et al.*, 2023), and maintain skin moisture.

CONCLUSION

In conclusion, the presence of parotoid glands can demonstrate that the species is a toad species and seromucous glands are the most abundant glands present in all four analysed skin regions of *Duttaphrynus melanostictus* and *Fejervarya limnocharis*. The dermal bones found in *D. melanostictus* are also able to differentiate them. It is possible to distinguish *D. melanostictus* and *F. limnocharis* based on the variation in the thickness of the epidermis and dermis, as well as gland distribution. In addition, the seromucous glands are the most abundant glands present in all four analysed skin regions of *D. melanostictus* and *F. limnocharis*. The enumeration of seromucous glands allows the seromucous glands to distinguish between these two species. The number and area of glands also can determine their adaptation to the environments. Further study and research might explore more on the different types of urban anuran species. In addition, future studies also can focus on the dermal bone within the skin structure, as there is only little research about this has been done.

ACKNOWLEDGEMENTS

This project was funded by the Malaysian Ministry of Higher Education's Fundamental Research Grant Scheme (FRGS/1/2020/SKK0/UNIMAS/01/1) with a research permit from the Sarawak Biodiversity Council (SBC-2021-RDP-34-AHR) and the Sarawak Forestry Department (WL08/2022). The animal ethics approval (UNIMAS/AEC/R/F07/043) was issued by the Animal Ethics Committee of Universiti Malaysia Sarawak. Special thanks to the Faculty of Resource Science and Technology (FRST) and Department of Pathology, Faculty of Medicine and Health Sciences (FMHS) for technical support.

REFERENCES

Avise, J.C. (2009). Phylogeography: retrospect and prospect. *Journal of Biogeography,* 36(1): 3-15. DOI: 10.1111/j.1365-2699.2008.02032.x

Barlian, A., Anggadiredja, K., Kusumorini, A. & Ekawati, U. (2011). Structure of *Duttaphrynus melanostictus* frog skin and antifungal potency of the skin extract. *Journal of Biological Sciences,* 11(2): 196-202. DOI: 10.3923/jbs.2011.196.202

Bowler, J. (2019). *Scientists Have Discovered*

These Toxic Frogs Have Bones Glowing Through Their Skin. Retrieved June 1, 2023, from https://www.sciencealert.com/these-cute-little-orange-frogs-have-a-florescent-secret-under-their-skin

Bradley, C.A. & Altizer, S. (2007). Urbanization and the ecology of wildlife diseases. *Trends in Ecology and Evolution,* 22(2): 95-102. DOI: 10.1016/j.tree.2006.11.001

Campbell, C.R., Voyles, J., Cook, D.I. & Dinudom, A. (2012). Frog skin epithelium: electrolyte transport and chytridiomycosis. *The International Journal of Biochemistry and Cell Biology,* 44(3): 431-434. DOI: 10.1016/j.biocel.2011.12.002

Cömden, E.A., Yenmis, M. & Cakir, B. (2023). The complex bridge between aquatic and terrestrial life: skin changes during development of amphibians. *Journal of Developmental Biology,* 11(1): 1-15. DOI: 10.3390/jdb11010006

Elias, H. & Shapiro, J. (1957). *Histology of the skin of some toads and frogs.* New York, USA: American Museum of Natural History.

Garg, A.D., Hippargi, R. & Gandhare, A.N. (2008). Toad skin-secretions: potent source of pharmacologically and therapeutically significant compounds. *The Internet Journal of Pharmacology,* 5(2): 17.

Goutte, S., Mason, M.J., Antoniazzi, M.M., Jared, C., Merle, D., Cazes, L., Toledo, L.F., el-Hafci, H., Pallu, S., Portier, H., Schramm, S., Gueriau, P. & Thoury, M. (2019). Intense bone fluorescence reveals hidden patterns in pumpkin toadlets. *Scientific Reports,* 9(1): 5388. DOI: 10.1038/s41598-019-41959-8

Inger, R.F., Stuebing, R.B., Grafe, T.U. & Dehling, J.M. (2017*). A field guide to the frogs of Borneo.* Third Edition. Sabah, Malaysia: Natural History Publications (Borneo).

Jaafar, I., Teoh, C.C., Mohd Sah, S.A. & Md. Akil, M.A.M. (2009). Checklist and simple identification key for frogs and toads from District IV of the MADA Scheme, Kedah, Malaysia. *Tropical Life Sciences Research*, 20(2): 49-57.

Junqueira, L.C. & Carneiro, J. (2005). *Basic histology.* Eleventh Edition. New York, USA: McGraw-Hill Companies, Inc.

Lillywhite, H.B. & Licht, P. (1975). A comparative study of integumentary mucous secretions in amphibians. *Comparative Biochemistry and Physiology Part A: Physiology,* 51(4): 937-941. DOI: 10.1016/0300-9629(75)90077-8

Maderson, P.F.A. (2010). Histological changes in the epidermis of snakes during the sloughing cycle. *Journal of Zoology,* 146(1): 98-113. DOI: 10.1111/j.1469-7998.1965.tb05203.x

Mailho-Fontana, P.L., Antoniazzi, M.M., Rodrigues, I., Sciani, J.M., Pimenta, D.C., Brodie, E.D., Rodrigues, M.T. & Jared, C. (2017). Paratoid, radial, and tibial macroglands of the frog *Odontophrynus cultripes*: differences and similarities with toads. *Toxicon,* 129: 123-133. DOI: 10.1016/j.toxicon.2017.02.022

Mariano, D.O.C., Messias, M.D.G., Spencer, P.J. & Pimenta, D.C. (2019). Protein identification from the parotoid macrogland secretion of *Duttaphrynus melanostictus*. *Journal of Venomous Animals and Toxins including Tropical Diseases,* 25(1): 1-12. DOI: 10.1590/1678-9199-jvatitd-2019-0029

Mills, J.W. & Prum, B.E. (1984). Morphology of the exocrine glands of the frog skin. *American Journal of Anatomy,* 171(1): 91-106. DOI: 10.1002/aja.1001710108

Moreno-Gómez, F., Duque, T., Fierro, L., Arango, J., Peckham, X. & Asencio-Santofimio, H. (2014). Histological description of the skin glands of *Phyllobates bicolor* (Anura: Dendrobatidae) using three staining techniques. *International Journal of Morphology,* 32(3): 882-888.

Ponssa, M.L., Barrionuevo, J.S., Alcaide, F.P. & Alcaide, A.P. (2017). Morphometric variations in the skin layers of frogs: an exploration into their relation with ecological parameters in *Leptodactylus* (Anura, Leptodactylidae), with an emphasis on the Eberth-Kastschenko layer. *The Anatomical*

Record, 300(10): 1895-1909. DOI: 10.1002/ar.23640

Rais, S.M. (2012). *Extracting high-quality DNA and PCR amplification from anuran skin (Bornean toads)* (Final Year Project Report), Universiti Malaysia Sarawak, Malaysia.

Rasit, A.H., Sungif, N.A.M., Zainudin, R. & Ahmad Narihan, M.Z. (2018). The distribution and average size of granular gland in poisonous rock frog, *Odorrana hosii*. *Malaysian Applied Biology Journal,* 47(1): 23-28.

Rasit, A.H., Tham, V., Zainudin, R. & Ahmad Narihan, M.Z. (2023). The relationship between *Odorrana hosii* skin histology and habitat water quality in different locations of Sarawak. *Borneo Journal Resource Science and Technology,* 13(2): 42-52. DOI: 10.33736/bjrst.5524.2023

Razali, S.R. (2017). *Skin structure difference in tree-frogs (genus Polypedates) at Kubah National Park, Sarawak, Borneo* (Final Year Project Report), Universiti Malaysia Sarawak, Malaysia.

Suhyana, J., Artika, I.M. & Safari, D. (2015). Activity of skin secretions of frog *Fejervarya limnocharis* and *Limnonectes macrodon* against *Streptococcus pneumoniae* multidrug resistant and molecular analysis of species *F. limnocharis*. *Current Biochemistry,* 2(2): 90-103. DOI: 10.29244/cb.2.2.99-112

Sungif, N.A.M. (2017). *Histology of selected Bornean frogs' skin in Sarawak, Malaysia.* (Master thesis), Universiti Malaysia Sarawak, Malaysia.

Toledo, R.C., Jared, C. & Junior, A.B. (1992). Morphology of the large granular alveoli of the paratoid glands in toad (*Bufo ictericus*) before and after compression. *Toxicon,* 30(7): 745-753. DOI: https://doi.org/10.1016/0041-0101(92)90008-S

Varga, J.F.A., Bui-Marinos, M.P. & Katzenback, B.A. (2019). Frog skin innate immune defences: sensing and surviving pathogens. *Frontiers in Immunology,* 9: 3128. DOI: 10.3389/fimmu.2018.03128

Yang, M., Huan, W., Zhang, G., Li, J., Xia, F., Durrani, R., Zhao, W., Lu, J., Peng, X. & Gao, F. (2023). Identification of protein quality markers in toad venom from *Bufo gargarizans*. *Molecules,* 28(8): 3628. DOI: 10.3390/molecules28083628

Zainudin, R., Deka, E.Q., Awang Ojep, D.N., Su'ut, L., Ahmad Puad, A.S., Jayasilan, M.A. & Rasit, A.H. (2018). Histological description of the Bornean horned frog *Megophrys nasuta* (Amphibia: Anura: Megophryidae) skin structure from different body regions. *Malaysia Applied Biology,* 47(1): 51-56.

Zhang, W., Li, B., Shu, X., Xie, H., Pei, E., Yuan, X., Sun, Y., Wang, T. & Wang, Z. (2015). A new record of *Kaloula* (Amphibia: Anuran: Microhylidae) in Shanghai, China. *Asian Herpetological Research,* 6(3): 240-244. DOI: 10.16373/j.cnki.ahr.140070